1-1-2011

Histological evaluation of putative biomarkers in prostate cancer

Gillian O'Hurley
Royal College of Surgeons in Ireland

"Histological evaluation of putative biomarkers in prostate cancer"

Gillian O'Hurley B.Sc. (Hons), M.Sc.

The thesis is submitted to the Royal College of Surgeons in Ireland for the degree of Ph.D. in the Faculty of Science.

August 2011

Based on research carried out at

Department of Pathology,

RCSI Education & Research Centre,

Beaumont Hospital,

&

School of Biotechnology,

Dublin City University,

Dublin 9,

Ireland.

Prof. Elaine Kay (RCSI/Beaumont Hospital), Supervisor,

Prof. Richard O'Kennedy (DCU), Co-Supervisor.

Acknowledgments

Firstly, I wish to express my appreciation and gratitude to Prof. Elaine Kay and Prof. Richard O'Kennedy. This thesis would not have been possible without the expert knowledge, direction, support and patience of my supervisor, Elaine Kay and the good advice and guidance of my co-supervisor, Richard O'Kennedy. It has been an invaluable experience working with both of you on both an academic and a personal level, for which I am extremely grateful.

I would also like to acknowledge and thank Dr. Tony O'Grady, Mr. Robert Cummins, Ms. Etain Daly, Prof. Mary Leader and everyone who was a member of the RCSI Histopathology Department during my four years in Beaumont Hospital for their assistance, support and friendship during my time there. I am especially grateful to Tony O'Grady for his endless guidance, wisdom and encouragement throughout my Ph.D.

I would also like to thank all the members (too many to name individually) of the Applied Biochemistry Group and the School of Biotechnology in DCU for their welcoming attitude, all their friendship and support in the last two years of my Ph.D. Special thanks to Dr. Stephen Hearty for all his assistance during my time in the DCU Lab.

In addition, I wish to thank the Irish Cancer Society and the Prostate Cancer Research Consortium who funded and supported this work. Special thanks to Prof. William Watson, Dr. Antoinette Perry, Prof. Orla Sheils, Prof. John O'Leary, Prof. Mark Lawler and all collaborators and colleagues within the Prostate Cancer Research Consortium for their insights and direction throughout my project.

Most importantly, I would like to thank my parents, family and friends for all their help, endless support and advice in the course of this Ph.D. Only by their constant effort and encouragement am I able to complete this Ph.D.

Table of contents

List of Abbreviations

Ab – antibody

Abs – absorbance

ABP – albumin binding protein

AD – allelic discrimination

ADep – androgen-dependent

AI – androgen-independent

AMACR – alpha methylacyl –Coenzyme A racemase

AP – alkaline phosphatase

AR – androgen receptor

BCH – basal cell hyperplasia

BCR – biochemical recurrence

BIMS – biobank information management system

BMP– bone morphogenetic protein

BSA – bovine serum albumin

BPH – benign prostatic hyperplasia

cDNA – complementary deoxyribonucleic acid

CDR – complementary determining region

CH_1 – constant region 1 of heavy chain

CH_2 – constant region 2 of heavy chain

CH_3 – constant region 3 of heavy chain

CL – constant light chain

CP – chronic prostatitis

CPPS – chronic pelvic pain syndrome

CRD – cysteine rich domain

CRPC – castration-resistant prostate cancer

cTnI – cardiac troponin I

DAB – 3, 3'-diaminobenzidine

DCU– Dublin City University

DMSO – dimethyl sulfoxide

DNA – deoxyribonucleic acid

DRE – digital rectal examination

Dsh – Dishevelled

DT T – Dithiothreitol

E. coli – Escherichia coli

EDC – N-ethyl-N'-(dimethylamiopropyl) carbodiimide

EDTA – ethylenediaminetetraacetic acid

ELISA – enzyme-linked immunosorbent assay

ER-α – estrogen receptor alpha

Fc – constant fragment (of antibody)

Fv – variable fragment (of antibody)

Fab – antigen binding fragment (of antibody)

FAM – 6-carboxyflourescein

FCA – Freund's complete adjuvant

FCIA – Freund's incomplete adjuvant

FDA – Food and Drug Administration

FFPE – formalin fixed paraffin embedded

FISH – fluorescent *in situ* hybridization

FR – framework region

fPSA – free prostate specific antigen

Fzd – frizzled

GSK – glycogen synthase kinase 3

GST – glutathione-s-transferase

G3 – Gleason grade 3

G4 – Gleason grade 4

G5 – Gleason grade 5

HA – haemagglutinin

HDAC – histone deacetylase

HER-2 – human epidermal growth factor 2

hFABP – heart fatty acid binding protein

HMWK – high molecular weight kininogen

HRP – horseradish peroxidase

HSA – human serum albumin

HV – hypervariable

H&E – haematoxylin and eosin

Ig – immunoglobulin

IHC – immunohistochemistry

IL – interleukin

IMAC – immobilised metal affinity chromatography

IMM – Institute of Molecular Medicine

IFN – interferon

IPTG – isopropyl-β-D-galactopyranoside

IP – immunoprecipitation

ISH – *in situ* hybridization

ISUP – International Society of Urological Pathology

JNK – cJun N-terminal kinase

JOE – 6-carboxy-4,5-dichloro-2,7-dimethoxyfluorescein

KLH – keyhole limpet hemocyanin

KNG-1 – kininogen 1

LCM – laser capture microdissection

LRP – LDL- receptor related protein

mAb – monoclonal antibody

MALDI-TOF MS – matrix-associated laser desorption/ionization

MBD – methyl-binding domain protein

MHC- major histocompatibility complex

mRNA – messenger RNA

MTA – Multiplex Tissue Immunoblotting

MW – molecular weight

MWCO – molecular weight cut-off

NFAT – nuclear factor of activated T-cells

NFQ – non-fluorescent quencher

NIH – National Institutes of Health

NTA – nitrilotriacetic acid

OD – optical density

O/N – overnight

pAb – polyclonal antibody

PAP – prostate specific acid phosphatase

PAGE – polyacrylamide gel electrophoresis

PBS – phosphate buffered saline

PCR – Polymerase Chain Reaction

PCRC – Prostate Cancer Research Consortium

PEG – polyethylene glycol

PIN – prostatic intraepithelial neoplasia

PKC – protein kinase C

PMSF – phenylmethanesulphonyl fluoride

PSA – prostate specific antigen

PSAP – prostate specific acid phosphatase

PSMB-6 – proteasome subunit beta type 6

PURE – protein synthesis using recombinant elements

QIF – quantitative immunoflourescence

RBS – ribosomal binding site

RCSI – The Royal College of Surgeons in Ireland

RNA – ribonucleic acid

RPM – revolutions per minute

RPPA – reverse phase protein lysate array

RQ – relative quantitation

RT-PCR – "real-time" polymerase chain reaction

SCNC – small cell (neuroendocrine) carcinoma

SB – super broth

scAb – single chain antibody fragment

scFv – single chain variable fragment

SDS – sodium dodecyl sulphate

SELDI-TOF MS – surface-enhanced laser desorption/ionization

SFRP-2 – secreted frizzled related protein 2

SNPs – single-nucleotide polymorphisms

SOE – splice by overlap extension

TAMRA – 6-carboxy-N,N,N',N'-tetramethylrhodamine

TB – terrific broth

TCC –Transitional Cell Carcinoma

TEMED – Tetramethylethylenediamine

TET – 6-carboxy-4,7,2',7'-tetrachlorofluorescein

TGF – transforming growth factor

T_H – T helper

tPSA – total prostate specific antigen

TMA – tissue microarray

TMB – tetramethylbenzidine dihydrochloride

TNF – tumour necrosis factor

tRNA – transfer ribonucleic acid

TURP – transurethral resection of the prostate

T – tween

UCC – urothelial cell carcinoma

UCD – University College Dublin

UV – ultra violet

VDBP – vitamin D binding protein

V_H – variable heavy chain (of antibody)

V_L – variable light chain (of antibody)

VDR– vitamin D receptor

WB – Western blot

Wnt – Wingless

ZAG – zinc-α-2- glycoprotein

Units

amp – amplification

°C – degrees Celcius

cm – centimetre

g – gram

h – hour

kDa – kilo Dalton

kg – kilogrm

L – litre

µg – microgram

µL – microlitre

µm – micrometre

m – metre

M – molar

mg – milligram

min – minute

mL – millilitre

mm – millimetre

ms – millisecond

MV – megavolt

mW – milliwatt

nM – nanomolar

pM – picomolar

sec – second

V – volt

v/v – volume per unit volume

x g – centrifugal acceleration

w/v – weight per unit volume

List of Figures

List of Tables

Publications and Presentations

Publications

O'Hurley G, Perry AS, O'Grady A, Loftus,B, Smyth P, O'Leary JJ, Sheils O, Fitzpatrick JM, Hewitt SM, Kay EW. **The role of SFRP-2 expression in Prostate Cancer.** Histopathology, 2011 (accepted manuscript in press)

O'Hurley G, O'Grady A, Smyth P, Byrne J, O'Leary JJ, Sheils O, Watson RW, Kay EW. **Evaluation of Zinc-alpha-2-Glycoprotein and Proteasome Subunit beta-Type 6 Expression in Prostate Cancer Using Tissue Microarray Technology.** Appl Immunohistochem Mol Morphol. 2010 Jul:18(6):512-517.

Smyth LG, **O'Hurley G**, O'Grady A, Fitzpatrick JM, Kay E, Watson RW. **Carbonic anhydrase IX expression in prostate cancer.** Prostate Cancer Prostatic Dis. 2010 Jun;13(2):178-81.

Difranco MD, **O'Hurley G**, Kay EW, Watson RW, Cunningham P. **Ensemble based system for whole-slide prostate cancer probability mapping using color texture features.** Comput Med Imaging Graph. 2011 Jan 24. [Epub ahead of print]

Perry AS, **O'Hurley G**, Raheem OA, Kennedy AM, Barrett C, Marignol L, Murphy TM, Sullivan L, Foley R, Brennan K., Loftus B, FitzPatrick JM, Hollywood D, Lawler M. **Gene expression and epigenetic discovery screen reveal transient expression of SFRP2 during prostate cancer progression.** International Journal of Cancer, 2011 (submitted manuscript).

Conference Publications

Perry AS*, **O'Hurley G***, Raheem OA, O'Grady A, Kennedy AM, Barrett C, Marignol L, Murphy TM, Sullivan L, Loftus B, Hewitt SM, Kay EW, Lawler M. *These authors contributed equally. **Epigenetic discovery screen identifies SFRP-2 as a novel biomarker of high grade prostate cancer.** American Association of Cancer Research (AACR), 2010, Washington DC, USA.

O'Hurley G, Perry A, O'Grady A, Smyth P, O'Leary J, Sheils O, Lawler M, Kay EW. **The role of SFRP-2 expression in Prostate Cancer – A predictor of prognosis and biochemical recurrence.** RCSI Annual Research Day, Dublin, 2010, Ireland.

O'Hurley G, Perry A, O'Grady A, Smyth P, O'Leary J, Sheils O, Lawler M, Kay EW. **The role of SFRP-2 expression in Prostate Cancer – A predictor of prognosis and biochemical recurrence.** Irish Association of Cancer Research (IACR) Annual Conference, Galway, 2010, Ireland. *Awarded a Travel Award to attend the IACR based on abstract presentation*

O'Hurley G., O'Grady A, Smyth P, O'Leary J, Sheils O, Watson, W, Kay E. **Zinc-alpha-2-glycoprotein is a potential biomarker of Prostate Cancer.** RCSI Annual Research Day, 2009, Dublin, Ireland.

O'Hurley G, O'Grady A., Smyth P, O'Leary J, Sheils O, Watson W, Kay E. **Zinc-alpha-2-glycoprotein is a potential biomarker of Prostate Cancer.** Irish Association of Cancer Research (IACR) Annual Conference, Athlone, 2009, Ireland.

O'Hurley G, O'Grady A, Smyth P, O'Leary J, Sheils O, Watson W, Kay E. **Zinc-alpha-2-glycoprotein is a potential biomarker of Prostate Cancer.** 9th International Cancer Conference, 2009, Dublin, Ireland. *Awarded Best Poster Presentation*

O'Hurley G, O'Grady A, Watson W, Kay E. **Tissue Validation of Potential Biomarkers in Prostate Cancer.** Pathology Society Winter Meeting, 2009, London, United Kingdom.

O'Hurley G, O'Grady A, Watson W, Kay E. Tissue **Validation of Potential Biomarkers in Prostate Cancer.** RCSI Annual Research Day, 2008, Dublin. Ireland. *Awarded Best First Year Post Graduate Poster Presentation*

Presentations

O'Hurley G, O'Grady A, Hearty S, Perry AS, Watson RW, O'Kennedy R., Kay, EW. **Tissue Validation within the Prostate Cancer Research Consortium.** Prostate Cancer Research Consortium Review Meeting. Molecular Medicine Ireland, March 2011.

O'Hurley G, Hearty S, O'Grady A, Kay EW, O'Kennedy R. **Production of an SFRP-2 fusion protein – an immunogen for SFRP-2 recombinant antibody production.** Prostate Cancer Research Consortium Biannual Meeting. Molecular Medicine Ireland, December 2010

O'Hurley G, Hayes C, O'Grady A, Kay EW, O'Kennedy R. **SFRP-2 recombinant antibody generation using phage display technology.** Prostate Cancer Research Consortium Biannual Meeting. Molecular Medicine Ireland, December 2009.

O'Hurley G, O'Grady A, Smyth P, O'Leary J, Sheils O, Watson RW, Kay,EW. **The role of SFRP-2 in Prostate cancer- Update 2.** Prostate Cancer Research Consortium Biannual Meeting. Molecular Medicine Ireland, September 2009.

O'Hurley G, O'Grady A, Perry AS, Smyth P, O'Leary J, Sheils O, Lawler M, Kay EW. **The role of SFRP-2 in Prostate cancer.** Prostate Cancer Research Consortium Biannual Meeting. Molecular Medicine Ireland, December 2008.

O'Hurley G, O'Grady A, Smyth P, O'Leary J, Sheils O, Watson RW, Kay EW. **Tissue validation of identified epigenetic markers of Prostate cancer.** Research Consortium Biannual Meeting. University College Dublin. September 2008

O'Hurley G, O'Grady A, Byrne J, Fan Y, Watson W, Kay EW. **Tissue validation of identified serum markers of Prostate cancer.** Prostate Cancer Research Consortium Biannual Meeting. Beaumont Hospital. March 2008.

O'Hurley G, O'Grady A, Watson RW, O'Kennedy R, Kay EW. **Evaluation of novel targets as prognostic/predictive markers in Prostate cancer – Tissue validation approach.** Prostate Cancer Research Consortium Biannual Meeting. University College Dublin. November 2007.

1.0 Abstract

Prostate cancer is a significant cause of illness and death in males. Marked disease heterogeneity is associated with prostate cancer. Current detection strategies do not detect the disease at an early stage and cannot distinguish aggressive versus non aggressive prostate cancer leading to over-treatment of the disease and associated morbidity. Thus, prostate cancer is a disease that would benefit from the discovery of novel biomarkers for both early detection and treatment selection.

In October 2003, the Prostate Cancer Research Consortium (PCRC), a multi-disciplinary, trans-institutional collaboration composed of researchers from University College Dublin's Conway Institute, Trinity College Dublin's Institute for Molecular Medicine, the Royal College of Surgeons in Ireland and Dublin City University, was established. Using a comprehensive approach which involves utilizing genomic, transcriptomic and proteomic platforms and using a high-throughput biomarker validation approach, the consortium's overall aim is to identify novel biomarkers of prostate cancer. This PhD project aims to evaluate the potential prostate cancer biomarkers in tissue which are identified in the discovery projects within the PCRC.

Following previous proteomic analysis within the PCRC group, Zinc-α–2-glycoprotein (ZAG), Proteasome subunit β type 6 (PSMB-6), Vitamin D binding protein (VDBP) and Kininogen-1 (KNG-1) were found to be upregulated in the serum of prostate cancer patients. The tissue expression profile of these proteins was investigated to determine if ZAG, PSMB-6, VDBP and KNG-1 were also upregulated in prostatic tumour epithelial cells in the tissue of prostate cancer patients. ZAG expression in epithelial cells of the prostate was inversely associated with Gleason grade (BPH>G3>G4/G5). PSMB-6 was not expressed in either tumour or benign epithelium. However, strong PSMB-6 expression was noted in stromal and inflammatory cells. KNG-1 and VDBP were not found to be expressed in prostate tissue blood. These results indicate ZAG as a possible predictive marker of Gleason grade. The inverse association between grade and tissue expression with a rising serum protein level is similar to that seen with

PSA. In addition the results for all proteins (ZAG, PSMB-6, KNG-1 and VDBP) highlight the challenges in trying to associate the protein levels in serum with tissue expression.

Following methylation analysis of Wingless signalling (Wnt) molecules and their antagonists using Quantitative Methylation-Specific PCR (QMSP), secreted frizzled related protein 2 (SFRP-2) was found to be highly methylated in prostate cancer. The prostatic tissue expression profile of SFRP-2 was investigated to determine whether there was a correlation between SFRP-2 methylation and SFRP-2 expression in prostate cancer. Strong to moderate SFRP-2 expression was observed in benign prostatic hyperplasia (BPH) epithelial cells and negative to weak SFRP-2 expression observed in tumour epithelium particularly Gleason grade 3 and 4. However, in Gleason grade 5 carcinoma there was a 40:60 split in the immunoexpression of SFRP-2, where 40% displayed strong to moderate SFRP-2 expression and 60% displayed negative SFRP-2 expression in epithelial cells. A morphological difference was noted in the Gleason grade 5 tumours that had strong to moderate expression of SFRP-2 (Type A) and the Gleason grade 5 tumours that had no SFRP-2 expression (Type B). It was also noted that biochemical recurrence occurred after 5 years in patients that had strong to moderate SFRP-2 expression in Gleason grade 5 tumours and had "Type A" morphology. These preliminary results propose SFRP-2 as a possible marker of histologically benign glands and a possible subgroup of Gleason grade 5 tumours that may predict prognosis and biochemical recurrence.

The use of well-characterised antibodies is vital for clinical diagnostics and protein studies. One of the major challenges facing researchers and clinicians in the area of cancer research is the lack of high quality, well characterised antibodies to novel proteins. Successful antibody generation depends on the use and availability of high quality antigen. However, like antibodies to novel proteins in cancer research, there is also a lack of high quality, well characterised, commercially available antigens to these proteins. Thus, generating antibodies to these targets is not straightforward and often requires heterologous production of recombinant proteins. SFRP-2 is a novel marker in prostate cancer and paucity of quality antigen and antibody is an impediment to research on this marker. An

antigen grade recombinant protein was designed, produced and used as an immunogen in an avian immune model to determine whether a recombinant antibody against SFRP-2 can be generated based on the polyclonal serum response of the chicken. The first strategy taken to produce the SFRP-2 antigen involved using a prokaryotic *(E. coli)* expression system. Both a pGS21-a vector containing a glutathione-s-transferase (GST) tag and a pET-28b(+) vector modified to contain a heart fatty acid binding protein (hFABP) tag were transformed into *E. coli* cells for soluble SFRP-2 recombinant fusion protein expression which could be subsequently used as an immunogen in an avian immune model. However, both fusion proteins were insoluble in the form of bacterial fusion proteins trapped within the bacterial cell periplasm. The second strategy taken to produce a soluble SFRP-2 antigen involved using a "cell-free" translation expression system. "Cell-free" translation is an *in vitro* expression system that does not require the use of a host cell to express the target protein. Soluble expression of SFRP-2 was achieved. However, the yield of the soluble protein was too low for its use as either an immunogen or in molecular applications. The challenges and difficulties faced in this study may reflect the lack of high quality, well characterised, commercially available antibodies to novel cancer targets such as SFRP-2.

Chapter 1 – Introduction and Aims of the Study

1.1 The Prostate

1.1.1 Histology of the Prostate

The prostate is the largest accessory gland in the male reproductive system. It is a compound tubuloalveolar exocrine gland which is located below the bladder and in front of the rectum and is pierced by the urethra and the ejaculatory ducts (Gartner, 2001) (see Figure 1). It is responsible for producing a slightly alkaline white fluid (pH 7.29) that makes up part (25-30%) of semen. This fluid, which protects, carries and nourishes sperm cells, is rich in lipids, proteolytic enzymes, acid phosphatase, fibrolysin and citric acids (Gartner, 2001). The majority of seminal fluid is produced by the seminal vesicles which are located directly behind the prostate gland. The prostate also contains some smooth muscle which helps expel semen during ejaculation. The active form of testosterone, dihydrotestosterone, regulates the formation, synthesis and release of prostatic secretion (Gartner, 2001).

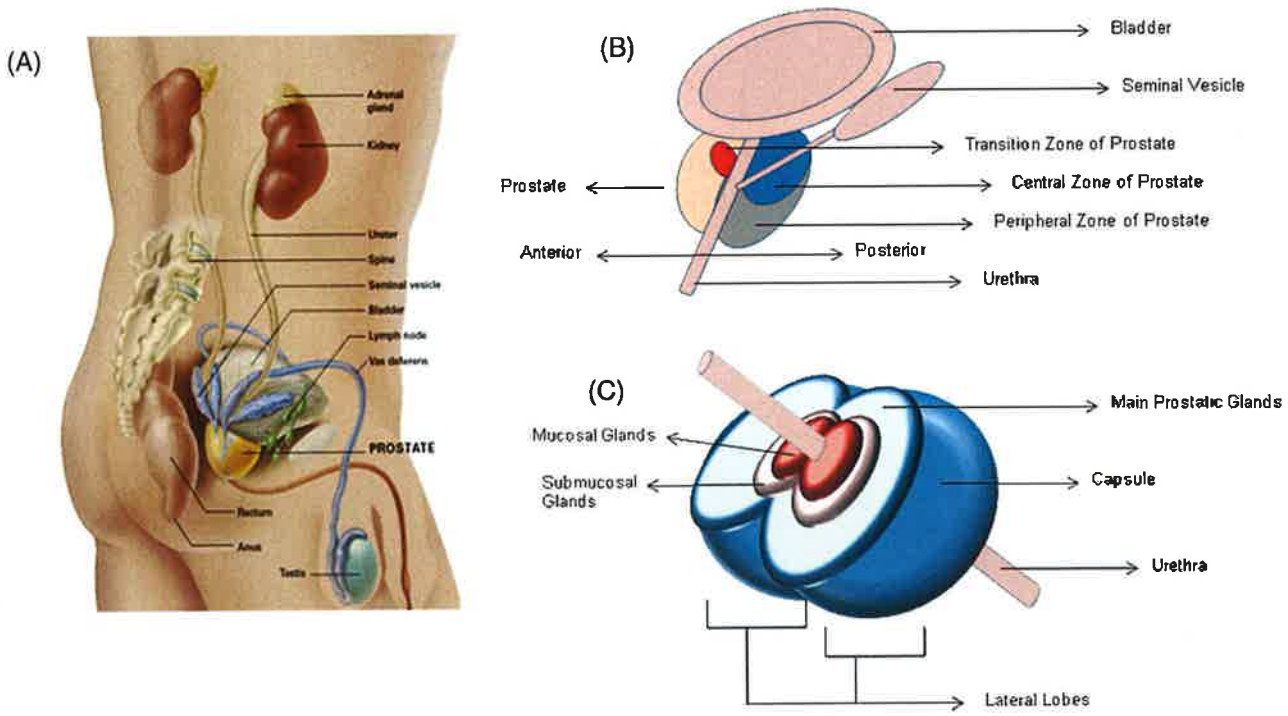

Figure 1: The Prostate

(A) Location of the prostate in the human body obtained from the website (www.urology.uci.edu/prostate/prostate.html)

(B) Zones of the prostate

(C) Schematic diagram of the prostate gland illustrating the mucosal, submucosal and main prostatic glands

There are three major glandular regions within the prostate gland; the peripheral zone, the central zone and the transition zone which differ biologically and histologically (McNeal, 1988). The anterior fibro-muscular zone is the fourth zone of the prostate but is usually devoid of glandular components and is composed only of muscle and fibrous tissue. Each glandular zone has specific architectural and stromal features. Ducts and acini are lined by secretory epithelium embedded in stroma in all glandular zones (see Figure 2). The stroma of the gland is derived from the capsule (membrane covering the prostate that merges with surrounding soft tissues, including nerves) and is enriched by smooth muscle fibres in addition to connective tissue cells. There is a layer of basal cells beneath the secretory lining in each zone, as well as interspersed endocrine-paracrine cells (McNeal, 1988) (see Figure 3). The lumina of the tubuloalveolar glands often contain oval prostatic concretions, corpora amylacea (see Figure 5), composed of calcified glycoproteins, the number of which increases with a man's age (Gartner, 2001).

The three separate groups of compound tubuloalveolar glands found in the prostate are mucosal, submucosal and main prostatic glands and they are arranged concentrically around the urethra. The mucosal glands form the inner periurethral layer and open directly into the urethra over its entire surface. Submucosal glands form the outer periurethral layer and drain through short ducts into the urethral sinuses. Main prostatic glands constitute the bulk of the organ occupying two-thirds of the gland. These glands drain into the urethra via long ducts. The submucosal and mucosal layers form the central glandular zone while the peripheral glandular zone is composed of main prostatic gland.

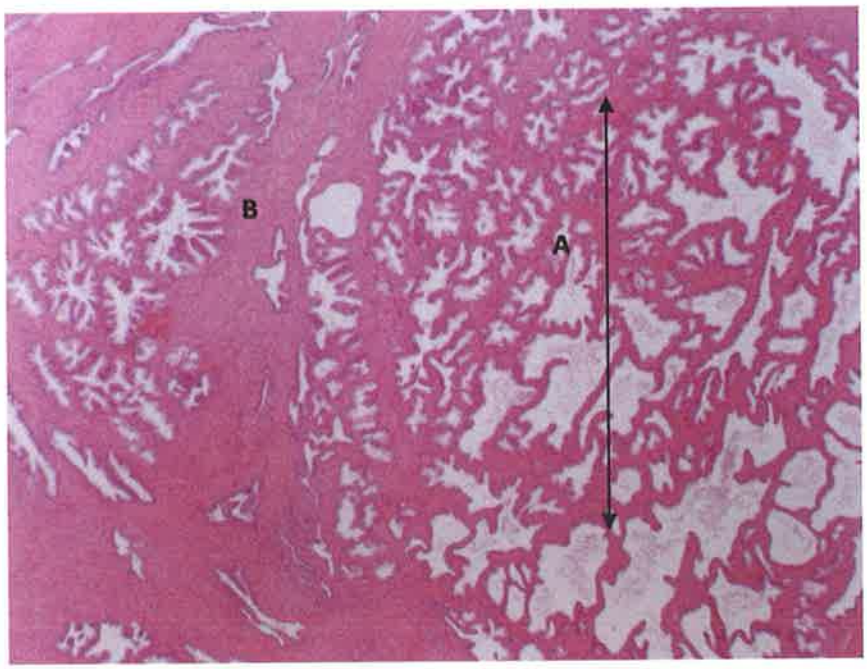

Figure 2: Low power image of normal/benign histology of the prostate

The whole section stained with Haematoxylin and Eosin (H&E) displays (A) tubuloalveolar glands and (B), fibromuscular stroma [X40 Magnification]. The glands are seen in cross section to be rounded to irregularly branching. These glands represent the terminal tubular portions of long tubuloalveolar glands that radiate from the urethra.

Simple to pseudostratified columnar epithelium lines the components of the prostate glands. The cells that make up the epithelium are well endowed with organelles responsible for the synthesis and packaging of protein and, therefore, have an abundant rough endoplasmic reticulum, a large Golgi apparatus, numerous secretory granules and many lysosomes (Gartner, 2001).

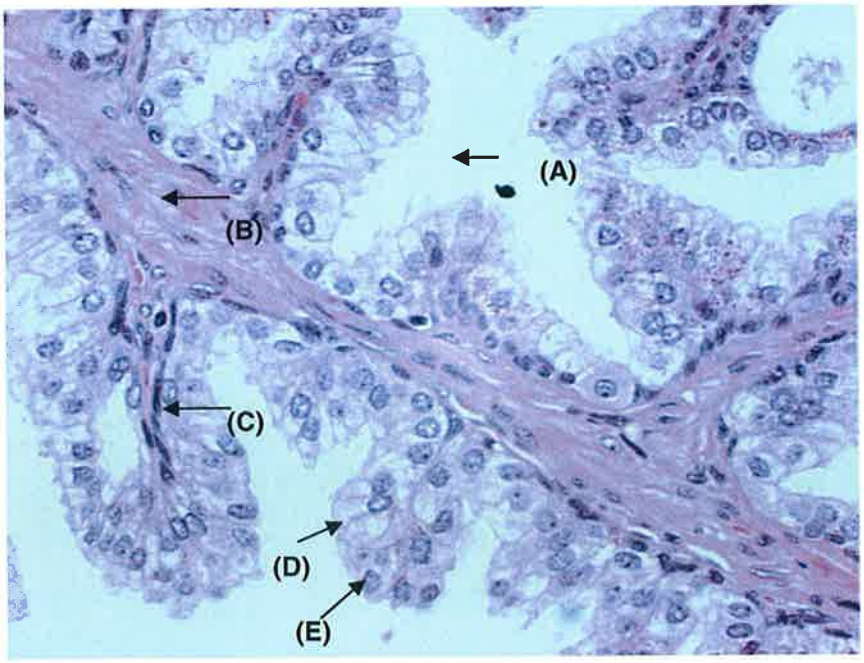

Figure 3: High power image of normal/benign histology of the prostate

Benign prostatic hyperplasia (BPH) from a Tissue Microarray core. The section was stained with Haematoxylin and Eosin (H&E). [X400 Magnification]

(A) = Lumen of gland, (B) = Stroma, (C) = Basal cell layer, (D) = Epithelial cell, (E) = Nucleus of Epithelial cell.

1.1.2 Pathology of the Prostate

Prostate disorders are usually associated with ageing. Disorders of the gland are among the most common of men's health complaints after the age of 50. Young men are rarely affected by prostate problems. The main prostate disorders include inflammatory disorders, hyperplasia and carcinoma.

1.1.2.1 Prostatitis

Inflammation of the prostate is known as prostatitis. There are 4 categories of prostatitis; acute prostatitis, chronic bacterial prostatitis, chronic prostatitis/chronic pelvic pain syndrome and asymptomatic inflammatory prostatitis. Infection in the prostate from Gram-negative organisms, such as *Escherichia coli* and *Proteus* species, causes a condition known as acute prostatitis which results in swelling of the acutely inflamed gland (Selius and Subedi, 2008). Chronic bacterial prostatitis is a relatively rare condition which presents as recurrent urinary tract infections originating from a chronic bacterial infection in the prostate. Chronic prostatitis/chronic pelvic pain syndrome (CP/CPPS) is the most common type of prostatitis (Pontari and Ruggieri, 2004). Genitourinary pain with or without voiding symptoms in the absence of uropathogenic bacteria, as detected by standard microbiological methods, or another identifiable cause such as malignancy is the current National Institute of Health (NIH) definition of CP/CPPS (Pontari and Ruggieri, 2004). Asymptomatic inflammatory prostatitis is a symptomless microscopic condition of the prostate where patients have no genitourinary pain complaints but leucocytosis is present in the gland. The treatment is different for the four types of prostatitis; therefore, the correct diagnosis is very important. Infectious prostatitis will not be cured without antimicrobial treatment and noninfectious prostatitis will not be cured with anti-microbial treatment. Alpha blockers or changes in diet can be used to treat noninfectious prostatitis.

1.1.2.2 Benign prostatic hyperplasia (BPH)

Benign prostatic hyperplasia (BPH) is a very common condition in older men (Edwards, 2008). It occurs when the prostate gland increases in size as a result of proliferation of epithelial cells within the basal cell layer, probably due to an alteration in hormone balance (accumulation of dihydrotestosterone) (Wheater, 1985). BPH is not considered to be a premalignant lesion. The

disease has stromal and glandular components (Ziada *et al.*, 1999) and is characterised histologically by the presence of discrete nodules in the periurethral zone/mucosal glands of the prostate (Edwards, 2008) but can extend to involve the lateral lobes. Symptoms include urinary hesitancy or frequent urination. Symptoms of BPH, such as impaired voiding, are caused by extrinsic compression of the prostatic urethra (Edwards, 2008). BPH, as with other abnormalities of the urinary tract, can predispose to infection and also stone formation (Wheater, 1985). Anatomic or microscopic evidence of BPH is present in approximately 20%, 40%, 55%, 80% and 90% of men aged 40–50, 50–60, 60–70, 70–80 and 80–90 years respectively, according to autopsy data (Ziada *et al.*, 1999). However, approximately only 25–50% of those with microscopic evidence of disease present with clinical manifestations (Ziada *et al.*, 1999). Age, race, ethnicity, family history, cigarette smoking and chronic disease such as hypertension, coronary artery disease and diabetes mellitus are some of the potential risk factors for BPH (Ziada *et al.*, 1999). Drug therapies for BPH include drugs that inhibit the enzyme 5-alpha reductase, which converts testosterone to dihydrotestosterone within cells and alpha adrenergic blockers which lead to relaxation of smooth muscle in prostate and help to relieve obstruction. The gold standard surgical treatment of BPH is transurethral resection of the prostate (TURP) which has a symptom improvement rate of 85-100% and mortality risk of 2% (Ziada *et al.*, 1999). This surgical procedure involves removing tissue from the prostate via a resectoscope inserted through the urethra. Examples of BPH are seen at low power in Figure 2 and at high power in Figure 3. Basal cells are usually present as a thin layer located at the base of secretory cells. These basal cells have the ability to proliferate leading to a condition known as basal cell hyperplasia (BCH) (Yang *et al.*, 2003). Basal cell proliferation is commonly noted in a benign hyperplastic prostate gland and is usually found near areas of inflammation in the prostate (Yang *et al.*, 2003).

1.1.2.3 Prostate Cancer

1.1.2.3.1 Epidemiology of Prostate Cancer

The incidence of prostate cancer varies largely between racial/ethnic groups, highest among Africans, intermediate among Caucasians and lowest among Asians (Ntais *et al.*, 2003). The strongest known risk factor, apart from age and ethnic origin, is a positive family history.

The first case of prostate cancer that was diagnosed by histological evaluation was reported in 1853 (Lytton, 2001). It was initially regarded as a very rare cancer but this may well be due to the fact that prostate cancer went largely unrecognised until the turn of the last century (Lytton, 2001). In developed countries today, prostate cancer is the second most frequently diagnosed cancer and the third most common cause of death from cancer in men (Damber and Aus, 2008). In Europe, an estimated 2.6 million new cases of cancer are diagnosed each year. Prostate cancer constitutes about 11% of all cancers in Europe and accounts for 9% of all cancer deaths among the male population within the EU (Aus *et al.*, 2005). The incidence and mortality numbers world-wide are approximately 679,000 and 221,000, respectively (Aus *et al.*, 2005) (Zhu *et al.*, 2006). Prostate cancer is the most common malignancy among men in Ireland and is associated with significant morbidity and mortality. Annual incidence of prostate cancer in the Republic of Ireland is approximately 2,500 with a mortality in excess of 550 cases per annum (www.nc (www.ncri.ie). It is predicted that the incidence of prostate cancer will increase by 275%, with figures approaching 6,000 new cases in Ireland by 2020, due to an ageing population (www.ncri.ie).

1.1.2.3.2 Types of Prostate Cancer

Prostatic adenocarcinoma is the most common form of prostate cancer which accounts for ~ 80%-90% of all prostate cancers and mainly involves the peripheral zone of the gland. Prostatic adenocarcinoma is an uncontrolled and abnormal malignant growth in the glandular tissue of the prostate. Adenocarcinoma may grow to involve the entire gland and then metastasise to other parts of the body especially the lymph nodes and the bones.

A diagnosis of "prostate cancer" or "carcinoma of the prostate", implies adenocarcinoma to most urologists and pathologists. However, there are other forms of prostate cancer which are summarized in Table 1, including small cell carcinoma, squamous cell carcinoma and transitional cell carcinoma but these types of prostate cancer are all rare and are excluded from this study.

Table 1: Rare Types of Prostate cancer

Type of Prostate Cancer	Disease Description	Incidence
Small-cell (neuroendocrine) carcinoma (SCNC)	SCNC is a rare malignancy of neuroendocrine cell lineage arising in the human prostate. SCNC is typically aggressive with a median survival time ranging from 6 to 17 months following diagnosis and this type of prostate tumour does not usually secrete prostate-specific antigen (PSA) unlike adenocarcinomas (Brownback *et al.*, 2009). It often causes lytic bone lesions, and more frequently is complicated by visceral metastases.	0.5–2% of all primary prostatic tumours (Brownback *et al.*, 2009)
Squamous cell carcinoma	Squamous cell carcinoma is a rare neoplasm of the prostate gland. It is as an aggressive tumour with short survival time. It differs from adenocarcinomas in its biological behaviour, therapeutic response and prognosis. The histological criteria for diagnosis are keratinisation, epithelial pearls and intercellular bridges (John *et al.*, 2005). The transitional epithelium of the urethra and periurethral ducts is widely accepted as the cell of origin (John *et al.*, 2005).	0.5% of all prostatic malignancies (John *et al.*, 2005)
Primary transitional cell carcinoma (TCC)/ urothelial cell carcinoma (UCC) of the prostate	TCC/UCC is a rare male malignancy originating in the transitional epithelial cells of the intraprostatic periurethral ducts. Transitional cell carcinoma is characterised by large cords of anaplastic tumour cells (Rubenstein and Rubnitz, 1969).	This rare cancer accounts for 2-4% of all prostatic carcinomas. (Rubenstein and Rubnitz, 1969).

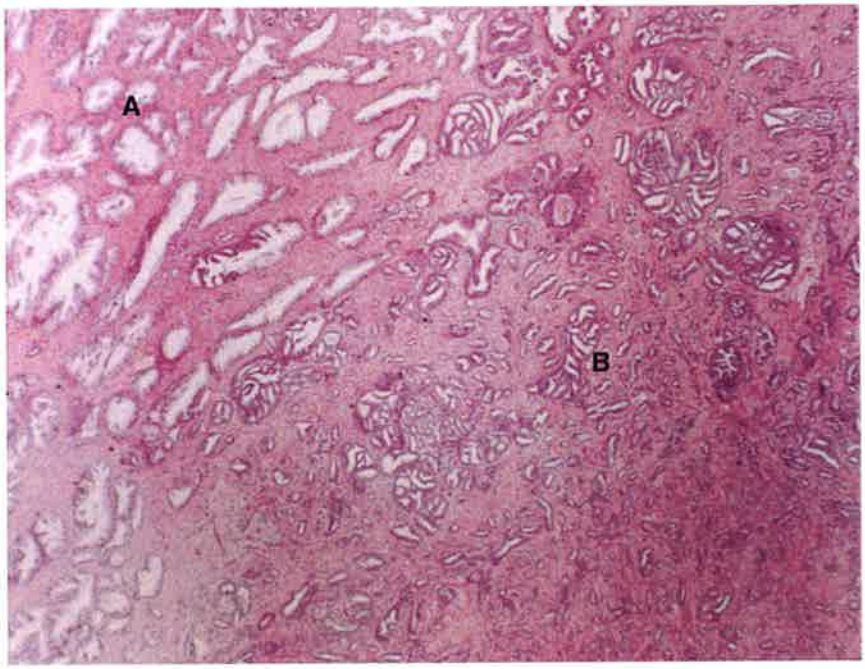

Figure 4: Low power image of normal/benign glands of the prostate beside prostatic adenocarcinoma

The whole section stained with Haematoxylin and Eosin (H&E) displays (A), benign glands of the prostate and (B), prostatic carcinoma [X40 Magnification]

1.1.2.3.3 Prostatic intraepithelial neoplasia (PIN)

Prostatic intraepithelial neoplasia (PIN) is defined as a cytological alteration in architecturally normal glands that comprises an intraluminal proliferation of the secretory epithelium revealing a spectrum of atypical cytological changes ranging from minimal changes to those that are indistinguishable from carcinoma. PIN is divided into two grades; low grade PIN (formerly grade 1) and high grade PIN (formerly grades 2 and 3). PIN, especially high grade PIN, is considered to be a precursor to malignancy. As high grade PIN has a high predictive value as a marker for adenocarcinoma, repeat biopsies are warranted if detected on initial biopsy (Dabbs, 2006). It has been reported by Bostwick *et al.* (2004) that carcinoma will develop in most patients with high

grade PIN within 10 years and that the incidence and extent of PIN appear to increase with patient age (Dabbs, 2006).

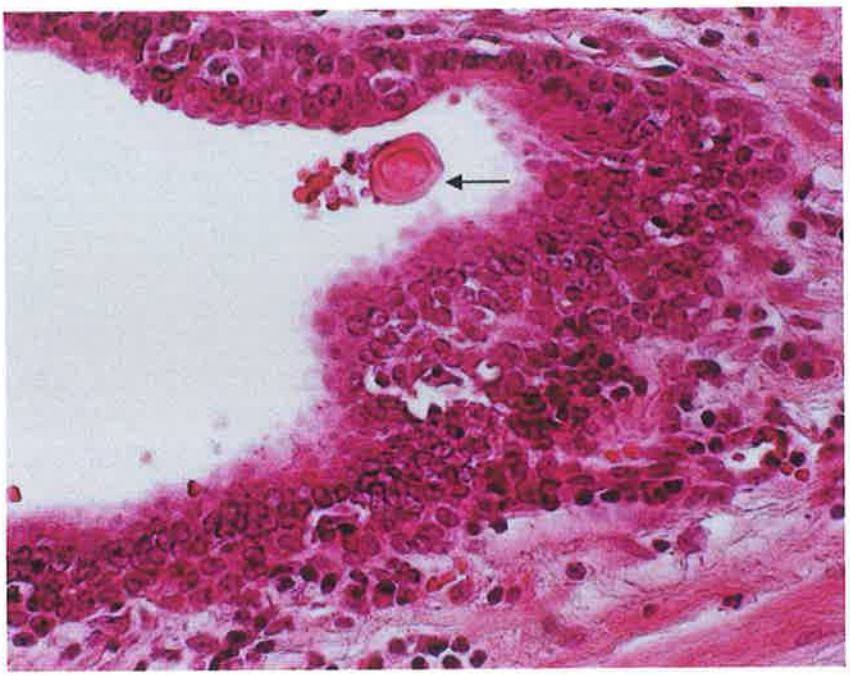

Figure 5: Prostatic Intraepithelial Neoplasia (PIN)

The section was stained with Haematoxylin and Eosin (H&E). [X400 Magnification]

The arrow indicates corpora amylacea.

1.1.2.3.4 Prognosis and treatment of Prostate cancer

Clinically, prostate cancer is diagnosed as local or advanced. There is marked disease heterogeneity associated with prostate cancer. Some men progress rapidly to metastatic disease while others may live relatively asymptomatically for many years. Thus a large percentage of men die with, rather than from, the disease. The outcome of prostate cancer is principally determined by metastases. Treatment options for prostate cancer are based on factors such as the patient's life expectancy and tumour characteristics (Damber and Aus, 2008) including tumour stage (see Table 2), aggressiveness of tumour and PSA level (see section 1.2.2). The four types

of standard treatment used for prostate cancer are watchful waiting, surgery, radiation therapy and hormone therapy. Watchful waiting involves closely monitoring a patient's condition without giving any treatment. This form of treatment is the usual preferred treatment for elderly men with early stage prostate cancer. Radical prostatectomy is a surgical procedure that involves removing the prostate, surrounding tissue and seminal vesicles. This form of treatment is an option for patients in good health and who have confined, localized disease. Radiation therapy uses high energy x-rays or another form of radiation to kill cancer cells. The two types of radiation therapy that exist for prostate cancer are external radiation and branchytherapy (internal radiation therapy using radioactive needles, seeds, wires or catheters). Hormone therapy is a treatment that systematically removes the body's testosterone (androgen ablation). There are four methods of androgen ablation: castration, oestrogens, anti-androgens and combined androgen blockade (uses both anti-androgens and castration).

Table 2: Stages of Prostate cancer

Adapted from the National Cancer Institutes website
(http://www.cancer.gov/cancertopics/pdq/treatment/prostate/HealthProfessional/page3)

Stage	Description
TX	Primary tumour cannot be assessed.
T0	No evidence of primary tumour.
T1	Clinically inapparent tumour neither palpable nor visible by imaging.
T1a	Tumour incidental histologic finding in ≤ 5% of tissue resected.
T1b	Tumour incidental histologic finding in > 5% of tissue resected.
T1c	Tumour identified by needle biopsy (e.g., because of elevated PSA).
T2	Tumour confined within prostate.
T2a	Tumour involves ≤ one-half of one lobe.
T2b	Tumour involves > one-half of one lobe but not both lobes.
T2c	Tumour involves both lobes.
T3	Tumour extends through the prostate capsule.
T3a	Extracapsular extension (unilateral or bilateral).
Nx	Regional lymph nodes were not assessed.
N0	No regional lymph node metastasis.
N1	Metastases in regional lymph node(s).
M0	No distant metastasis.
M1	Distant metastasis.
M1a	Nonregional lymph node(s).
M1b	Bone(s).
M1c	Other site(s) with or without bone disease.

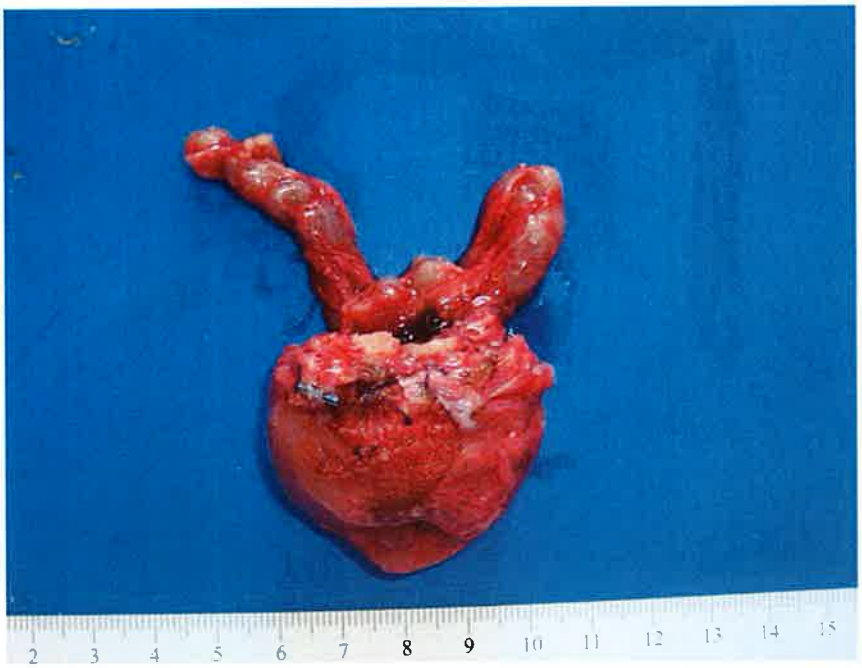

Figure 6: Prostate Gland with seminal vesicles removed by radical prostatectomy

1.1.2.3.5 Diagnosis of Prostate Cancer

In addition to the basic recognition of malignancy it has long been recognised that various patterns of tumour proliferation are associated with tumour aggressiveness and patient outcome. This is the basis of the Gleason grading system. Current clinical practice in making a tissue diagnosis of prostate cancer is based on examination of histopathological specimens from the gland by a pathologist. The most common method to obtain the necessary prostate tissue specimen from the patient is by several systematic transrectal core biopsies, with guidance by transrectal ultrasound (Damber and Aus, 2008). When cancer occurs epithelial cells replicate in an uncontrolled way, which results in the regular arrangement of gland units being disrupted (Scardino *et al.*, 1992). A combination of architectural, cytological, as well as ancillary features is the main basis of prostate cancer diagnosis on needle biopsy (Che M, 2003). The typical acinar-type prostatic adenocarcinoma is characterised by a proliferation of small infiltrating glands lined by a single-layered epithelium with enlarged nuclei, amphophilic

cytoplasm, prominent nucleoli and absence of basal cells as reported by Che *et al.* (2003).

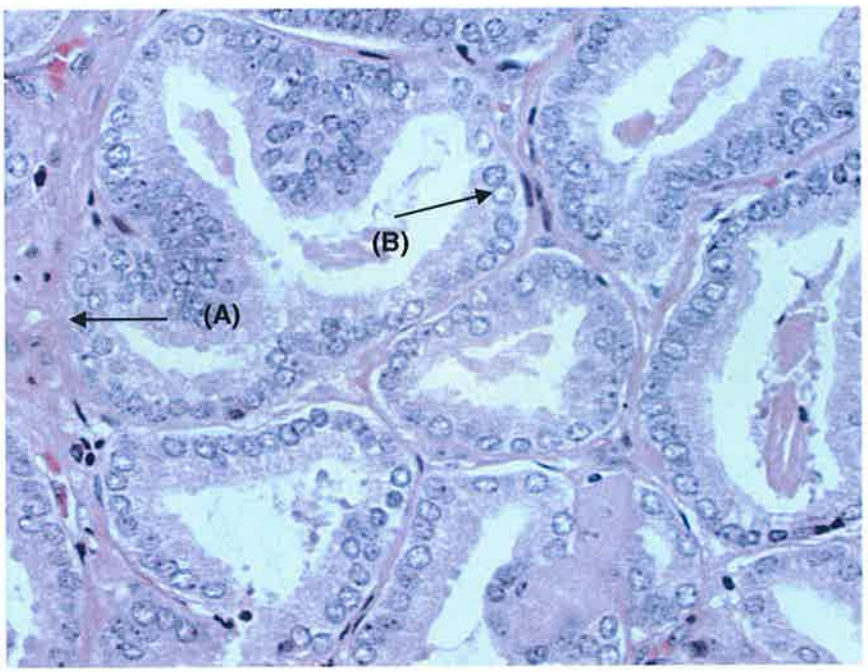

Figure 7: Histology of prostate tumour tissue

Prostate tumour tissue (Gleason grade 3) from a Tissue Microarray core constructed as part of this project. Haematoxylin and Eosin [X400 magnification].

(A) Absent Basal Cell Layer (B) Single-layered Epithelium

1.1.2.3.6 The Gleason grading System

Tumour grading is essentially a reflection of how closely tumour cells resemble their cell of origin and in almost all human tumours tumour grade has an impact on disease behaviour. Histological grading is therefore extremely valuable to physicians as it aids the prediction of the extent of the disease, correlates well with patient survival and helps with determining the most appropriate treatment options. In 1966, Donald F. Gleason created a unique grading system for prostatic carcinoma. This was based on the architectural pattern of the tumour alone (Epstein *et al.*, 2005). This system is

known as Gleason grading and is the most common method for histological grading of prostate cancer. The Gleason grading system classifies the tissue into five grades, 1 to 5, based on tumour differentiation, i.e. the degree of tumour resemblance to normal tissue. The Gleason grade increases with increasing malignancy level and, therefore, cancer aggressiveness. Grade 1 corresponds to well differentiated tumour (tissue with the highest degree of resemblance to normal tissue and indicates a high chance of patient survival) while grade 5 corresponds to poorly differentiated tumour (indicating a low chance of survival) (Tabesh *et al.*, 2007). Prognosis of the disease is associated with the overall Gleason score which ranges from 2 to 10. The Gleason score represents the sum of the most prominent and second most prominent Gleason grades present in the tissue section. As reported by Damber and Aus., (2008), on needle biopsy, the worst grade should always be included even if present in less than 5% of the tissue sampled. Gleason grading remains one of the most significant factors in the clinical decision-making on needle biopsy specimens and after radical prostatectomy is performed. It has the ability to predict pathological stage, margin status, biochemical failure, local recurrences, lymph node involvement, disease progression, or distant metastasis after prostatectomy (Lopez-Beltran *et al.*, 2006).

Due to its heavy reliance on human interpretation, Gleason grading is prone to subjectivity and limited intra- and inter-pathologist reproducibility. Some cases exist that are right at the interface between two different patterns according to the original description of the Gleason grading system, leading to interobserver and possibly intraobserver variability (Lopez-Beltran *et al.*, 2006). Distinguishing between Gleason grade 3 and 4 and Gleason grade 4 and 5 becomes a difficulty when faced with this dilemma particularly when determining the percentage of each Gleason grade in the specimen. This problem is so significant among pathologists that it has even led to the establishment of a new Gleason grade termed Gleason grade 4/5 and following the 2005 International Society of Urological Pathology (ISUP) Consensus Conference on Gleason Grading and Prostatic Carcinoma, it has

been proposed that pathologists should record the percentage pattern 4/5 especially on radical prostatectomy as it is predictive of prognosis (Epstein *et al.*, 2005). Patterns 3 and 4 are often noted to be intimately mixed leading to assessment of the percent of pattern 4 becoming difficult (Epstein *et al.*, 2005). Over and under grading of specimens in particular on biopsy is a major issue among pathologists also. Because radiation therapy, radical prostatectomy, other therapies and overall prognosis of the disease are initially based on the Gleason score, these problems are a huge concern in prostate cancer diagnosis and better molecular markers that can make the distinction between Gleason grades would be hugely beneficial.

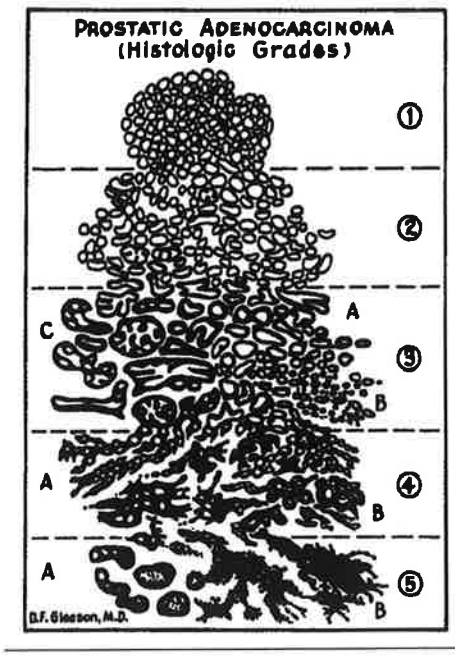

Figure 8: Gleason Grading Diagram (Tabesh *et al.*, 2007)

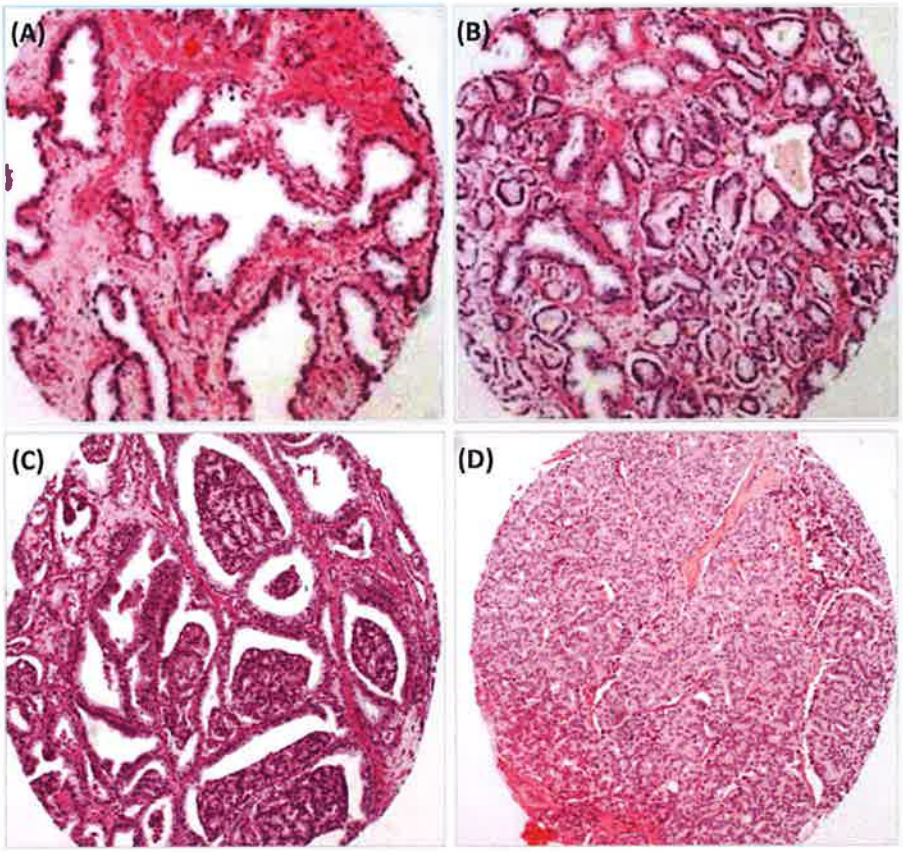

Figure 9: Gleason Grades

Benign Prostatic Hyperplasia (BPH), Gleason grade 3, 4 and 5 displayed on Tissue Microarray cores constructed as part of PhD project stained with Haematoxylin and Eosin [X100 Magnification]. (A) BPH, (B) Gleason grade 3 invading BPH, (C) Gleason grade 4, (D) Gleason grade 5.

1.1.2.3.7 Molecular Biology of Prostate Cancer

Every carcinoma focus is presumed to reflect a progressive and cumulative genetic alteration from a single cell which affects regulatory genes resulting in a growth or survival advantage. Multiple classes of cancer-associated genes contribute to the carcinogenic process when their functions are perturbed by either genetic or epigenetic mechanisms (Isaacs and Kainu, 2001). Such classes of cancer-associated genes are oncogenes and tumour suppressor genes.

Proto-oncogenes are involved in normal cell proliferation. They encode a variety of proteins that function as growth factors, growth factor receptors, modifiers of protein function, regulators of replication or transcription or other signalling pathways (Karayi and Markham, 2004). When a proto-oncogene becomes mutated, translocated or amplified it becomes activated and is known as an oncogene. Oncogenes are pro-carcinogenic and only require the alteration of one allele as they function in a dominant manner (Karayi and Markham, 2004). Examples of oncogenes include *K-RAS* which is widely studied in many cancers including urological neoplasms and *C-ERB-B2* (also called *HER-2/NEU*) in breast cancer.

Tumour suppressor genes are anti-oncogenes. They are protective genes that normally limit the growth of tumours. When tumour suppressor genes are inactivated there is a loss or reduction in their function contributing to cancer formation. Tumour suppressor genes function in a recessive manner. Therefore, if one copy of the gene is already missing because of an inherited defect, then loss of the remaining gene results in the absence of that gene's product which may lead to carcinoma (Karayi and Markham, 2004). An example of a well characterised tumour suppressor gene is the *P53* gene which is the cause of Li-Fraumeni syndrome when absent in the germ line and which is implicated in many other cancers. "Gatekeeper" genes directly regulate the growth of tumours through promoting cell death and inhibiting growth (Karayi and Markham, 2004). The inactivation of a "gatekeeper" gene results in tissue-specific distribution of cancer. Examples of "gatekeeper" genes include the *APC* gene in colon carcinoma and the *RB* gene in retinoblastoma. "Caretaker" genes regulate genomic repair. Genomic instability results from mutations in "caretaker" genes. Tumour initiation is not promoted by the

inactivation of "caretaker" genes but the resulting genomic instability leads to the higher mutation rates in other genes such as "gatekeeper" genes. Thus, an individual with a hereditary mutation of a "caretaker" gene is at greater risk of developing tumours than the general population (Karayi and Markham, 2004). *BRCA1* and *BRCA2* are examples of "caretaker" genes associated with breast cancer.

Like all carcinomas, prostate cancer arises in differentiated epithelial cells and/or progenitor cells in which embryonic pathways are reactivated through the activation of oncogenes and the loss of tumour suppressor genes, which leads to a growth and survival advantage (Taichman *et al.*, 2007). The process of prostate carcinogenesis is the result of DNA damage that occurs in either a differentiated cell or a stem cell through a complex interplay of genes, the cellular microenvironment and the macroenvironment such as external agents and/or ingestion of carcinogens (Taichman *et al.*, 2007). It is postulated that prostate carcinogenesis is a multistep process requiring a subset of "hits" or mutations in putative precursor lesions or latent cancers in order for progression to fully malignant phenotype (Isaacs and Kainu, 2001). Molecular and cytogenic analysis reveal that multiple metastases in the same patient are clonally related, implying that advanced prostate cancer is monoclonal, despite the phenotypic heterogeneity of metastatic prostate cancer (Shen and Abate-Shen, 2010). Classic oncogenes and tumour suppressor genes are rarely mutated in prostate cancer. However, several molecular and genetic changes both inherited (e.g. *RNASEL* and *MSR1*) and somatic (e.g. *RB1* and *PTEN*) have been directly involved in prostate carcinogenesis but none of these has yet been explicitly linked to prostate cancer initiation or progression (DeMarzo *et al.*, 2003). These molecular and genetic changes in prostate cancer are summarised in Tables 3 and 4.

Table 3: Genes proposed to be involved in prostate cancer carcinogenesis or in modifying the risk of prostate cancer

Adapted from (DeMarzo *et al.*, 2003)

Gene	Proposed function
Mutations causing decreased activity	
MSR1	Anti-infectious, scavenger receptor
RNASEL	Anti-infectious, apoptosis
ELAC2	Metal-dependent hydrolase
Promotor hypermethylation resulting in gene silencing	
GSTP1	Carcinogen detoxification
Loss of heterozygosity and point mutation	
PTEN	Cell survival and proliferation
TP53 (also P53)	Cell survival and proliferation, genome stability
Loss of heterozygosity and haploinsufficiency	
NKX3-1	Cell differentiation and proliferation
CDKN1B (P27KIP1)	Cell differentiation
Point mutations	
COPEB (also KLR6)	Transcription regulator
AR	Cell proliferation, survival and differentiation
Amplification	
AR	Cell proliferation, survival and differentiation
Overexpressed at mRNA and protein level	
HTERT	Cell immortality
HPN	Transmembrane protease
FASN	Fatty-acid synthesis
AMACR	Fatty-acid metabolism, branched chain
EZH2	Transcription repressor, cell proliferation
MYC	Cell proliferation
BCL2	Cell survival
Polymorphism affecting prostate cancer risks	
AR	Cell proliferation, survival and differentiation
CYP17	Androgen metabolism
SRD5A2	Androgen metabolism

Table 4: **Molecular progression in prostate cancer**

Adapted from (Karayi and Markham, 2004)

Normal prostate cells

Presence of predisposed alleles (e.g. *RNASEL*)
Methylation of tumour suppressor gene promoters leading to epigenetic silencing
Chromosome 8p loss
AR CAG repeat alterations
Vitamin D Receptor reduced activity
5α reductase (*SRD4A2*) increased activity
CAPB (1p36) mutation
HPC1 (1q24-25) mutation
MSR1 (8p22-23) mutation
KLF6 (10p15) mutation
ELAC2 (17q11.2) mutation
HPC20 (20q13) mutation
HPCX mutation

Localised prostate cancer

Chromosome 16q loss
Altered E-Cadherin expression (16q)
RB1 (13q) loss
p53 (17p) inactivation
GSTP1 (11q13) inactivation

Metastatic prostate cancer

Over expression of EZH2 polycomb protein
Transcriptional silencing of many genes by histone deacetylation
Increased BCL-2 expression
Increased availability of adrenal steroids
Loss of *KAI-1 (11p)*
PTEN mutation
AR gene amplification
AR mutation
Abnormal phosphorylation of AR by 2nd messenger systems

Androgen-independent prostate cancer

1.2 Biomarkers of Prostate Cancer

1.2.1 Biomarkers of disease

The term "biomarker" is defined by the National Institute of Health as "a characteristic that is objectively measured and evaluated as an indicator of normal biological processes, pathogenic processes or pharmacologic responses to a therapeutic intervention or other health care intervention". A biomarker can be produced by the diseased organ or elsewhere in the body in response to disease. They can be found in biological fluids or tissue in higher-than-normal amounts in patients with a certain disease (Issaq *et al.*, 2010). There are three types of biomarkers; Type 0 biomarker, Type 1 biomarker and surrogate end point (Type 3 biomarkers). Type 0 biomarkers refer to a marker of the natural history of the disease and correlates longitudinally with known clinical indices (Vasan, 2006). A Type 1 biomarker refers to marker that captures the effect of a therapeutic intervention in accordance with its mechanism of action (Vasan, 2006). A "surrogate marker" (surrogate end point/Type 2 biomarker) is defined as "a laboratory measurement or physical sign that is used in therapeutic trials as a substitute for a clinically meaningful endpoint that is a direct measure of how a patient feels, functions, or survives and is expected to predict the effect of the therapy". The main difference between a "surrogate marker" and a "biomarker" is that a biomarker is a "candidate" surrogate marker, while a surrogate marker is a test used to measure the effects of a specific treatment (Katz, 2004). Examples of some well known biomarkers of diseases currently used in the clinic include high blood pressure, which can indicate risk of stroke and high cholesterol levels, which can indicate risk for cardiovascular disease.

Molecular biomarkers, in cancer research, refer to substances that are indicative of the presence of cancer in the body (Maruvada *et al.*, 2005). They can include changes in mRNA, DNA methylation, patterns of single-nucleotide polymorphisms (SNPs), protein or metabolite abundances providing that these patterns of change can be shown to correlate with the characteristics of the disease preferably produced only by the malignant tissue (Issaq *et al.*, 2010). Biomarkers are extremely valuable

clinical tools which can be used to detect cancer, examine biological behaviour, predict clinical outcome and/or monitor therapeutic response and disease progression. An ideal diagnostic biomarker should have a sensitivity and specificity close to 100% and a high predictive value in order to be clinically relevant. It should also be accurate, economical, easy to perform, reproducible by different laboratories and measured within a non-invasive or semi-invasive collected specimen (Issaq *et al.*, 2010). Many biomarkers have been approved by the Food and Drug Administration (FDA) to monitor specific cancers (see Table 5). However, the majority of discovered biomarkers are not sensitive and/or specific enough to be used for population screening (Issaq *et al.*, 2010).

Table 5: Examples of Biomarkers in Cancer research

Adapted from Marduva *et al.* 2005

Biomarker	Technology	Biomarker Application and Cancer Affecting Organ
Genomic		
BRCA-1 and *BRCA-2* mutations (blood)	DNA sequencing	Risk assessment and prognosis (breast)
Chromosomal damage (blood, white cells)	Commet assay, micronucleus assay	Diagnosis and risk assessment (acute myeloid leukaemia, acute lymphoma)
Osteopontin (blood)	Microarray	Detection, diagnosis and prognosis (ovaries)
Ras mutation (blood)	Short oligonucleotide mass analysis (SOMA), PCR primer-introduced restriction with enrichment for mutant alleles	Risk assessment (colon and lung)
Her-2/neu (tissue, serum)	Fluorescent In Situ Hybridization (FISH), PCR	Prognosis and treatment (breast)
Glutathione S-transferase (*GSTP1*) polymorphisms (blood)	PCR restriction fragment-length polymorphism assay (PCR-RFLP assay)	Risk assessment, prognosis and treatment (breast and prostate)
Cytochrome P450 mutations, *CYP3A4* polymorphisms (blood)	DNA sequencing	Diagnosis (breast)
Epigenomic		
Methylation markers *RASSF1A*, *TWIST*, *cyclin D2*, *HIN1* (blood)	Methyl-specific PCR	Diagnosis (breast)
Proteomic		
PSA (serum)	Immunoassay	Detection, diagnosis and prognosis (prostate)
CA-125 (serum)	Immunoassay	Detection, diagnosis and prognosis (ovary)
Cancer antigen-19 (CA-19) (serum)	Immunoassay	Diagnosis and prognosis (pancreas and colon)
Carcinoembryonic antigen (CEA) (serum)	Immunoassay	Detection, diagnosis and prognosis (colon, lung and breast)
Protein profiling (serum)	SEILDI, MALDI	Detection and diagnosis (multiple organs)
Her-2/neu (tissue and serum)	Immunohistochemistry (IHC) and immunoassay	Prognosis and treatment (breast)
EGFR (serum)	Immunoassay	Prognosis and treatment (lung)
Haptoglobin (serum)	IHC, immunoassay	Diagnosis, treatment response (lung, colon and breast)

Metabolic		
Cotinine (serum, urine)	High-performance liquid chromatography (HPLC)	Exposure (lung)
1-Hydroxypyrene (urine)	HPLC	Exposure (lung)
Aflatoxin M1 (blood)	HPLC	Exposure (liver)
Deoxynivalenol (DON) (serum)	Mass spectrometry	Exposure and risk assessment (oesophagus)
Lysophosphatidic acid (LPA) (serum)	Mass spectrometry	Detection, diagnosis and prognosis (ovary)
Metabolomic		
Metablolomic profiling (serum)	1H NMR spectroscopy	Early detection and diagnosis (ovary)
Stable isotype-based dynamic metabolin profiling (SIDMAP) of glucose (tumour cells)	Mass spectrometry	Drug discovery and treatment (pancreas)
Metabolic profiling (tumour)	1H NMR spectroscopy	Diagnosis (brain)

1.2.2 Prostate Cancer screening and PSA

Prostate cancer screening is performed in an effort to detect unsuspected cancer which may lead to more specific diagnostic follow up tests such as a biopsy. The two main screening methodologies for prostate cancer are digital rectal examination (DRE) and the prostate specific antigen (PSA) blood test.

A DRE is a physical examination of the prostate gland by a clinician. During a DRE, a clinician inserts a lubricated, gloved finger into the patient's rectum in order to detect hard nodules on the prostate or prostate enlargement. The latter typically indicating BPH or prostatitis and the former typically relating to prostate cancer (Baumgart *et al.*, 2010). DRE plays an integral role in the detection of prostate cancer.

The measurement of serum levels of prostate-specific antigen (PSA) is the most widely used indicator to detect prostate cancer (Nadler *et al.*, 1995). PSA is a serine protease that is synthesised by epithelial cells of the prostate under normal conditions and is secreted into seminal fluid. Its function is thought to be liquefaction of seminal fluid through enzymatic action (Vihinen, 1994). In normal conditions, PSA can only enter blood circulation by leaking into the extracellular fluid and diffusing into veins and capillaries. However, in cancerous prostatic tissue, tumour growth disrupts the basal cell layer and cell polarity is altered. The direction of PSA secretion is disturbed and PSA is released freely into the circulatory system.

PSA is a 34 kilo Dalton (kDa) glycoprotein and consists of 237 amino acids. PSA is found in the serum in several isoforms including free PSA (complete PSA protein with no modifications), complexed PSA (PSA that form complexes with various serum proteins), pro PSA (a precursor form of PSA), benign PSA (contains 2 internal peptide bond cleavages at lysine 145 and 182) and intact non native PSA (a non native form of PSA that is not cleaved at lysines 145). Raised levels of serum PSA (0.4ng/mL of total PSA as the upper limit of normal

(Makarov *et al.*, 2009)) are suggestive of prostate cancer, however, diagnostic confirmation requires a transrectal prostatic needle biopsy (Roddam *et al.*, 2005). PSA is not a cancer-specific protein therefore its presence is not unique to cancerous cells (Jung *et al.*, 2000). PSA is also very accurate and sensitive in detection of residual cancer, recurrence and cancer progression following treatment (Dabbs, 2006). Serum PSA concentration exceeding 0.2 ng/mL following radical prostatectomy is often considered as evidence of biochemical recurrence (Dabbs, 2006).

Although serum PSA screening has emerged as the most useful tumour marker in all of oncology (Brawer *et al.*, 1998), its poor specificity has led to prostate cancer not being detected early enough and aggressive versus non aggressive disease not being distinguished e.g. one third of men with prostate cancer have normal PSA levels. Many non-malignant prostate conditions, including benign prostatic hyperplasia (BPH) and prostatitis, often lead to serum PSA elevations, limiting the specificity of PSA elevation for cancer detection (Makarov *et al.*, 2009) - only one in four men with a PSA of greater than 0.4 ng/mL have biopsy proven prostate cancer. Thus, determining which patients require treatment and determining which patients to treat aggressively remains a significant dilemma. For this reason, better molecular markers that can make this distinction are urgently required if screening for this disease is to continue (Downes *et al.*, 2007). This will help to select patients suitable for appropriate therapy and reduce unnecessary surgical interventions (Downes *et al.*, 2007).

1.2.3 Protein detection in tissue – Immunohistochemistry

Immunohistochemistry (IHC) is a method for localizing specific antigens/proteins in tissues or cells based on antigen-antibody recognition; it seeks to exploit the specificity provided by the binding of an antibody with its antigen at a light microscopic level (Dabbs, 2006). IHC is a more certain means of validating

morphological judgements by pathologists by identifying the presence or absence of proteins associated with morphological attributes. The basic principle of IHC is a sharp localization of target components in cell and tissue using an antigen specific primary antibody and a detection method usually consisting of a secondary antibody and an enzymatic label such as horseradish peroxidase, which in the presence of a suitable chromogenic substrate system allows the visualization of labelled antibodies by light microscopy (Dabbs, 2006).

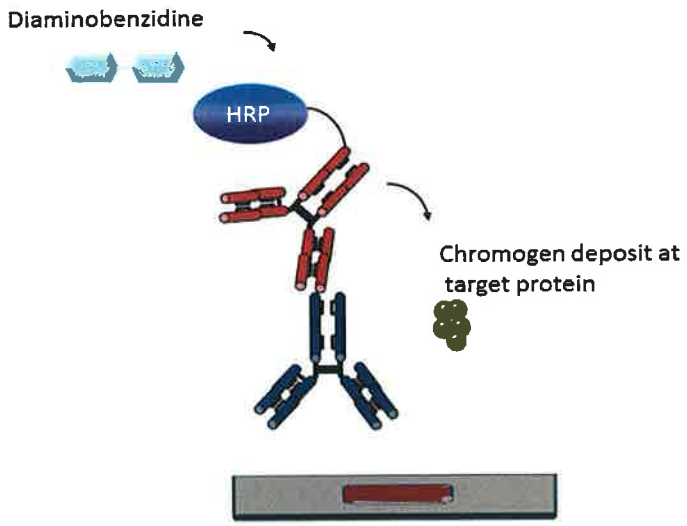

Figure 10: An example of an immunohistochemical method used by the BondMax™ automated IHC platform (Leica Microsystems))

Primary antibody binds to surface antigen on tissue (blue antibody in diagram), anti-primary antibody/secondary antibody (red antibody in diagram) binds to the primary antibody. The secondary antibody has a polymer tail with horseradish peroxidise attached. With the addition of an appropriate substrate e.g. diaminobenzidine (DAB) chromogen a brown end colour results which allows the visualization of the antigenic site by light microscope.

1.2.3.1 Prostate cancer tissue markers

Accurate pathologic diagnosis of prostate cancer is vital for optimal patient treatment. Diagnosis of the disease can usually be made on morphologic features such as growth pattern, nuclear atypia and the absence of basal cells. However, due to the heterogeneous nature of the disease, often in morphologically equivocal cases the use of IHC is applied by the histopathologist to resolve differential diagnosis (Varma and Jasani, 2005). IHC is used essentially in two different clinical settings in prostate cancer: (i) to distinguish low-grade prostatic cancer from benign mimics, in particular on needle biopsies and (ii) in transurethral resection specimens or metastatic tumour samples, to establish the prostatic origin of a poorly differentiated carcinoma (Varma and Jasani, 2005). Some of the key antigens used in the diagnosis of prostate cancer include PSA, keratin 34βE12, alpha-methylacyl-Coenzyme A racemase (AMACR/P504S), P63 and PSAP.

Raised levels of serum PSA, as discussed in the previous section, are suggestive of prostate cancer. PSA is also a useful antigen used by IHC to assist prostate cancer diagnosis. In the normal and hyperplastic prostate, PSA is uniformly expressed at the apical portion of the glandular epithelium of secretory cells (Dabbs, 2006). The intensity of PSA expression is decreased in poorly differentiated carcinoma as seen in Figure 11(A). PSA is also expressed in extra prostatic tissues but this expression is usually very weak. It can also detect metastatic tumours of prostatic origin elsewhere in the body which is very useful in the differential diagnosis of poorly differentiated or undifferentiated carcinomas (Dabbs, 2006).

The earliest serum marker of prostate cancer was prostate specific acid phosphatase (PSAP/PAP) (Makarov *et al.*, 2009). PSAP detection is also used to assist prostate cancer diagnosis by IHC. PSAP like PSA is expressed in normal and hyperplastic glandular epithelial cells. There is usually more intense

and uniform staining in glandular epithelium of well-differentiated adenocarcinoma, however, less intense and more variable staining is observed in moderate and poorly differentiated adenocarcinoma.

Another antigen used for IHC to assist prostate cancer diagnosis is AMACR. AMACR gene product, which is also referred to as P504S protein, is an enzyme involved in β-oxidation of branched-chain fatty acids. This gene product was reported to have been strongly expressed in 80 - 100% of small prostate cancers on biopsy in recent studies (Makarov *et al.*, 2009). The staining intensity and percentage of AMACR in prostatic adenocarcinoma was significantly higher than those in benign prostatic tissue (Makarov *et al.*, 2009). AMACR is also expressed in high grade PIN.

The presence of basal cells around prostate glands is indicative of benign glands. Therefore the use of basal cell markers in IHC is extremely valuable to pathologists in assisting prostate cancer diagnosis. Keratin 34βE12 is a high molecular weight cytokeratin expressed in the cytoplasm of basal cells. Monoclonal basal cell-specific anti-keratin 34βE12 stains positively in almost all normal basal cells of the prostate with no staining in secretory or stromal cells (Dabbs, 2006). Recently, p63, a nuclear basal cell protein, was shown to be a useful basal cell marker and was reported to be as specific and sensitive in detecting basal cells in diagnostic prostate specimens as keratin 34βE12. It was demonstrated by Zhou *et al* that dual staining of 34βE12 and p63 increased the sensitivity of the basal cell detection and reduced staining variability, thus rendering basal cell immunostaining more consistent (Dabbs, 2006). Cocktail staining of AMACR (absent in benign tissues) with p63 and/or 34βE12 (absent in cancer tissues) is increasingly being carried out in histopathology laboratories as a diagnostic assay in difficult cases.

Although there are some drawbacks associated with IHC involving standardizing fixation, processing and antigen retrieval techniques of tissue specimens and also involving objective quantitative measurement for target antigens, ultimately

the widespread application of IHC has revolutionized diagnostic surgical pathology.

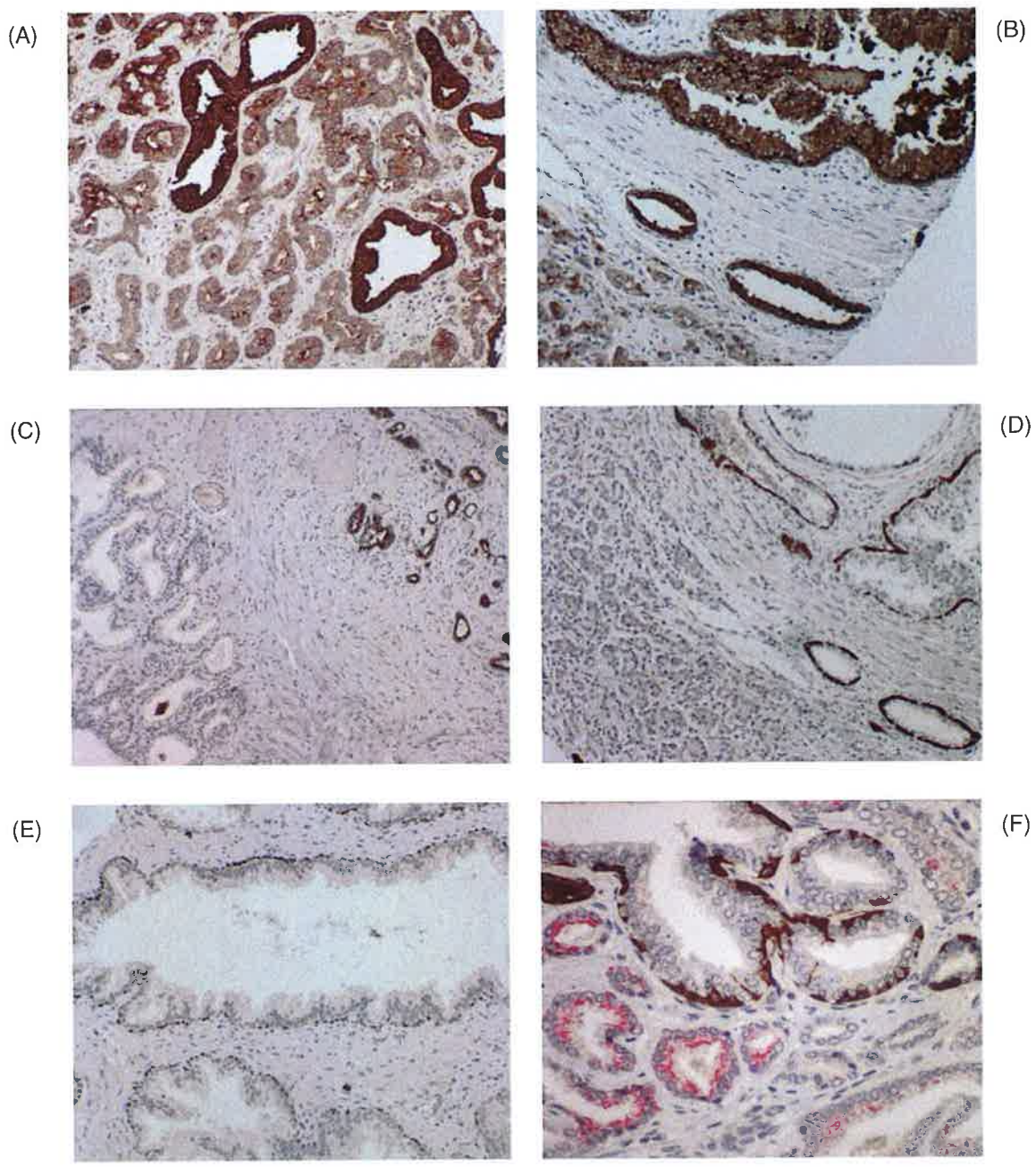

Figure 11: Tissue microarray cores stained with diagnostic markers used routinely to detect prostate cancer

(A) Strong expression of PSA in benign epithelia with weaker expression observed in adjacent tumour. (B) Strong expression of PSAP in benign epithelia with weaker expression observed in adjacent tumour, (C) AMACR expression in tumour with no expression observed in adjacent benign glands, (D) Keratin 34βE12 expression observed in the cytoplasm of basal cells in benign glands with no basal cells noted in adjacent tumour, (E) Nuclear P63 expression in basal cells of benign glands, (F) Cocktail staining of AMACR and keratin 34βE12: Keratin 34βE12 (brown colour) expression observed in benign glands and AMACR expression (red colour) observed in tumour cells. [(A)-(F) X200 Magnification]

1.2.4 Novel antibodies for cancer research

The use of well characterised antibodies is vital for clinical diagnostics and protein studies. Antibodies are routinely used for Western blotting (WB), immunoprecipitation (IP), enzyme-linked immunosorbent assays (ELISA), quantitative immunofluorescence (QIF), and immunohistochemistry (IHC) in research and are also extremely important tools in clinical management with extensive use in both laboratory medicine (ELISA assays and flow cytometry) and anatomic pathology (immunohistochemistry) (Bordeaux *et al.*, 2003). IHC, as previously discussed, serves as a diagnostic, prognostic and predictive method to assist pathologists. Such examples include oestrogen receptor α (ER-α) and human epidermal growth factor-2 (HER-2) assessment by IHC in breast cancer to determine whether patients are suitable candidates to receive certain therapies that can cost as much as $100,000 per year (Bordeaux *et al.*, 2003).

One of the major challenges facing researchers and clinicians in the area of cancer research is the lack of high quality, well characterised antibodies to target proteins. Although commercial production of antibodies is well established, the market has been driven so far by the popularity of particular antibody targets (Blow, 2007) due to the fact that antibody companies are likely to make profit on more popular targets. For example more than 1,000 antibodies against the tumour suppressor p53 are available commercially but the less sought-after targets frequently have none (Blow, 2007). Therefore, antibodies do not exist for the majority of proteins in the human genome. The production and validation of specific antibodies is very challenging, costly and time consuming and this also may account for the lack of specific antibodies to less popular targets.

Biomarker discovery, particularly in cancer research, requires the rapid validation of markers identified in studies to allow markers to be more quickly moved towards clinical utilisation. However due to the lack in availability of antibodies to novel markers/proteins this makes validation of potential biomarkers identified in

cancer research extremely difficult. Therefore, there is an urgent requirement for more well-characterised antibodies to be generated against less popular novel target proteins. The development of a novel antibody is a major component of this project and this is dealt with in detail in section 1.3 and chapter 5.

1.2.5 Prostate Cancer Research Consortium

Prostate cancer is a major health issue for patients, physicians, healthcare providers and policy makers and it is imperative to convert knowledge of the disease process to tangible benefits through clinical research initiatives. This requires translation of current discovery to clinically applicable diagnostic tools and new therapeutic approaches. A critical bridge for enabling this translational research is the establishment of a collaborative infrastructure from the clinic to the research bench and the availability of bioresources or biobanks of clinically relevant samples from patients at different stages of the disease.

In October 2003, the Prostate Cancer Research Consortium (PCRC) was created with funding from the Irish Cancer Society and within the structure of the Dublin Molecular Medicine Centre. It is a multi-disciplinary, trans-institutional collaboration composed of researchers from University College Dublin's Conway Institute, Trinity College Dublin's Institute for Molecular Medicine, Royal College of Surgeons in Ireland and Dublin City University. This consortium brings together clinicians, pathologists, scientists, research nurses and allied health care professionals with a common goal of understanding the molecular and cellular basis for prostate cancer development and progression. The overall aim of the PCRC is to translate this information to improve detection, prognosis and treatment of prostate cancer. A key component of the PCRC is the establishment of a multi-site prostate cancer bio-resource at The Mater Misericordiae University Hospital, St James's Hospital, St Vincent's University Hospital and Beaumont Hospital which contain tissue, matched serum/plasma

and urine samples with comprehensive clinical information and follow up from patients with different stages of prostate cancer.

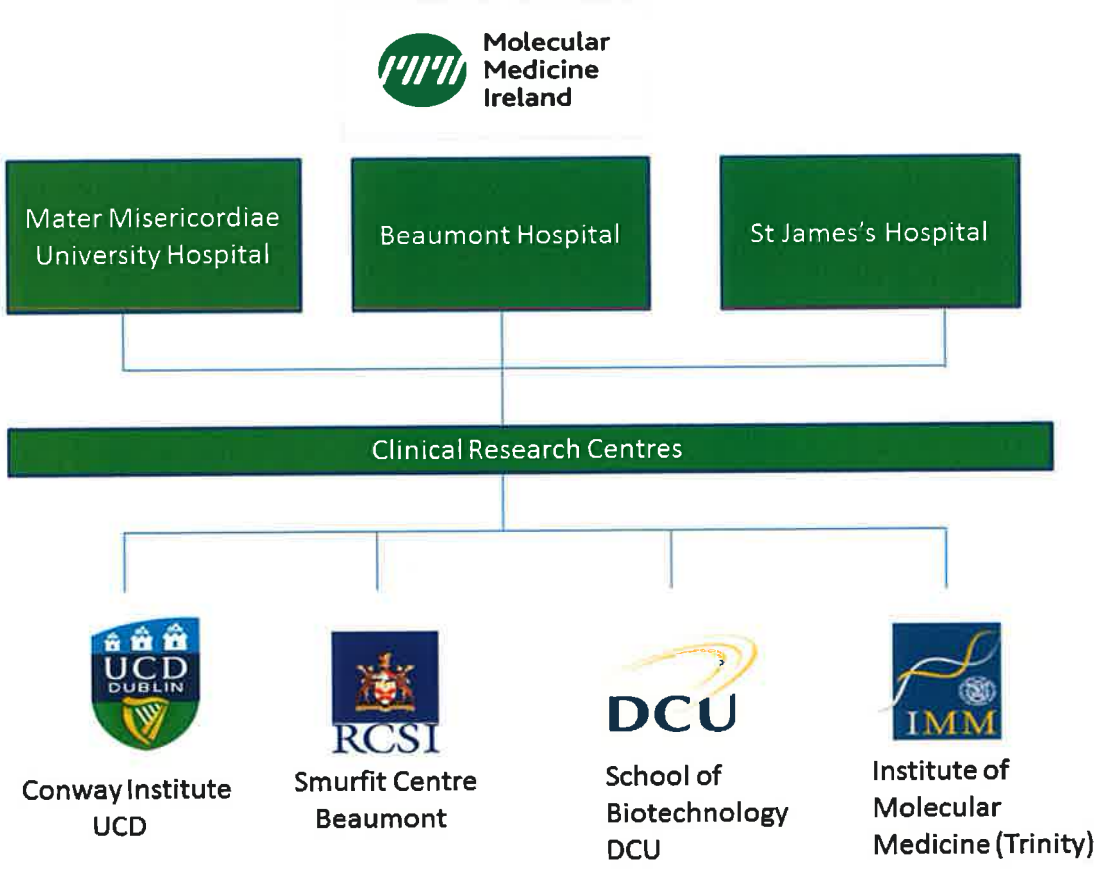

Figure 12: Participating Institutions in the Prostate Cancer Research Consortium

The research focus of the PCRC has been primarily driven by the need to address urgent clinical questions. The limitations of PSA as a marker of prostate cancer have highlighted the need for new biomarkers of this heterogeneous

disease. One of the PCRC's main aims is to identify novel cancer biomarkers which will permit early diagnosis of disease and provide critical information for stratification and clinical intervention using a comprehensive approach which involves utilizing genomic, transcriptomic and proteomic platforms and using a high-throughput biomarker validation approach. The PCRC hypothesise that appropriate diagnosis of prostate cancer using biomarkers is a multi-step algorithm. The biomarker discovery workflow of the PCRC is shown in Figure 13.

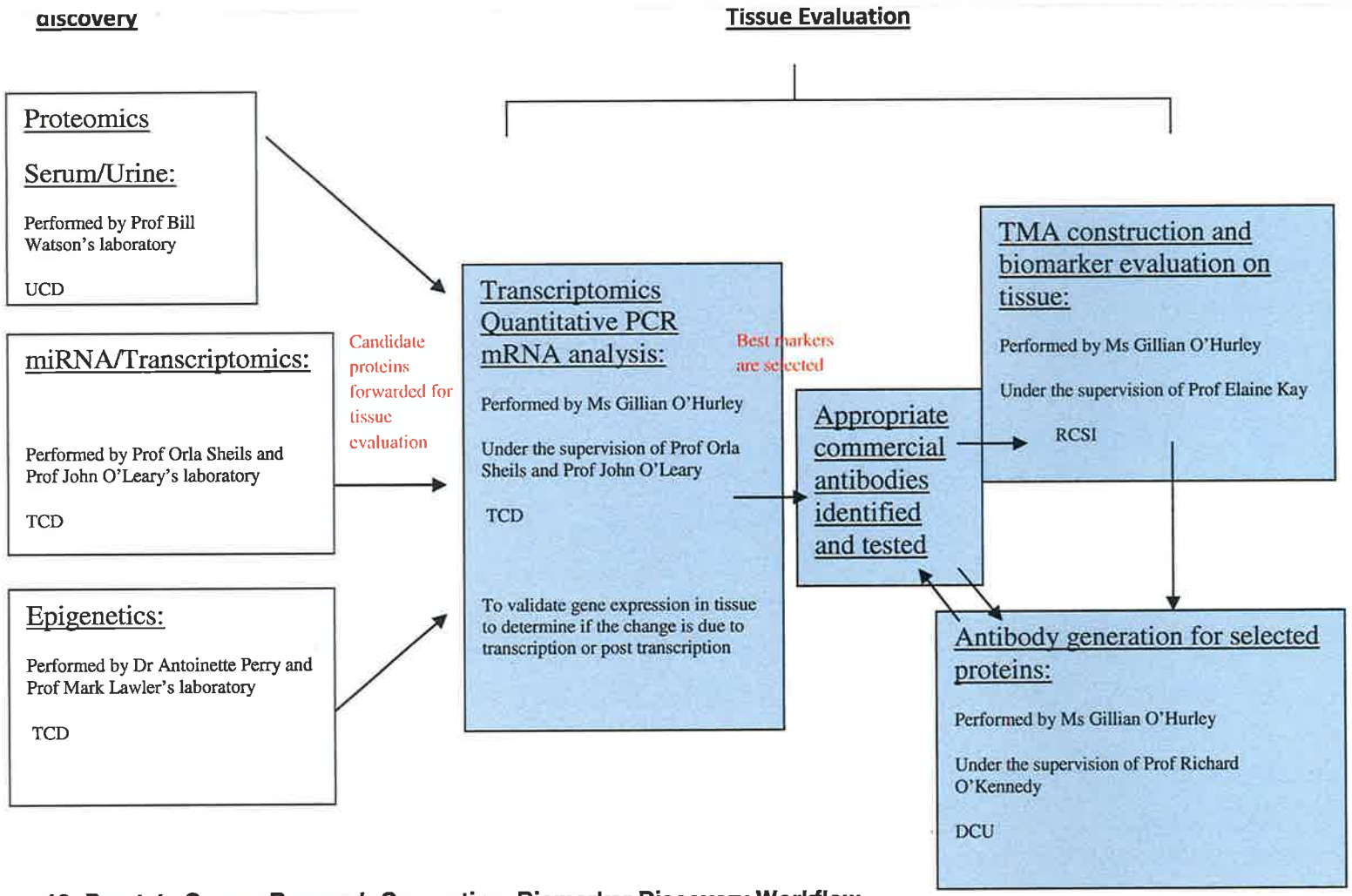

Figure 13: Prostate Cancer Research Consortium Biomarker Discovery Workflow

Candidate proteins/biomarkers of prostate cancer are forwarded for tissue validation from the Proteomic study (UCD Conway Institute), the Transcriptomic study (Trinity College Dublin Institute for Molecular Medicine) and the Epigenetic study (Trinity College Dublin Institute for Molecular Medicine). The first step in the tissue evaluation level is mRNA analysis using quantitative PCR to validate the gene expression in the tissue (RCSI/TCD institute for molecular medicine). Following this markers are selected for immunohistochemical analysis on prostate cancer tissue microarrays constructed from the PCRC's bioresources (RCSI). Antibodies are generated (DCU/RCSI) to the identified markers if no suitable antibodies for Immunohistochemistry exist for the markers. All the above studies will be carried out on serum/urine and tissue samples from the same cases of prostate cancer from the PCRC's bioresources.

1.3 Antibody Generation

1.3.1 Introduction

A major component of this project is antibody development to novel markers of prostate cancer. This is discussed in detail in Chapter 5. The following section gives some background to antibodies and their structure and also describes the issues relevant to antibody production.

1.3.2 Innate and acquired immunity

Immunity is the ability to resist infection. The innate immune system is a general non-specific response to foreign molecules that is passed on from mother to offspring and includes systems such as phagocytosis (macrophages), cell lysis (natural killer cells) and a host of chemical and physical elements (Conroy *et al.*, 2009). The first of the innate mechanisms is the barrier functions of the body's epithelia, e.g. skin, which can simply prevent an infection from being established. It also consists of mucosal immunity e.g. saliva, tears, nasal secretions and lysozyme, an enzyme in perspiration that causes cell lysis in Gram positive bacteria. Next, there are cells and molecules such as eosinophils, basophils, macrophages, cytokines and chemokines, available to control or destroy the pathogen once it has breached the body's natural barriers. The inflammation process is initiated by cytokines and chemokines released by innate immune cells such as mast cells (Luster *et al.*, 2005). Heat, pain, redness and swelling are all associated with the inflammation process and all reflect the effects of cytokines and other inflammatory mediators on blood vessels. Increased blood flow and leakage of fluid results from vasodilation and increased permeability of blood vessels during inflammation to increase permeability and allow inflammatory cells to migrate to the site of infection in the tissue. This accounts for the heat,

redness and swelling associated with inflammation. Only if a pathogen can breach these early lines of defence will the adaptive immune response ensue.

Acquired/adapted immunity involves a cascade of events involving B and T cell lymphocytes. B lymphocyte cells are derived from the stem cells of the bone marrow and produce antibodies. T lymphocyte cells are produced in the bone marrow but processed in the thymus and constitute the basis of cell-mediated immunity. The main difference between innate and adaptive immunity is the ability of the adaptive immune system to improve after exposure to specific molecules (Conroy *et al.*, 2009). During cell-mediated immunity, antigen presenting cells such as dendritic cells engulf the antigen, process it internally and display part of the antigen on their surface through major histocompatibility complex (MHC) molecules (see Figure 14).

(A)

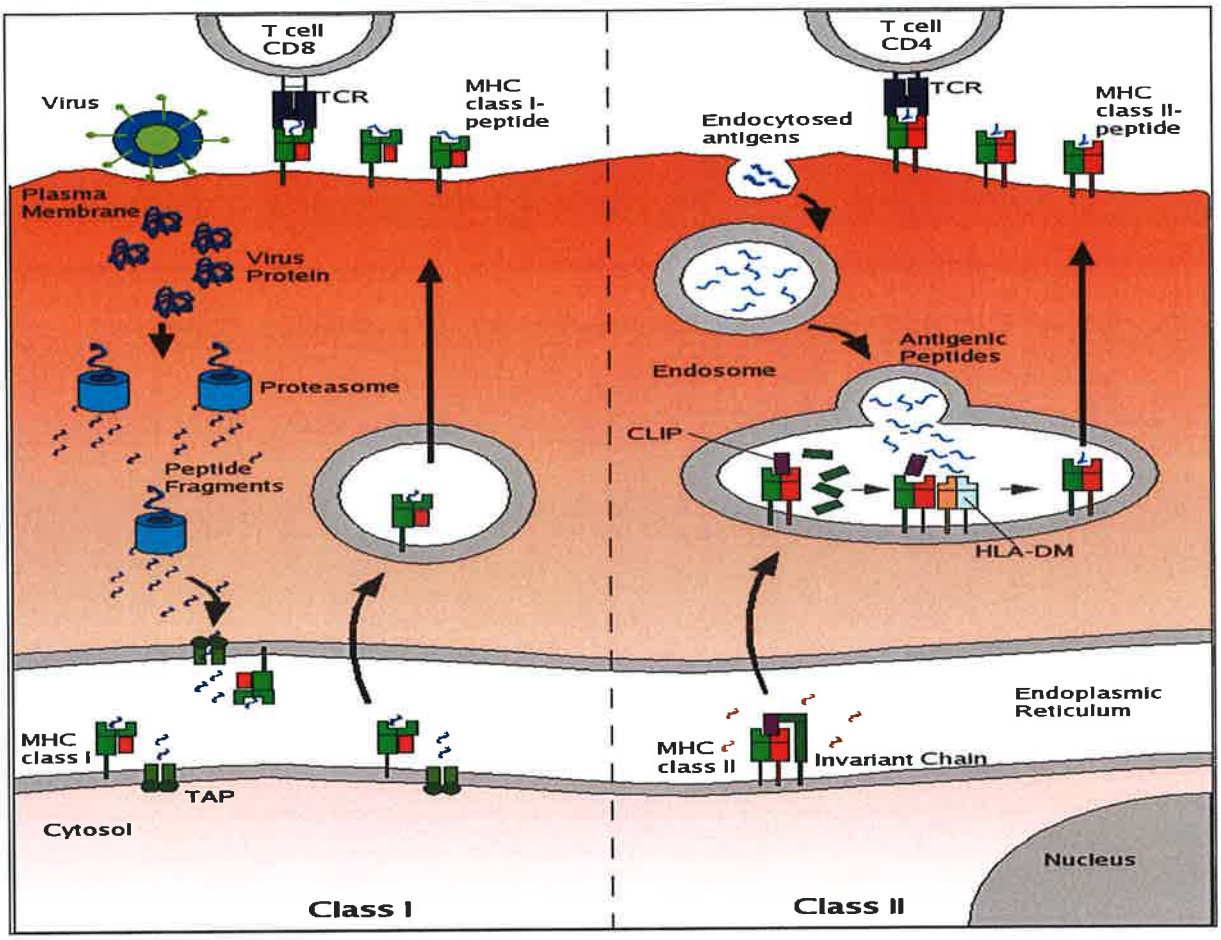

Figure 14: Antigen presenting by MHC molecules (http://www.lesc.ic.ac.uk/projects/appp.html)

MHC class I:

Intracellular cytosolic antigen is broken down into peptides by the proteasome. Peptides are then transported to the endoplasmic reticulum where they bind to MHC I which is then transported to the cell surface for antigen presenting to T cells.

MHC class II:

Extracellular antigen is taken up into intracellular vesicles. In early endosomes of neutral pH endosomal proteases are inactive. Acidification of vesicles activates proteases to degrade antigen into peptide fragments. Vesicles containing peptides fuse with vesicles containing MHC class II molecules and this is then transported to the cell surface for antigen presenting to T cells.

Several types of effector T cells have been discovered which are specialized to deal with different classes of pathogen. CD8 cytotoxic cells kill target cells that display peptide fragments of cytosolic pathogens, most notably viruses,

bound to MHC class I molecules at the cell surface. Helper T (T_H) cells express the CD4 co-receptor and recognize fragments of antigens degraded within intracellular vesicles displayed at the cell surface by MHC class II molecules. Unlike CD8 cytotoxic cells, T_H cells do not kill target cells directly but guide the immune response by secreting lymphokines that encourage cytotoxic T cells and B cells to grow and divide, attract neutrophils and boost the ability of macrophages to engulf and destroy microbes. They also stimulate immature B lymphocytes to maturity when an antigen binds to their surface receptors. There are five subsets of T_H cells categorised based on their cytokine secretion capacity and their function; T_H1, T_H2, T_H9, T_H17, and T_H22. Originally, only two subsets of T_H lymphocytes were described; T_H1 and T_H2. However, newly described proinflammatory T_H17 or T_H9 cell lineages and well-characterized Tregs have been reported as important players in immune regulation (Jutel and Akdis, 2011). Dendritic cells are essential for the differentiation of naive T cells into the T_H cell subsets through the release cytokines and other cofactors (see Figure 15) (Jutel and Akdis, 2011).

- T_H1 cells activate macrophages, enabling them to destroy intracellular microorganisms more efficiently. They can also activate B cells to produce strongly opsonising antibodies.

- T_H2 cells, in contrast, drive B lymphocytes to differentiate and produce immunoglobulins of all other types, and are responsible for initiating B lymphocyte responses by activating naïve B lymphocytes to proliferate and secrete IgM.

- T_H17 cells produce interleukin 17 (IL-17) and are thought to play a role in inflammation (Steinman, 2007). Excessive amounts of T_H17 cells are thought to play a major role in autoimmune disease.

- T_H9 cells produce IL-9 and IL-10 and have been shown to induce tissue inflammation In autoimmune diseases (Jutel and Akdis, 2011).

- Another novel T-cell subset T_H22 has been demonstrated in T cell. This T_H cell independently expresses IL-22 and low levels of IL-17 (Jutel and Akdis, 2011). T_H22 lymphocytes play a role in atopic dermatitis.

- Regulatory T cells (T_{reg}, also known as suppressor T cells) inhibit the production of cytotoxic T cells and memory T cells recognise and respond to a further infection of the same pathogen.

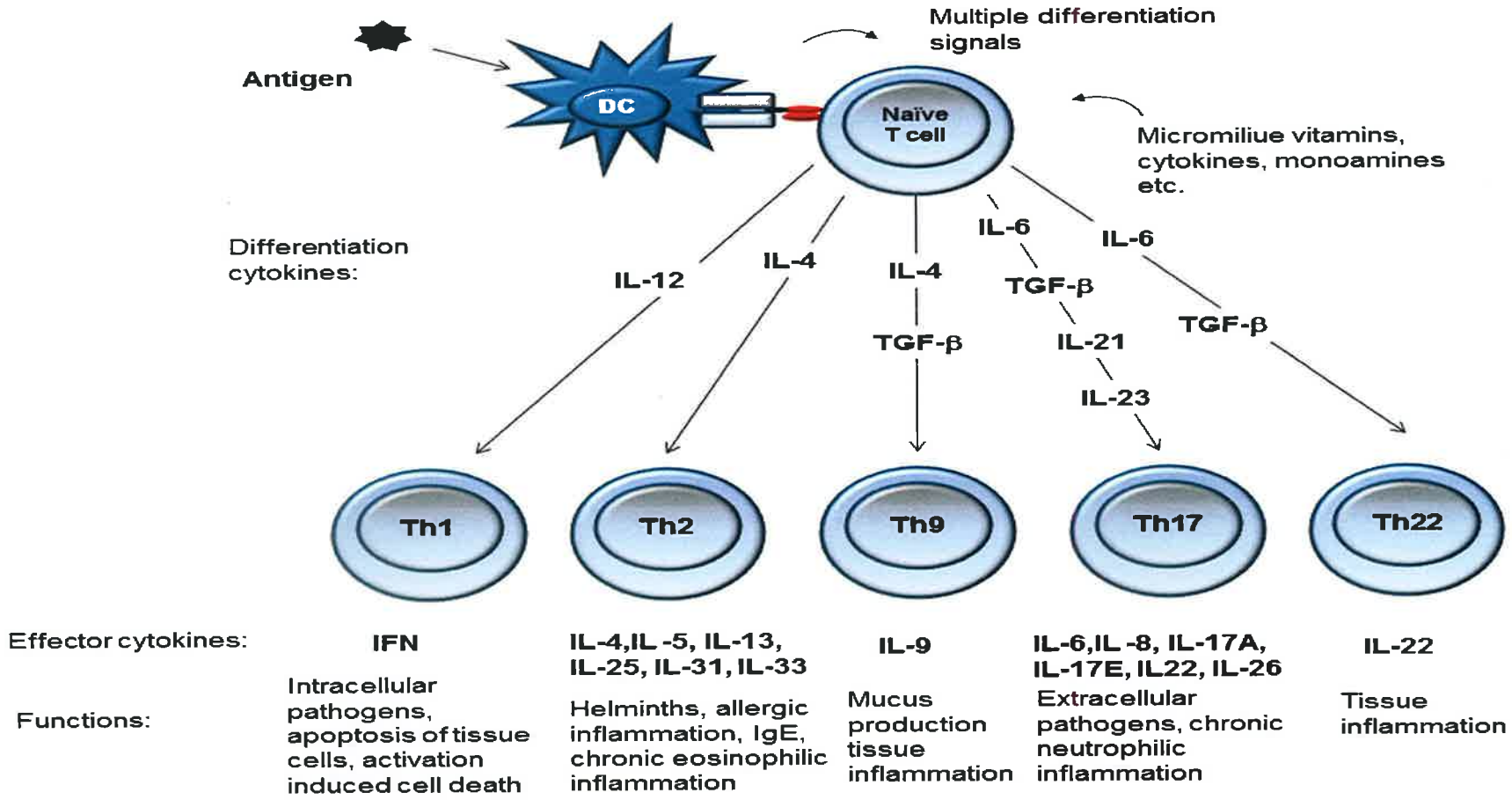

Figure 15: T_H cell subsets

Naive T cells differentiation. Naive T cells can differentiate into T_H1, T_H2, T_H9, T_H17, and T_H22 types of T helper cells depending on the substances co-exposed with the antigen and status of the cells and cytokines in the microenvironment. Based on their respective cytokine profiles, responses to chemokines, and interactions with other cells, these T-cell subsets can promote different types of inflammatory responses.

(IFN = interferon, IL = interleukin, TGF = transforming growth factor, TNF = tumour necrosis factor)

1.3.3 Antibodies and their structure

Adaptive immunity is mediated by lymphocytes (in particular white blood cells) that are responsible for secreting antibodies (immunoglobulins) upon exposure to a foreign entity such as infection or immunisation (Conroy *et al.*, 2009). An antibody is a glycoprotein that binds specifically to a particular substance – an antigen. The three methods by which antibodies eliminate and destroy hazardous pathogens are neutralization, opsonisation or complement activation. All antibodies have the same general overall structure and are known collectively as immunoglobulins or Igs. The basic structure of an antibody is shown in Figure 16.

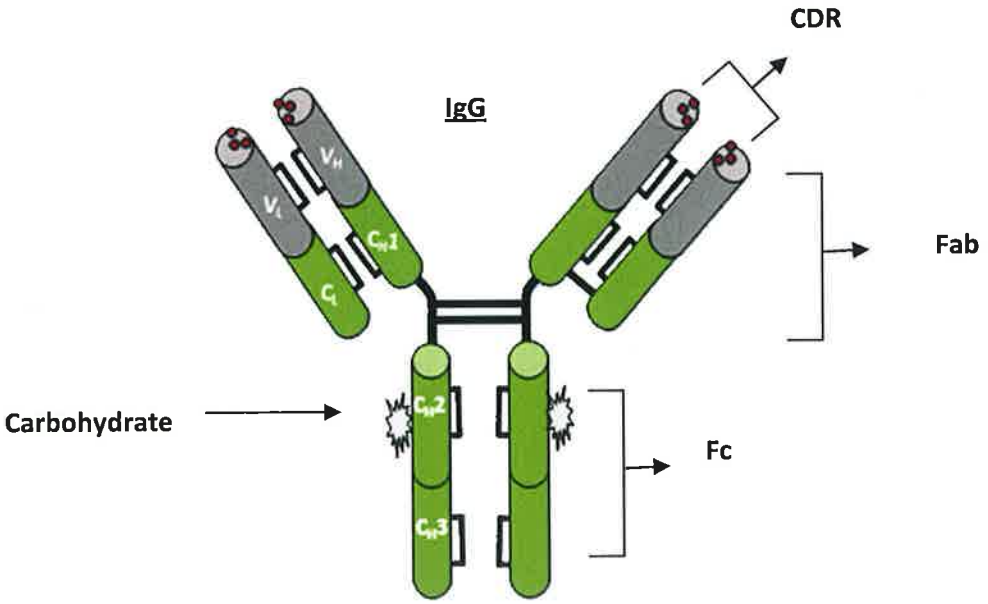

Figure 16: Structure of the immunoglobulin G (IgG) molecule

The molecule consists of two identical heavy (H) chains (approximately 50 kDa) and two identical copies of a light chain (25 kDa). Each light chain is attached to a corresponding heavy chain by a disulphide bond. Both heavy chains are covalently linked by interchain disulphide bridges located near the hinge axis. The heavy chain is divided into 4 domains (1 x V_H and 3 x C_H domains) and the light chain is divided into 2 domains (1 x V_L and 1 x C_L). The V_H and V_L domains confer antigenic binding specificity. The complementary determining regions (CDR) which form the antigen binding site, antigen binding fragment (Fab), and constant fragments (Fc) are labelled.

Polyclonal antibodies are a mixture of immunoglobulins (Ig) that recognise different epitopes of the antigen, while monoclonal antibodies bind to a single epitope of the antigen. Monoclonal antibodies were first reported by Georges Kohler and Cesar Milstein in 1975. Since then many advances have generated recombinant antibody fragments namely, the single chain variable fragments (scFv), antigen binding fragment (Fab) and the single chain antibody fragment (scAb). These fragments retain antigenic specificity due to the complementary determining region (CDR) of the antibody without compromising binding affinity.

1.3.4 Antibody Classes

The 5 major classes/isotypes of antibody (immunoglobulin/Ig) are IgM, IgG, IgA, IgD and IgE which differ in both their structure and immune function. IgM is so called because of its size: although monomeric IgM is only 190 kDa, it normally forms pentamers, known as macroglobulins (hence the M) (Janeway, 2005). Clinically IgMs are significant because they are predominant in early immune responses to most antigens. IgA dimerizes to give a molecular mass of approximately 390 kDa (Janeway, 2005) and is the predominant immunoglobulin in secretions e.g. saliva, tears, nasal mucosa, prostatic fluid and many other bodily fluids. IgA is further classified into 2 isotypes IgA1 and IgA2 (Correia, 2011). IgA1 is the predominant IgA subclass found in serum (~90% of serum IgA). The principle difference between IgA1 and IgA2 is that the heavy and light chains are linked with noncovalent bonds in IgA2 whereas they are linked by disulfide bonds in IgA1. IgD antibodies are monomeric and trace amounts are present in serum and are found on the surface of human B lymphocytes. IgE antibodies represent only a small fraction of total antibodies in blood. They are present in serum in a monomeric form. IgEs are involved in the production and release of vasoactive mediators e.g. histamine and other chemicals that cause an inflammatory reaction. In humans, IgG antibodies are further subdivided into 4 subclasses; IgG1, IgG2, IgG3 and

IgG4 (Correia, 2011) and are named in order of their abundance in serum. The basic IgG structure is made up of four polypeptide chains with two identical heavy (H) chains and two identical light (L) chains connected by disulphide bonds. The IgG structure differs depending on the isotype (see Figure 16).

IgY is the major serum Ig of birds, amphibians and reptiles (Purzel *et al.*, 2009). The structure of avian IgY (~180 kDa) is similar to mammalian IgG, with 2 heavy ("nu" chains, ~67-70 kDa) and 2 light chains (22-30 kDa). However, IgY has an extra heavy chain constant domain.

The variable region of an antibody varies greatly in amino acid sequence in different antibodies. The hypervariable (HV) and framework (FR) regions make up the variable region. Three HV regions exist (HV 1, 2 and 3) and these HV regions are collectively known as complementary determining regions (CDRs). The CDRs are interspersed by FRs which provides a backbone structure for the antibody. They can also have an influence on antigenic specificity. Six HV loop structures which structurally form antigen-binding surfaces result from the conformation of the V_H and V_L chain CDRs.

Antibodies are ideal biorecognition elements due to their specificity and affinity for cognate antigen (Conroy *et al.*, 2009). Virtually any substance can be the target of an antibody response. The capability of the body to generate an enormous diversity of antibodies accounts for the remarkable adaptive nature of the immune system. It is because of the unique genetic mechanisms governing antibody synthesis that the body is capable of producing these highly specific molecules to foreign entities. The V_H and V_L chains retain this diversity. V_L chain genes are composed of two loci, the variable (V) and joining (J) loci. The V_H genes are composed of three loci, the V and J loci and diversity (D) locus. These different regions combine randomly to produce a huge range of diverse antibodies. Different combinations of the various VDJ sequences in the V_H chain and VJ sequences in the V_L chain results in the formation of diverse conformations in the binding sites (Storb *et al.*, 2001) (Figure 17). This mechanism is called somatic recombination. In addition,

nucleotides are randomly added and/or removed at joints between gene segments which create junctional diversity. Upon activation by antigens, mature B cells initiate a process of somatic point mutation of the V region DNA, which creates numerous variants of the original assembled V region (Janeway, 2005).

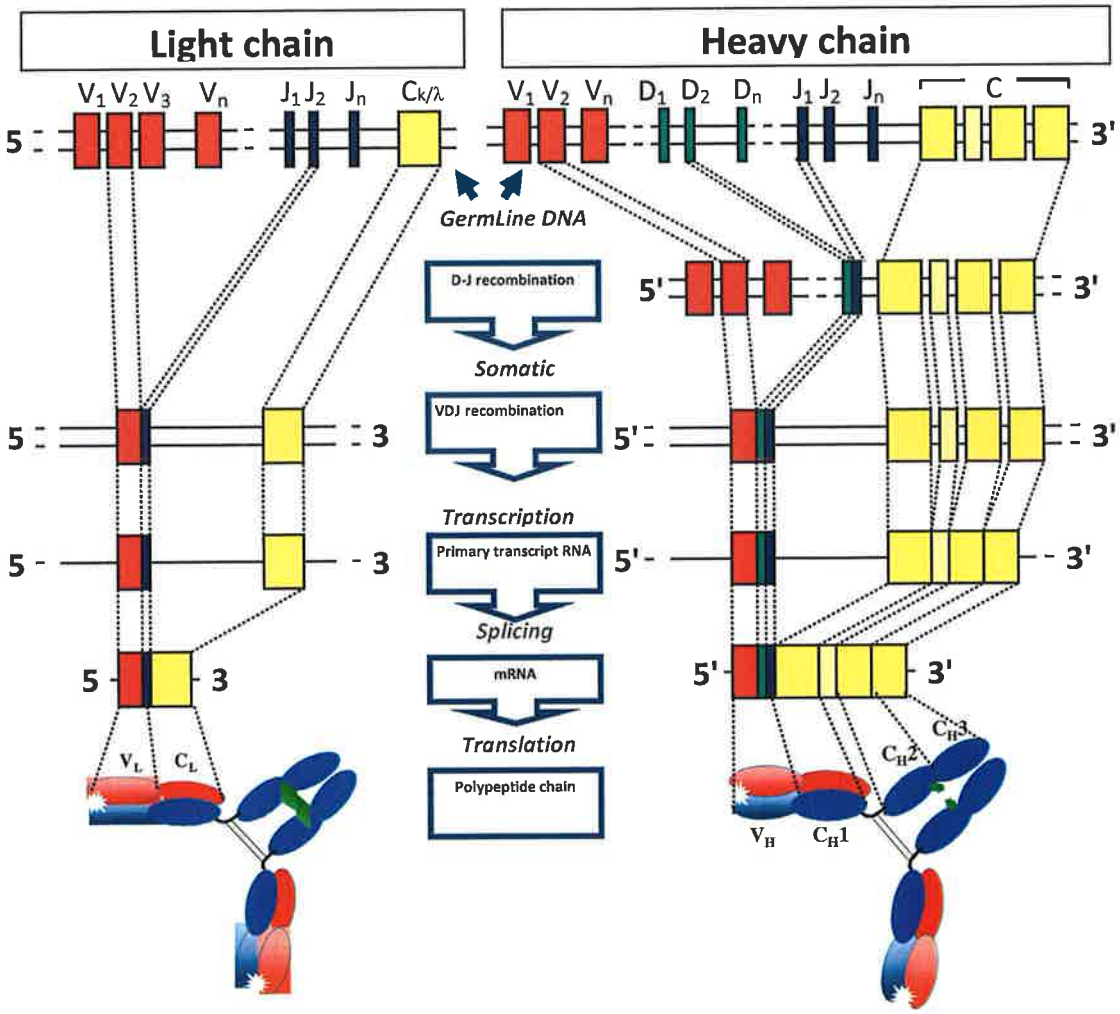

Figure 17: Somatic recombination of the separate gene segments for the construction of the variable genes

Light chain genes are constructed whereby a variable (V) and joining (J) gene segment are combined to form a complete light-chain V-region gene. The constant (C) is encoded on a separated gene locus and is attached to the variable region exon through splicing of the light-chain RNA to remove the J and C introns. Heavy chain genes are constructed using three gene segments, diversity (D), J and C. Firstly the D and J gene segments are joined followed by the combination of the V gene segment to form a complete heavy-chain exon. The heavy chain C-region genes are encoded by numerous exons which are spliced to the heavy chain C-region during processing of the heavy-chain transcript. The light and heavy chain genes are translated into large polypeptide chains that associate to form the antibody molecule. The diagram was adapted from Janeway, *2005*.

1.3.5 Recombinant antibodies

Recombinant antibody fragments are becoming important tools in research biotechnology, medicine and therapeutics due to their intrinsic properties. Recombinant antibodies have the ability to maintain antigen recognition, are relatively easy to produce and their small size leads to greater penetration capabilities when compared with the complete antibody.

Recombinant antibody fragments can be generated by amplifying the variable genes from the cDNA from the lymphocytes of an immunised source. They can also be generated by directly cloning the heavy and light chain variable domains from a monoclonal antibody-producing hybridoma cell. A single-chain variable fragment (scFv) consists of variable heavy and variable light chain domains of the full immunoglobulin joined together using a flexible glycine-serine linker (see Figure 18). The scFv fragment which is 30 kDa maintains specificity and affinity of the full antibody fragment (150 kDa) despite the lack of the constant domains. An antigen-binding fragment (Fab) consists of the variable heavy and light chain genes joined with the constant heavy and light chain genes developing a more stable antibody construct. A major choice facing an investigator is whether to construct a library in a scFv or Fab format (Barbas, 2001). Fab fragments are generally seen as a more functional and stable version of recombinant antibody than the scFv. However, the advantages of scFv format over Fab fragments are several: (i) the scFv libraries are quicker to construct as they involve fewer PCR steps, (ii) they are smaller fragments so they are flexible and have greater penetration capabilities and so can access their antigen better, (iii) yields from *E. coli* tend to be better for scFvs than Fabs and (iv) scFvs have the ability to multimerize which can enhance avidity for antigen and facilitate selection against certain antigens such as cell surface antigens (Barbas, 2001).

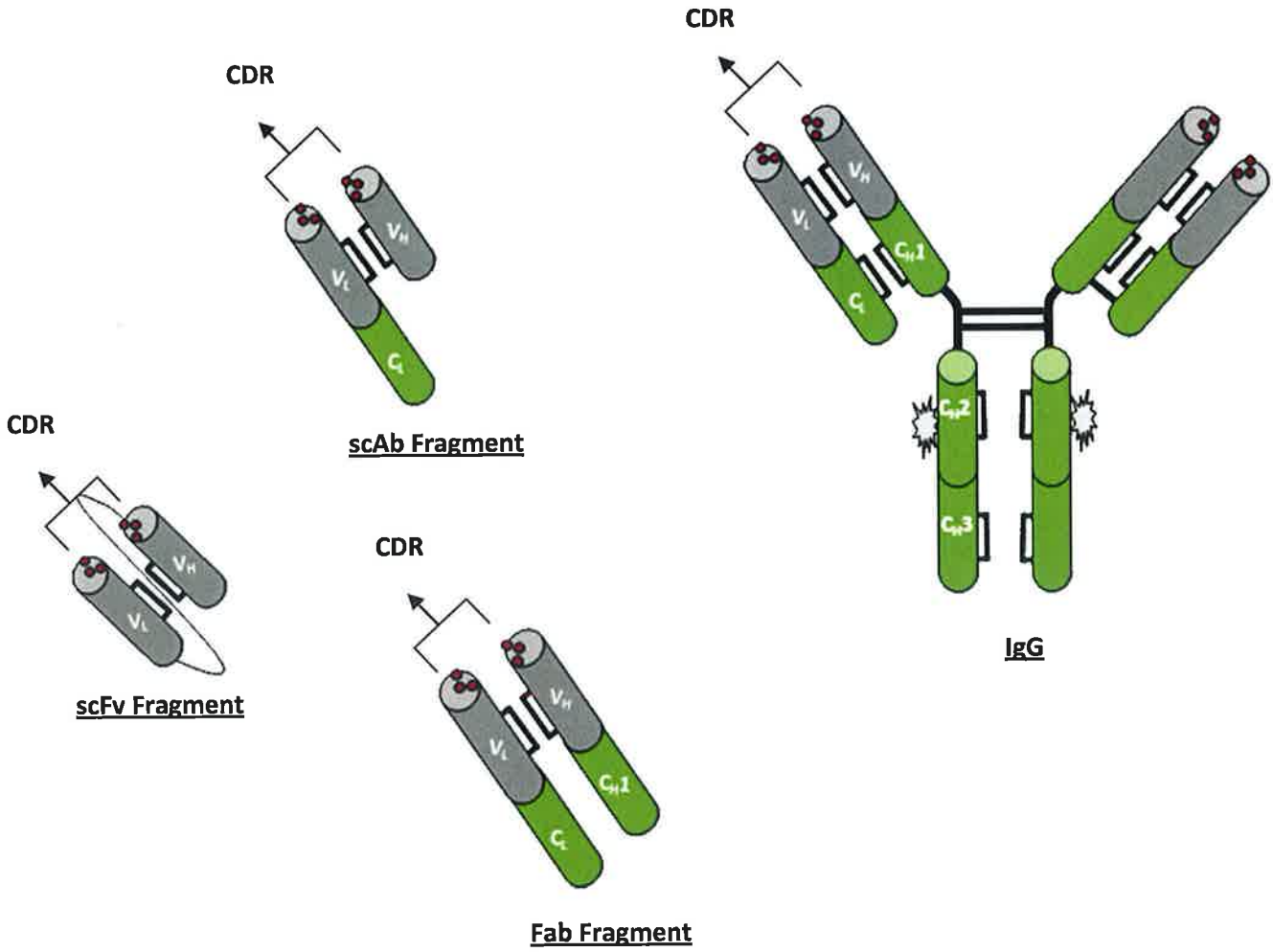

Figure 18: Genetically-derived recombinant antibodies which retain antigen specificity

The smallest of these recombinant antibody fragments is a scFv fragment consisting of the V_H and V_L chain of the full IgG molecule bound by a glycine-serine linker. The Fab fragment is similar in structure to the scFv fragment but is a more stable construct. A scAb fragment consists of linking a constant kappa domain to the scFv fragment. The CDR regions of the antibody fragment are responsible for binding to the epitope on the antigen.

1.3.6 Phage display

Phage display has become a widely used selection platform for antibodies (Conroy *et al.*, 2009). Phage display was first reported in 1985 (Smith, 1985) and since then has been largely developed and implemented in many fields of research. Phage display is based on two pivotal concepts:

(i) Phage, viruses that infect bacteria, can be used to link protein recognition and DNA replication. The protein (or peptide)/antibody is displayed on the surface of the phage particle and the gene encoding the protein is contained within the particle (Barbas, 2001).

(ii) Large libraries of the DNA encoding these molecules can be cloned into phage. Individual phage can then be rescued from libraries through interaction of the displayed protein/antibody with the cognate ligand and the phage can be amplified by infection of bacteria (Barbas, 2001).

The fact that a highly comprehensive library of antibody fragments can be generated from which an antibody with high specificity for the antigen can be selected is one of the main advantages of recombinant technology for antibody production (Hoogenboom *et al.*, 1998).

Phage display involves using a filamentous bacteriophage (see Figure 19) which is a virus that contains a circular single stranded DNA genome encased in a long protein capsid cylinder (Barbas, 2001). Foreign DNA can be inserted into regions of the genome and expressed on the surface as fusion coat proteins. Thus, there is a direct link between the genotype and phenotype.

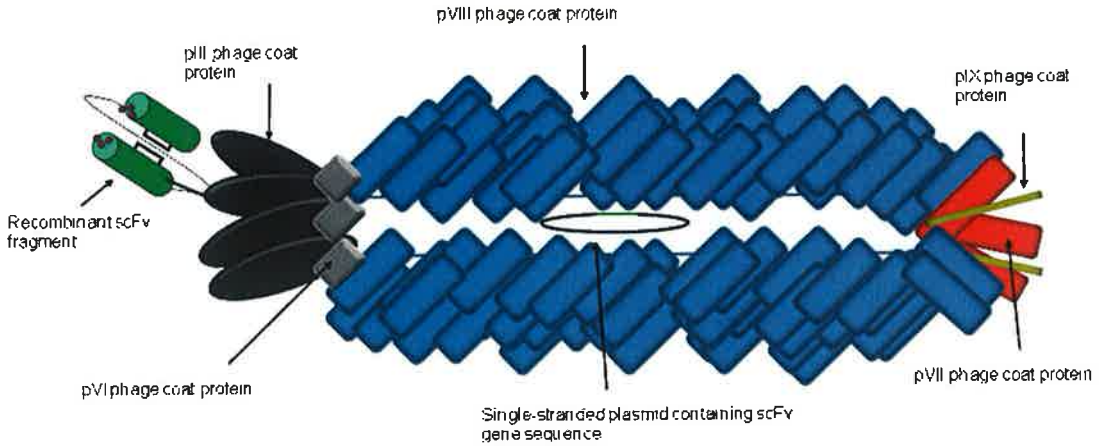

Figure 19: The recombinant scFv expressed on the surface of a bacteriophage and the gene encoding the fusion protein within the virion

Schematic representation of a bacteriophage expressing a scFv antibody fragment on the pIII phage coat protein. 2700 copies of the major coat protein (pVIII) encapsulate a single stranded DNA genome. The antibody genes are shown in-frame with gene III.

Phage display libraries can be developed synthetically or by using an immunised source. Generally, cDNA is generated from the mRNA extracted from the spleen or bone marrow of an immunised animal. The heavy and light chain genes are amplified by polymerase chain reaction (PCR) and the antibody fragment is then ligated into a phagemid vector (into one of the encoding genes for surface coat proteins). The phagemid DNA is then transformed into competent *E. coli* cells for expression. The coat protein fusions are integrated into new phage particles assembled in the bacterium after expression. This enables phage particles to be replicated as ssDNA in the presence of helper phage. Helper phage provides the required viral tools for packaging of phagemid DNA into phage particles. These phage express the antibody fragment/protein (encoded in the phagemid) onto the surface coat of the phagemid. Helper phage contains a defective origin of replication which reduces the ability of helper phage to replicate. Phage particles are harvested from the infected cells and positive clones with desired affinities selected by a process known as 'biopanning' which is described in Figure 21

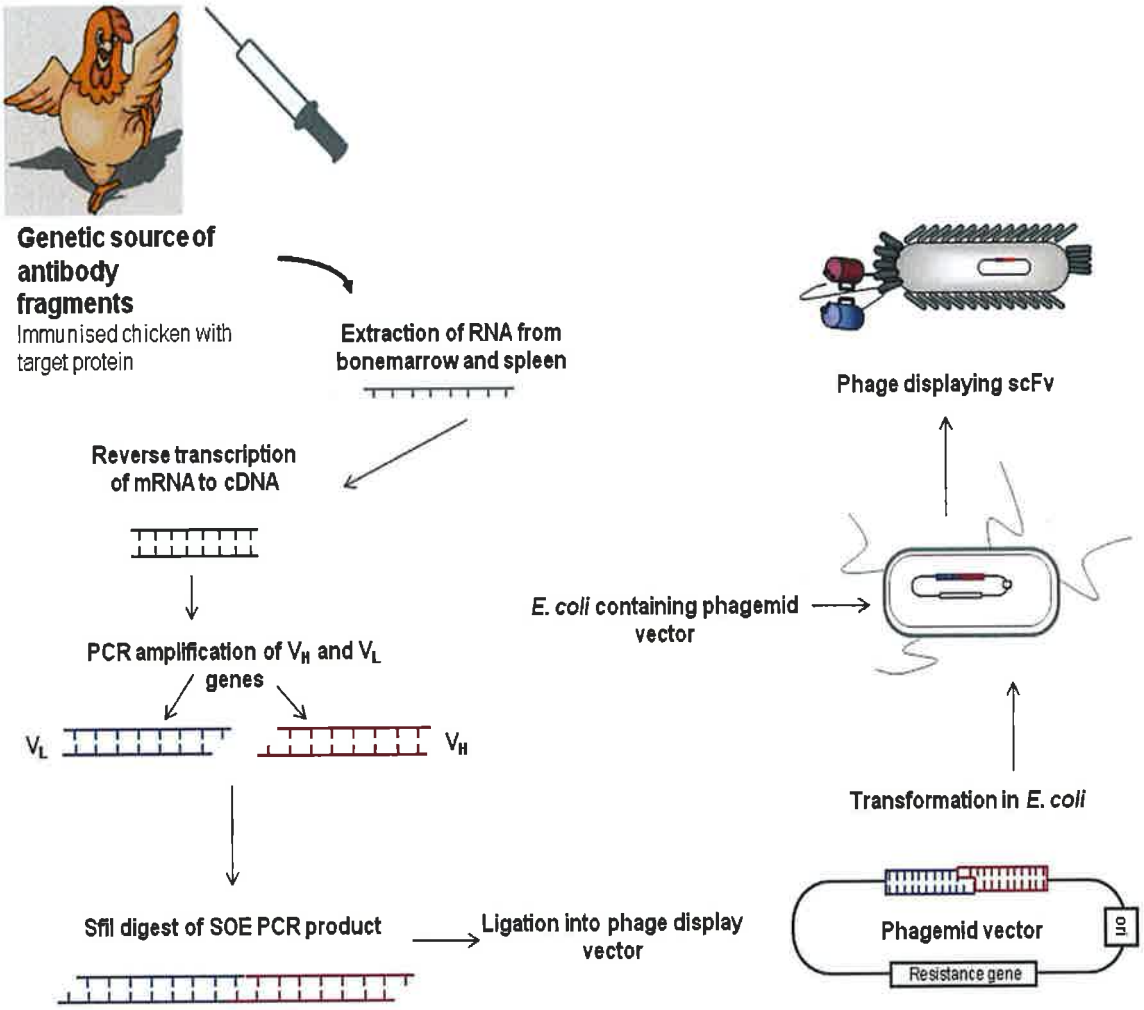

Figure 20: Schematic representation of the production of a phage display library

An immune model is selected for immunisation (e.g. an avian model). Bone marrow and spleen is removed from immune source following immunisations with target protein. RNA from bone marrow and spleen is extracted. The RNA is reverse transcribed to cDNA. The variable light (V_L) and variable heavy chains (V_H) are amplified in the cDNA with appropriate primers. The V_H and V_L amplified DNA is then spliced together following splice overlap extension (SOE) PCR. The PCR product and a phagemid vector are then digested with a *Sfi*I enzyme and ligated together. The phagemid containing the scFv gene is then transformed into *E. coli* cells. Selection of specific phage is carried out by a process called "biopanning" described in detail in Figure 21.

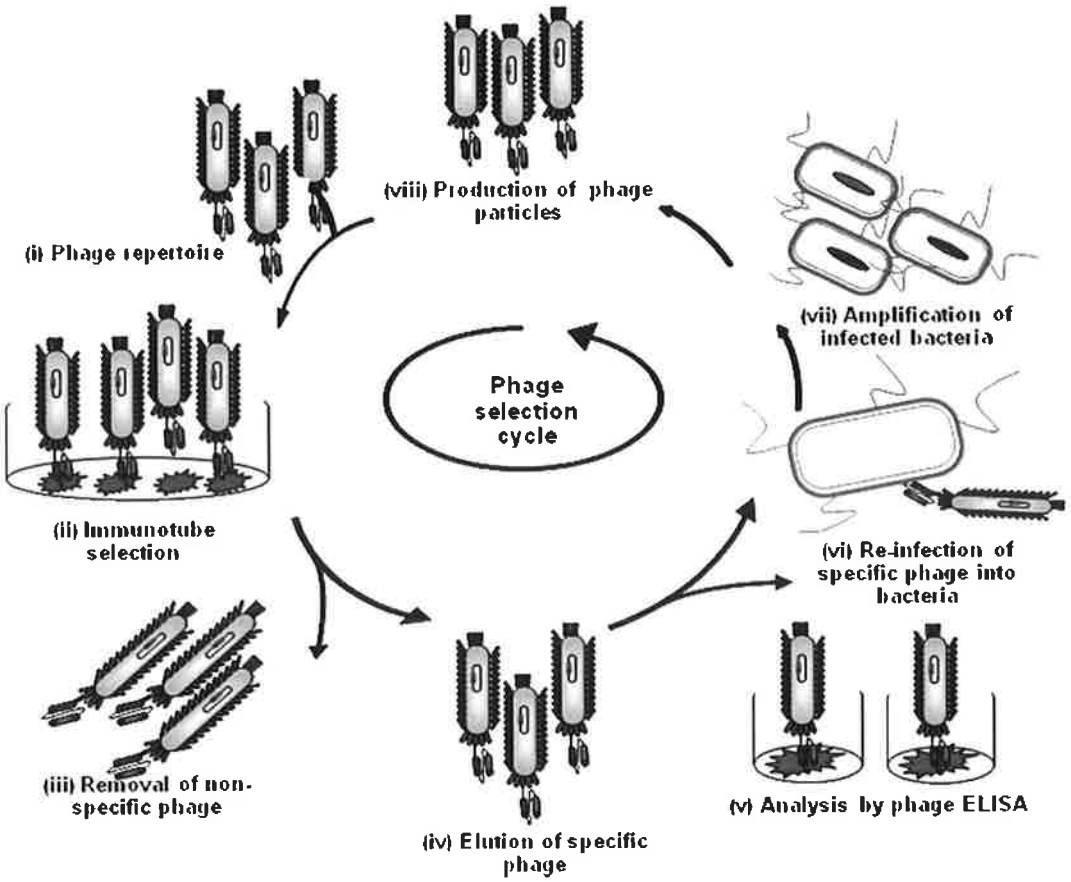

Figure 21: Individual phage particles displaying the scFv – pIII fusion proteins are selected by 'biopanning'

This process involves incubating the phage-scFv particle in an immunotube coated with the antigen and washing away non-specific phage particles. The antigen-specific phage particles are eluted and re-infected into *E. coli* cells for propagation and analysis in subsequent rounds of selection. The stringency is increased by decreasing the antigen concentration and increasing the washing steps to select high affinity recombinant antibody fragments. (Fitzgerald, 2007)

Antigen-specific antibody fragment enrichment is confirmed by analysing the phage pools from each round of selection ELISA. Individual clones are analysed, screened, sequenced and affinities determined.

1.4 Summary

Prostate cancer is a significant cause of illness and death in Irish males. Annual incidence of prostate cancer in Ireland is approximately 2,500 and the mortality rate is approximately 550 cases per annum. Statistics recently released from the National Cancer Registry in Ireland predict a 275% increase in incidence of the disease between 2000 and 2020 (www.ncri.ie).

Marked disease heterogeneity is associated with prostate cancer with some men progressing rapidly to metastatic disease whilst others may live relatively asymptomatically for many years. Current detection strategies do not reliably detect the disease at an early stage and cannot distinguish aggressive versus non-aggressive prostate cancer leading to over-treatment of the disease and associated morbidity. This indicates prostate cancer as an appropriate disease to pursue novel markers for disease detection and determining appropriate therapeutic strategies.

In October 2003, the Prostate Cancer Research Consortium (PCRC) was created with funding from the Irish Cancer Society. It is a multi-disciplinary, trans-institutional collaboration bringing together researchers from University College Dublin, Trinity College Dublin, Royal College of Surgeons in Ireland and Dublin City University. One of the PCRC's main aims is to identify novel cancer biomarkers which will permit early diagnosis of disease and provide critical information for stratification and clinical intervention using a comprehensive approach which involves utilizing genomic, transcriptomic and proteomic platforms and using a high-throughput biomarker validation approach.

1.5 Project Aim

The aims of the work presented in this thesis are to evaluate the tissue expression profile of potential markers of prostate cancer forwarded for tissue validation from the biomarker discovery projects within the PCRC. This involves:

- Constructing tissue microarrays (TMAs) from a range of Gleason grades of prostate cancer using the PCRC bioresources.
- Performing immunohistochemistry (IHC) on these TMAs with antibodies to potential markers discovered in biomarker discovery projects within the PCRC and assessing the protein's expression across the different tumour grades.
- In parallel with IHC, confirmatory gene analysis will be carried out on laser captured material from selected whole sections used in TMAs using quantitative PCR to ensure what is observed at a protein level corresponds to the gene level.
- And finally, generating, selecting and characterizing a recombinant antibody to a novel protein marker of prostate cancer progression discovered in the Ph.D. project using phage display technology.

Chapter 2 - Materials and Methods

2.1 Introduction

This chapter describes all the methodologies employed in this project, accompanied by background information on some of the techniques. Several techniques are used in a number of chapters. The full description of the technique is restricted to this chapter, with specifics for the histopathology analysis appearing in chapters 3 & 4.

2.2 Background Information

2.2.1 Key Histological Methods

2.2.1.1 Tissue Microarray (TMA) Technology

While new technologies have resulted in an exponential increase in the number of novel genes implicated in carcinogenesis, there has been extensive delay between identification of individual genes and their validation as clinically useful prognostic markers (Horvath and Henshall, 2001)(Kononen *et al.*, 1998). The laborious process required to assess gene expression using conventional methodologies such as immunohistochemistry on individual tissue sections is largely responsible for this bottleneck. TMA technology was developed to replace this one slide/one section approach and facilitate the rapid assessment of several molecular markers in hundreds of tumours (Horvath and Henshall, 2001). A TMA consists of paraffin blocks in which up to 1000 different tissue cores are assembled in an orderly fashion. Sections from this block are then sectioned and mounted on microscope slides to allow multiplex histological analysis.

The construction of a TMA is shown schematically in Figure 22(B). The essential idea is to identify the target area (areas of interest) on the donor paraffin block after Haematoxylin and Eosin (H&E) staining. Tissue cores ranging from 0.6 to 2 mm diameter are then sampled from the donor block

(target area) and arrayed into a recipient paraffin block. Up to 1000 specimens can be arrayed per recipient block, representing a number of different pathologies and tissue types, both benign and malignant (Horvath and Henshall, 2001). Therefore, TMAs make the analysis of histological samples easy by having all the information on a single slide.

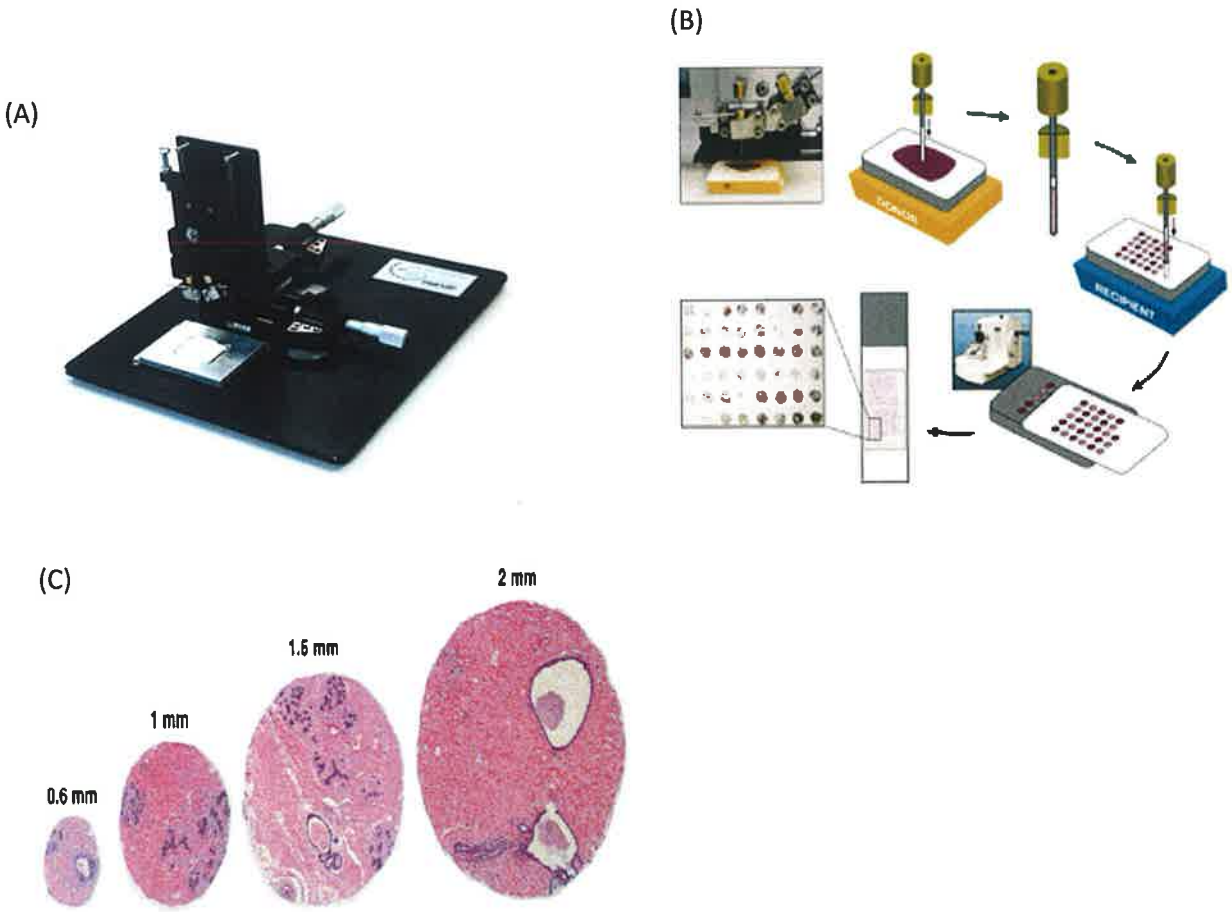

Figure 22: Pictorial representation of the tissue microarraying process

(A) Beecher Instrument Manual Tissue Arrayer

(B) Small tissue core biopsies are punched from selected regions of donor blocks using a 1mm donor pin. H&E stained sections overlaid on the surface of the donor blocks guide sampling. The tissue cores are then transferred to a readymade hole on the recipient block. 4 µm sections of the TMA are cut using a microtome and transferred to a glass slide. (Taken from (http://www.microarraystation.com/tissue-microarray/)

(C) Potential core needle sizes that can be used for tissue microarray construction

2.2.1.2 Laser Capture Microdisection (LCM)

Laser capture microdissection is a technique that permits the rapid and reliable procurement of pure populations of cells from tissue sections, in one step, under direct microscopic visualisation (Curran *et al.*, 2000). The basic principles of LCM are as follows;

A histological section is placed on the stage of a specialized microscope and a pathologist selects the target tissue area for extraction. A transparent ethylene vinyl acetate layer at the bottom of a LCM cap is apposed to the tissue section. A low power infrared laser beam is directed at the target cells. The film directly above the target area transiently melts and the long chain polymers in the film surround and tightly hold the cells which remain embedded in the film after removal from the section (Curran *et al.*, 2000).

(A)

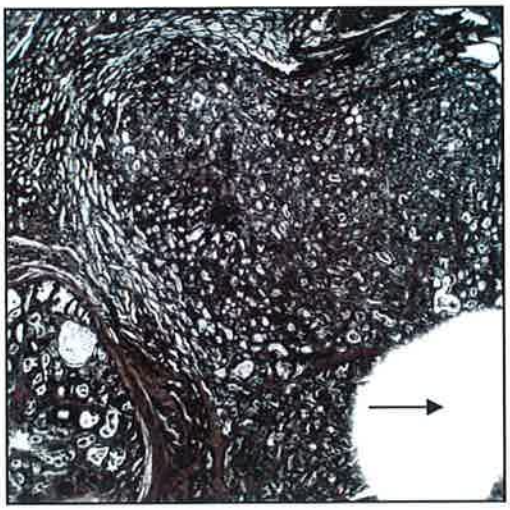

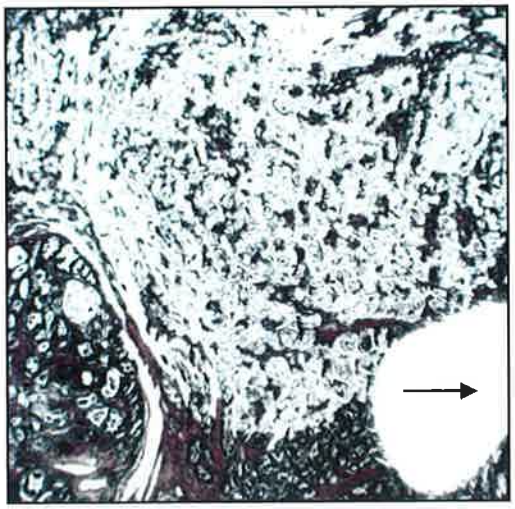

(B)

Figure 23: Laser capture microdissected section

(A) 7 µm prostate cancer whole section before laser capture microdisection

(B) 7 µm prostate cancer section after laser capture microdisection

*Arrow indicates where TMA core was taken

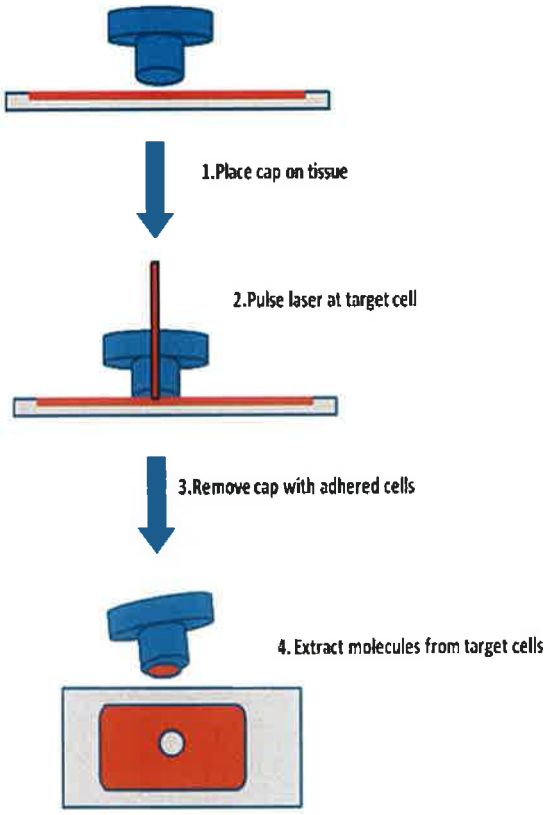

Figure 24: The laser capture microdissection process

2.2.1.3 Taqman® PCR

A TaqMan® PCR-based system was selected for mRNA quantitation in this study. This system was chosen for two reasons.

- Firstly Taqman® PCR and Reverse-Transcriptase (RT) PCR requires only a few nanograms of target DNA/RNA. This is highly significant since the amount of DNA/RNA extractable from formalin fixed and paraffin embedded (FFPE) archival material is low.

- Secondly, Taqman PCR and RT-PCR products are small (generally less than 200 bp) and thus can be used to amplify partially degraded or fragmented DNA/RNA such as that obtained from FFPE material.

Taqman® PCR exploits the 5´ nuclease activity of AmpliTaq Gold® DNA Polymerase to cleave a TaqMan probe during PCR. The TaqMan probe contains a reporter dye at the 5´ end of the probe and a quencher dye at the 3´ end of the probe. During the reaction, cleavage of the probe separates the reporter dye and the quencher dye, resulting in increased fluorescence of the reporter. Accumulation of PCR products is detected directly by monitoring the increase in fluorescence of the reporter dye.

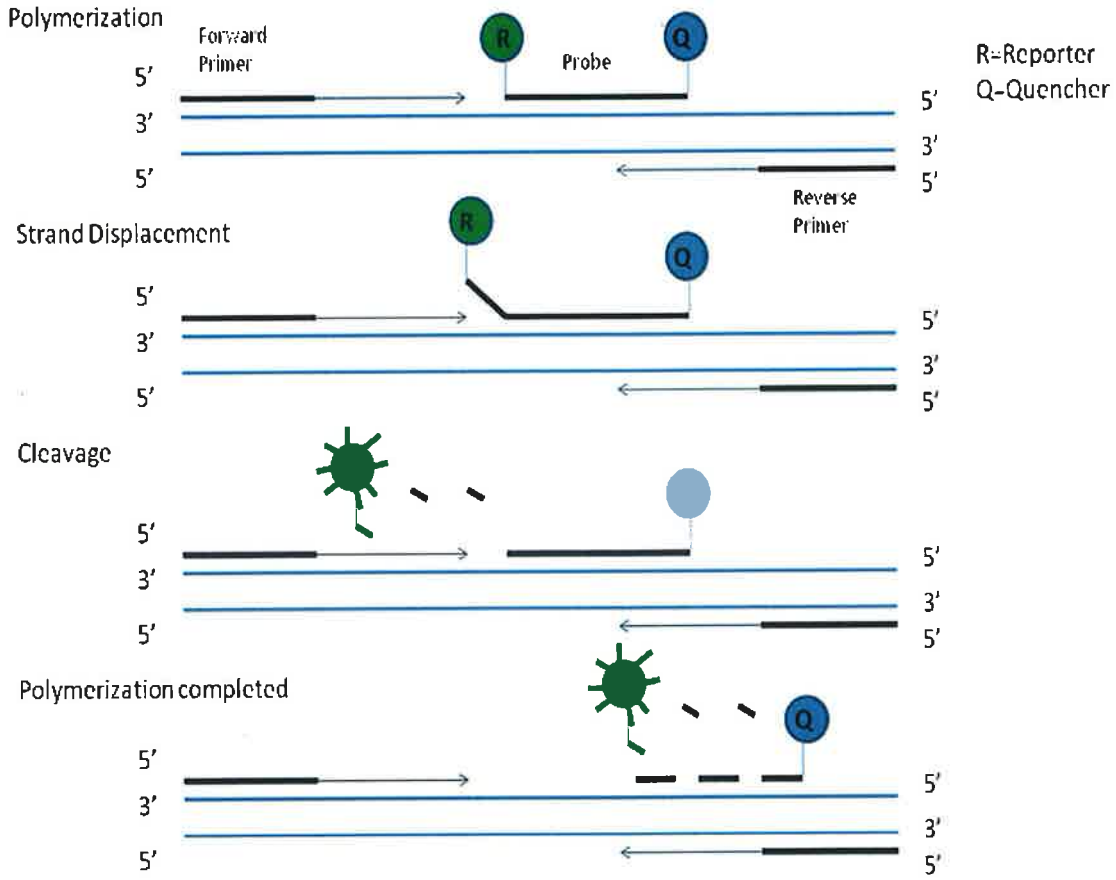

Figure 25: The forklike-structure-dependent, polymerisation-associated, 5´–3´ nuclease activity of AmpliTaq Gold DNA polymerase during PCR

When the probe is intact, suppression of the reporter fluorescence occurs due to the proximity of the reporter dye to the quencher dye. During PCR, the probe specifically anneals between the forward and reverse primer sites if the target of interest is present.

The 5´-3´ nucleolytic activity of the AmpliTaq Gold DNA Polymerase cleaves the probe between the reporter and the quencher only if the probe hybridises to the target. The probe fragments are then displaced from the target, and polymerisation of the strand continues. The 3´ end of the probe is blocked to prevent extension of the probe during PCR. This process occurs in every cycle and does not interfere with the exponential accumulation of product.

The probe consists of an oligonucleotide with a 5´-reporter dye and a 3´-quencher dye. A fluorescent reporter dye, such as FAM (6-carboxyfluorescein), is covalently linked to the 5´ end of the oligonucleotide. JOE (6-carboxy-4,5-dichloro-2,7-dimethoxyfluorescein), TET (6-carboxy-4,7,2´,7´-tetrachlorofluorescein) and VIC are also used as reporter dyes. Reporters are quenched by TAMRA (6-carboxy-N,N,N´,N´-tetramethylrhodamine) at the 3´ end in older Taqman® probes. Newer Taqman® MGB probes are recommended for genotyping/allelic discrimination (AD) purposes and when conventional probes exceed 30 bp. These MGB probes use a non-fluorescent quencher (NFQ) at the 3´ end.

2.2.1.4 Real-time quantitative Taqman® RT-PCR

Real-time RT-PCR is defined as the ability to monitor the progress of the PCR as it occurs in real time. Therefore rather than collecting data at the end of the PCR the data is collected throughout the PCR process. In real-time RT-PCR, reactions are characterised by the point in time during cycling when amplification of a target is first detected as opposed to the amount of target accumulated after a fixed number of cycles. The higher the starting copy number of the nucleic acid target, the sooner a significant increase in fluorescence is observed. An endpoint assay (also called a "plate read assay") measures the amount of accumulated PCR product at the end of the PCR cycle. RT-PCR can be one-step or two-step.

Little change in fluorescence signal is observed in the initial cycles of PCR. This defines the baseline for the amplification plot. The detection of accumulated target is indicated when an increase in fluorescence above the baseline occurs. A fixed fluorescence threshold can be set above the baseline. The parameter C_T (threshold cycle) is the fractional cycle number at which the fluorescence passes the fixed threshold.

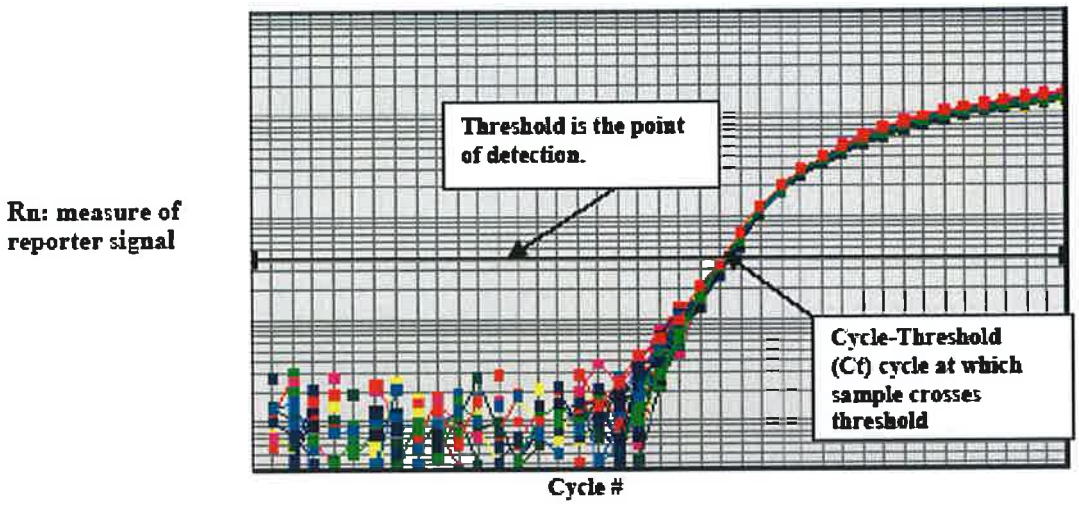

Figure 26: Example of an amplification plot

A sample of known concentration is used to construct a standard curve from which the quantity of an unknown sample can be extrapolated. The standards used depend on whether absolute or relative quantitation (RQ) is used.

In relative quantitation, quantity is expressed relative to a base sample, such as a calibrator. Quantity of all experimental samples are determined from the standard curve and divided by the quantity of the calibrator. Thus, the calibrator becomes the 1X sample and all other quantities are expressed as an n-fold difference relative to the calibrator.

Standard curves are prepared for both the target and the endogenous reference for quantitation normalized to an endogenous control. The amount of target and endogenous reference is determined from the appropriate standard curve for each experimental sample. The target amount is then divided by the endogenous reference amount to obtain a normalized target value. One of the experimental samples is the calibrator, or 1X sample. Each of the normalized target values is divided by the calibrator normalized target value to generate the relative expression levels (RQ values) (Livak and Schmittgen, 2001). For the quantitation of gene expression, researchers have

used β-actin, glyceraldehyde-3-phosphate dehydrogenase (GAPDH), ribosomal RNA (rRNA), or other RNAs as an endogenous control.

2.2.2 Key Antigen Production Methods

2.2.2.1 Bacterial expression systems

Unlike small molecules, which can typically be synthesized by chemical means, most proteins are sufficiently complex to necessitate their production in living systems (Gerngross, 2004). These complex proteins can be synthesised in expression hosts, typically bacteria, yeast or fungi. The choice of recombinant expression hosts usually depend on: (i) the cost of manufacturing and purification (ii) the ability to control the final product including its post-translational processing (iii) the time required from gene to purified protein (iv) the regulatory path to approve a drug/protein produced on a given expression platform and (v) the overall royalties associated with the production of a recombinant product in a given host. In general, the choice of protein expression system is not necessarily based on the ease of initial production but by the ultimate use of the product (Gerngross, 2004).

The use of bacterial expression systems has proven to be powerful in terms of the successful production of various mammalian proteins (Larsson *et al.*, 1996). These systems involve cloning a target gene fused to the gene encoding the affinity tag into an expression vector. This vector is then transformed into bacterial cells which express the fusion protein (see Figure 27). Finally the gene product is affinity purified. This method of bacterial expression of gene products constitutes a strategy that has been used extensively in different fields of research (Larsson *et al.*, 1996) and is a very popular technique employed by antibody companies to generate immunogens for antibody production.

Escherichia coli (*E. coli*) is usually the principal bacterium of choice for cloning genes and recombinant proteins (Billman-Jacobe, 1996). It is a popular host for heterologous gene expression as it is well characterised, many of its biological processes are understood and there are many genetic tools readily

available for its manipulation (Billman-Jacobe, 1996). However, *E. coli* is unlikely to be suitable for every application and the choice of host bacteria is primarily influenced by the required application. Many bacteria may function as alternative hosts to *E. coli* but the availability of tools for their genetic manipulation generally determines the extent of their utilization (Billman-Jacobe, 1996). Regardless of approach, *E. coli* remains the expression host of choice due to its advantages of high growth and production rates, ease of use, cheapness and widespread availability (Hammarstrom *et al.*, 2002). However, there are disadvantages associated with using *E. coli* as an expression host such as difficulties in expression of eukaryotic proteins, most post-translational modifications are absent, and the product is often generated in the form of inclusion bodies (Hammarstrom *et al.*, 2002). When selecting an affinity system choosing an affinity tag with a high affinity for specific ligand is desired as the affinity tag should allow affinity purification in buffers containing chaotrophic agents such as guanidine hydrochloride or urea, used for solubization of proteins precipitated in inclusion bodies (Larsson *et al.*, 1996). The affinity tags should also be resistant to proteolysis. A commonly used strategy to increase solubility of a protein is to fuse the protein to another protein that is known to have high solubility. There are several fusion proteins/affinity tags that have been shown to increase solubility in *E. coli* such as glutathione-S-transferase (GST), the maltose binding protein (MBP) and the Z-domain from protein A (Hammarstrom *et al.*, 2002).

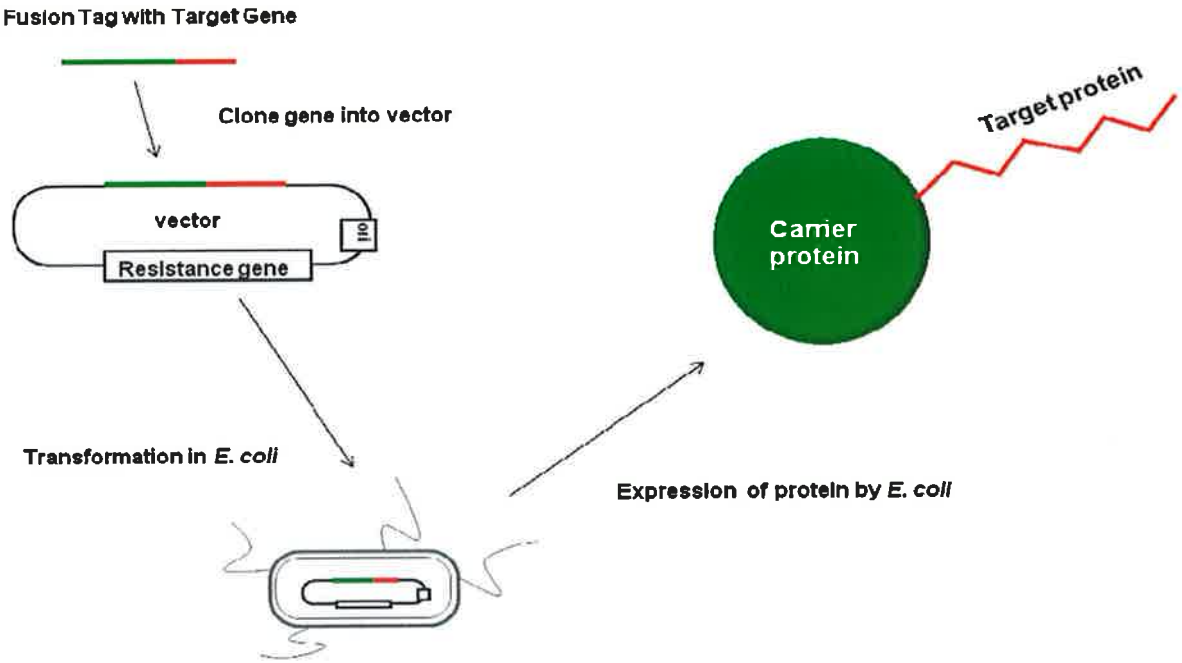

Figure 27: Basic bacterial expression systems

The target gene sequence which is conjugated to a fusion tag is cloned into a vector. The vector is transformed into *E. coli*. *E. coli* express the fusion protein (carrier protein fused to target protein) and following lysisof the bacteria, the protein is affinity purified from bacterial lysate.

2.2.2.2 "Cell-free" translation

The development of "cell-free" translation has become an important tool in biotechnology by playing a central role in a wide variety of applications (Katzen *et al.*, 2005). *In vitro* translation systems are based on the early revelation that cell integrity is not essential for protein synthesis to occur (Katzen *et al.*, 2005). Translation can be achieved using crude lysate from any given organism (that provides the translational machinery, accessory enzymes, tRNA and transcription factors) in combination with exogenously added RNA template, amino acids and an energy supply (Katzen *et al.*, 2005). "Cell-free" systems for *in vitro* gene expression and protein synthesis have been demonstrated for both prokaryotic and eukaryotic systems. These "cell-free" systems are based on crude cell extract derived from either rabbit reticulocytes or wheat germ (eukaryotic systems) or *E. coli* (prokaryotic system). The choice of the system should be determined by the biochemical nature and origin of the protein and the specifics of the downstream application. *E. coli*-based systems provide higher yields and more-homogeneous samples suitable for structural studies (Katzen *et al.*, 2005).

There are several advantages to "cell-free" protein synthesis over traditional cell-based expression methods. The main advantage of "cell-free" protein synthesis is that it is an extremely fast way to obtain an expressed phenotype (protein) from a genotype (gene) compared to protein production in living cells. This method of translation is independent of the host cell, such as *E. coli*; therefore proteins which are toxic or prone to proteolytic degradation can be readily prepared *in vitro*. Moreover, inclusion body formation is not an issue with "cell-free" expression. Other advantages include the ease of modification of reaction conditions to favour protein folding and decreased sensitivity and improvements in translation efficiency have resulted in yields that exceed a milligram of protein per millilitre of reaction mix (Katzen *et al.*, 2005). However, the cell extract system has been described as a "black box" where numerous uncharacterised activities may modify or interfere with subsequent downstream assays. Such activities include rapid depletion of energy charge independent of peptide bond formation and degradation of

protein products or template nucleic acids by proteases or nucleases (Shimizu *et al.*, 2001).

In 2001, Shimizu *et al.* (2001) accomplished the first *in vitro* reconstitution of protein translation from *E. coli.* This alternative "cell-free" protein synthesis approach reconstitutes protein synthesis from purified recombinant components of the translation machinery in *E. coli* (Shimizu *et al.*, 2001). Except for the purified *E. coli* ribosomes and tRNAs, all the factors for translation are tagged with a hexahistidine (His-tagged) ensuring that no unknown components are present within the reaction and allowing the synthesized protein to be easily purified by removal of the His-tagged factors and ribosomes using metal affinity resin and ultrafiltration membrane, respectively. This also ensures that no unexpected effects of tags such as misfolding or aggregation will arise. This "cell-free" system is known as the "PURE" (Protein synthesis Using Recombinant Elements) system and commercialized as the PURESYSTEM® by the Post Genome Institute (PGI) (Tokyo, Japan). An overview of this technique is illustrated in Figure 28.

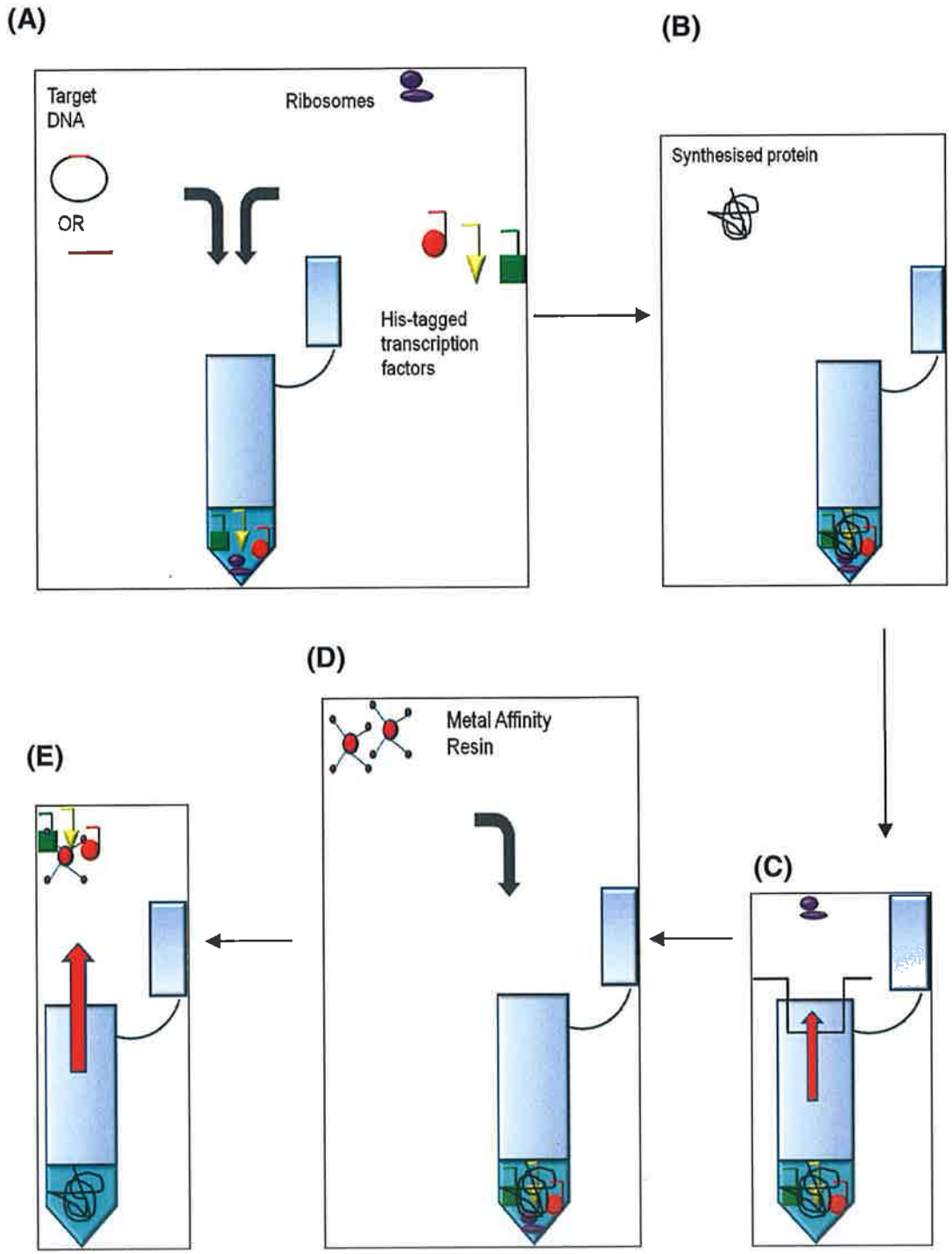

Figure 28: PURESYSTEM® Cell-free translation (*in vitro* expression)

(A) Addition of DNA template and His-tagged translation factors and ribosomes

(B) Protein synthesis

(C) Ribosomes are removed by ultrafiltration using a membrane with a cut-off of 100kDa

(D) All histidine-tagged components are eliminated by passage through a Ni^{2+} column

(E) Translation product (purified protein) isolated in PCR tube

2.3. Materials

All reagents were purchased from Sigma-Aldrich Co., Poole, Dorset, England except where otherwise stated below.

Table 6: Materials and Suppliers

Reagent	Supplier
DNA ligase Restriction enzymes	New England Biolabs, Wilbury Way, Hitchin, Hertfordshire, SG4 0TY, UK.
PCR primers	Integrated DNA Technologies, Interleuvenlaan, 12A B-3001 Leuven Belgium.
Nulceospin Extract II	Macherey-Nagel GmbH & Co. KG, Neumann-Neander-Str. 6-8, 52355 Düren, Germany.
PURESYSTEM® Kit PURE2004C	Cosmo, bio Co. Ltd, Toyo 2Chome, koto-ku, Tokyo, 135-0016, Japan.
PAGE Ruler	Fermentas UK, Sheriff House, Sheriff Hutton Industrial Park, York Y060 6RZ, UK.
IMAC Resin	Novagen® affiliated with Merck KGaA, Frankfurter Straße 250, 64293 Darmstadt, Germany.
GST Purification kit	GenScript USA Inc., 860 Centennial Ave. Piscataway, NJ 08854, USA.
RecoverAll™ Total Nucleic Acid Isolation Kit	Ambion Inc., 2130 Woodward St Ste 200, Austin, TX, USA.

cDNA Archive kit Taqman PreAmp Master Mix kit	Applied Biosystems, 850 Lincoln Centre Drive, Foster City, CA 94404, USA.
Polymer detection kit-BondMax™	Leica Microsystems, Balliol Business Park West Benton Lane, Newcastle Upon Tyne NE12 8EW, UK.

Table 7: Antibodies/Antigen and suppliers

Antibody	Supplier
Rabbit anti-SFRP-2 pAb Rabbit anti-KNG-1 pAb SFRP-2-ABP Antigen (Kindly donated by Atlas Antibodies)	Atlas Antibodies AB, AlbaNova University Center, SE-106 91 Stockholm Sweden. (in Partnership with Prestige® Antibodies)
Chicken anti-hFABP (scFv)	Kindly donated by Dr. Vijayalakshmi Ayyar (Applied Biochemistry Group, School of Biotechnology, Dublin City University, Ireland.)
Mouse anti-cTnI (HRP-labelled)	HyTest Ltd, Joukahaisenkatu 6, 20520, Turku, Finland.
Mouse anti-PSMB-6 mAb	Abcam PLC, 204 & 330 Cambridge Science Park, Cambridge, CB4 0FW, UK.
Mouse anti-ZAG mAb	Santa Cruz Biotechnology Inc., 2145 Delaware Avenue, Santa Cruz, CA. 95060 USA.

Rat Anti-HA (HRP- labelled)	Roche Applied Sciences, 9115 Hague Road, Bldg. B, IN 46250, USA.
Mouse Anti-His (HRP labelled) mAb Rabbit Anti-GST (HRP-labelled) pAb HRP-labelled anti-rabbit pAb HRP-labelled anti-chicken	Sigma Aldrich, Co., Poole, Dorset, UK.

Table 8: Culture media formulation

Media	Ingredients
Luria Broth (LB)	Tryptone 10 g/L Yeast Extract 5 g/L NaCl 5 g/L
Terrific Broth	Tryptone 12 g/L Yeast Extract 24 g/L Glycerol 4 mL KH_2PO_4 2.31 g/L (0.017M) K_2HPO_4 12.54 g/L (0.072M)

2.3.1 Buffer composition

2.3.1.1 Phosphate buffered saline (PBS) (150 mM, pH 7.4)

0.15 M NaCl

2.5 mM KCl

10 mM Na_2HPO_4

18 mM KH_2PO_4

Reagents were dissolved in 800 mL ultra pure H_2O, pH was adjusted to 7.4 and volume made up to 1 litre with ultra pure H_2O.

2.3.1.2 PBS-Tween (PBST)

Tween 20 detergent (Sigma) was added to PBS to give a final concentration of 0.05% (v/v).

2.3.1.3 Tris Buffered Saline (TBST)

0.05 M Tris

0.15 M NaCl

The Tris and NaCl were dissolved in 800 mL ultra pure H_2O. The pH was adjusted to 7.6 using NaOH and made up to 1 L with ultrapure H_2O.

2.3.1.4 TBS-Tween (PBST)

Tween 20 detergent (Sigma) was added to TBS to give a final concentration of 0.05% (v/v).

2.3.1.5 Tris-acetic acid-EDTA buffer (TAE) (400 mM, pH 8.3)

A 10X stock (100mL) solution of TAE buffer, supplied by Sigma, was diluted to 1 L with ultra pure H_2O. All agarose gels for DNA visualisation were prepared and resolved in 1X TAE buffer.

2.3.1.6 SDS Gels

12.5% (w/v) Separation gel	**1gel/6 mL**
1 M TrisHCl, pH 8.8	1.500 mL
30% (w/v) acrylamide (Acrylagel)	2.500 mL
2% (w/v) methylamine bisacrylamide (Bis-Acrylagel)	1.000 mL
Water	0.934 mL
10% (w/v) sodium dodecyl sulfate (SDS)	0.030 mL
10% (w/v) APS	0.030 mL
TEMED	0.006 mL

4.5% (w/v) Stacking gel	**1gel/2.5 mL**
1 M TrisHCl, pH 6.8	0.300 mL
30% (w/v) acrylamide (Acrylagel)	0.375 mL
2% (w/v) methylamine bisacrylamide (Bis-Acrylagel)	0.150 mL
Water	1.740 mL
10% (w/v) SDS	0.024 mL
10% (w/v) APS	0.024 mL
TEMED	0.0025 mL

2.3.1.7 (10X) electrophoresis buffer

50 mM Tris pH, 8.3	30 g
196 mM Glycine	144 g
0.1% (w/v) SDS	10 g
dH_2O to 1 L	

2.3.1.8 Loading buffer (4X)

Tris 0.5 M, pH 6.8	2.5 mL
Glycerol	2.0 mL
2 mercaptoethanol	0.5 mL
20% (w/v) SDS	2.5 mL
Bromophenol blue	20 ppm
dH_2O	2.5 mL
Final Volume of 10 mL	

2.3.1.9 Coomassie stain dye/ 500mLs

Coomassie blue R-250	1 g
Methanol	225 mL
dH_2O	225 mL
Acetic acid	50 mL

2.3.1.10 Coomassie destain/L

Acetic acid	250 mL
Methanol	250 mL
Water	650 mL

2.3.1.11 Transfer Buffer

80% (1X) Electrophoresis buffer	400 mL
20% (v/v) Methanol	100 mL

2.3.2 Bacterial strains used

All bacterial strains cultured and expressed in different nutrient broth solutions are listed in Table 9.

Table 9: Bacterial strains

Bacterial Strain	Supplier and Strain Properties
E. coli Tuner(DE3) cells	Novagen – Merck F^- *ompT hsdS*$_B$ ($r_B^- m_B^-$) *gal dcm lacY1*
E. coli BL-21(DE3) cells	Novagen – Merck F^- *ompT hsdS*$_B$ ($r_B^- m_B^-$) *gal dcm lacY1(DE3)plysS* (*Cam*^{R})
E. coli BLR(DE3) cells	Novagen – Merck F^- *ompT hsdS*$_B$ ($r_B^- m_B^-$) *gal dcm lac ile (DE3)Δ(srl-recA)306::Tn10(Tet*^{R})
E. coli Nova Blue(DE3) cells	Novagen – Merck F^- *ompT hsdS*$_B$ ($r_B^- m_B^-$) *gal dcm lacY1*
E. coli HMS(DE3)174	Novagen – Merck F^- *recA1 hsdR*($r_{K12}^- m_{K12}$(*Rif*^{R})

2.3.3 Equipment list

Table 10: Equipment list

Equipment	Supplier
Tissue-Arrayer™	Beecher Instruments, Silver Spring, MD, USA.
Nikon Eclipse E400 Microscope Nikon DXM 1200 digital camera	Nikon Instruments Inc., Melville, NY 11747-3064, USA.
Leica Bond-Max™ automated Immunohistochemistry Instrument Rotary Microtome	Leica Microsystems, Newcastle Upon Tyne NE12 8EW, UK.
Arcturus Pixcell II® System	Acturus Engineering Inc., Mountain View, CA, USA.
ABI Prism® 7000 sequence detection system	Applied Biosystems, Foster City, CA 94404, USA.
Balances (Chyo JK-180) (Mettler PJ300)	Medical Supply Company Ltd, Damastown, Mulhuddart, Dublin 15, Ireland.

PX2 thermal cycler	Thermo Electron Corporation, Waltham, MA 02454,USA.
Blood tube rotator SB1	Stuart Scientific, Beacon Road, Stone, Staffordshire, ST15 0SA, UK.
HermLe Z233MK-2 refrigerated centrifuge	HermLe Labortechnik GmbH, Wehingen, 78564, Germany.
ND-1000 Spectrophotometer (Nanodrop)	A,btech International Ltd, Acorn House, The Broyle, Ringmer, East Sussex, BN8 5NN, UK.
Tomy Autoclave (SX-700E High Pressure Steam Sterilizer)	Tomy Digital Biology, Ikenohata Taito-ku, Tokyo, Japan.
Tecan Saffire 2 Plate reader	Tecan Austria GmbH, Untersbergstrasse, 5082 Grödig, Austria.
Water bath (Y6 model)	Grant instruments (Cambridge) Ltd, Shepreth, Royston, Herts., SG8 6PZ, UK.
SDS Bio-Rad Min-Protean® 3 Cell Trans-Blot®SD Semi-Dry Transfer cell Bio-Rad Powerpac Basic	Bio-Rad Laboratories, 2000 Alfred Nobel Drive, Hercules, CA 94547, USA.
Vibra Cell™ sonicator	Sonics and Materials Inc., Newtown, CT 06470-1614, USA.

2.4 Histological Materials and Methods

2.4.1 Sample Collection

Prostate cancer cases were obtained from Beaumont Hospital, St James's Hospital and the Mater Misericordiae University Hospital Histopathology archives dating from 2002 - 2008.

Ethics approval was granted from all participating hospitals. The PCRC BIMS (Biobank Information Management Systems) is a database which consists of a central Biobank data repository for the perpetual storage and easy retrieval of anonymous clinical information on patients along with information on their biosamples within the PCRC. This system was also searched for appropriate cases to include in the study.

All tissue samples were routinely fixed and processed to paraffin wax. The reports on all cases were reviewed and superficial sections were cut and stained with haematoxylin and eosin to confirm the diagnosis.

The cases chosen to include in the study consisted of a variety of Gleason scores ranging from 5 to 10. Suitable formalin fixed paraffin embedded blocks of each case representing as many Gleason grades as possible were selected. The corresponding Haematoxylin and Eosin (H&E) stained sections were reviewed by a pathologist to select for appropriate cases to include in tissue microarray construction.

2.4.2 Tissue Microarray (TMA) Construction

Three 1 mm diameter cores of benign prostatic hyperplasia (BPH) and Gleason grade 3, 4 and 5 carcinoma were taken from every case where available. The tissue microarrays were assembled using the Beecher Instruments Tissue-Arrayer^{TM} (Beecher Instruments, Silver Spring, MD) Figure 22(A).

2.4.3 Immunohistochemical Analysis

A detailed overview of the principles of immunohistochemistry is described in section 1.2.3.

Deparaffinization, antigen retrieval and immunohistochemistry were performed on the paraffin-embedded 4 μm tissue microarray sections on an automated IHC platform (Bond Max^{TM} - Leica Microsystems). A polymer-based detection system was used with 3, 3' Diaminobenzidine (DAB) as the chromogen resulting in a brown end colour. The optimal antigen retrieval and optimal concentrations of primary antibody were determined by serial dilution and serial antigen retrieval methods optimising for maximal signal without background immunostaining using the appropriate positive controls. Negative controls included exclusion of the primary antibody and replacement with a non-immune mouse antibody of identical isotype. Sections were counterstained with haematoxylin.

The immunohistochemical reactivity of the proteins was scored in a blinded fashion with regard to histological diagnosis by a two independent observers. Cores that had less than 10% prostatic epithelium were excluded. Immunoreactivity of the proteins was assessed in benign prostatic hyperplastic epithelium and tumour epithelium across all Gleason grades.

2.4.4 Statistical Methods

Chi square tests were performed on contingency tables using GraphPad INSTAT-3^{TM} software version 3.02 (Graph Pad Software Inc, San Diego, USA).

2.4.5 Validation of Immunohistochemical results

To validate the IHC results, LCM and Taqman PCR were carried out on selected prostate cancer cases used in IHC analysis to confirm mRNA expression. Seven micrometer whole sections were mounted on uncharged slides, dewaxed and H&E stained. Pure cell populations from areas of BPH, Gleason grade 3, 4 and 5 were laser capture microdissected (PixCell II® System (Acturus Engineering Inc., CA)) according to a standard protocol: laser spot size = 30 μm, pulse power = 40 mW, pulse width = 1.5 ms, threshold voltage = 285 MV.

Total RNA was extracted from the captured cells using the RecoverAll™ Total Nucleic Acid Isolation Kit (Ambion Inc, Austin, TX) according to manufacturer's instructions and quantified using a Nanodrop® ND-1000. Using a high capacity cDNA Archive Kit (Applied Biosystems, Foster City, CA), RNA was reverse transcribed to single-stranded cDNA in 25 μL reactions. An Applied Biosystems TaqMan® PreAmp Master Mix Kit was used to increase the quantity of cDNA for the gene expression study.

TaqMan gene expression assays were performed on the ABI Prism® 7000 sequence detection system using the following cycles; 2 min at 50°C, 10 min at 95°C and 40 cycles each at 95°C for 15 sec and 60°C for 1 min. The $2^{-\Delta\Delta C}{}_T$ method was used for analysis of the relative gene expression data with cyclin dependent kinase inhibitor 1 B (CDKN1B) as the endogenous control assay. Box plots of the fold increase or decrease of gene expression from the calibrator sample (BPH sample 1) were plotted for the usable data using SPSS 15.0 for Windows®.

2.5 Antigen & Antibody Production Materials and Methods

2.5.1 Antibody & Antigen Production Methods

2.5.1.1 E. coli Expression Systems

2.5.1.1.1 Vector Design

2.5.1.1.1.1 pGS-21a Vector

An optimised DNA sequence corresponding to amino acids 165-295 on the human SFRP-2 protein was cloned into a pGS-21a vector using the *Nco I* and *Hind III* restriction sites by Genscript USA Inc (USA). This is the most immunogenic proportion of the SFRP-2 gene and was successfully used by Atlas antibodies to produce their fusion protein which generated their SFRP-2 polyclonal antibody.

A wide variety of factors can regulate and influence gene expression levels in *E. coli*, including synonymous codon bias. Synonymous codon bias refers to differences in the frequency of occurrence of synonymous codons in coding DNA. Different organisms can demonstrate particular preferences for one of the several codons that encode the same amino acid. In fast growing organisms such as *E. coli* it is thought that the codon preference reflects the composition of their tRNA pool and help to achieve faster translation rates and high accuracy.

The native DNA sequence of the SFRP-2 gene employs tandem rare codons that can reduce the efficiency of translation or even disengage the translational machinery due to synonymous codon bias in *E. coli.* Codon optimisation was performed using Genscript software for the SFRP-2 gene to allow for synonymous codon bias in *E. coli* to improve translation efficiency (see optimized gene sequence following).

Original SFRP-2 gene

5'ATGGCCACCGAGGAAGCTCCAAAGGTATGTGAAGCCTGCAAAAATAAA
AATGATGATGACAACGACATAATGGAAACGCTTTGTAAAAATGATTTTGC
ACTGAAAATAAAAGTGAAGGAGATAACCTACATCAACCGAGATACCAAAA
TCATCCTGGAGACCAAGAGCAAGACCATTTACAAGCTGAACGGTGTGTC
CGAAAGGGACCTGAAGAAATCGGTGCTGTGGCTCAAAGACAGCTTGCAG
TGCACCTGTGAGGAGATGAACGACATCAACGCGCCCTATCTGGTCATGG
GACAGAAACAGGGTGGGGAGCTGGTGATCACCTCGGTGAAGCGGTGGC
AGAAGGGGCAGAGAGAG3'

Optimized SFRP-2 gene cloned into PGS21a vector (Codon changes shown in red)

5'ATGGCGACCGAAGAAGCCCCGAAAGTTTGCGAAGCATGTAAAAACAAA
AACGATGACGATAACGACATTATGGAAACGCTGTGCAAAAACGATTTCGC
TCTGAAAATCAAAGTCAAAGAAATCACCTACATCAACCGTGACACGAAAA
TTATCCTGGAAACCAAATCCAAAACGATTTACAAACTGAATGGCGTCAGC
GAACGCGACCTGAAAAAATCTGTGCTGTGGCTGAAAGATAGTCTGCAGT
GCACCTGTGAAGAAATGAACGATATTAATGCCCCGTATCTGGTGATGGG
CCAGAAACAAGGCGGTGAACTGGTGATCACGAGCGTTAAACGTTGGCAG
AAAGGTCAACGCGAA3'

The pGS-21a vector consists of a T7 promoter, lac operator, His-tag, GST-tag, enterokinase, restriction sites including *Nco I* and *Hind III* restriction sites and a T7 terminator, as shown in Figure 29.

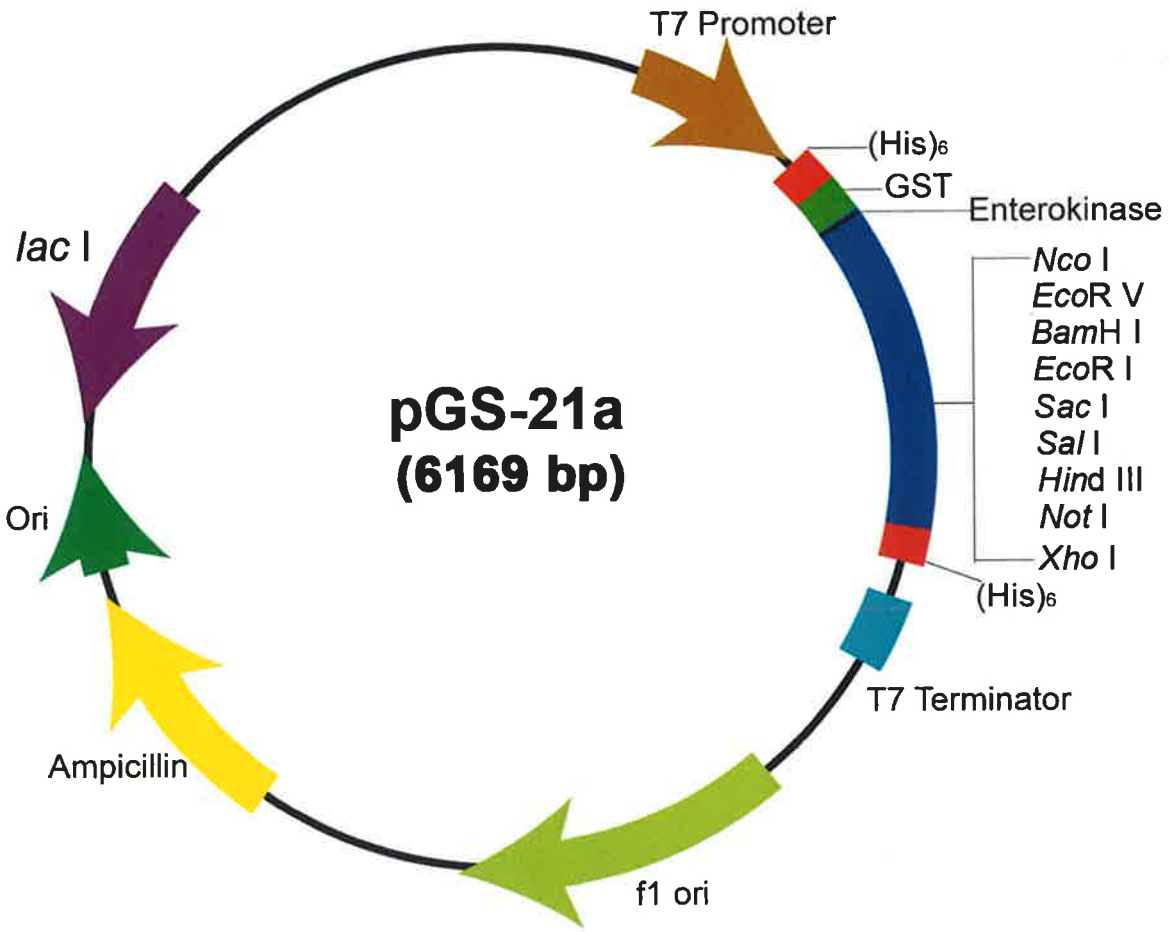

Figure 29: Map of pGS-21a vector (Genscript USA Inc. (USA))

The pGS-21a vector map designed by Genscript USA Inc. (USA). The map locates the T7 promoter, the lac operator, 2 His-tags, the GST-tag, enterokinase, the T7 terminator and the restriction sites including *Nco I* and *Hind III*.

2.5.1.1.1.2 pUC57 Vector

The optimised DNA sequence corresponding to amino acids 165-295 on the human SFRP-2 protein, including the *Nco I* and *Hind III* restriction site (detailed in section 2.5.1.1.1.1), was cloned into a pUC57 vector using *EcoRV* restriction enzyme by Genscript USA Inc (USA) (see Figure 30).

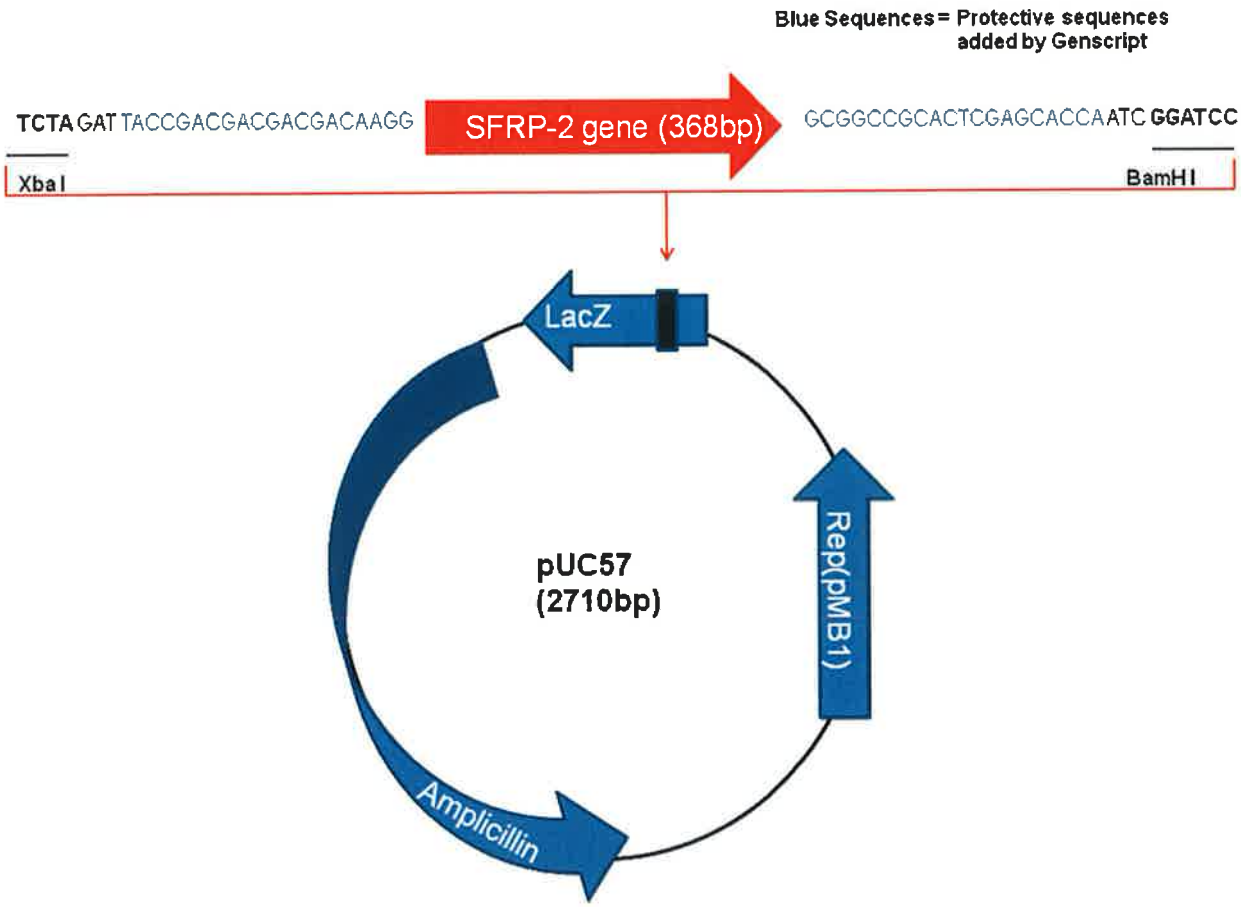

Figure 30: Map of Puc57 vector (designed and produced by Genscript USA Inc (USA))

The Puc57 vector map designed by Genscript USA Inc. (USA). The map locates where the optimised DNA sequence corresponding to amino acids 165-295 on the human SFRP-2 protein was cloned into the Puc57 vector. The map also locates the pMB 1 replication origin, the amplicillin resistant gene and the lac Z gene.

2.5.1.1.1.3 pET-28b(+)-hFABP Vector

For the purpose of this study, purified plasmid containing an unrelated peptide sequence (cTnI) in a pET-28b(+) backbone was prepared by Mr. Paul Conroy. This novel fusion construct was designed by Dr. Stephen Hearty.

The gene that was cloned into a pET-28b(+) by Genscript consisted of a *Nco I* restriction site, hFABP gene sequence, a *BamH I* restriction site, a linker DNA

sequence, a *Sac* I restriction site, a cTnI gene sequence and a *Not* I restriction site. The gene was cloned into the pET-28b(+) vector using the *Nco I* and *Not* I restriction sites

CC*ATGG*TGGACGCTTTCCTGGGCACCTGGAAGCTAGTGGACAGCAAGA
ATTTCGATGACTACATGAAGTCACTCGGTGTGGGTTTTGCTACCAGGCAG
GTGGCCAGCATGACCAAGCCTACCACAATCATCGAAAAGAATGGGGACA
TTCTCACCCTAAAAACACACAGCACCTTCAAGAACACAGAGATCAGCTTT
AAGTTGGGGGTGGAGTTCGATGAGACAACAGCAGATGACAGGAAGGTC
AAGTCCATTGTGACACTGGATGGAGGGAAACTTGTTCACCTGCAGAAAT
GGGACGGGCAAGAGACCACACTTGTGCGGGAGCTAATTGATGGAAAACT
CATCCTGACACTCACCCACGGCACTGCAGTTTGCACTCGCACTTATGAG
*AAAGAG****GGATCC****GGTGGTTCCTCTAGATCTTCCTCCTCTGGTGGCGGTG*
GCTCGGGCGGTGGTGGG***GAGCTC***AACTATCGCGCGTATGCGACCGAAC
CGCATGCGAAAAAAAAAAGCAAAATTAGCGCGAGCCGCAAACTGCAGCT
GAAAACC***GCGGCCGC***

Figure 31: Gene sequence of the pET-28b(+) vector that contained the cTnI sequence

The novel gene construct contained a gene sequence that corresponded to a hFABP DNA sequence (blue text), a cTnI peptide DNA sequence (red text), a linder DNA sequence (non-bold/italics/underlined black text) and restriction sites (bold, italics and underlined black text (***CCATGG*** = *Nco* I, ***GGATCC*** = *Bam*H I, ***GAGCTC*** = *Sac* I *and* ***GCGGCCGC*** = *Not* I)).

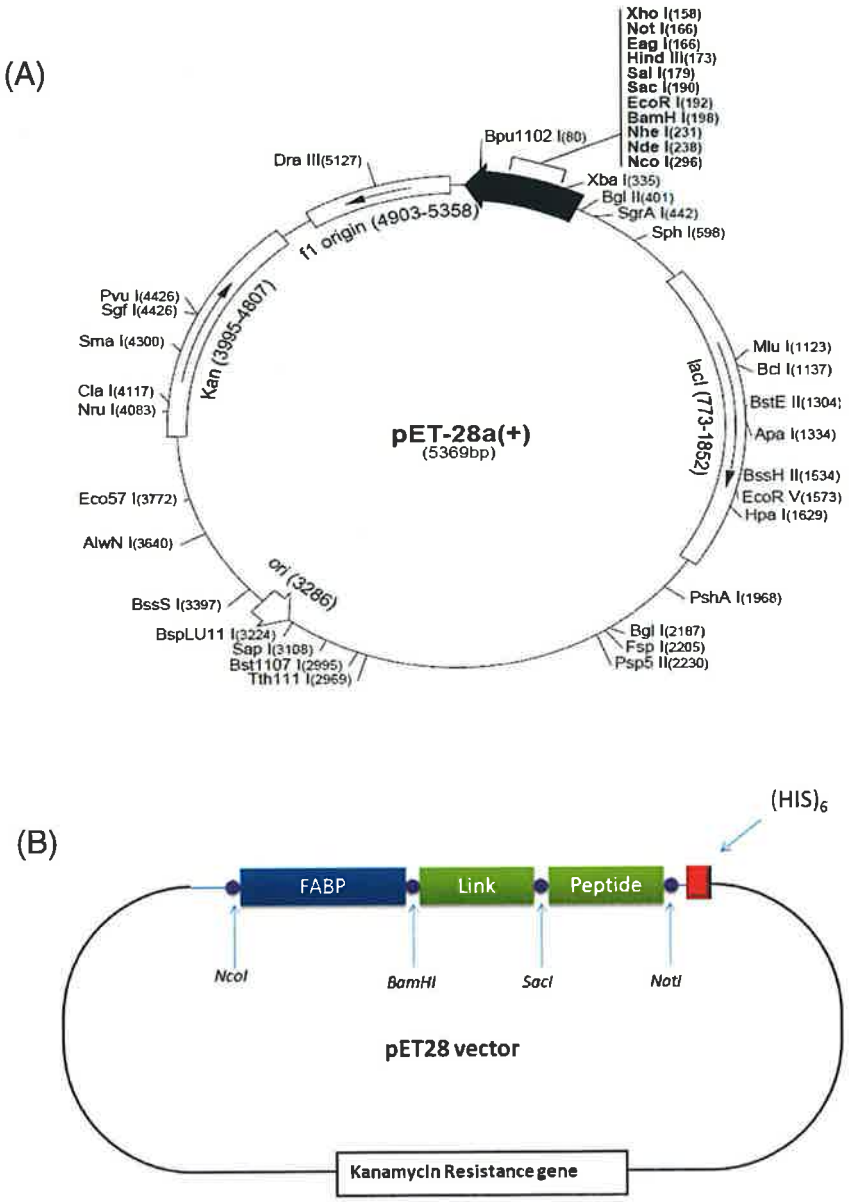

Figure 32: pET-28b(+)-hFABP vector

(A): **Map of pET-28a(+)vector (Merck KGaA, Darmstadt, Germany):**

The maps for pET-28b(+) is the same as pET-28a(+) with the following exception; pET-28b(+) is a 5368bp plasmid; subtract 1bp from each site beyond *Bam*H I at 198. The pET-28b(+) vector carries an N-terminal His-Tag, thrombin and a T7-Tag configuration. Unique sites are shown on the vector map. The cloning region of the coding strand transcribed by T7 RNA polymerase is reversed on the circular map. The f1 origin is oriented so that infection with helper phage will produce virions containing single-stranded DNA that corresponds to the coding strand.

(B): **Map of pET-28b(+)-hFABP vector:**

The map locates the hFABP gene, the linker sequence, the peptide sequence (cTnI), the His-Tag, the kanamycin resistant gene and the restriction sites (*Nco* I, *Bam*H I, *Sac* I and *Not* I) on the pET28(+) vector.

2.5.1.1.2 PCR primers for SFRP-2 amplification

The primers listed below were designed to amplify the optimized SFRP-2 gene cloned into the pUC57 vector, as described in section 2.5.1.1.1.2.

Primers:

Sense Primer for optimized SFRP-2 gene amplification:

5'GAG GAG GAG GAG CGA GCT CGC GAC CGA AGA AGC CCC GAA3'

Antisense Primer for optimized SFRP-2 gene amplification:

5'GAG GAG TCC TTT TGC GGC CGC TTC GCG TTG ACC TTT CTG CCA3'

The above sense primer contains a sequence tail that corresponds to the *Sac* I restriction site and the above antisense primer contains a sequence tail that corresponds to the *Not* I restriction site for ligation into pET-28b(+)-hFABP vector.

2.5.1.1.3 Annealing temperature optimisation of the sense and anti-sense primers for the SFRP-2 gene amplification from pUC57 vector

PCR was performed using an annealing temperature gradient of 55°C, 58°C and 62°C to select the optimal primer annealing temperature for SFRP-2 gene amplification.

The 1X reaction components and volumes for SFRP-2 gene amplification were as follows:

Component	50 µL volume
Vector DNA (20 ng/mL)	2 µL
dNTP	1 µL
GoTaq (5 x Buffer)	10 µL

$MgCl_2$	3 µL
Sense Primer (60 pM)	0.5 µL
Anti-sense Primer (60 pM)	0.5 µL
H_2O	32.75 µL
GoTaq polymerase	0.25 µL

The PCR conditions for the amplification of the SFRP-2 gene by PCR were as follows:

Steps	Temperature (°C)	Time
1	94	5 min
2	94	30 sec
3	Temperature gradient (55,58,62)	30 sec
4	72	30 sec
Repeat Steps 1→ 4 twenty five times		
5	72	10 min
6	4	Pause

2.5.1.1.4 Large-scale SFRP-2 gene amplification from pUC57 vector

Amplification of the SFRP-2 gene was performed as stated above in section 2.5.1.1.3, using a 15X reaction to increase the amount of amplified SFRP-2

gene product for purification. However, instead of a temperature gradient, an annealing temperature of 62°C was chosen to perform the gene amplification.

After successful amplification of the SFRP-2 gene, the PCR product was stored overnight at -20°C. It was centrifuged at 12,465 x g for 10 minutes at 4°C and the pellet washed using 70% (v/v) ice cold ethanol. The mixture was centrifuged at 12,465 x g for 10 minutes at 4°C and the pellet resuspended in 80 µL of molecular grade H_2O. After precipitation the DNA was resuspended in a small volume of water to ensure a high DNA concentration. The DNA was then resolved on a 1% (w/v) agarose gel and purified using the Promega gel "clean up" kit.

2.5.1.1.5 Purification of SFRP-2 gene

The SFRP-2 gene was purified from a 1% (w/v) agarose gel by excising the amplified size fragment of the SFRP-2 gene at 365bp. The gel slices were weighed and binding buffer (x 3 times the volume of the excised gel fragment) added. The mixture was incubated in a water bath for 10 minutes at 50°C. The guanidine isothiocyanate-containing binding buffer allows for sufficient binding of the DNA to the silica membrane columns. A volume of isopropanol equal to the weight of the excised fragment was added and the resulting mixture added to a collection column. Isopropanol encourages DNA precipitation of the excised fragment. The column was centrifuged at 12,465 x g for 1 minute to remove any remaining residual buffer and the "flow-through" discarded. The column was washed with 750 µl wash buffer, centrifuged at 12,465 x g for 1 minute and washed with 250 µl wash buffer. The column was centrifuged at 12,465 x g for 2 minutes and the DNA eluted from the column using 30 µl molecular grade H_2O into a clean 1.5 mL sterile centrifugation tube. The purified DNA absorbance was measured at 260 nm using the Nanodrop ND-1000 and the concentration calculated using the Beer-Lambert law.

2.5.1.1.6 SFRP-2 gene restriction using Sac I *and Not* I *enzyme and ligation into pET28(+)-hFABP vector*

The gel-purified SFRP-2 gene and pET-28b(+)-hFABP vector were cut using *Sac* I and *Not* I restriction enzymes. The restriction enzymes allows for the unidirectional cloning of the SFRP-2 into the pET-28b(+)-hFABP vector. *Sac* I recognises 6 bases (5'GAGCTC3') and *Not* I recognises 8 bases (5'GCGGCCGC3'). The pET28-hFABP vector and SFRP-2 gene were incubated with the digestion enzymes at 50°C for 1 hour in a water bath.

The pET-28b(+)-hFABP vector and SFRP-2 were digested using *Not* I *and Sac* I as follows:

Components	33.3 µL volume
SFRP-2 gene	25 µL
10 x Fast digest buffer	3.3 µL
H_2O	1 µL
Sac I	2 µL
Not I	2 µL

Components	50 µL volume
pET-28b(+)-hFABP vector	5 µL
10 x Fast digest buffer	5 µL
H_2O	36 µL
Sac I	2 µL
Not I	2 µL

Following large-scale digestion, the restricted pET28b-(+)-hFABP vector and SFRP-2 gene were purified from a 1% (w/v) agarose gel using the Promega gel "clean up" kit. The DNA concentrations were determined on the Nanodrop and the purified SFRP-2 gene was ligated into the purified pET28b-(+)-hFABP vector with a ratio of 3:1 (insert to vector) using T4 DNA ligase overnight at RT.

The ligation mixture contained the following components;

Components	20 µL volume
pET28b-(+)-hFABP vector	1.7 µL
SFRP-2 gene	2.1 µL
10 X ligase buffer	2 µL
H_2O	13.7 µL
T4 DNA ligase	0.5 µL

2.5.1.1.7 Transformation of vectors into E. coli cells

One microlitre (10 ng) of vector was added to 20 µL of the appropriate *E. coli* cells and mixed by gently tapping. The tube was incubated on ice for 30 min and then incubated in a water bath at 42°C for 30 sec. Following this the tube was placed back on ice and 80 µl of SOC media was added. The tube was then incubated at 37°C for 60 min shaking at 250 rpm (for all *E. coli* strains except NovaBlue) and plated on LB agar containing either 100 µg/mL carbenicillin or 50 µg/mL kanamycin for the pGS21a and pET28b-(+)-hFABP vectors, respectively.

Individual colonies (8-10 in total from each cell line) were picked from the LB plates and inoculated overnight (O/N) at 37°C and 230 rpm into TB media containing 100 µg/mL carbenicillin or 50 µg/mL kanamycin and 2% (v/v) glucose for the pGS-21a and pET-28b(+)-hFABP vectors, respectively. The O/N culture was then subcultured into 5 mL of fresh TB media containing 1X 505 supplement (0.5% (v/v) glycerol, 0.05% (w/v) glucose final concentration), 1 mM $MgSO_4$ and 100 µg/mL carbenicillin or 50 µg/mL kanamycin for the appropriate vector. These cultures were incubated at 37°C and 230 rpm until the cells appeared turbid at ~0.6 (OD600 nm). Expression was then induced by adding IPTG to a final concentration of 1 mM and transferring to 30°C (180 rpm) O/N. The cultures that were induced overnight were centrifuged at 3,220 x g for 10 minutes at 4°C. The pellets were resuspended in 500 µL of 1X PBS. The resuspended pellets were then sonicated on ice using the appropriate setting (40 amp for 90 sec with 3 sec intervals). Following this sonicated-lysate was centrifuged at 10,685 x g for 10 min and the supernatant was transferred to fresh centrifugation tubes. Twenty microlitres of the lysates from each transformant were then analysed using SDS gel and Western blotting described in sections 2.5.1.1.8 and 2.5.1.1.9. The remainder of the lysate from each transformant was centrifuged at 10,685 x g for 10 min at 4°C and the pellets were resuspended in 200 µL LB media supplemented with 20% (v/v) glycerol and stored at -80°C.

2.5.1.1.8 Sodium dodecyl sulphate polyacrylamide gel electrophoresis (SDS-PAGE)

The following stock solutions were prepared for gel casting: 30% (w/v) acrylamide containing 0.8% (w/v) bis-acrylamide, 1.5 M Tris-HCl, pH 8.8, 0.4% (w/v) SDS, 0.5 M Tris-HCl, pH 6.8, 0.4% (w/v) SDS and 10% (w/v) ammonium persulfate. The glass plates were washed with acetone and sealed with a gasket and grips. Free radical-induced polymerisation of the resolving gel acrylamide (see section 2.3.1.6) was catalysed by addition of ammonium persulphate and the accelerator TEMED and the gel added to the

space between the plates and covered with a layer of ethanol. Following polymerisation of the gel, the ethanol was removed and the stacking gel placed directly onto the resolving gel. A plastic comb was placed in this gel creating the wells for sample application. Once the gel had fully polymerised, the plates were then placed in an electrophoresis chamber, the comb was removed, the chamber and wells filled with electrophoresis buffer (25 mM Tris, 250 mM glycine (electrophoresis grade), pH 8.3 and 0.1% (w/v) SDS) and samples were loaded and run at 100V for 1-2 hours.

The gel was removed from the casting tray apparatus and stained using Coomassie blue solution for 1 hour. The gel was transferred to destain solution and incubated until the protein bands were clearly visible (approximately 1 hour).

2.5.1.1.9 Western blotting

An SDS-PAGE gel was resolved and the proteins transferred to nitrocellulose paper. The gel, extra thick blotting paper and nitrocellulose were incubated in transfer buffer for 30 min before the actual transfer. For each transfer, 2 pieces of extra thick blotting paper (Sigma - P7176) were placed on the bottom of the transfer apparatus, the nitrocellulose was carefully placed on top of the blotting paper, the SDS-PAGE gel was added on top of the nitrocellulose and 2 pieces of extra thick blotting paper placed over the SDS-PAGE gel. The proteins were transferred to the nitrocellulose using 15 V for 15 min. The nitrocellulose was carefully removed from the apparatus and placed in 5% (w/v) dried milk (Marvel) in PBS. The nitrocellulose membrane was blocked for 1 hour by constantly shaking the membrane at room temperature in 5% (w/v) dried milk in PBS. The membrane was washed once with 1X PBST followed by 1X PBS. The membrane was then incubated for 1 hour with appropriate primary antibody (see Table 11) in 1% (w/v) dried milk (Marvel) in PBST. Following this, the membrane was washed 3 times with 1X PBST and 3 times with 1X PBS. An appropriate HRP-labelled secondary

antibody in 1% (w/v) dried milk in PBST was then applied to the membrane and incubated for 1 hour at room temperature (this step was skipped for directly labelled HRP antibodies). Following this, it was washed 5 times with 1X PBST and once with 1X PBS and TMB liquid substrate carefully added to the blot and allowed to develop. Once sufficient development had occurred the reaction was stopped by multiple washes with distilled water.

Table 11: Antibodies used for Western blotting

Primary Antibody	Secondary Antibody	Primary Antibody Dilution	Secondary Antibody Dilution
Rabbit anti-SFRP-2 HPA002652 Atlas Antibodies (Prestige Antibodies®)	HRP- labelled anti-Rabbit A6154 Sigma	1/500	1/2,000
Rabbit anti-GST HRP A7340 Sigma	–	1/5,000	–
Mouse anti-His HRP A7058 Sigma	–	1/2,000	–
Mouse anti-cTnI HRP 19c7 hrp conjugate Hytest	–	1/2,000	–
Chicken anti-hFABP (scFv) (3.G9) ABG DCU	Rat anti-HA HRP 12013819001 Roche Applied Sciences	1/5000	1/2000

2.5.1.1.10 Large-scale expression of SFRP-2 fusion protein

A glycerol stock of the selected transformant was inoculated overnight (O/N) at 37°C and 230 rpm into 5 µL TB media containing 100 µg/mL carbenicillin or 50 µg/mL kanamycin for the appropriate vector and 2% (v/v) glucose. The O/N culture was then subcultured into 1 L of fresh TB media containing 1X 505 supplement (0.5% (v/v) glycerol, 0.05% (w/v) glucose final concentration), 1 mM $MgSO_4$ and 100 µg/mL carbenicillin or 50 µg/mL kanamycin for the appropriate vector. The culture was incubated at 37°C and 230 rpm until the cells appeared turbid at ~0.600 (OD600 nm). Expression was then induced by adding IPTG to a final concentration of 1 mM and transferring to 30°C (180 rpm) O/N. The culture was transferred equally to 6 centrifuge sorvals and spun at 3,220 x g for 10 min at 4°C and supernatant was discarded.

2.5.1.1.11 SFRP-2 fusion protein purification using a GST purification kit

Pellets were resuspended in 3 mL of 1X PBS containing 5 mM DTT per 50 mL of culture. Four microlitres of resuspended pellet was aliquoted into 15 mL centrifugation tubes and each sample sonicated on ice using the appropriate setting (40 amp for 45 sec with 3 sec intervals). The sonicated lysate was then centrifuged at 3,220 x g for 10 min at 4°C and the lysate was passed through a 0.2 µm filter. A total of 4 GST columns containing 1 mL of GST resin (Genscript, USA Inc) slurry were prepared and equilibrated with 2 mL of equilibration/wash buffer (125 mM Tris, 150 mM sodium chloride, pH 8.0) by centrifuging the columns in a 15 mL centrifugation tube at 700 x g for 2 min at 4°C and discarding the "flow-through". Filtered lysate (3 mL) was mixed with 3 mL equilibration/wash buffer and added to each column of resin and the tubes were rolled at 4°C O/N to allow time for the GST to bind with the resin. The tubes were then centrifuged at 700 x g for 2 min at 4°C and the "flow-through" was collected. The tubes were then washed with 2 mL of equilibrating buffer/wash buffer by centrifuging the tubes at 700 x g for 2 min

at 4°C and collecting the wash/"flow-through". This step was repeated 5 times to remove any non-specifically binding proteins. The recombinant protein was eluted by adding 2 mL of 1X glutathione elution buffer (184 mg of reduced glutathione dissolved in equilibration/wash buffer) and then centrifuging the columns at 700 x g for 2 min at 4°C. The eluted protein was collected and added to a spin column with a 5,000 Dalton molecular weight cut-off (MWCO). This was centrifuged at 3,220 x g at 4°C until concentrated to a volume of 500 µL. Five mL of filtered PBS was added to the column. This was stored on ice overnight at 4°C. The following day the sample was centrifuged at 3,220 x g at 4°C until concentrated to a 500 µL volume. The concentration of protein was calculated on the Nanodrop and an SDS-PAGE and a Western blot performed to ensure protein purity. The recombinant fusion protein was stored in 20 µL aliquots at -20°C until required.

2.5.1.1.12 SFRP-2 fusion protein purification using immobilised metal affinity chromatography (IMAC) purification kit

Sorval tubes (used for centrifugation) containing a culture of cells induced overnight (500 mL SB media) was spun at 10,685 x g for 10 minutes at 4°C. The pellets were resuspended in 30 mL of sonication buffer (1X PBS + 0.5 M NaCl + 20 mM imidazole). The resuspended pellet was aliquoted into thirty 2 mL centrifugation tubes (thirty 1 mL samples) and each sample sonicated on ice using the appropriate setting (40 amp for 45 seconds with 3 second intervals). The sonicated lysates were centrifuged at 12,465 x g for 10 minutes at 4°C and the lysate was passed through a 0.2 µm filter to reduce clogging of the nickel resin. A 4 mL column of nickel-nitrilotriacetic acid (NTA) resin slurry (Qiagen) was prepared and equilibrated with 30 mL of running buffer (sonication buffer + 1% (v/v) Tween). The filtered lysate was passed through the column once and the "flow-through" collected. The column was washed with 30 mL of running buffer to remove any non-specifically binding proteins. The recombinant antibody fragment was eluted with 20 mL of 100 mM sodium acetate solution, pH 4.4. The eluted fusion protein was collected

in 1.5 mL centrifugation tubes (final volume 500 µL in each tube) containing 50 µL 10X PBS (filtered through a 0.2 µm filter) and 50 µL 100 mM NaOH. The fractions were pooled together and added to a spin column with a 5,000 Da MW "cut off". The spin column was centrifuged at 3,220 x g at 4°C until concentrated to a volume of 500 µL. Five mL of filtered PBS was added to the column. This was stored on ice overnight at 4°C. The following day the sample was centrifuged at 3,220 x g at 4°C until concentrated to a 500 µL volume. The concentration of protein in PBS was calculated on the Nanodrop and an SDS-PAGE and Western blot performed to ensure protein purity. The recombinant fusion protein was stored in 20 µL aliquots at -20°C until required.

2.5.1.1.13 Purification of bacterial SFRP-2 inclusion bodies

Sorval tubes (used for centrifugation) containing a culture of cells induced overnight (200 mL SB media) was spun at 10,685 x g for 10 minutes at 4°C. The pellets were resuspended in 4 mL of lysis buffer (50 mM Tris-HCL pH 8.1 + 100 mM NaCl + 1mM EDTA). The resuspended pellet was transferred into a 15 mL centrifugation tube and the sample was frozen O/N at -80°C. After thawing, phenylmethanesulphonyl fluoride (PMSF) (1 mL, 100 mM) and 1 mg/ml lysozyme were added and incubated at 37°C and 230 rpm for 2 hours. One millilitre of Triton X-100 was added (0.5% (w/v) Triton X-100) and incubated at RT for 1 hour. Following this, the mixture was ice-jacketed, and 5 cycles of sonication was performed for 10 min at 40% amplitude at 0.5 sec intervals. After sonication, 50 µL of Tween-20 was added to the rest of the suspension and samples were incubated at 4°C for 1 h. Then, DNA was removed with DNase (150 µL, 1 mg/ml) and $MgSO_4$ (150 µL, 1 M) for 45 min at 37°C and 230 rpm. Finally, samples transferred to 1.5 mL centrifuge tubes and centrifuged at 4°C at 15,000 g for 15 min. The pellet containing pure SFRP-2 inclusion bodies were washed once with 1 mL of lysis buffer

containing Triton X-100 (0.5%). After a final centrifugation at 15,000 g for 15 min at 4°C, pellets were stored at -80°C until analysis.

2.5.1.1.14 Solubilisation of SFRP-2 inclusion bodies

Purified SFRP-2 inclusion bodies were resuspended in 1 mL of urea (8M). Following this, the mixture was ice-jacketed, and 2 cycles of sonication were performed for 45 sec at 40% amplitude under 3 sec intervals. The sonicated mixture was then dialysed overnight at 4°C in 5 L of PBS using dialysis tubing cellulose (D9652- Sigma Aldrich). The solubilised SFRP-2 was then analysed by Western blot and stored at -20°C until required.

2.5.1.2 "Cell-free" Translation

2.5.1.2.1 PCR Primers

The primers listed below were obtained from IDT Ltd and were designed to amplify the optimized SFRP-2 gene cloned into pUC57 vector described in section 2.5.1.1.1.2.

Primers:

Sense Primer for optimized SFRP-2 gene amplification for cell-free translation

5'AAG AGA TAT ACC AAT GGC GAC CGA AGA AGC CCC GAA AGT TT3'

Antisense Primer for optimized SFRP-2 gene amplification for cell-free translation

5'TAT TCA TTA TTC GCG TTG ACC TTT CTG CC3'

Universal Primer for optimized SFRP-2 gene amplification for cell-free translation

5'GAA ATT AAT ACG ACT CAC TAT AGG GAG ACC AC TCC CTC TAG AAA TAA TTT TGT TTA ACT TTA AGA AGG AGA TAT ACC A3'

The template DNA used for "cell-free" translation can be generated by 2-step PCR using the above primers. Using the sense primer in the first PCR, an adapter sequence containing the ribosomal binding site (RBS) is added at 5'-terminus of the SFRP-2 gene and all the regulatory sequences including the T7 promotor are added in the second PCR using the universal primer listed above.

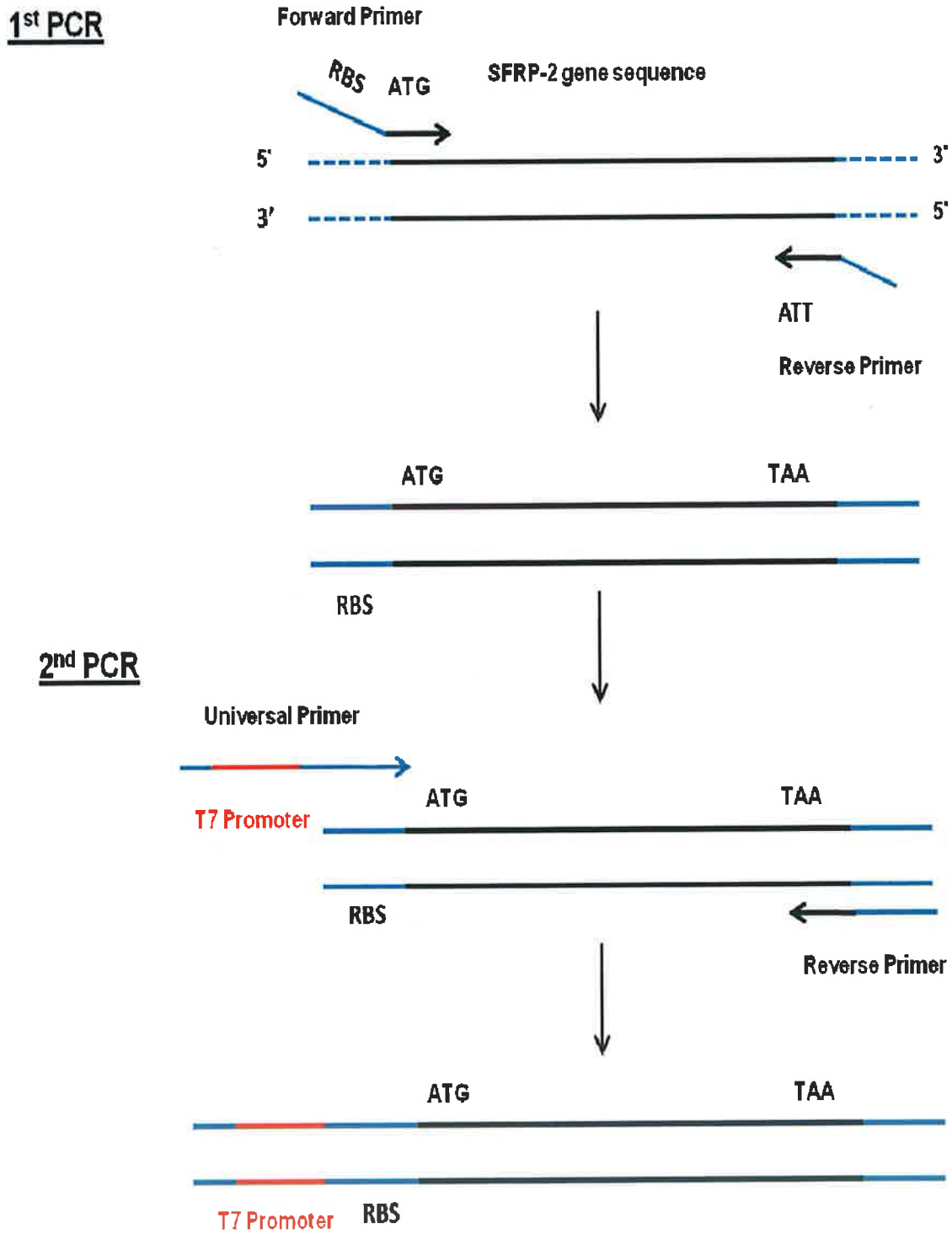

Figure 33: Generation of template DNA for cell-free expression by 2-step PCR

Template DNA for "cell-free" translation can be generated by 2-step PCR. The adaptor sequence (in blue) is added to at 5'- terminus of target gene in the first PCR and all the regulatory sequences, including the T7 promotor (in red), are added in the second PCR

2.5.1.2.2 Annealing temperature optimisation of the sense and anti-sense primers for SFRP-2 gene amplification from pUC57 vector (1st PCR)

The 1X reaction components and volumes for SFRP-2 gene amplification were as follows:

Component	50 µL volume
Vector DNA (20ng/mL)	0.5 µL
dNTP	5.0 µL
Velocity (5X Buffer)	10.0 µL
Sense Primer (60pM)	0.5 µL
Anti-sense Primer (60pM)	0.5 µL
H_2O	32.5 µL
Velocity polymerase	1.0 µL

The PCR conditions for the amplification of the SFRP-2 gene by PCR were as follows:

Steps	Temperature (°C)	Time
1	94	5 min
2	94	30 sec
3	Temperature gradient (55, 58,62)	30 sec
4	72	30 sec
Repeat Steps 1→ 4 twenty five times		
5	72	10 min
6	4	Pause

2.5.1.2.3 DMSO concentration optimisation of the sense and anti-sense primers for SFRP-2 gene amplification from pUC57 vector (1st PCR)

Two 50 µl (1X) reaction components and volumes for SFRP-2 gene amplification were as follows:

Component	Reaction 1	Reaction 2
Vector DNA (20ng/mL)	0.5 µL	0.5 µL
dNTP	5.0 µL	5.0 µL
Velocity (5X Buffer)	10.0 µL	10.0 µL
Sense Primer (60pM)	0.5 µL	0.5 µL
Anti-sense Primer (60pM)	0.5 µL	0.5 µL
H_2O	32.5 µL	31.0 µL
DMSO	–	1.5 µL
Velocity polymerase	1.0 µL	1.0 µL

The PCR conditions for the amplification of the SFRP-2 gene by PCR were as follows:

Steps	Temperature (°C)	Time
1	94	5 min
2	94	30 sec
3	62	30 sec
4	72	30 sec
Repeat Steps 1→ 4 twenty five times		
5	72	10 min
6	4	Pause

2.5.1.2.4 Annealing temperature optimisation of the universal primer (2nd PCR)

The 1X reaction components and volumes for SFRP-2 gene amplification were as follows:

Component	50 µL volume
Amplified DNA (from 1st PCR))	1.0 µL
dNTP	5.0 µL
Velocity (5X Buffer)	10.0 µL
Universal Primer (60pM)	0.5 µL
Anti-sense Primer (60pM)	0.5 µL
H_2O	32.0 µL
Velocity polymerase	1.0 µL

The PCR conditions for the amplification of the SFRP-2 gene by PCR were as follows:

Steps	Temperature (°C)	Time
1	94	5 min
2	94	30 sec
3	Temperature gradient (56,58,60,62)	30 sec
4	72	30 sec
Repeat Steps 1→ 4 twenty five times		
5	72	10 min
6	4	Pause

2.5.1.2.5 Large-scale SFRP-2 gene amplification universal primer (2nd PCR)

Amplification of the SFRP-2 gene (5X reaction) using the universal primer was performed, as described in section 2.5.1.2.4. However, instead of a temperature gradient, an annealing temperature of 62°C was chosen to perform the gene amplification. After successful amplification of the SFRP-2 gene, the PCR product was stored overnight at -20°C. It was centrifuged at 12,465 x g for 10 minutes at 4°C and the pellet washed using 70% (v/v) ice cold ethanol. The mixture was centrifuged at 12,465 x g for 10 minutes at 4°C and the pellet resuspended in 80 µL of molecular grade H_2O. After precipitation the DNA was resuspended in 20 µL of H_2O to ensure a high DNA concentration. The DNA was then resolved on a 1% (w/v) agarose gel and purified using the Promega gel "clean up" kit.

2.5.1.2.6 Purification of SFRP-2 gene

Purification and quantification of the SFRP-2 gene with the universal primer was performed, as described in section 2.5.1.1.5.

2.5.1.2.7 SFRP-2 protein synthesis/translation

The reaction components and volumes for SFRP-2 protein translation were as follows:

Component	50 µL volume
Amplified DNA (1 pM)	2.0 µL
Solution A	25.0 µL
Solution B	10.0 µL
H_2O	13.0 µL

The reaction was incubated at 37°C for 1 hour and deactivated by placing on ice for 20 mins.

2.5.1.2.8 SFRP-2 protein purification

An equal volume of H_20 was added to the reaction (50 µL) and transferred to a fresh tube (2 mL round-bottomed tube). Exactly 0.1 volume (10 µl) of IMAC resin was added to the tube and vortexed at 4°C for 1 hour. The tube was then centrifuged at 4°C for 30 minutes at 1,500 xg and the supernatant was recovered. The cell-free translated protein was then analysed by anti-SFRP-2 Western blotting, as described in 2.5.1.1.9, to determine if the protein was successfully translated.

2.5.1.3 Immunisation of Leghorn chickens with SFRP-2 and antiserum titre determination

This work was passed by the ethics committees of the School of Biotechnology Dublin City University and the licence subsequently granted by the Department of Health and Children. Extreme care was taken to minimise stress levels to the animal. A chicken (Leghorn female between the age of 5 – 8 weeks) was used for production of recombinant antibodies to SFRP-2. The chicken was initially immunised in the peritoneal cavity with a final concentration of 200 µg/mL of Tuner (DE3) *E. coli* lysate containing SFRP-2 conjugated to GST in 800 µL PBS, mixed in a 1:1 ratio with Freund's complete adjuvant. The mixture was vigorously shaken to ensure a completely homogenous solution. Freund's Complete Adjuvant (FCA) is an emulsified mineral oil antigen solution used as an immunopotentiator. Subsequent injections were performed with 200 µg/mL SFRP-2 conjugated to hFABP purified inclusion bodies mixed in a 1:1 ratio with Freund's incomplete Adjuvant (FICA). A bleed was taken from the chicken 7 days after the second booster administration to confirm that the animal was responding to the immunisations and that antigen-specific antibodies were being produced.

2.5.1.4 SFRP-2 antibody response determination by Enzyme-Linked Immunosorbent Assay (ELISA)

A 96 well ELISA plate (Maxisorp™, Nunc) coated with 100 µL per well of 2 µg/mL SFRP-2 conjugated to ABP was incubated O/N at 4°C. The SFRP-2 solution was decanted and the plate was blocked with 3% (w/v) BSA in PBS for 1 hour at 37°C. A 100 µL volume of each of the diluted chicken sera was added in tripicate to the ELISA plate and incubated for 1 hour at 37°C. Following the incubation of the sera, the plate was washed 3 times with both PBST and PBS. Next, 100 µL of 1/2,000 dilution of a HRP-conjugated anti-

chicken IgY (IgG) antibody (Sigma A9046) in 1% (w/v) BSA-PBST was added to each well and incubated for 1 hour at 37°C. The specific complex was then detected by the addition of 100 µL of TMB substrate and allowed to develop for 10 mins at 37°C. Finally, the reaction was quenched using 100 µL of 1 M HCl and the absorbance values read at 450 nm on a Tecan Saffire 2 Plate reader.

Chapter 3 - Evaluation of Zinc-α-2-Glycoprotein (ZAG), Kininogen-1 (KNG-1), Vitamin D Binding Protein (VDBP) and Proteasome Subunit β Type 6 (PSMB-6) expression in prostate cancer

3.1 Summary

There is continued debate over the efficacy of prostate specific antigen (PSA) as a diagnostic marker. Its poor specificity has led to prostate cancer not being detected early enough and aggressive versus non aggressive disease not being distinguished leading to over-treatment of the disease and associated morbidity. The discovery of a novel biomarker of prostate cancer with expression in serum which correlates with expression in tissue and with Gleason grade would be extremely beneficial as it would mean that less invasive diagnostic procedures could be carried out on patients to measure the biomarker's expression level. Given the heterogeneous nature of prostate cancer a combination of biomarkers may provide better prediction regarding the disease and allow for more appropriate intervention with improved outcome.

Zinc-α-2-glycoprotein (ZAG), Kininogen-1 (KNG-1), Vitamin D Binding Protein (VDBP) and Proteasome Subunit β Type 6 (PSMB-6) were found to be up-regulated in the serum of prostate cancer patients with higher grade tumours following 2D-DIGE analysis. The aim of this study was to investigate if ZAG, KNG-1, VDBP and PSMB-6 were also overexpressed in prostatic tumour tissue of prostate cancer patients.

Immunohistochemical analysis was performed on prostate cancer tissue microarrays with samples from 199 patients. Confirmatory gene expression profiling for ZAG, KNG-1, VDBP and PSMB-6 was performed on 4 cases using Laser Capture Microdissection and TaqMan® Real-Time PCR. ZAG expression in prostate cancer epithelial cells was inversely associated with Gleason grade (BPH>G3>G4/G5). PSMB-6 was not expressed in either tumour or benign epithelium. However, strong PSMB-6 expression was noted in stromal and inflammatory cells. KNG-1 and VDBP were not expressed in BPH or prostate cancer tissue.

The results presented in this chapter indicate ZAG as a possible predictive marker of Gleason grade. The inverse association between grade and tissue expression with a rising serum protein level is similar to that seen with PSA. In addition the results for all proteins (ZAG, PSMB-6, KNG-1 and VDBP) highlight the challenges in trying to associate the protein levels in serum with tissue expression.

3.2 Introduction

3.2.1 Prostate Cancer Serum Markers

Although management of prostate cancer patients has improved significantly, early detection is a crucial parameter in contributing to increased survival. It has become increasingly important to have reliable ways to diagnose the disease, as aggressive therapies can lead to significant risk of treatment-related side effects which will impact on the patient's quality of life. The widespread use of prostate specific antigen (PSA) as a screening tool for prostate cancer has led to a decline in death rates due to the disease and a decrease in the prevalence of advanced stage disease at diagnosis (Byrne *et al.*, 2009, Thompson *et al.*, 2003). However, there is continued debate over the efficacy of PSA as a diagnostic marker as its poor specificity has led to prostate cancer not being detected early enough and aggressive versus non aggressive disease not being distinguished leading to over-treatment of the disease and associated morbidity (see section 1.2.2). Several other markers have been implicated as potential biomarkers of prostate cancer including α-methylacyl coenzyme A racemase (AMACR) which has been shown to be significantly up-regulated in prostate cancer serum and tissue, however, no individual marker has proven as good or better than PSA.

The discovery of a novel biomarker of prostate cancer with expression in serum which correlates with expression in tissue and with Gleason grade would be extremely beneficial as it would mean that less invasive diagnostic

procedures could be carried out on patients to measure the biomarker's expression level. Given the heterogeneous nature of prostate cancer a combination of biomarkers may provide better prediction regarding the disease and allow for more appropriate intervention with improved outcome. Comparative serum proteomic analysis has the potential to reveal protein expression changes present at different stages of prostate cancer progression (Byrne *et al.*, 2009). Such markers could have the potential to tackle the central clinical dilemma within this disease: distinguishing clinically indolent disease from aggressive forms of prostate cancer that are most likely to benefit from clinical intervention (Byrne *et al.*, 2009).

3.2.2 Increased expression of Zinc-α-2-Glycoprotein (ZAG), Kininogen-1 (KNG-1), Vitamin D Binding Protein (VDBP) and Proteasome Subunit β Type 6 (PSMB-6) serum markers in the progression of prostate cancer

Within the prostate cancer research consortium (PCRC), the proteomic biomarker discovery group (UCD Conway Institute of Biomolecular and Biomedical Research) identified a number of differentially expressed proteins in serum samples from two well-defined histological cohorts, namely Gleason score 5 and Gleason score 7. This study was carried out on a small cohort (N = 12) using 2D-Difference Gel Electrophoresis (2D-DIGE) analysis by Byrne *et al.* (2009). 2D-Difference Gel Electrophoresis (2D-DIGE) is a protein separation technique which was first introduced in 1997 by Unla *et al.* (1997). 2D-DIGE has recently emerged as a powerful analytical tool within the field of proteomics, allowing for relative quantitation of protein spot intensity across carefully matched gels (Byrne *et al.*, 2009). The proteins that were found to be significantly up-regulated between the two cohorts of Gleason score 5 and 7 patients were Zinc-α-2-glycoprotein (ZAG), Kininogen-1 (KNG-1), Vitamin D Binding Protein (VDBP) and Proteasome Subunit β Type 6 (PSMB-6).

Table 12: Differentially expressed proteins identified in serum samples of Gleason score 5 versus Gleason score 7 prostate cancer patients by Byrne *et al.* (2009)

Protein	Expression in Gl 7 vs. Gl.5	Fold-Change
Proteasome subunit beta type 6	Increased	2.53
Zinc-alpha-2-glycoprotein	Increased	1.36
Pigment epithelium-derived factor	Decreased	1.76
Clusterin	Decreased	2.12
Interalpha trypsin inhibitor heavy chain	Decreased	1.55
Dermicidin	Decreased	1.66
Kininogen-1	Increased	2.8
AMBP protein / Inter Alpha Trypsin Inhibitor	Decreased	1.32
Alpha-2-macroglobulin	Decreased	1.48
Vitamin D binding protein	Increased	2.44
monocyte differentiating antigen CD14	Decreased	9.7
Insulin like grow th factor binding protein 7 / IFGBPRP1	Decreased	3.7

Given that in most scientific experiments it is easier to detect the presence of a substance or its up-regulation than to prove its absence we focused this study on those proteins that were found to be up-regulated in prostate cancer serum by Byrne *et al.* (2009). In this study/chapter the prostatic tissue expression of the up-regulated proteins in prostate cancer serum (namely ZAG, KNG-1, VDBP and PSMB-6) is investigated to determine if they are also up-regulated in prostate cancer tissue, if there is a difference in their expression across the different Gleason grades of prostate cancer and to investigate whether the proteins' presence in serum is originating from the tumour/ tissue. ZAG, KNG-1 and PSMB-6 tissue expression was assessed at both a protein and mRNA level. However VDBP was only assessed at an mRNA level as no reliable commercially available antibodies applicable for IHC were available to Vitamin D Binding Protein at the time of the study.

3.2.3 Zinc-α-2-Glycoprotein (ZAG)

ZAG is a 41 kDa secreted, soluble protein present in blood and many other bodily fluids (Tada *et al.*, 1991, Descazeaud *et al.*, 2006). It was first identified and purified over forty years ago as an abundant protein in serum and subsequently identified as a major protein constituent of sweat, seminal fluid, breast cyst fluid (Delker *et al.*, 2004), cerebrospinal fluid and urine (Bondar *et al.*, 2007). It is also found in secretory epithelial cells of the liver and the gastrointestinal tract (Bondar *et al.*, 2007) and is over-expressed in certain human malignant tumours (Descazeaud *et al.*, 2006). Biochemically, ZAG is known to stimulate lipid degradation in adipocytes and appears to be involved in cachexia, a wasting syndrome that can affect people with cancer, AIDS and other terminal illnesses (Bondar *et al.*, 2007). ZAG was recognized as a homolog of the class I major histocompatibility complex (MHC) heavy chain and its crystal structure purified from human serum confirmed that ZAG has an MHC-like fold (Delker *et al.*, 2004). ZAG protein has been found to be immunoreactive within the cytoplasm of normal secretory epithelial cells, including breast, prostate and liver (Hale *et al.*, 2001, Tada *et al.*, 1991).

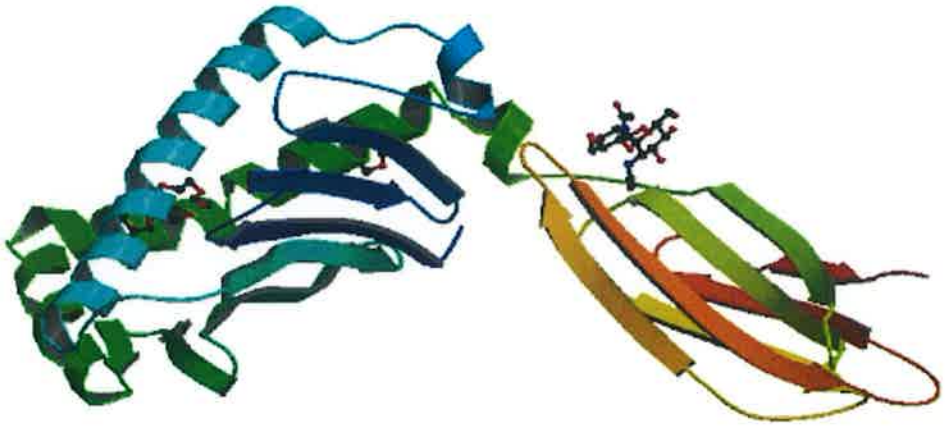

Figure 34: Crystal structure of Zinc-α-2 glycoprotein (www.pdb.org/pdb/home/home.do)

Purified forms of ZAG do not contain a bound endogenous ligand, but the ZAG groove is capable of binding hydrophobic molecules, which may relate to its function.

3.2.4 Kininogen 1 (KNG-1)

Kininogen-1 is also known as high molecular weight kininogen, Williams-Fitzgerald-Flaujeac factor, Alpha-2-thiol proteinase inhibitor, Fitzgerald factor and KNG-1. It is a secreted glycoprotein which contains three cystatin domains. Kininogen-1/KNG1 is approximately 120 kDa and circulates in plasma at a concentration of ~90 µg/ml (McCrae *et al.*, 2005). It adsorbs to the surface of biomaterials that come in contact with blood *in vivo*. It plays an important role in blood coagulation as well as the kinin-kallikrein system by

positioning prekallikrein and factor XI near factor XII (Houlihan *et al.*). Structurally, KNG-1 consists of heavy and light chains, which contain domains that are linked by domain 4, the domain which contains the vasoactive nonapeptide, bradykinin (BDK) (McCrae *et al.*, 2005). BDK is a peptide that causes vasodilation and is released from KNG-1/HMWK following cleavage by plasma kallikrein (McCrae *et al.*, 2005).

Defects in the KNG-1 gene are the cause of high molecular weight kininogen deficiency (HMWK deficiency) which is an autosomal recessive coagulation defect (Houlihan *et al.*). Patients with HWMK deficiency exhibit abnormal surface-mediated activation of fibrinolysis.

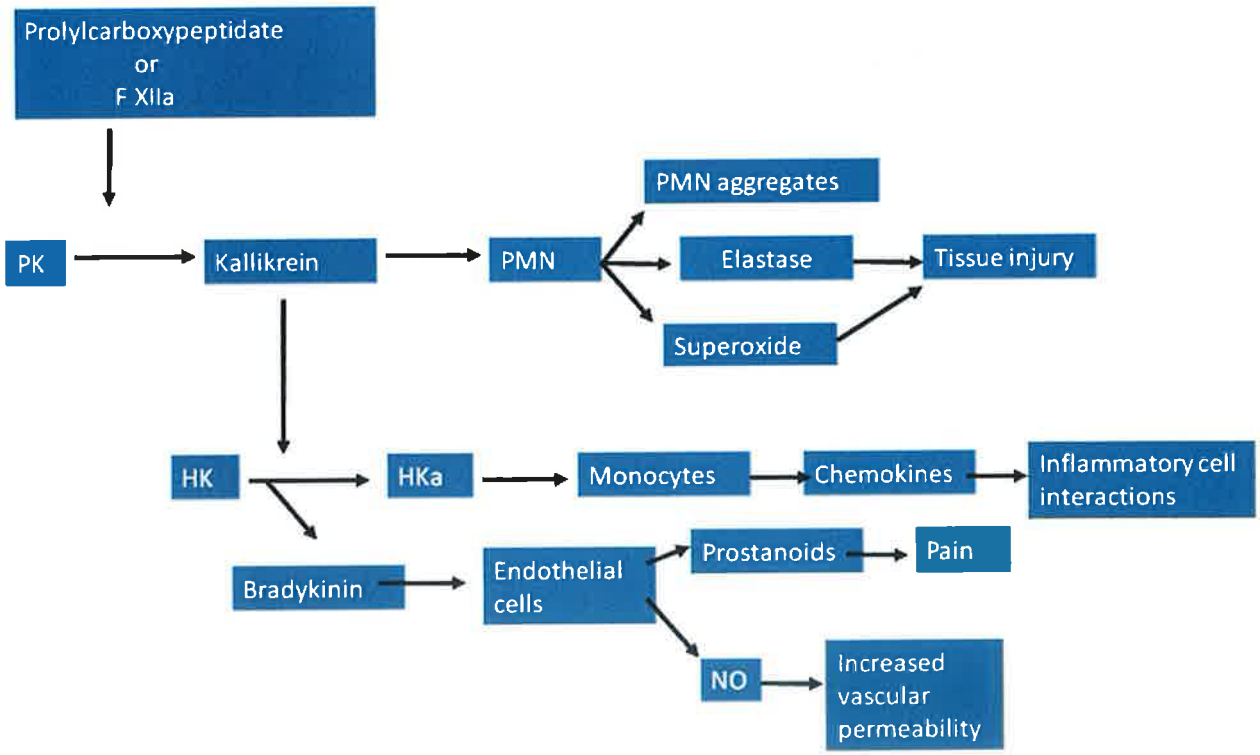

Figure 35: Kallikrein–kinin system (KKS) adapted from (Keith *et al.*, 2005)

The KKS is initiated by factor XIIa (FXIIa) or prolylcarboxypeptidase on the endothelial cell and leukocyte (polymorphonuclear cell (PMN)) surface, generating the enzyme kallikrein, which in turn cleaves high-molecular-mass kininogen (HK) to yield bradykinin (BK) and cleaved high-molecular-mass kininogen (HKa). Kallikrein is chemotactic, aggregates neutrophils, and stimulates the release of elastase and superoxide (potent inducers of tissue injury). BK stimulates vasodilation, mediates pain through the release of prostaglandins, and stimulates vascular permeability through the generation of nitrous oxide (NO). PK, prekallikrein.

3.2.5 Vitamin D Binding Protein (VDBP)

Vitamin D is a secosteroid hormone and is a key physiological modulator of calcium and phosphate homeostasis (Ma *et al.*, 2004). Most vitamin D is obtained by the conversion, by UV radiation, of 7-dehydroxycholesterol in the skin (Gann *et al.*, 1996). Vitamin D is then hydroxylated by the liver to 25-hydroxyvitamin-D3 (25(OH)D3) and a very small portion of circulating 25(OH)D3 is then further hydroxylated again in the kidney to form 1,25-dihydroxyvitamin-D3 (1,25(OH)2D3) which is 500 - 1000 times more potent than 25(OH)D3 at regulating calcium metabolism (Gann *et al.*, 1996).

The vitamin D receptor (VDR) mediates the biological actions of 1,25(OH)2D3. VDRs which are ligand-dependent transcription factors are present in many tissues essential to calcium and phosphate metabolism, including bone, parathyroid glands, small intestine and kidney (Ma *et al.*, 2004). They are also present in a variety of other tissues, including uterus, ovary, testis, breast and prostate, where 1,25(OH)2D3 is involved in cellular functions unrelated to calcium metabolism (Ma *et al.*, 2004). Both normal and cancerous prostate epithelial cells have VDRs, indicating that they are target cells and can respond to vitamin D (Ma *et al.*, 2004). 1,25(OH)2D3, the active form of vitamin D, inhibits growth of normal and cancerous prostate cells (Ma *et al.*, 2004).

It has been hypothesised that vitamin D metabolites inhibit cancer development at various tissue sites. Regarding prostate cancer, this hypothesis is compatible with the observation that certain high risk populations, including the elderly, African-Americans and residents of northern latitudes, all tend to have reduced levels of vitamin D formation (Gann *et al.*, 1996).

Vitamin D and metabolites of vitamin D (including 25(OH)D3 and 1,25(OH)2D3) are poorly soluble in blood and are transported in the circulation almost entirely bound to serum proteins (Schwartz, 1994). Vitamin D binding protein (VDBP) is the principal transport protein for the metabolites.

VDBP is an alpha globulin also known as group specific component which is synthesized in the liver and also has an effect on inflammation. Eighty five percent of total circulating 1,25(OH)2D3 is bound to VDBP, 14.6% is bound to albumin and only 0.4% is free (Schwartz, 1994). It is generally thought that the bound 1,25(OH)2D3 is physiologically inactive and the physiologically active hormone is the free 1,25(OH)2D3, estimated as the ratio of total 1,25(OH)2D3 to VDBP (Schwartz, 1994). An essential way for assessing the effective vitamin D status of an individual is to measure serum levels of VDBP. Both in normal individuals and individuals with various diseases, serum levels of total 1,25(OH)2D3 and VDBP are correlated positively (Schwartz, 1994).

Vitamin D binding protein belongs to the albumin gene family. It is multifunctional and found in plasma, ascitic fluid and cerebrospinal fluid and on the surface of many cell types. VDBP is a glycosylated alpha-globulin which is approximately 58 kDa in size (Verboven *et al.*, 2002). The three most common phenotypes of VDBP, $Gc1_{fast}$, $Gc1_{slow}$ and Gc2, combine to form 6 genotypes 1F/1F, 1F/1S, 1F/2, 1S/1S, 1S/2, 2/2. Each polymorphism is thought to have similar affinity for 1,25(OH)2D3 (Corder *et al.*, 1995).

Figure 36: Crystal structure of uncomplexed vitamin D-binding protein

(www.pdb.org/pdb/home/home.do)

3.2.6 Proteasome Subunit β Type 6 (PSMB-6)

Proteasome Subunit β Type 6 (PSMB-6) is a core beta subunit of the 20S and 26S proteasomes. Proteasomes are large ATP dependent multisubunit proteases (Kloetzel, 2001). They are the central proteolytic machinery of the cell responsible for degradation of proteins. Proteasomes are also involved in a number of cell processes including cell cycle, transcription, signalling, metabolism, antigen processing and apoptosis (Dahlmann *et al.*, 2001).

The 20S proteasome is referred to as the core structure of the proteasome. It is cylinder shaped and is composed of multiple subunits; four stacked rings

with seven subunits in each ring (see Figure 37(A)). In eukarya, the outer two rings are made of seven different α subunits, while the two inner rings are composed of seven different β subunits where only the $\beta1$, $\beta2$ and $\beta5$ subunits contain protease activities (Wu, 2002). PSMB-6 is the 6^{th} β subunit ($\beta6$) forming part of these two inner rings. The protease activities of the 20S proteasome are located in the inner cavity of the cylinder and are thus insulated by the cylinder wall which prevents indiscriminate digestion of proteins that are not to be eliminated (Wu, 2002). The 20S proteasome degrades unfolded proteins or short peptides only in an ATP-independent fashion (Wu, 2002).

In Eukaryotic cells most proteasomes are in a 26S form. The 26S proteasome is composed of the 20S core with a 19S regulatory complex attached to each of its ends. The 26S proteasome digests intact but ubiquitinated proteins. The 26S proteasomal regulatory complex has intrinsic ATPase activity that seems to play an essential role in its function for the selective degradation of target proteins (Tanaka and Tsurumi, 1997). The 26S proteasome is present in cytoplasm as well as in nuclei and degrades about 70 – 90% of cellular proteins (Wu, 2002). The 19S complex is responsible for recognizing ubiquitinated protein substrates and also contains ATPase activity (Wu, 2002).

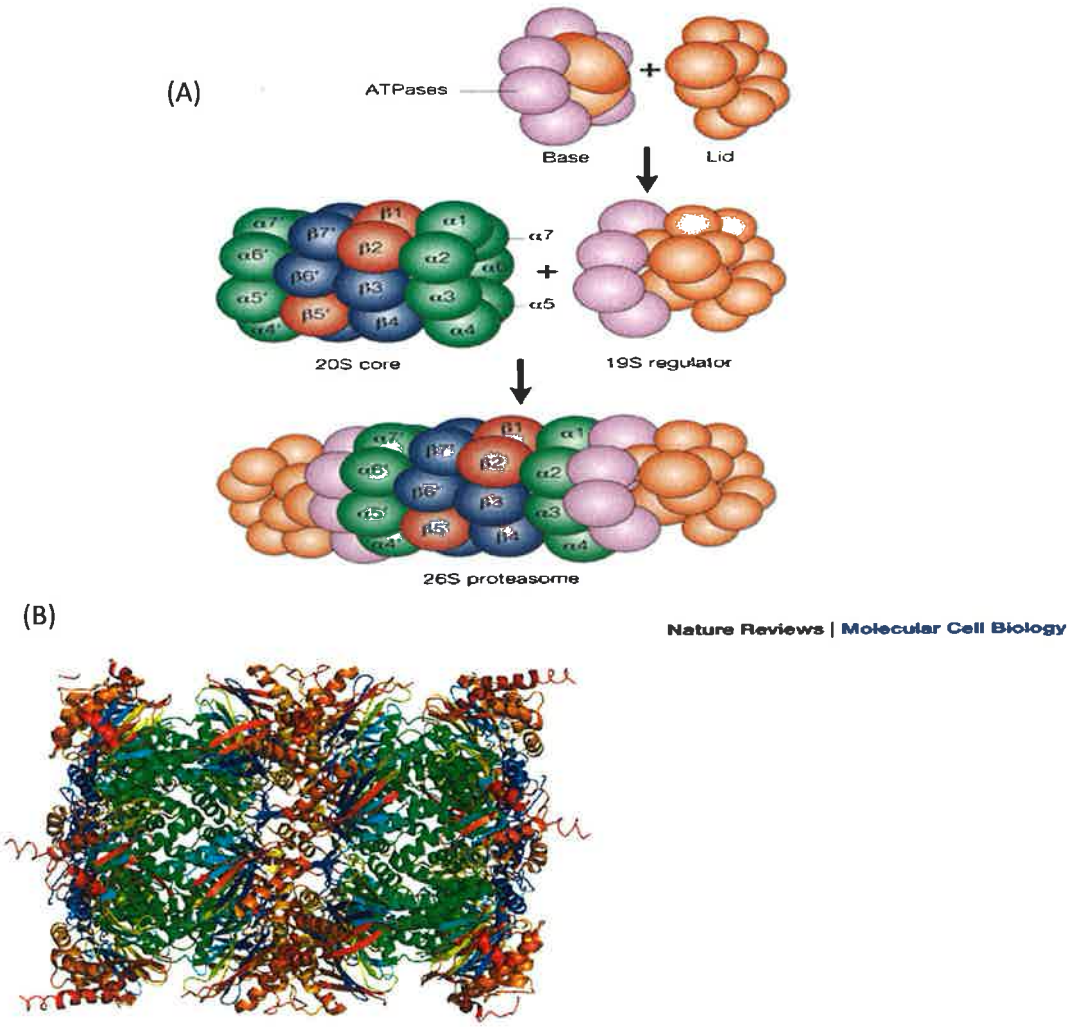

Figure 37: Proteasomes

(A) 19S, 20S and 26S proteasomes

The 20S proteasome consists of 28 (14 different) subunits, which are arranged as four heptameric staggered rings. The two outer rings contain the α subunits (green), the amino termini of which protrude into the central opening of the cylinder, as shown by X-ray structure analysis of the yeast proteasome. The two inner rings contain two copies of the β-subunits (blue and red), three of which (β1, β2 and β5; red) harbour the six active sites. The 19S subunit comprises two substructures. The base, which attaches to the two α-rings, is composed of six ATPase (purple) and two non-ATPase subunits (orange). The lid, which contains up to ten non-ATPase subunits (orange), is responsible for substrate binding and has poorly understood regulatory functions (Kloetzel, 2001).

(B) Crystal structure of mammalian 20S proteasome (Unno *et al.*, 2002)

3.2.7 Aim

The aim of this study is 3-fold:

(i) To determine if ZAG, KNG-1, VDBP and PSMB-6 are also up-regulated in prostate cancer tissue in parallel with the increase in the serum of prostate cancer patients identified by Byrne *et al.* (2009)

(ii) To establish if there is a difference in the protein expression between prostatic tumour tissue and BPH.

(iii) To determine if there is a difference in the expression of these proteins across the different Gleason grades of prostate cancer.

3.3 Materials and Methods

3.3.1 Sample Collection/Tissue Microarray Construction

One hundred and ninety nine prostate cancer cases (age range 43-74 years) were obtained from the Beaumont Hospital and the Mater Misericordiae University Hospital Histopathology archives dating from 2002 - 2008. This cohort of 199 cases included 4 cases which had ZAG, PSMB-6, KNG-1 and VDBP proteomic serum analysis performed from the initial proteomic study by Byrne *et al.* (2009), and another 15 cases which had further ZAG proteomic serum analysis performed by Byrne *et al.* (2009). The 199 cases included a variety of Gleason scores ranging from 5 to 10. Suitable formalin fixed paraffin embedded blocks of each case representing as many Gleason grades as possible were selected. The corresponding Haematoxylin and Eosin (H&E) stained sections were reviewed by a Pathologist. Three 1 mm cores of benign prostatic hyperplasia (BPH) and Gleason grade 3, 4 and 5 carcinoma were taken from every case where available. The tissue microarrays were assembled using the Beecher Instruments Tissue-Arrayer^{TM} (Beecher Instruments, Silver Spring, MD).

3.3.2 Immunohistochemistry

Immunohistochemistry was performed on the paraffin-embedded 4 μm tissue microarray sections using an automated Immunohistochemistry (IHC) platform (Bond Max^{TM} - Leica Microsystems), as described in section 2.2.4. Table 13 shows the optimal antigen retrieval and optimal concentrations of primary antibodies determined for immunohistochemistry. Sections were counterstained with haematoxylin.

Table 13: Optimal antigen retrieval and optimal concentrations of primary antibodies determined for immunohistochemistry

Protein	Antibody	Supplier	Optimal Dilution	Optimal Epitope Retrieval for Bond Max™
ZAG	anti-ZAG mAb (1D4) sc-13585	Santa Cruz Biotechnology	1/4000	ER 2 for 20 min
PSMB-6	anti-PSMB-6 mAb ab58079	Abcam	1/400	ER 1 for 10 min
KNG-1	anti-KNG-1 pAbl HPA001616	Atlas Antibodies *(Prestige Antibodies®)*	1/500	ER 2 for 10 min

3.3.3 Scoring of ZAG, KNG-1 and PSMB-6 Protein Expression

Immunoreactivity for ZAG and KNG-1 was assessed in benign prostatic hyperplastic epithelium and tumour epithelium across all Gleason grades. For the purpose of statistical analysis, immunoexpression of the proteins was graded according to the following scales:

ZAG: 0, absence of reactivity, 1, faint but clearly detectable reactivity in > 10% of epithelial cells, 2, moderate reactivity in > 10% of epithelial cells and 3, strong reactivity in > 10% of epithelial cells.

KNG-1: 0, absence of reactivity and 1, faint but clearly detectable reactivity in > 10% of epithelial cells.

PSMB-6: Immunoreactivity was assessed only in the stroma as no expression was noted in tumour epithelium or benign prostatic hyperplastic epithelium. However, its expression in the stroma was not scored.

3.3.4 Statistical Analysis

Often more than one histological grade of prostate tissue was present on a single TMA core. Due to this, individual cores were not scored for immunohistochemical staining as a whole; instead the different histological areas present on the core representing more than 10% of the core were graded separately. Thus, altogether 1489 histological areas/Gleason grades were scored for each variable (663=BPH, 418=G3, 266=G4 and 142=G5).

For statistical analysis of immunoreactivity of ZAG versus histopathological features the staining intensity of the epithelial cells was divided into two groups: low expression (immunohistochemical score of 0 or 1) included those with negative or weak reactivity, and high expression (immunohistochemical score of 2 or 3) included those with moderate or strong reactivity. Chi square tests were performed on contingency tables using GraphPad INSTAT-3^{TM} software version 3.02 (Graph Pad Software Inc, San Diego, USA) to test the association of the prostate cancer samples, BPH samples and tumour grade with immunohistochemical score (positive (2/3) and negative (0/1)).

3.3.5 Laser Capture Microdissection, total RNA extraction and Taqman PCR

To validate the immunohistochemical results, four of the 199 prostate cancer cases were selected on which to perform mRNA analysis. Areas of BPH and all Gleason grades of tumour (Gleason grade 3, 4 and 5) were present on each of the 4 cases selected. Laser capture microdissection, RNA extraction and Taqman PCR were carried out on 7μm whole sections from the 4 cases, as described in section 2.2.8, using assay context sequences described in Table 14.

Table 14: TaqMan® context sequences of primers and probes designed by Applied Biosystems™, Foster City, CA

Reaction	Context Sequence	Assay I.D.
ZAG (FAM labelled) TaqMan®	TTACAACGACAGTAACGGGTC TCAC	*Hs00426651_m1
VDBP (FAM labelled) TaqMan®	CTTTAGAGAGAGGCCGGGATT ATGA	*Hs00167096_m1
PSMB-6 (FAM labelled) TaqMan®	TCCAGAACAACCACTGGGTCC TACA	*Hs00382586_m1
KNG-1 (FAM labelled) TaqMan®	ACAACTAGTCACCTAAGGTCC TGCG	*Hs00949376_m1
CDKN1B (FAM labelled) TaqMan®	AACCGACGATTCTTCTACTCA AAAC	*Hs00153277_m1

*Suffix "_m" indicates that the assay's probe spans an exon junction and will not detect genomic DNA

3.4 Results

3.4.1 ZAG Expression

ZAG protein expression was observed in epithelial cells for both BPH and prostate cancer and the immunoreactivity pattern for ZAG varied from diffusely cytoplasmic in BPH to granular cytoplasmic with increasing Gleason grade. ZAG expression showed an inverse association with Gleason grade (BPH > G3 > G4/G5) as shown in Figure 38.

- Out of a total of 663 BPH areas analysed, 590 displayed positive expression of ZAG (score of 2/3) and 73 areas lacked expression for ZAG (score of 0/1).
- 248 areas of Gleason grade 3 displayed positive expression of ZAG out of a total of 418 and 176 lacked expression.
- Out of a total of 408 areas of > Gleason grade 3 (G4+G5), 270 lacked expression of ZAG and 138 displayed positive expression.

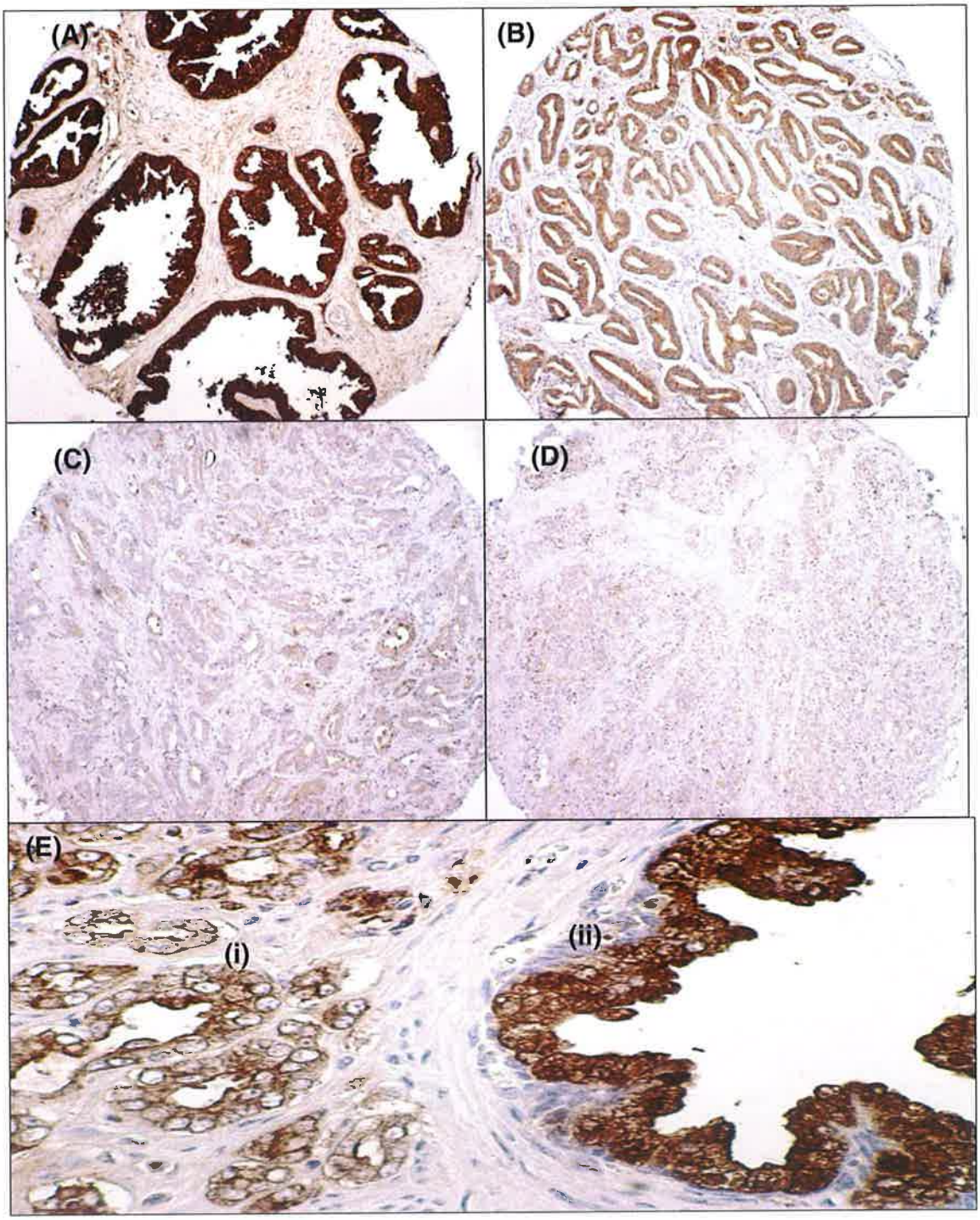

Figure 38: ZAG protein expression assessed by IHC on prostate tissue

BPH, Gleason grade 3, 4 and 5 immunoreactive with ZAG on TMA cores: (A) BPH displaying strong expression of ZAG in epithelial cells [X100 Magnification], (B) Gleason grade 3 displaying moderate ZAG expression [X100 Magnification], (C) Gleason grade 4 displaying moderate/weak ZAG expression epithelial cells [X100 Magnification], (D) Gleason grade 5 displaying weak expression ZAG [X100 Magnification], (E) High power image of (i) tumour epithelium displaying weak difuse to granular ZAG expression and (ii) BPH epithelium displaying strong diffuse ZAG expression [X200 Magnification].

To statistically assess the hypothesis that ZAG expression is inversely associated with Gleason grade, 2 two-way contingency tables were set up as shown in Table 15, which classified the test variables into categories; Gleason grade 3 versus Gleason grade > 3 (G4 and G5) and Gleason grade 5 versus Gleason grade < 5 (G3 and G4). To test the association of the categories with immunohistochemical score (positive (2/3) and negative (0/1)) a Chi square test was performed on the contingency tables. The level of significance used for analyses was 0.01. Both tests gave highly significant two-sided P values of <0.0001. This suggests that ZAG expression is inversely associated with Gleason grade.

Table 15: Two-way Contingency tables comparing ZAG immunohistochemical scores (0/1 = Negative 2/3 = Positive)

Test	Histology	Score of ZAG 0/1	Score of ZAG 2/3
Gleason grade 3 vs. Gleason grade 4+5	Gleason grade 3 n = 418	176 (21%)	248 (30%)
Chi Square P value < 0.0001	Gleason grade >3 n = 408	270 (32%)	138 (17%)
Gleason grade 5 vs. Gleason grade 3+4	Gleason grade 5 n = 142	103 (12%)	39 (5%)
Chi Square P value < 0.0001	Gleason grade <5 n = 684	337 (41%)	347 (42%)
BPH vs. Tumour (G 3+4+5)	Normal/BPH n = 663	73 (5%)	590 (40%)
Chi Square P value < 0.0001	Cancer n = 826	440 (30%)	386 (26%)
BPH vs. Gleason grade 3	Normal/BPH n = 663	73 (6%)	590 (55%)
Chi Square P value < 0.0001	Gleason grade 3 n = 418	170 (16%)	248 (23%)

To determine if there is a statistical difference in association of ZAG expression in BPH epithelium and ZAG expression in prostate cancer epithelium another two way contingency table was set up as shown in Table 15 and a Chi square test was performed on the contingency table. The test gave a highly significant P value of < 0.0001 which supports the hypothesis

that there is a significant difference in expression of ZAG between BPH and prostate cancer.

Finally, a fourth two-way contingency table was set up as shown in Table 15 to determine if there was a significant difference in association of ZAG expression in BPH epithelium and Gleason grade 3 epithelium and a Chi square test was performed on the contingency table. Again the test returned a highly significant P value of < 0.0001 which supports the hypothesis that there is a significant difference in ZAG expression in BPH epithelium compared with Gleason grade 3 adenocarcinoma epithelium.

The presence of ZAG at the gene level was confirmed by TaqMan® Real-Time PCR as seen in 39. A significant fold decrease in ZAG gene expression was noted for Gleason grade 5 tumour cells compared with BPH, Gleason grade 3 and Gleason grade 4 cell populations. No fold decrease or increase in ZAG gene expression was noted among BPH, Gleason grade 3 and 4 cell populations.

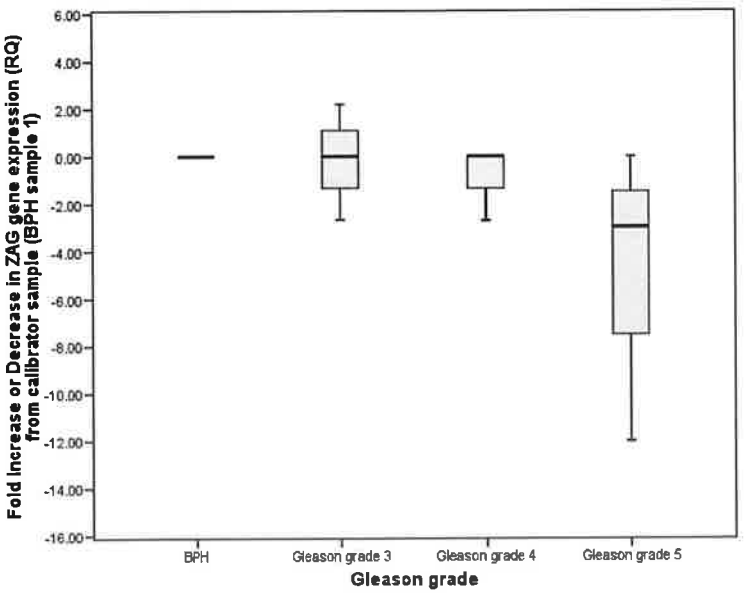

Figure 39: RQ Taqman data ($2^{-\Delta\Delta CT}$ method) graphically represented as a box plot

The box plot compares ZAG gene expression in BPH, Gleason grade 3, 4 and 5 as fold difference from the ZAG gene expression of the calibrator sample (BPH from case/sample 1).

3.4.2 KNG-1 Expression

KNG-1 immunostaining displayed inconsistent negative to weak expression in epithelial cells for both BPH and all Gleason grades. Where staining was observed, KNG-1 displayed granular cytoplasmic expression. No statistical significance was observed between BPH/normal and cancer or across the Gleason grades of prostate cancer.

KNG-1 was not present at the gene level in the 4 cases analysed by TaqMan® Real-Time PCR.

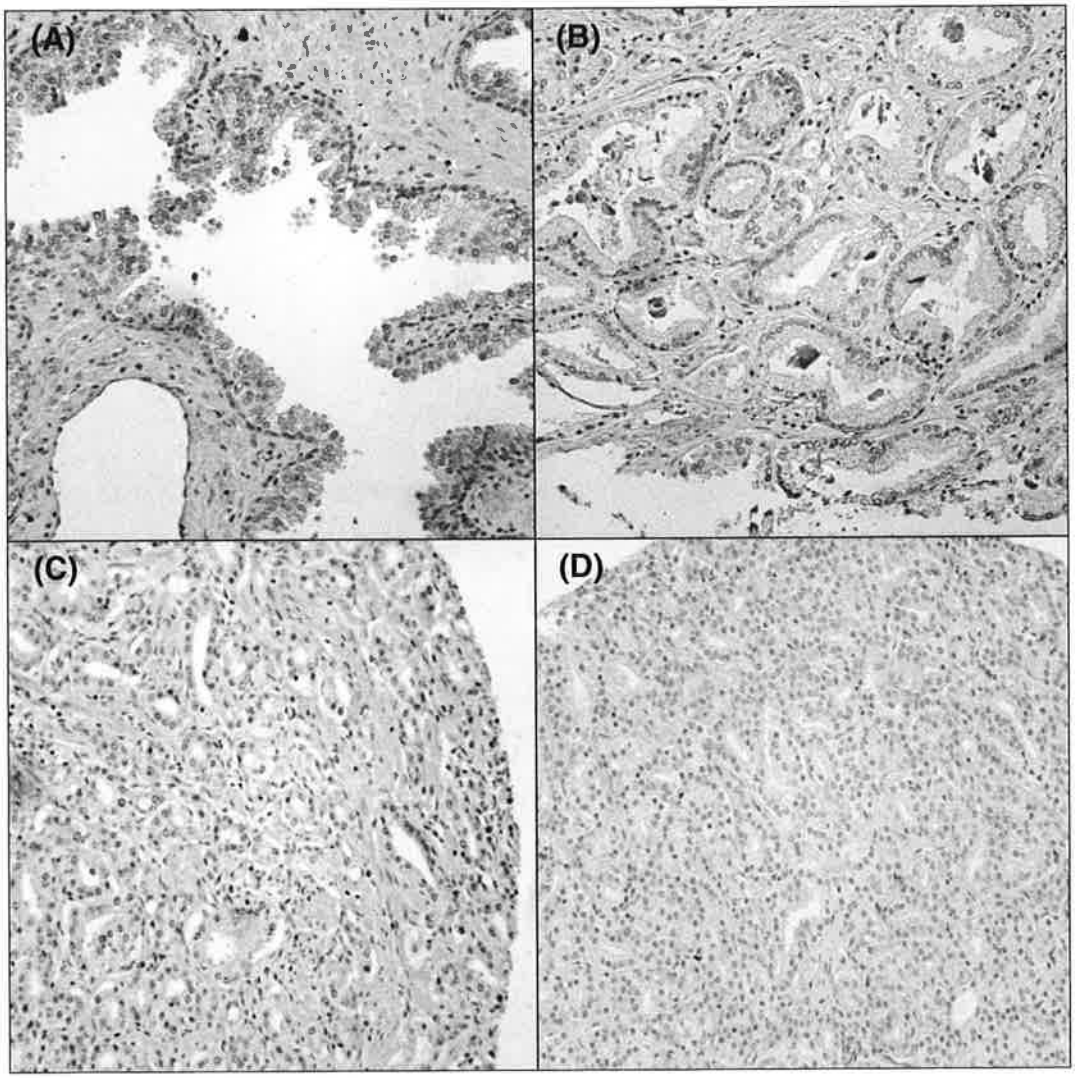

Figure 40: KNG-1 protein expression assessed by IHC on prostate tissue

(A) BPH lacking KNG-1 expression in epithelial cells (B) Gleason grade 3 lacking KNG-1 expression in epithelial cells (C) Gleason grade 4 lacking KNG-1 expression (D) Gleason grade 5 lacking KNG-1 expression [X200 Magnification].

3.4.3 VDBP Expression

VDBP could not be assessed at the protein level in tissue as no appropriate commercial antibody to VDBP applicable for IHC was available at the time of the study. However, mRNA analysis was carried out on 4 cases which contained BPH and all grades of prostate cancer (G3, G4 and G5). VDBP was not present at the gene level in the 4 cases analysed by TaqMan® Real-Time PCR as seen in Figure 41.

(A)

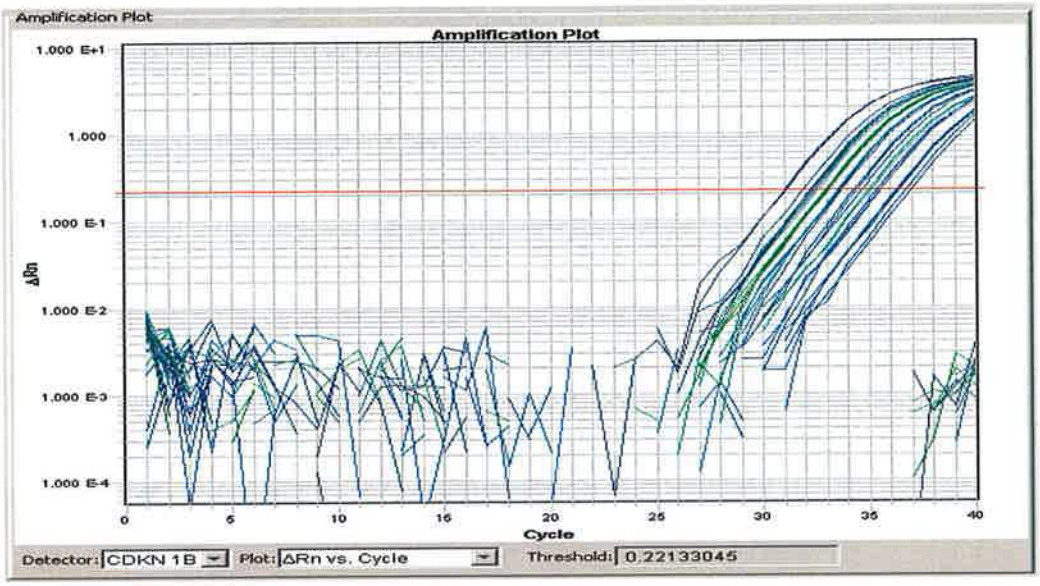

(B)

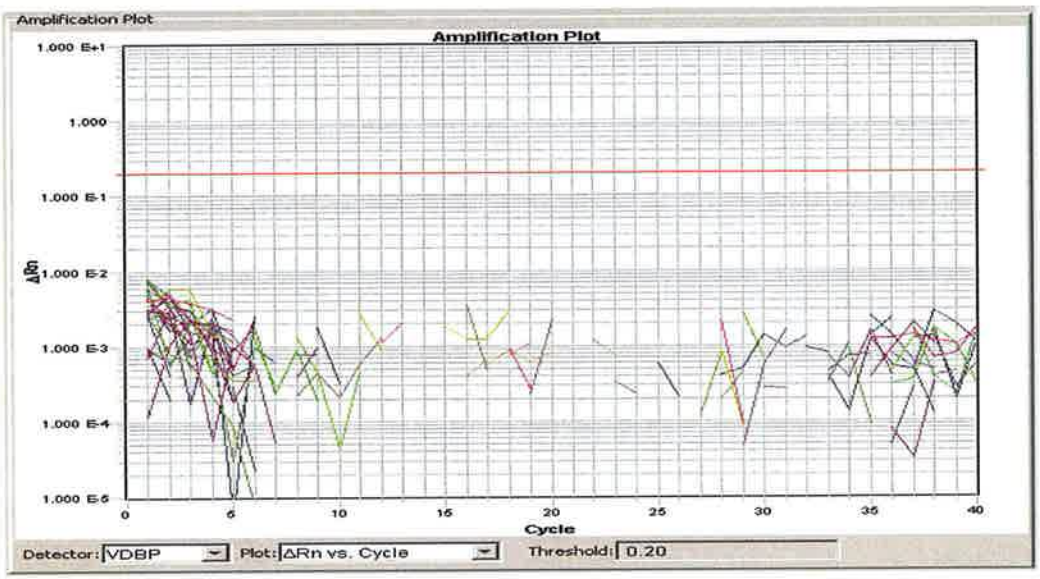

Figure 41: Taqman gene expression amplification Plots

(A) CDKN1B (Endogenous control) – All 4 cases (16 samples) expressing CDKN1B (crossing the threshold after approximately 32 PCR cycles)

(B) VDBP (Target gene) – All 4 cases (16 samples) did not express VDBP

3.4.4 PSMB-6 Expression

PSMB-6 IHC was negative in epithelial cells in both BPH and all grades of tumour. However, strong PSMB-6 protein expression was noted in stromal and inflammatory cells around BPH and tumour nests as shown in Figure 42.

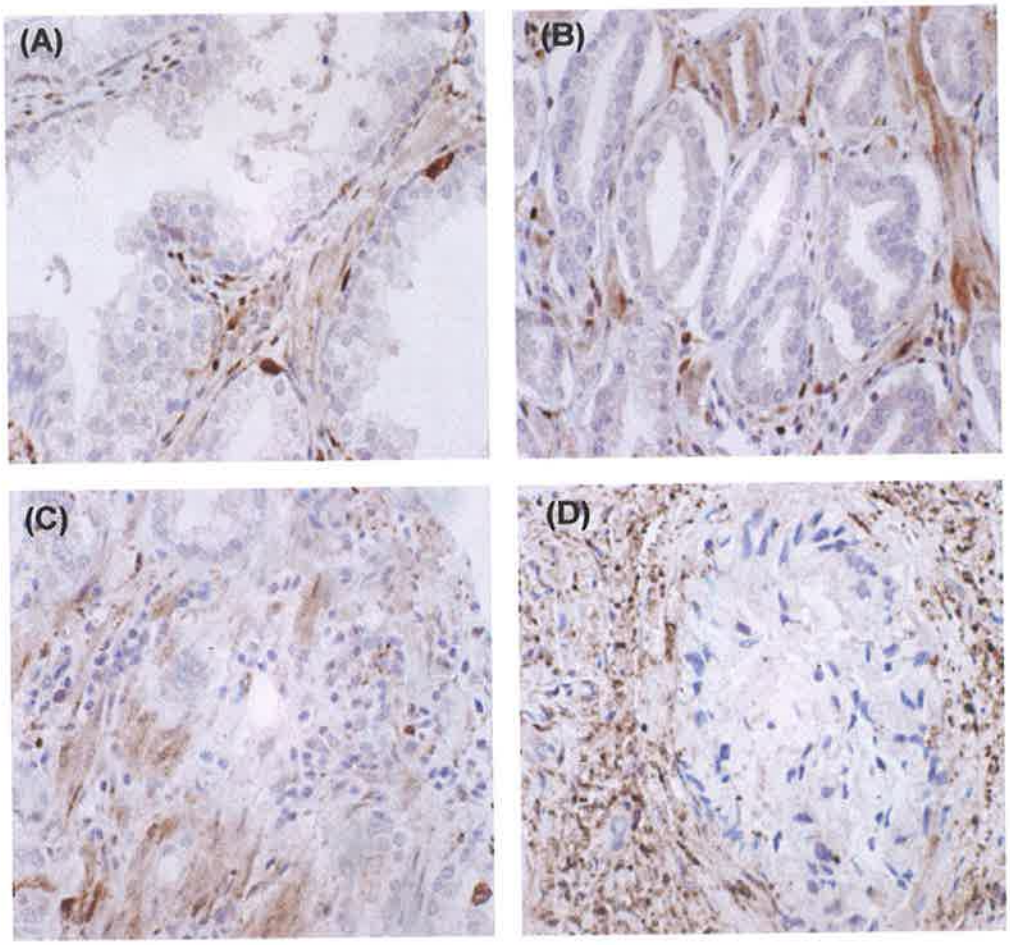

Figure 42: PSMB-6 protein expression assessed by immunohistochemistry on prostate tissue

BPH, Gleason grade 3, 4 and 5 immunoreactive with PSMB-6 on TMA cores: Epithelial cells lacking expression for PSMB-6 (Stromal cells positive) [X400 magnification]: (A) =BPH, (B) =G3, (C) =G4, (D) =G5.

Laser capture microdissection was used to extract areas of different histological grades of prostate cancer but did not separate tumour stroma from tumour epithelium. Therefore, a mixture of stroma and epithelium was extracted for mRNA analysis and confirmed PSMB-6 gene expression in all samples analyzed as seen in Figure 43. Overall no significant fold difference in the gene expression was noted between cases of BPH and all Gleason grades.

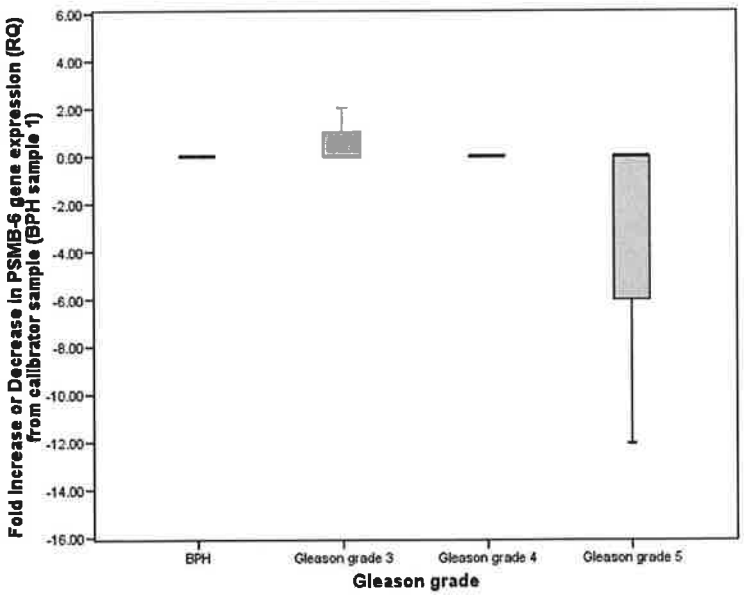

Figure 43: RQ Taqman data ($2^{-\Delta\Delta CT}$ method) graphically represented as a box plot

The box plot compares PSMB-6 gene expression in BPH, Gleason grade 3, 4 and 5 gene expression as fold difference from the PSMB-6 gene expression of the calibrator sample (BPH from case/sample 1).

3.5 Discussion

In this study, we investigated the tissue expression profiles of four proteins in prostate cancer; ZAG, KNG-1, VDBP and PSMB-6, which had been previously found to be up-regulated in the serum of prostate cancer patients with Gleason score 7 compared with Gleason score 5 following proteomic analysis by Byrne *et al.* (2009). The aim of this study was to characterise ZAG, KNG-1, VDBP and PSMB-6 expression in the different Gleason grades of prostate cancer (G3, G4 and G5) and BPH using immunohistochemical analysis and tissue microarray technology and Taqman® RT quantitative PCR to determine their role as potential biomarkers of prostate cancer.

The immunohistochemical evaluation of ZAG as a putative marker of prostate cancer has previously been demonstrated. However, conflicting conclusions exist among reports concerning ZAG as a prognostic marker of prostate cancer and predictive marker of Gleason grade. Gagnon *et al.* (1990) and Lapointe *et al.* (2004) found no association with ZAG expression and tumour stage or grade, whereas Hale *et al.* (2001) and Byrne *et al.* (2009) reported an association with tumour grade and decreased ZAG production. Descazeaud *et al.* (2006) found ZAG expression to have independent prognostic value for pT2N0M0 patients. Our study investigated the association of ZAG expression across the different Gleason grades of prostate cancer focussing alone on Gleason grade independent of Gleason score, tumour stage and recurrence.

The immunohistochemical results for ZAG show its expression in epithelial cells of the prostate was inversely associated with Gleason grade (BPH>G3>G4/G5). The results concur with previous observations by *Hale et al.* (2001) that ZAG production is associated with tumour differentiation status with decreased or absent ZAG expression in more poorly differentiated tumours. Intensity of immunoreactivity of ZAG was variable within the same Gleason grade between cases occasionally but there was no variability within cases. The decrease in ZAG tissue expression was not reflective of the increase in ZAG serum levels observed in prostate cancer by Byrne *at al.* (2009). These inverse results for tissue and serum were also observed by

Hale *et al.* (2001) where elevated levels of serum ZAG were observed relative to their normal age - and race - matched controls and a decrease in ZAG tissue expression was observed with increasing Gleason grade. This may be due to transformation in phenotype of normal epithelium to tumour epithelium resulting in leakage of ZAG into the serum or that the increase in serum ZAG is not prostatic in origin as suggested by Hale *et al.* (2001). It is also possible those metabolic alterations due to prostate cancer may result in its release from the liver (Tada *et al.*, 1991, Byrne *et al.*, 2009) or that the altered tissue expression may be a result of altered transcription of the ZAG gene. ZAG gene expression demonstrated a significant fold decrease in Gleason grade 5 tumours compared with BPH, Gleason grade 3 and Gleason grade 4 which supports the immunohistochemical data and the hypothesis that decreased ZAG expression is associated with high grade tumours. No fold decrease in ZAG gene expression was determined for Gleason grade 3 and 4 compared with BPH. However, the immunohistochemical scores of ZAG in BPH, Gleason grade 3 and 4 from the 4 cases used for mRNA analysis all had identical moderate expression of ZAG. This implies that the consistent gene expression of ZAG observed for BPH, Gleason grade 3 and 4 may be due to the particular cases selected and the low number of cases used for mRNA analysis.

The study of PSMB-6, VDBP and KNG-1 expression in prostate cancer is significant as these proteins have not been previously characterised in the disease. Therefore, their role as potential biomarkers has not been extensively determined.

Like ZAG, the results for KNG-1 were also not reflective of serum analysis. All cases showed either negative or sporadic weak expression in epithelial tissue for both BPH and prostate cancer. Its expression was inconsistent in prostate tissue for BPH and all grades of tumour, thus, no true association of staining was demonstrated for either BPH versus cancer or Gleason grade. It is possible that KNG-1 was not detected in prostate epithelium as its expression was below the immunohistochemistry detectable threshold. However, the presence of KNG-1 at a gene level was not confirmed by Taqman PCR which

may suggest that KNG-1 is not present in prostate tissue. KNG-1 plays an important role in blood coagulation as well as the kinin-kallikrein system so it is also possible that alterations in the blood due to prostate cancer may contribute to the increase in serum KNG-1 observed.

VDBP gene expression was not observed in either BPH or prostate cancer. This could suggest that VDBP is not expressed in prostate tissue. VDBP functions as a transporter of vitamin D metabolites in circulation and has an effect on inflammation so it is possible that the protein may only be found in circulation and that the reason for an increase in VDBP expression observed in serum samples between Gleason 5 and Gleason 7 patients by Byrne *et al.* (2009) may be due to alterations in the blood due to prostate cancer such as increased inflammatory cells in circulation. However, immunohistochemical evaluation of VDBP was not carried out on prostate tissue and the gene analysis was only carried out on 4 cases so the lack of VDBP gene expression may be due to case selection.

PSMB-6 protein expression was not observed in BPH or prostate cancer epithelium. It was, however, strongly expressed in stromal and inflammatory cells around BPH and tumour nests. The gene expression profile of PSMB-6 confirmed the presence of the protein and displayed no fold difference among BPH and all the Gleason grades. This PSMB-6 protein expression in stromal and inflammatory cells may explain its detection in serum from prostate cancer patients when analyzed by Byrne *et al.* (2009).

The results presented in this study raise some interesting issues. Although all markers showed an up-regulation in the serum of prostate cancer patients the markers did not behave the same way in the tissue. ZAG was found to be increased in the serum of prostate cancer patients but significantly decreased in tissue expression with increasing Gleason grade. This pattern of serum elevation with decreased tissue expression is very similar to that seen with PSA. At a tissue level, the ZAG expression profile would suggest that it is associated with increasing Gleason grade. However, there is significant overlap among Gleason grades and expression of ZAG so further studies with

larger patient cohorts need to be carried out with this marker to explore its potential role as a marker of grade progression. Although PSMB-6 was found to be up-regulated in the serum of prostate cancer patients it was found to be expressed in stromal and inflammatory cells only in the prostate cancer tissue indicating that PSBM-6 is not prostate specific. This suggests that PSMB-6 can be of no specific value in the serum to detect prostate cancer and may in fact be more a marker of inflammation.

Overall, these results highlight the importance of prostate tissue validation models in the assessment of prostate serum markers to determine whether serum markers are coming directly from the tumour. This principle is of relevance to all such studies attempting to identify disease-specific serum markers.

Chapter 4 - The role of SFRP-2 expression in Prostate Cancer

4.1 Summary

It is well established that cancer is a disease driven by progressive genetic and epigenetic abnormalities. Therapeutically, targeting epigenetic regulation of gene expression has become a very appealing topic of investigation in diseases such as cancer. Moreover, the detection and quantification of specific methylation patterns of genes in biopsies or bodily fluids such as urine and serum could be hugely beneficial diagnostically. As prostate cancer is an extremely heterogeneous disease both at the genetic and epigenetic level the use of a panel of methylated loci may potentially be used as a prognostic marker to identify prostate cancer that will progress to symptomatic or metastatic disease.

Following methylation analysis of Wingless signalling (Wnt) molecules and their antagonists using Quantitative Methylation-Specific PCR (QMSP), secreted frizzled related protein 2 (SFRP-2) was found to be highly methylated in prostate cancer. In this study the prostatic tissue expression of SFRP-2 is investigated at both a protein and mRNA level to determine whether there is a correlation between SFRP-2 methylation and SFRP-2 expression in prostate cancer.

Immunohistochemical analysis was performed on prostate cancer tissue microarrays with samples from 216 patients. Confirmatory gene expression profiling for SFRP-2 was performed on 8 cases using Laser Capture Microdissection and TaqMan® Real-Time PCR.

Strong to moderate SFRP-2 expression was observed in benign prostatic hyperplasia (BPH) epithelial cells and negative to weak SFRP-2 expression observed in tumour epithelium particularly Gleason grade 3 and 4. However, in Gleason grade 5 carcinoma there was a 40:60 split in the immunoexpression of SFRP-2, where 40% displayed strong to moderate SFRP-2 expression and 60% displayed negative SFRP-2 expression in epithelial cells. A morphological difference was noted in the Gleason grade 5 tumours that had strong to moderate expression of SFRP-2 (Type A) and the Gleason grade 5 tumours that had no SFRP-2 expression (Type B). It was also noted that biochemical

recurrence occurred after 5 years in patients that had strong to moderate SFRP-2 expression in Gleason grade 5 tumours with "Type A" morphology and no evidence of biochemical recurrence occurred in patients with negative SFRP-2 expression in Gleason grade 5 tumours with "Type B" morphology.

The preliminary results presented in this study propose SFRP-2 as a possible marker of histologically benign glands and a possible subgroup of Gleason grade 5 tumours that may predict prognosis and biochemical recurrence. However further methylation analysis and IHC is required on more Gleason grade 5 tumours with follow-up to confirm these results.

4.2 Introduction

4.2.1 Epigenetic abnormalities in Prostate cancer

It is well established that cancer is a disease driven by progressive genetic and epigenetic abnormalities. DNA methylation, histone modifications, nucleosome remodelling and gene targeting by micro RNAs are all epigenetic modifications. Epigenetic modifications in cancer manifest as both changes in chromatin packaging and changes in specific gene promoters that influence the transcription of genes important to the neoplastic process (Ting *et al.*, 2006). CpG methylation is a common biochemical modification of eukaryotic DNA. Hypermethylation of normally unmethylated gene promoters can inhibit transcription initiation by directly excluding transcription factors from binding to the promoter (Chalitchagorn *et al.*, 2004, Ehrlich, 2002, Jarrard *et al.*, 1995) and by attracting methyl-binding domain proteins (MBDs) that interact with both histone deacetylases (HDACs) and chromatin remodelling factors to bring about chromatin condensation, so the promoter becomes inaccessible to the transcriptional machinery. Targeting epigenetic regulation of gene expression has become a very appealing topic of investigation in diseases such as cancer therapeutically. Moreover, the detection and quantification of specific methylation patterns of genes in biopsies or bodily fluids such as urine and serum could be hugely beneficial diagnostically (Hoque *et al.*, 2004). Prostate cancer is an extremely heterogeneous disease. This applies both at the genetic and epigenetic level which suggests that the use of a panel of methylated loci may potentially be used as a prognostic marker to identify prostate cancer that will progress to symptomatic or metastatic disease. Several reviews have recently assessed the importance of epigenetics in prostate cancer initiation and progression (Brooks *et al.*, 1998, Kang *et al.*, 2004, Perry *et al.*, 2007). Promotor hypermethylation in prostate cancer is especially documented leading to silencing many classic tumour suppressor genes such as p16, APC, RASSF1A, as well as steroid hormone receptors like AR, ER, RARβ2, cell adhesion genes such as CD44, ECAD, TIG1,

TSLC1, cell cycle control genes including CCND2, CDKN4, 14-3-3-σ and anti-apoptotic genes such as DCR1, DCR2, DAPK, RTVP1 (Brothman *et al.*, 2005).

4.2.2 Wnt/Wingless signalling

The Wnt (wingless) signalling pathway is made up of a complex network of proteins that can regulate the production of Wnt signalling molecules. It is involved in diverse biological processes required for embryonic development and adult homeostasis including determination, proliferation, migration and differentiation (Verheyen and Gottardi, 2009). At least three distinct intracellular pathways induce Wnt signals; the Wnt/β-Catenin pathway, the Wnt/Ca^{2+} pathway and the Wnt/JNK pathway (Miller, 2002). The Wnt/β-Catenin pathway is known as the Canonical pathway and the Wnt/Ca^{2+} and the Wnt/JNK pathways are known as the Non-Canonical pathways. Wnt signal reception and transduction requires the binding of a Wnt molecule to members of two distinct families of cell surface receptors; the Fzd (Frizzled) gene family and the LRP (LDL-receptor related protein) family (Miller, 2002). Each Wnt pathway is activated by the binding of distinct sets of Wnt and Fzd ligand receptor pairs inducing a unique cellular response (Miller, 2002). Wnt1, Wnt3, Wnt3a, Wnt7a, Wnt7b, Wnt8 activate the Canonical pathway and the Non-Canonical pathways are activated by Wnt5a, Wnt4, Wnt11 (Pongracz and Stockley, 2006).

4.2.3 The Canonical Wnt signalling Pathway

The Canonical Wnt signalling pathway controls cell fate by regulating gene expression (Verheyen and Gottardi, 2009). The Canonical Wnt signalling pathway is activated when Wnt molecules bind to the Fzd and LRP5/6 coreceptors (Verheyen and Gottardi, 2009). This leads to the phosphorylation

of three domains of Dishevelled (Dsh), which is a family of cytosolic signal transducer molecules (Pongracz and Stockley, 2006). Activation of Dsh results in the phosphorylation and inhibition of glycogen synthase kinase 3 (GSK-3) which leads to stabilisation and consequently cytosolic accumulation of β-Catenin (Pongracz and Stockley, 2006). As a result the accumulated β-Catenin enters the nucleus to interact with members of the T Cell Factor (LEF1, TCF1, TCF3, TCF4) transcription factor family and transcription initiator p300 (Verheyen and Gottardi, 2009) which ultimately leads to gene activation. Matrix metalloproteinases (MMP2, MMP3, MMP7 and MMP9), cyclin D1, Cox-2, c-myc, c-jun, Fra-1 and VEGFR are some of the target genes involved in the Canonical β-Catenin pathway (Pongracz and Stockley, 2006). This pathway is summarized in Figure 44.

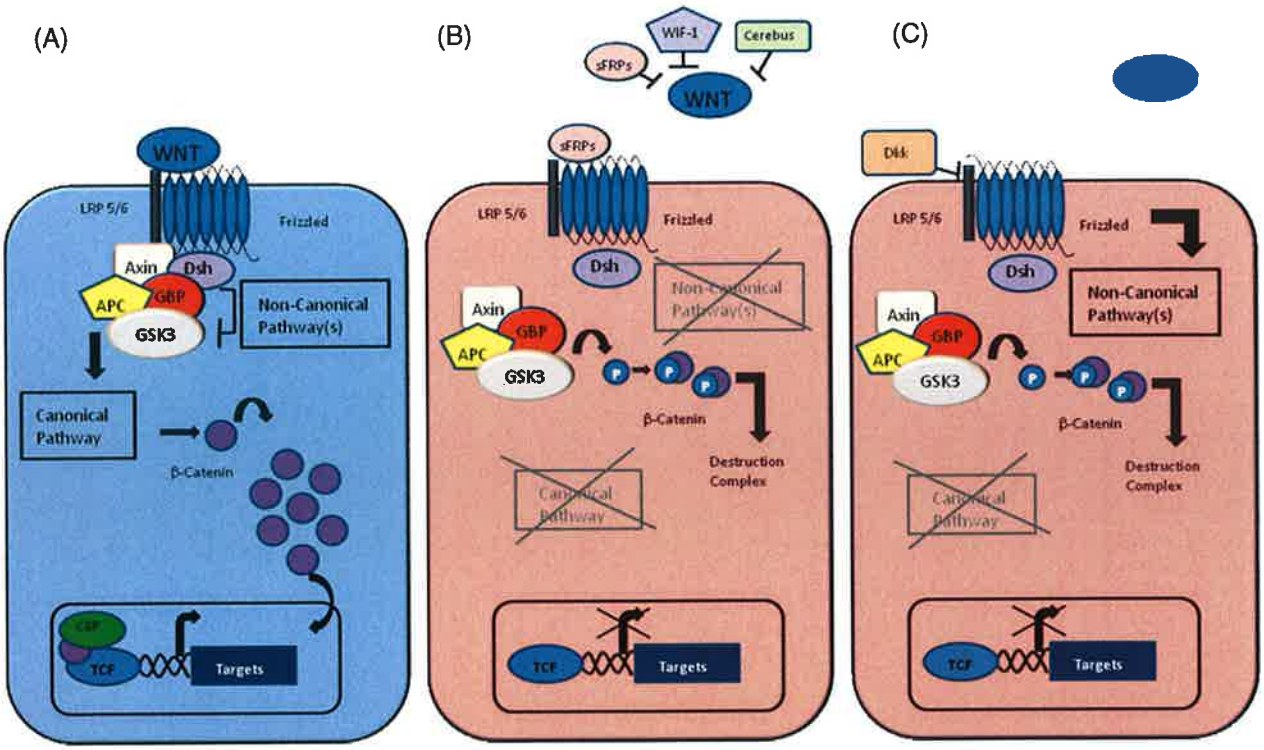

Figure 44: Wnt signal transduction pathways

(A) Wnts signal through Canonical & Non-Canonical pathways. Classic Wnt signalling (Wnt1, Wnt3, Wnt3a, Wnt7a, Wnt7b, Wnt8) causes dephosphorylation & stabilisation of β-Catenin, which then translocates to the nucleus and activates transcription of target genes (*c-myc*, *c-jun* and *cyclin D*). Non-Canonical Wnts (e.g. Wnt5a, Wnt4, Wnt11) activate other signalling pathways, such as the planar-cell-polarity like pathway that guides cell movement during gastrulation. (B) The sFRP class of Wnt antagonists bind directly to Wnts, thus blocking all Wnt signalling pathways. This leads to the phosphorylation of Beta-Catenin, which leads to its degradation through the ubiquitin proteosome pathway. (C) The Dkk class inhibits the Canonical Wnt cascade by binding to the LRP5/LRP6 component of the Wnt receptor complex.

4.2.4 The Non-Canonical Wnt signalling pathways

The Non-Canonical Wnt signalling pathways (see Figure 45), like the Canonical pathway, are activated by Wnt-Fzd binding but differ in their dependency on the type of G-protein they require for activation (Pongracz and Stockley, 2006). The Non-Canonical Wnt pathways do not signal through β-Catenin and also do not require phosphorylation of all three domains of Dsh for signal transduction. The two Non-Canonical pathways have the ability to antagonise the functions of Canonical Wnts (McDonald and Silver, 2009), can activate different signalling cascades and trigger the transcription of different gene-sets (Pongracz and Stockley, 2006).

4.2.4.1 The Non-Canonical Wnt/Ca^{2+} Pathway

The Non-Canonical Wnt/Ca2+ pathway controls protein kinase C (PKC) and calcium/calmodulin-dependent kinase II (CamKII) and regulates cell adhesion and motility (Schwarz-Romond *et al.*, 2002). The Wnt/Ca2+ pathway releases intracellular calcium following Wnt binding to a Fzd receptor resulting in the activation of enzymes such as CamKII, PKC and calcineurin before the activation of Nuclear factor of activated T-cells (NFAT) occurs. NFAT is a family of transcription factors who can regulate activation induced transcription of several immunologically important genes including interleukin-2, -4, IFN-γ, and TNF-α (Pongracz and Stockley, 2006).

4.2.4.2 The Non-Canonical Wnt/JNK Pathway

The Non-Canonical Wnt/JNK pathway depends on cJun N-terminal kinase (JNK) activity and controls cytoskeletal rearrangements (Schwarz-Romond *et al.*, 2002). The Wnt/JNK pathway is similar to the Wnt/Ca2+ pathway in utilizing Frizzled receptors and Dsh. Activation of Dsh leads to JNK and in

turn to AP1 activation (Pongracz and Stockley, 2006). AP1 is a complex of smaller proteins such as cJun, JunB, JunD, cFos, FosB, Fra1, Fra2, ATF2 and CREB which form homo and heterodimers to select gene targets for activation (Pongracz and Stockley, 2006).

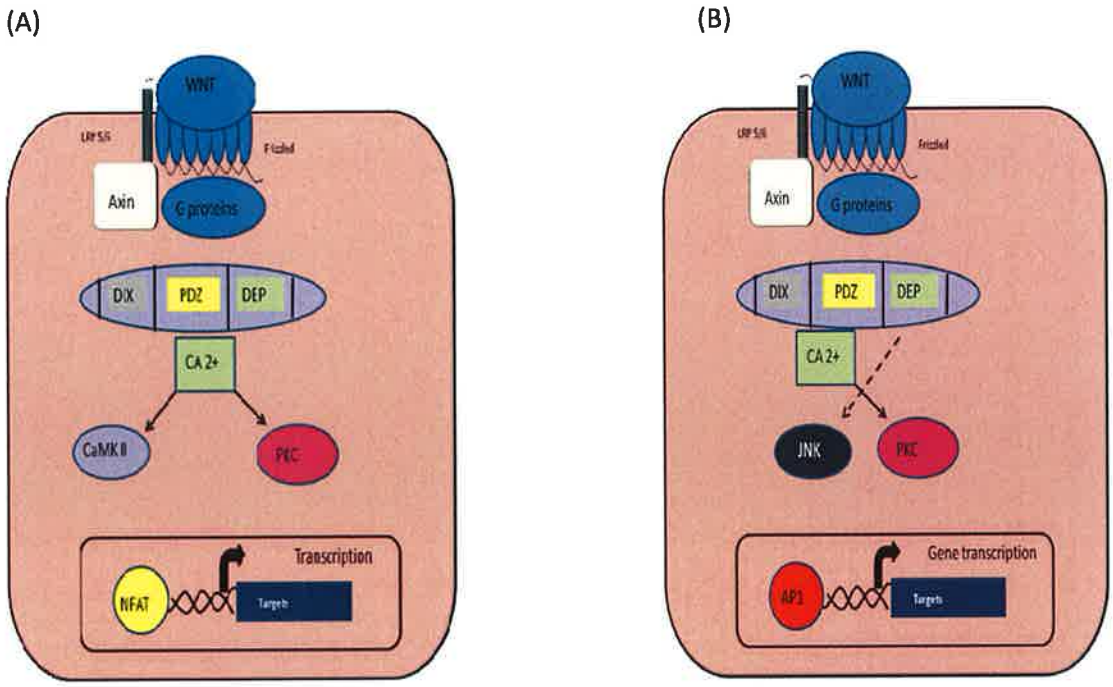

Figure 45: The Non-Canonical Wnt Signalling pathways

(A) The Non-Canonical Wnt/Ca2+ pathway

(B) The Non-Canonical Wnt/JNK pathway

4.2.5 Regulation of Wnt signalling pathway

The Wnt signalling pathway is tightly controlled by secreted extracellular (DKKs, SFRPs, WIF, CER) and intracellular, both cytosolic (ICAT, Nkd) and nuclear (Sox17), signal modulators (Pongracz and Stockley, 2006). There is also cross talk between the two Wnt Canonical pathways; the Non-Canonical pathways have the ability to antagonise the functions of the Canonical pathway. Regulation of Wnt signalling is also controlled through inhibitory Fzd pathways for example Fzd 1 inhibits Wnt signalling through a G-protein dependent manner and Fzd 6 inhibits Wnt dependent gene transcription through activating a calcium dependent signalling cascade (Pongracz and Stockley, 2006).

4.2.6 Secreted Frizzled Related Protein (SFRP) Family and SFRP-2

SFRPs are soluble modulators of Wnt signaling. The SFRP family, which is the largest family of Wnt inhibitors, is made up of five members; SFRP-1, SFRP-2, SFRP-3, SFRP-4 and SFRP-5. SFRP-1, SFRP-2 and SFRP-5 are encoded by exons on chromosomes 8p12-p11.1, 4q31.3 and 10q24.1 respectively and SFRP-3 and SFRP-4 are encoded by six exons on chromosomes 2q31-q33 and 7p14-p13, respectively (Bovolenta *et al.*, 2008).

SFRPs are modular proteins which fold into two separate domains (Bovolenta *et al.*, 2008). Their N-terminus contains a secretion signal peptide followed by a cysteine rich domain (CRD) which is composed of ten cysteine residues at conserved positions (Bovolenta *et al.*, 2008). These ten cysteine residues form a pattern of disulphide bridges identical to the extracellular CRD domains of Fzd (Bovolenta *et al.*, 2008). The C-terminal part of SFRP proteins contains segments of positively charged residues which confer heparin-binding and six cysteine residues that form three disulphide bridges (Bovolenta *et al.*, 2008). Post-translational modifications also contribute to differences that may further diversify the functions of the different SFRP family members (Bovolenta *et al.*, 2008).

Wnt antagonists, including SFRP-2, inhibit Wnt signalling by binding to Wnt ligands via their CRD preventing them from binding to Fzd receptors (Kawamoto *et al.*, 2008). Not only are SFRPs negative modulators of Wnt signalling they can also antagonise one another's activity, bind to Fzd receptors and provide axon-guidance information, interact with other receptors or matrix molecules and interfere with bone morphogenetic protein (BMP) signalling by acting as proteinase inhibitors (Bovolenta *et al.*, 2008). Carcinogenesis can result from the functional loss of Wnt antagonists through dysregulation of cell proliferation (Kawamoto *et al.*, 2008). The expression levels of SFRPs are altered in different types of cancers such as bone pathologies, retinal degeneration and hypophosphataemic diseases which suggests SFRP activity is fundamental for tissue homeostasis (Bovolenta *et al.*, 2008).

4.2.7 Identification of secreted frizzled related protein-2 (SFRP-2) hypermethylation in Prostate cancer

Recent methylation analysis of Wnt molecules and their antagonists by the epigenetic biomarker discovery group (Prostate Molecular Oncology, Institute of Molecular Medicine, Trinity College Dublin) within the PCRC using Quantitative Methylation-Specific PCR (QMSP) revealed hypermethylation of Wnt antagonist SFRP-2 (Secreted Frizzled-Related Protein 2) in 65% (48/74) of pooled tumours, 30% (6/20) of high-grade prostatic intraepithelial neoplasia, 11% of BPH glands from prostate cancer patients and 9% (7/69) of histologically benign tissues from patients with no evidence of prostate cancer (see Figure 46(A)). Individual Gleason grades (G3, G4 and G5 areas) were also microdissected from 33 patients to assess SFRP-2 methylation by QMSP within the individual Gleason grades of prostate cancer. Overall, 73% (24/33) of patients displayed SFRP-2 methylation in at least one tumour focus. Within individual grades, there was a slight trend in methylation frequency with hypermethylation more frequent in low grade rather than high grade disease (P=0.39) (Figure 46 (C)).

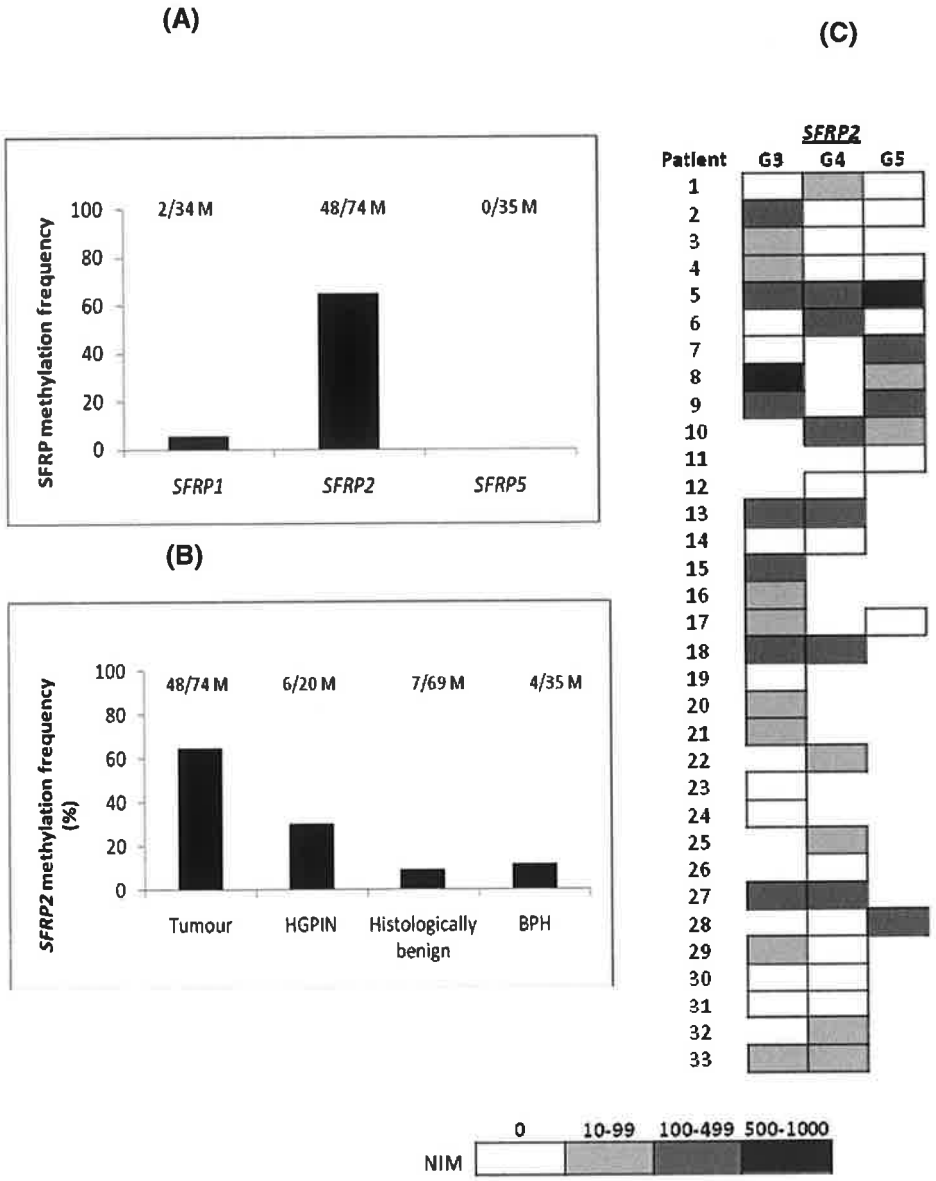

Figure 46: Methylation frequency in Prostate cancer by QMSP (Unpublished data)

(A) SFRP methylation frequency in Prostate cancer tissue.

(B) SFRP-2 methylation frequency in tumour tissue samples (pooled Gleason grades) from 74 patients, high grade PIN from 20 patients, histologically benign glands from 69 patients with no evidence of prostate cancer and BPH from 35 patients with prostate cancer.

(C) Analysis of SFRP-2 NIM (Normalized Index of Methylation) in individual Gleason grades.

4.2.8 Aim

The aim of this study is 3-fold:

(i) To investigate the prostatic tissue expression of SFRP-2 at both a protein and mRNA level to determine if there is a correlation between SFRP-2 methylation and SFRP-2 expression in prostate cancer tissue.

(ii) To establish if there is a difference in the expression of SFRP-2 between prostatic tumour tissue and BPH.

(iii) To determine if there is a difference in the expression of SFRP-2 across the different Gleason grades of prostate cancer.

4.3 Materials and Methods

4.3.1 Sample Collection/Tissue Microarray Construction

Two hundred and sixteen prostate cancer cases (age range 43-74 years) were obtained from the Beaumont Hospital, St. James's Hospital and the Mater Misericordiae University Hospital Histopathology archives dating from 2002 - 2008. The 216 cases included a variety of Gleason scores ranging from 5 to 10. Suitable formalin fixed paraffin embedded blocks of each case representing as many Gleason grades as possible were selected. The corresponding Haematoxylin and Eosin (H&E) stained sections were reviewed by a Pathologist. Three 1mm cores of benign prostatic hyperplasia (BPH) and Gleason grade 3, 4 and 5 carcinoma were taken from every case where available. The tissue microarrays were assembled using the Beecher Instruments Tissue-Arrayer^{TM} (Beecher Instruments, Silver Spring, MD).

For control purposes, benign prostatic hyperplasia (BPH) lesions from 37 men with no diagnosis of prostate cancer that underwent transurethral resection (TURP) of the prostate were also collected from the Adelaide & Meath Hospital, Incorporating the National Children's Hospital.

In order to ensure that the SFRP-2 expression observed on the TMAs was a true representative of SFRP-2 expression on prostate whole sections and not misrepresented by the heterogeneous nature of the prostate or sampling, whole sections from 13 of the 216 cases were selected on which to perform IHC. Representative whole sections of histologically benign glands and every Gleason grade present in the case were selected for analysis and for 5 of the 13 cases representative sections from both lobes of the prostate (left and right) were analysed.

Post operative PSA data was obtained for 22 patients from the cohort (10 of these patients had Gleason grade 5 tumours) to assess for biochemical recurrence.

4.3.2 Validation of SFRP-2 antibody (HPA002652, Prestige Antibodies)

To confirm specificity of the SFRP-2 antibody (HPA002652, Prestige Antibodies), it was subjected to Western blot analysis. Two Western blots were performed. The first Western blot was performed testing the antibody using a recombinant mouse SFRP-2 protein (Sino Biological Inc) which is 100% homologous with the human SFRP-2 protein to ensure that the antibody was specific for SFRP-2. The immunogen used to generate the antibody by Prestige Antibodies (SFRP-2 peptide conjugated to albumin binding protein (Larsson *et al.*, 1996)) was also tested in parallel with the unconjugated mouse recombinant SFRP-2 to ensure that the polyclonal antibody was specific for SFRP-2 alone and not albumin binding protein (ABP). The second was performed testing the antibody using prostate BPH and PC-3 cell lines.

4.3.2.1 SFRP-2 peptides

4.3.2.1.1 Recombinant mouse SFRP-2 protein

The recombinant mouse SFRP-2 protein (50028-M08H, Sino Biological Inc) used in the Western blot analysis is 100% homologous with the human SFRP-2 protein sequence below:

The recombinant mouse SFRP-2 consists of 282 amino acids after removal of the signal peptide and has a predicted molecular mass of 32.5 kDa.

4.3.2.1.2 SFRP-2 fusion protein conjugated to Albumin Binding Protein (ABP)

A SFRP-2 peptide conjugated to 6 Histidine-Albumin binding protein (His_6ABP) was kindly donated to us by the Human Protein Atlas - Prestige Antibodies (Sigma-Life Sciences and Atlas Antibodies). The SFRP-2 sequence is 118 amino acids and has position 162-282 on SFRP-2 (NCBI

gene ID: 6423). The conjugated SFRP-2 peptide was synthesised by Human Protein Atlas by cloning the SFRP-2 DNA sequence to the SFRP-2 amino acids 162-282 into a pT7-ABP vector which then was transformed into BL-21-DE3 *E .coli* cells to be expressed (Larsson *et al.*, 1996). The DNA fragment encoding the ABP in the pT7-ABP vector corresponds to the human serum albumin (HSA) binding region of streptococcal protein G (residues 146-266) (Larsson *et al.*, 1996). Therefore, purification of the fusion proteins was performed using HSA sepharose beads (Larsson *et al.*, 1996). ABP was chosen as the conjugate protein for the SFRP-2 fusion protein by human protein atlas for a number of reasons; (i) it is relatively small (18 kDa), which ensures a high product to tag ratio; (ii) its highly specific interactions for its ligand (HSA) enables efficient purification by affinity chromatography; (iii) it allows efficient recovery of gene products of low solubility since affinity chromatography can be performed after guanidine hydrochloride/urea mediated solubilisation and renaturing of precipitated products; (iv) ABP can be detected by blotting techniques after SDS-PAGE analysis by taking advantage of its HSA binding properties (using biotinylated HSA and conjugated streptavidin-alkaline phosphatase); (v) it is proven to be highly stable to proteolysis and contains no cysteins which could cause formation of unwanted disulfide-bridges complexes (Larsson *et al.*, 1996). The molecular mass of the SFRP-2 peptide and ABP conjugate were 14 kDa and 18 kDa respectively. The total SFRP-2 peptide sequence (in red) including the His_6ABP (in black) was as follows;

MGSSHHHHHHSSGLVPRGSHMASLAEAKVLANRELDKYGVSDYHKNLINN
AKTVEGVKDLQAQVVESAKKARISEATDGLSDFLKSQTPAEDTVKSIELAEA
KVLANRELDKYGVSDYYKNLINNAKTVEGVKALIDEILAALPGTFAHYMDPNS
SSVDKLAAATEEAPKVCEACKNKNDDDNDIMETLCKNDFALKIKVKEITYINR
DTKIILETKSKTIYKLNGVSERDLKKSVLWLKDSLQCTCEEMNDINAPYLVMG
QKQGGELVITSVKRWQKGQRE

4.3.2.2 Western Blot analysis using recombinant mouse SFRP-2 (50028-M08H, Sino Biological Inc) and an SFRP-2 peptide conjugated to ABP

Loading buffer was added to 30 µl of the samples (final concentration of 50µg of the mouse recombinant SFRP-2 protein and 100µg of the SFRP-2 peptide conjugated to ABP) and they were then boiled at 95°C for 5 min. Two SDS gels were run, as described in section 2.5.1.1.8. However, Coomassie blue stain was not applied to the second gel upon completion, as described in section 2.5.1.1.8. Instead the samples from the second gel were transferred to nitrocellulose paper and a Western blot using anti-SFRP-2 (HPA002652, Prestige Antibodies) was carried out, as described in section 2.5.1.1.9.

4.3.2.2 Western Blot analysis using BPH and PC-3 Cell lines

4.3.2.2.1 Cell Culture

Confluent PC-3 and BPH cell lines were kindly donated by the epigenetic biomarker discovery group within the PCRC (Prostate Molecular Oncology, Institute of Molecular Medicine, Trinity College Dublin). Both cell lines were maintained and cultured by the epigenetic biomarker discovery group in RPMI 1640 medium (Gibco, Paisley, UK) supplemented with 10% foetal calf serum (Globepharm Guildford, UK) and 1% streptomycin-penicillin (Gibco). Cells were routinely grown and passaged in 75 cm^2 vented tissue culture flasks at 37°C in a humidified atmosphere of 5% CO_2 until confluent.

4.3.2.2.2 Cell Lysis

Cells were plated onto 10 cm culture dishes and medium was poured off. Culture dishes were then placed on a tray of ice and 1 ml of PBS was added to the plates for I minute. Cells were then scraped to the edge of the plate and pipetted into ice cold 1.5 mL tubes. The tubes were then centrifuged at

3,220 x g for 30 seconds at 4°C. The supernatant was removed and pellet vortexed to break up the pellet. The pellet was then resuspended in 100 µl M2 lysis buffer (see Table 16), vortexed briefly and allowed to stand on ice. It was then sonicated on ice using the appropriate setting (power 10 for 10 seconds using a Sanyo Soniprep 150) centrifuged at 12,465 x g for 15 mins at 4°C and this process was repeated 3 times. The supernatant was then transferred to fresh 1.5mL tubes on ice. A Bradford assay was performed and absorbance of the sample was measured using a spectrophotometer.

Table 16: M2 Lysis Buffer Composition

Reagent	Stock Concentration	To make 200ml
20 mM Tris pH 7.6	1 M	4 ml
0.5% NP40	–	1 ml
250 mM NaCl	3 M	16.6 ml
EDTA	–	0.22 g
EGTA	–	0.23 g

4.3.2.2.3 Chemiluminescent Western Blot analysis

Loading buffer was added to 30 µl (final concentration of 500 µg) of the BPH and PC-3 cell line samples and they were then boiled at 95 °C for 5 min. An SDS PAGE gel was run, as described in section 2.5.1.1.8. However, Coomassie blue stain was not applied to the gel upon completion, as described in section 2.5.1.1.8. Instead the samples from the gel were transferred to nitrocellulose paper and a Western blot using anti-SFRP-2 (HPA002652, Prestige Antibodies) was carried out, as described in section

2.5.1.1.9. TBS and TBST were used to wash the membrane instead of PBS and PBST and 5% milk TBS was used in the blocking steps instead of 3% BSA PBS. Bands were detected using a chemiluminescent substrate, ECL (Amersham Biosciences, UK).

4.3.3 Immunohistochemistry

Immunohistochemistry was performed on the paraffin-embedded 4μm tissue microarray sections using an automated Immunohistochemistry (IHC) platform (Bond Max™ - Leica Microsystems), as described in section 2.2.4. Table 17 shows the optimal antigen retrieval and optimal concentrations of primary antibodies determined for immunohistochemistry. Sections were counterstained with haematoxylin.

Table 17: Optimal antigen retrieval and optimal concentrations of primary antibodies determined for immunohistochemistry

Protein	Antibody	Antibody Company	Optimal Dilution	Optimal Epitope Retreival for Bond Max™ - Leica Microsystems
SFRP-2	HPA002652	Atlas Antibodies (Prestige Antibodies®)	1\100	ER 1 for 10 min
PSA	A0562	DAKO	1\15,000	ER 1 for 20 min
Synaptophysin	0776	DAKO	1\20	ER 1 for 20 min

4.3.4. Scoring of SFRP-2 Protein Expression

Immunoreactivity for SFRP-2 was assessed in benign prostatic hyperplastic epithelium and tumour epithelium across all Gleason grades. For the purpose of statistical analysis, immunoexpression of the proteins was graded according to the following scales: 0, absence of reactivity in > 10% of epithelial cells, 1, faint but clearly detectable reactivity in > 10% of epithelial cells, 2, moderate reactivity in >10% of epithelial cells and 3, strong reactivity in >10% of epithelial cells.

4.3.5 Statistical Analysis

Often more than one histological grade of prostate tissue was present on a single TMA core. Due to this, individual cores were not scored for immunohistochemical staining as a whole; instead the different histological areas present on the core representing more than 10% of the core were graded separately. Thus, altogether 1603 histological areas/Gleason grades were scored for each variable (699=BPH, 439=G3, 321=G4 and 144=G5).

For statistical analysis of immunoreactivity of SFRP-2 versus histopathological features the staining intensity of the epithelial cells was divided into two groups: low expression (immunohistochemical score of 0 or 1) included those with negative or weak reactivity, and high expression (immunohistochemical score of 2 or 3) included those with moderate or strong reactivity. Chi square tests were performed on contingency tables using GraphPad INSTAT-3^{TM} software version 3.02 (Graph Pad Software Inc^{TM}, San Diego, USA) to test the association of the prostate cancer samples, BPH samples and tumour grade with immunohistochemical score (positive (2/3) and negative (0/1)).

4.3.6 Laser Capture Microdissection, total RNA extraction and Taqman PCR

To validate the immunohistochemical results, eight of the 216 prostate cancer cases were selected on which to perform mRNA analysis. Areas of BPH and all Gleason grades of tumour (Gleason grade 3, 4 and 5) were present on each of the 8 cases selected. Laser capture microdissection, RNA extraction and Taqman PCR were carried out on 7μm whole sections from the 4 cases, as described in section 2.4.5, using assay context sequences described in Table 18.

Table 18: TaqMan® context sequences of primers and probes designed by Applied Biosystems, Foster City, CA

Reaction	Context Sequence	Assay I.D.
SFRP-2 (FAM labelled) TaqMan®	CAGCCACCGAGGAAGCTCCA AAGGT	*Hs00293258_m1
CDKN1B (FAM labelled) TaqMan®	AACCGACGATTCTTCTACTCA AAAC	*Hs00153277_m1

*Suffix "_m" indicates that the assay's probe spans an exon junction and will not detect genomic DNA

4.4 Results

4.4.1 Validation of Polyclonal SFRP-2 antibody (HPA002652, Prestige Antibodies)

An SDS-PAGE (Figure 47(A)) was run in parallel with the Western blot (Figure 47 (B)) to ensure the SFRP-2 protein was present and to give an approximate location of where the band on the Western blot should be located. In lane 2 of the SDS-PAGE gel clean bands were observed at approximately 33 kDa (approximate molecular mass of the mouse recombinant SFRP-2) and at approximately 80 kDa. However, the SFRP-2 antibody (HPA002652, Prestige Antibodies) only detected the band at 33kDa in lane 2 on the Western blot (Figure 47 (B)) which indicates that the antibody is specific for SFRP-2. In lane 3 a clean band was observed at approximately 31 kDa (approximate molecular mass of the SFRP-2 peptide conjugated to ABP) and a weak band is observed at approximately 60 kDa on the SDS-PAGE. The 31 kDa protein in lane 3 was detected by the SFRP-2 antibody (HPA002652, Prestige Antibodies) on the Western Blot (Figure 47 (B)) and a weak smear was observed at 61 kDa.

The PC3 cell line had been tested by immunohistochemistry previously to ensure there was SFRP-2 in the cell line (data not shown). However, the BPH cell line was not tested by immunohistochemistry. The SFRP-2 antibody (HPA002652, Prestige Antibodies) detected a very weak band was at 38kDa (approximate molecular mass of human SFRP-2 protein) in the BPH cell line in lane 1 (Figure 47 (D)). In lane 2 (PC-3 cell line) the SFRP-2 antibody detected a strong band at 38 kDa also.

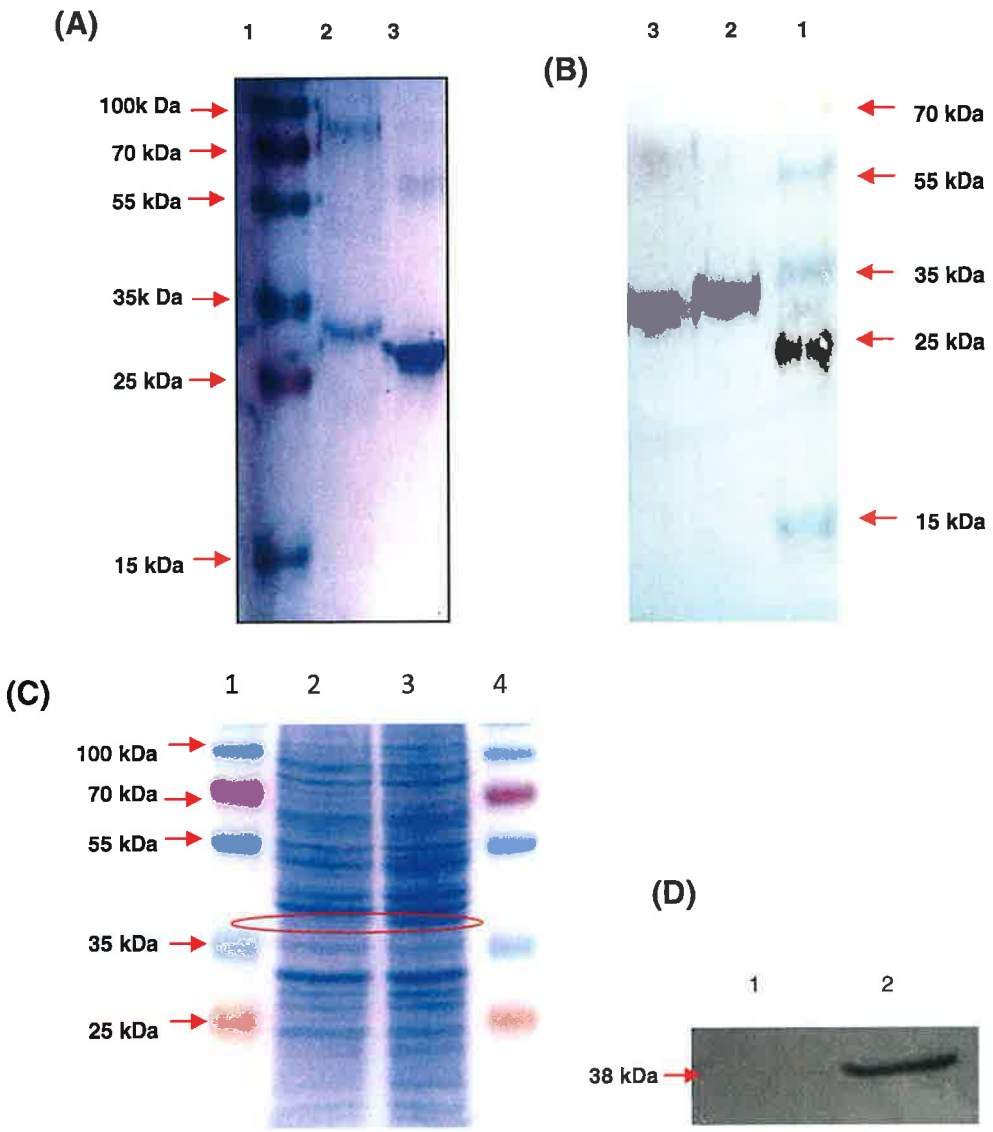

Figure 47: Western Blot analysis to validate SFRP-2 antibody

(A) SDS PAGE Gel: Lane 1 represents the fermentas pageruler^{TM}prestained marker for protein size determination, lane 2 represents the mouse recombinant SFRP-2 and lane 3 represents the SFRP-2 peptide conjugated to ABP. **(B) WESTERN BLOT using TMB chromogenic substrate detection:** Lane 1 represents the fermentas pageruler^{TM}prestained marker for protein size determination, lane 2 represents the mouse recombinant SFRP-2 and lane 3 represents the SFRP-2 peptide conjugated to ABP. **(C) SDS PAGE Gel:** Lane 1 and 4 represent the fermentas pageruler^{TM}prestained marker for protein size determination, lane 2 repersents BPH cell line and lane 3 represents PC-3 cell line. **(D) WESTERN BLOT using chemiluminescent blotting substrate (ECL) and X-ray film detection:** Lane 1 represents BPH cell line and lane 2 represents PC-3 cell line.

4.3.2 SFRP-2 protein expression

4.4.2.1 SFRP-2 is expressed in the cytoplasm of benign prostate epithelium and lost in low grade prostate tumours

In total, 13 TMAs were constructed from 216 prostate cancer patients. Immunohistochemical expression of SFRP-2 was first analyzed by histological area: either BPH or tumour. SFRP-2 expression was observed in the cytoplasm of prostate epithelial cells. The majority (77%) of BPH areas displayed moderate/strong (score 2/3) expression (Figure 48). By comparison, only 23% of tumour areas stained positively ($P<0.0001$). Further analysis across a spectrum of tumour grades revealed significant differences in expression between different Gleason grades. Acini of G3 and G4 largely displayed negative/weak (score 0/1) expression, whereas 40% of G5 acini showed moderate/strong expression ($P< 0.0001$).

The immunohistochemical score for the three TMAs cores taken from each histological feature (BPH and G3, G4 and G5 tumours) per case were next averaged to produce one score for each diagnostic entity/patient. The results were consistent with the analysis of individual areas. Eighty five percent of patients with moderate/strong SFRP-2 expression in their BPH glands displayed negative/weak expression in adjacent G3 acini. Ninety three percent of patients with negative/weak expression in their G5 acini also showed negative/weak SFRP-2 expression in G3 and/or G4 acini. Of note, 79% of patients who had positive immunostaining in their G5 acini had negative/weak immunostaining in their adjacent G3 and/or G4 acini.

Strong/moderate SFRP-2 expression was observed in epithelial cells of BPH glands on 95% of TURPs from patients with no evidence of prostate cancer.

To ensure that the SFRP-2 expression observed on the TMAs was truly representative of the entire prostate gland and not unduly influenced by the heterogeneous nature of prostate disease or by sampling error, whole

sections from 13 patients were also analyzed. In support of the TMA data, moderate/strong expression was observed in BPH epithelial cells, negative/weak immunoreactivity was detected in G3 and G4 acini, while G5 acini had moderate/strong expression in 6/12 sections. The immunohistochemical scores for SFRP2 on the whole sections showed 100% concurrence with those obtained for the corresponding TMAs for every case. In addition, identical SFRP-2 immunoexpression in corresponding histological grades in both left and right lobes of the prostate were noted in 5 cases selected for multifocal analysis.

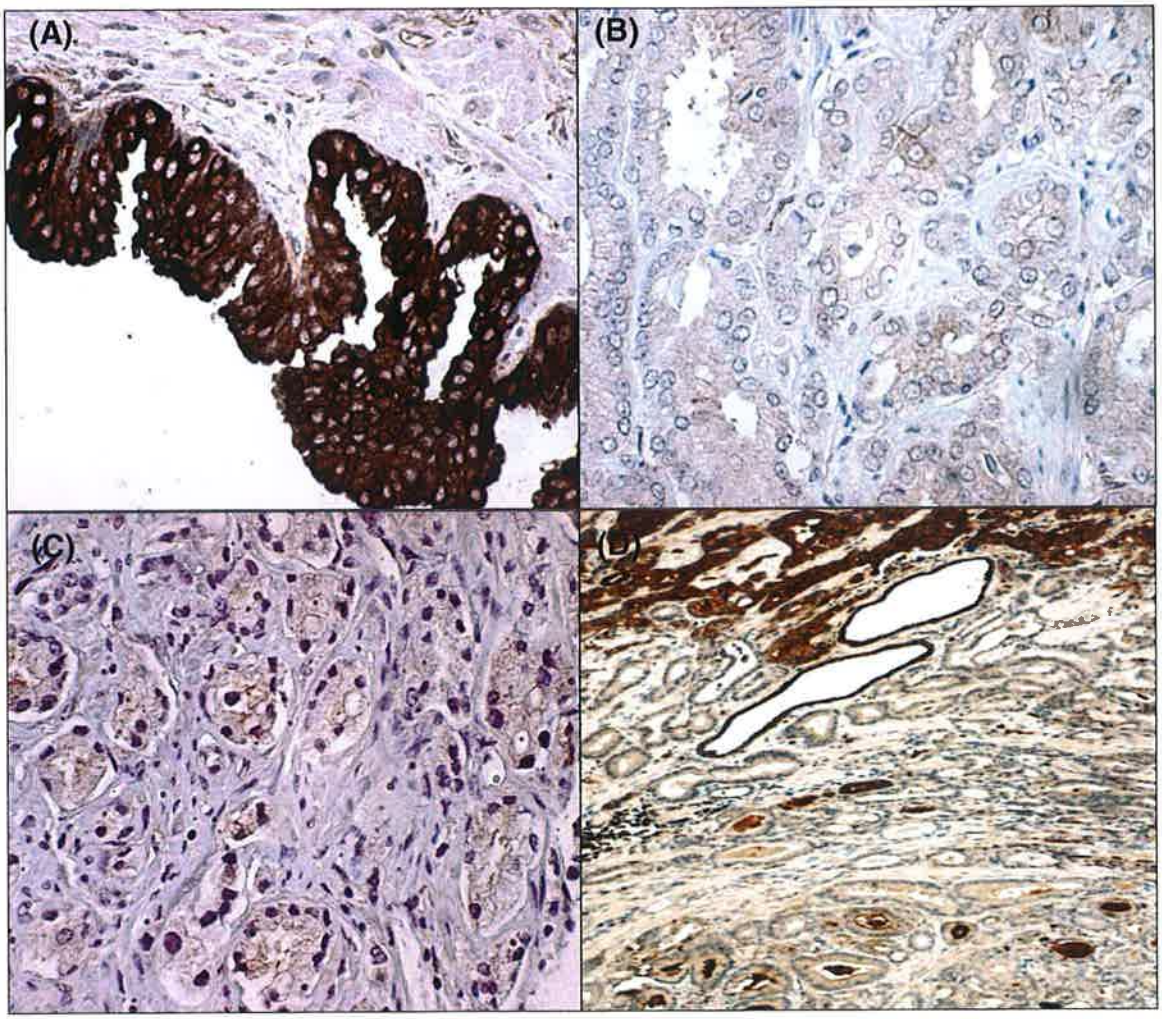

Figure 48: SFRP-2 protein expression assessed by IHC on prostate tissue

BPH, Gleason grade 3 and 4 immunoreactive with SFRP-2 on TMA cores: (A) BPH epithelium displaying strong cytoplasmic SFRP-2 expression [X400 Magnification], (B) Tumour epithelium with negative SFRP-2 expression [X400 Magnification], (C) Gleason grade 4 with negative SFRP-2 expression in epithelial cells [X400 Magnification], (D) Prostate whole section displaying Gleason grade 3 carcinoma with negative SFRP-2 expression surrounded by high grade tumour and two histologically benign glands displaying moderate SFRP-2 [X40 Magnification].

Table 19: Two-way Contingency tables comparing SFRP-2 Immunohistochemical scores (0/1 = negative 2/3 = Positive)

Test	Histology	Score of SFRP-2 0/1	Score of SFRP-2 2/3
Histologically Benign vs. Tumour (G 3+4+5)	Histologically Benign n = 699	161 (10%)	538 (34%)
Chi Square P value < 0.0001	Cancer n = 902	696 (43%)	208 (13%)
Gleason grade 5 vs. Gleason grade 3+4	Gleason grade <5 n = 760	610 (67%)	150 (17%)
Chi Square P value < 0.0001	Gleason grade 5 n = 144	58 (6%)	86 (10%)
Histologically Benign vs. Gleason grade 3	Histologically benign n = 699	161 (14%)	538 (47%)
Chi Square P value < 0.0001	Gleason grade 3 n = 439	371 (33%)	68 (6%)

4.4.2.2 Differential SFRP-2 expression identifies sub-categories of Gleason Grade 5 tumours

Further microscopic evaluation of G5 tumours revealed differences in morphological patterns, which corresponded with differential SFRP-2 expression (see Figure 49). The first subgroup ("Type A") appeared morphologically solid and displayed moderate/strong expression. The second

subgroup ("Type B") were morphologically more diffuse than "Type A" and did not express SFRP-2. Type A comprised approximately 40% of the G5 tumours and Type B the remaining 60%. To test whether Type A were neuroendocrine tumours, synaptophysin expression was assessed by IHC, however no correlation was found. Very aggressive, high Gleason score tumours lose the ability to secrete PSA. Therefore, they often escape detection for long periods of time as the PSA level in serum appears to be in the normal range. Some of these aggressive tumours have reverted to such a primitive state that they completely stop secreting PSA into the serum. A possible relationship between differential SFRP-2 expression and the ability to secrete PSA was also considered. Evaluation of PSA tissue expression in G5 tumours was assessed by IHC and PSA serum levels of the patients were documented. However, no correlation between the expression of PSA in the tumour epithelial cells and SFRP-2 expression in the subgroups of Gleason grade 5 tumours was noted.

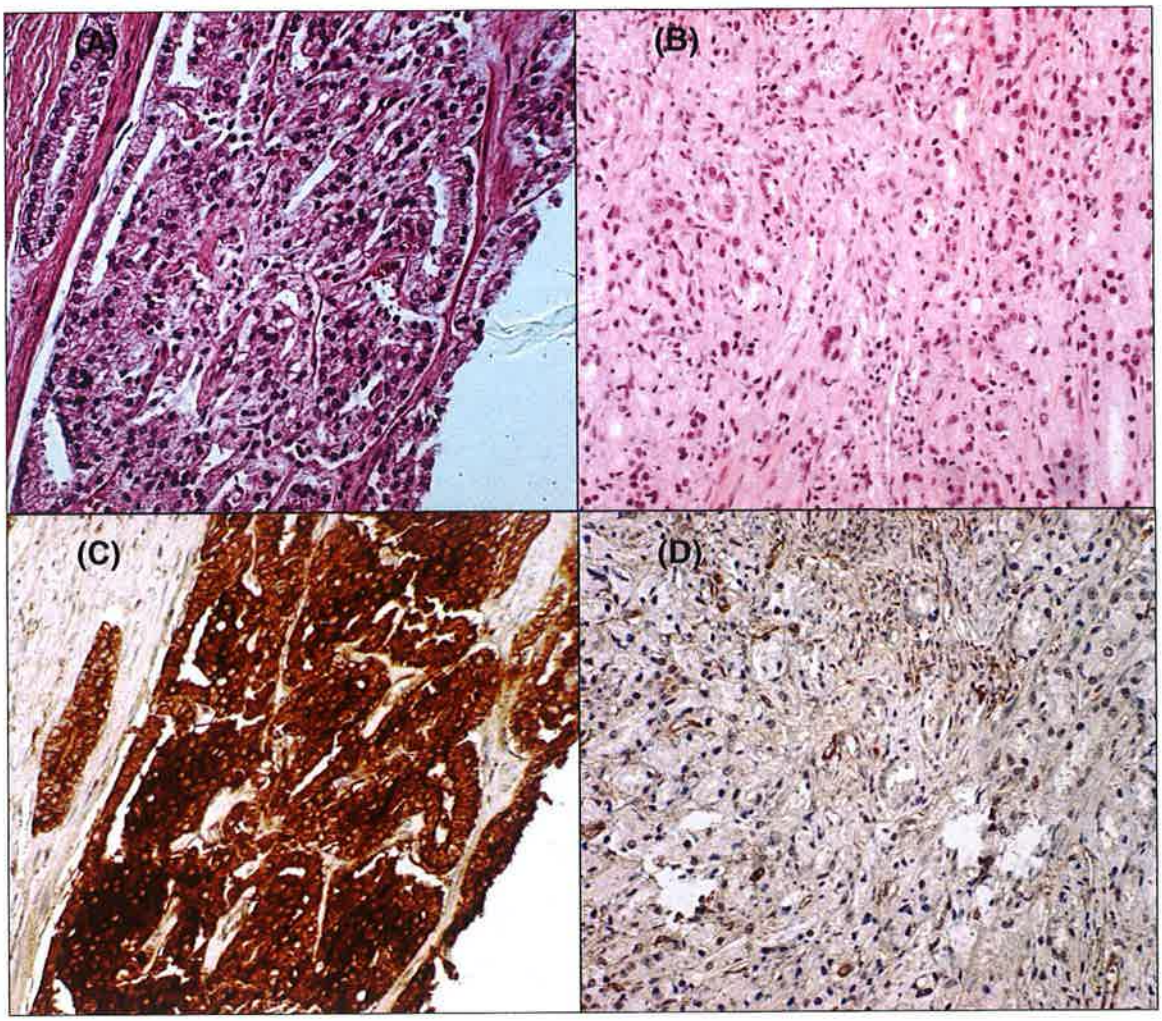

Figure 49: SFRP-2 Expression in Gleason Grade 5 Tumours

(A) and (C) = Examples of "Type A " Gleason grade 5 tumours [200X Magnification]

(B) and (D)= Examples of "Type B " Gleason grade 5 tumours [200X Magnification]

(A) and (B)= H&E TMA cores of the Gleason grade 5 subgroups [200X Magnification]

(C) and (D)= SFRP-2 IHC TMA cores of Gleason grade 5 subgroups [200X Magnification]

Table 20: SFRP-2 IHC score within the proposed subgroups of Gleason grade 5

SFRP-2 IHC Score	G5 "Type A"	G5 "Type B"	TOTAL
0\1	7	79	86
3\2	42	16	58
TOTAL	49	95	144

4.4.3 SFRP-2 gene expression

The presence of SFRP-2 at the gene level was confirmed by TaqMan® Real-Time PCR as seen in Figure 50. Although no significant fold change in SFRP-2 gene expression was noted as illustrated in Figure 50 (B), the trend in SFRP-2 gene expression correlated with what was observed at the protein level; a decrease in SFRP-2 gene expression was noted in Gleason grade 3 and 4 cell populations compared with histologically benign and Gleason grade 5 cell populations.

(A)

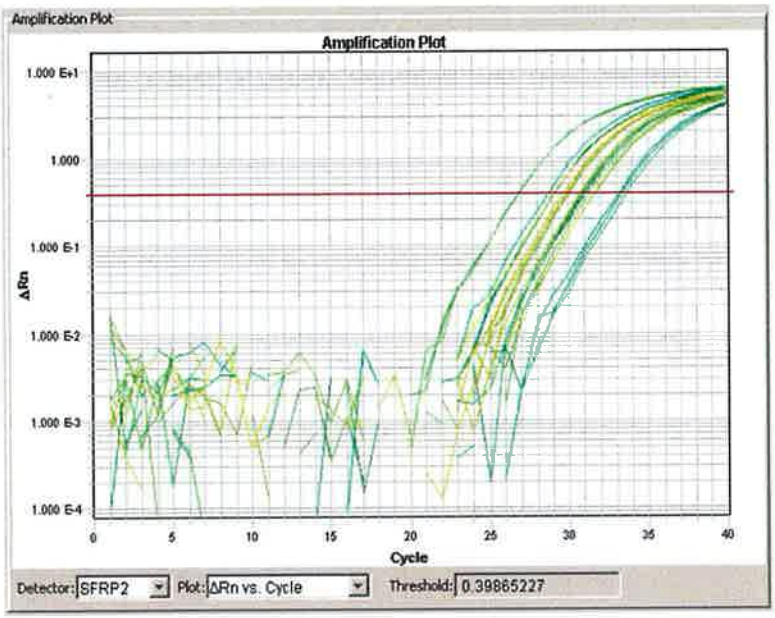

(B)

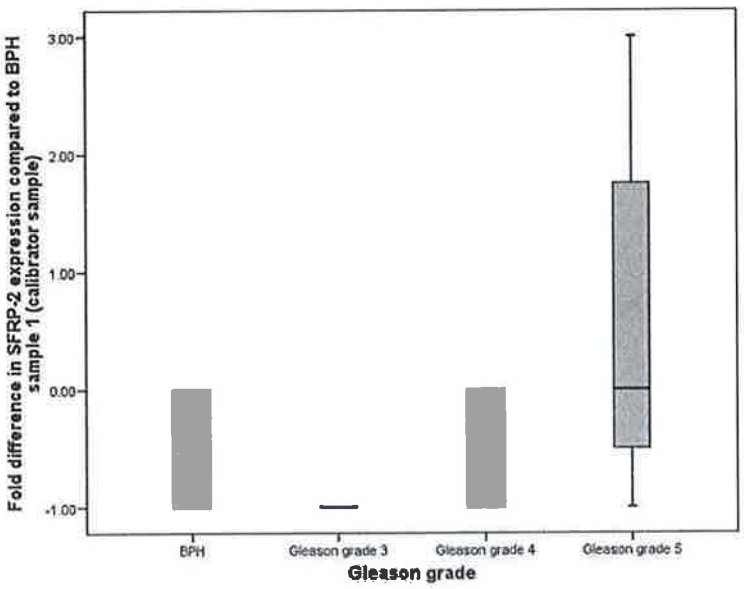

Figure 50: SFRP-2 Gene Expression

(A) TaqMan® Amplification plot of SFRP-2

(B) RQ Taqman data ($2^{-\Delta\Delta CT}$ method) graphically represented as a box plot:

The box plot compares SFRP-2 gene expression in BPH, Gleason grade 3, 4 and 5 gene expression as fold difference from the gene expression of the calibrator sample (BPH from case/sample 1).

4.4.4 SFRP-2 expression in Gleason grade 5 tumours is associated with biochemical recurrence

Five year post-operative PSA data were available for 22/216 patients; 9/22 patients experienced biochemical recurrence (BCR) and 10/22 patients had a G5 tumour. Consistent with the overall study cohort, 4/10 G5 tumours displayed moderate/strong SFRP-2 expression all of whom experienced BCR. In contrast, there was no evidence of BCR in any of the 6 patients with G5 negative/weak SFRP-2 expression.

4.5 Discussion

The evaluation of SFRP-2 as a putative marker of prostate cancer has not previously been demonstrated. In this study, the tissue expression profile of SFRP-2 in prostate cancer was evaluated. This protein had been previously found to be hypermethylated in prostate cancer following QMSP analysis by the epigenetic biomarker discovery group (Prostate Molecular Oncology, Institute of Molecular Medicine, Trinity College Dublin) within the PCRC. The aim of this study was to characterise SFRP-2 expression in the different Gleason grades of prostate cancer (G3, G4 and G5) and BPH glands using immunohistochemical analysis and tissue microarray technology and Taqman® RT quantitative PCR to determine its role as a potential biomarker of prostate cancer.

Western blot analysis was performed to validate the specificity of the polyclonal SFRP-2 antibody (HPA002652, Prestige Antibodies). The Western blot analysis confirmed that the SFRP-2 polyclonal antibody was specific for SFRP-2 protein. In lane 2 of the Western blot (Figure 46 (B)) the recombinant mouse SFRP-2 (33 kDa), which is 100% homologous with human SFRP-2, was detected by the antibody. This evidence for SFRP-2 specificity by the antibody was further strengthened by the detection of a band at 31 kDa

(approximate size of the immunogen used to generate the antibody, SFRP-2-ABP) in lane 3 in Figure 47 (B). A weak smear of antibody at approximately 60 kDa was detected in the Western blot in lane 3 in Figure 47 (B) which was also observed in the SDS-PAGE (Figure 46(A) lane 3). This could represent an unreduced dimer of the conjugated SFRP-2 peptide as it is approximately twice the molecular mass of the conjugated SFRP-2 (31 kDa). Further evidence of SFRP-2 specificity is demonstrated in Figure 47 (C) where BPH and PC-2 cell lines were lysed and a Western blot analysis was performed using the cell lysates. In Figure 47 (C) a weak band for the BPH cell line lysate is detected by the antibody at 38 kDa (molecular mass of human SFRP-2 protein) and a strong band is detected by the antibody at 38 kDa for the lysate of the PC-3 cell line. The weight of evidence in determining if the antibody is specific for SFRP-2 is strongly supportive.

The immunohistochemical results for SFRP-2 showed cytoplasmic SFRP-2 expression in epithelial cells of the prostate with overall strong to moderate SFRP-2 expression observed in BPH epithelial cells and negative to weak SFRP-2 expression observed in tumour epithelium particularly Gleason grade 3 and 4. However, in Gleason grade 5 carcinoma there was a 40:60 split in the immunoexpression of SFRP-2, where 40% (58/144) had strong to moderate SFRP-2 expression and 60% (86/144) had negative SFRP-2 expression in epithelial cells. Chi square tests performed on the contingency tables in Table 19 supported the hypotheses that there is a difference in SFRP-2 protein expression in histologically benign epithelium compared with tumour epithelium and between SFRP-2 expression in Gleason grade 5 tumours compared with Gleason grade 3 and 4 tumours. The gene expression profile of SFRP-2 confirmed the presence of the protein and the trend of SFRP-2 gene expression across BPH, Gleason grade 3, 4 and 5 correlated exactly with what was observed at the protein level which supports the immunohistochemical results. Immunohistochemical analysis of BPH glands from patients with no evidence of prostate cancer revealed that BPH epithelium had strong/moderate SFRP-2 expression in 95% of TURPs analysed. This indicates that BPH from cancer patients are suitable controls

for benign prostate tissue as they were behaving and expressing SFRP-2 in the same way as BPH from patients with no evidence of prostate cancer. Immunohistochemical analysis of SFRP-2 on 13 whole sections confirmed that the evaluation of SFRP-2 protein expression on TMAs was a valid model of the overall SFRP-2 immunoexpression on prostate tissue as identical immunoexpression was observed on the whole sections and the corresponding TMA cores. Analysis of SFRP-2 immunoexpression on both lobes of the prostate gland from 5 patients demonstrated that SFRP-2 immunoexpression was identical for a particular histological area on the left and right lobe of the prostate implying that there is uniform SFRP-2 expression for particular histological areas throughout the prostate. Averaging the SFRP-2 immunoexpression of each histological feature per case for the 216 patients presented very similar results to the histological area statistics which suggest that the immunoexpression of SFRP-2 across the different histological areas in the prostate is no 8t patient specific.

While the majority of prostate tumours overall showed reduced/absent SFRP-2 staining, an interesting observation was made for Gleason grade 5 adenocarcinoma. Within this specific cohort, 40% of G5 tumours showed strong positivity, compared with only 15% and 25% of G3 and G4 acini, respectively. Notably, a similar trend was observed for differences in methylation frequency between individual Gleason grades by the epigenetic biomarker discovery group (see Figure 46 (C)). Such differences in expression and methylation patterns are not uncommon between different stages of tumour progression (Lapointe *et al.*, 2004). However, epigenetic and gene expression changes have not been previously characterised within individual Gleason grades. These findings raise questions as to whether methylation patterns are clonally inherited during neoplastic transformation of the prostate and whether the SFRP-2 promoter becomes demethylated during tumour progression. Furthermore, it is not clear why a significant proportion of G5 carcinomas either retain or regain SFRP2 expression.

Further histological evaluation revealed notable morphological differences between G5 acini that corresponded with SFRP-2 staining patterns, leading to

a distinction between "Type A" G5 (solid tumours, strong SFRP-2 expression) and "Type B" G5 (diffuse tumours, weak/negative SFRP-2 expression). It was considered that the Gleason grade 5 subgroup "Type A" (nests of solid tumour) may represent a neuroendocrine subgroup of Gleason grade 5 tumour. However, no correlation between the subgroup and synaptophysin expression was observed. The ability of prostate tumours to secrete PSA was also examined in both Gleason grade 5 subgroups identified but no correlation between PSA expression and SFRP-2 expression in the subgroups of Gleason grade 5 tumours was noted. This pattern of SFRP-2 expression in morphologically dissimilar Gleason grade 5 tumours could suggest SFRP-2 as a surrogate marker of disease progression. Variation in tumour morphology and association with prognosis has previously been described in prostate cancer by Veltri *et al.*, (2007). They reported that Quantitative Nuclear Morphometry signatures illustrate alterations in nuclei structure, based upon nuclear morphometry within each Gleason grade patterns which might signify potential variations in prostate cancer disease risk of progression outcomes (Veltri *et al.*, 2007).

Another interesting result regarding Gleason grade 5 tumours and their subgroups was that "Type A" tumours with strong/moderate SFRP-2 expression were found to be associated with biochemical recurrence (4/4). However, follow up numbers with Gleason grade 5 tumours were small so further evaluation on larger patient numbers with longer follow-up will address whether SFRP-2 expression has prognostic relevance. If the results concur with preliminary biochemical results observed here, SFRP-2 could become a useful marker for predicting prognosis and biochemical recurrence, particularly in patients with advanced prostate cancer.

Expression patterns of SFRP-2 are not well defined in the literature. Similar loss of SFRP-2 expression pattern has been reported in the kidney by Kawamoto *et al.*, (2008). Kawamoto *et al* reported strong membranous expression in normal epithelium and loss of expression due to DNA methylation and histone modifications in renal cell carcinoma (Kawamoto *et al.*, 2008). It is possible that the loss of SFRP-2 expression noted in prostate

cancer in this study may be related to methylation of the SFRP-2 gene and that the 40% of G5 carcinomas that either retain or regain SFRP-2 expression may be due to demethylation of the gene. Overall the SFRP-2 tissue expression observed here was reflective of the SFRP-2 methylation frequency observed in prostate cancer by the epigenetic biomarker discovery group, where hypermethylation of SFRP-2 was noted in 65% of prostate cancer samples, 11% of BPH samples and 10% of histologically normal samples. Forty percent of Gleason grade 5 tumours displayed strong to moderate SFRP-2 expression following immunohistochemical analysis which may be because these Gleason grade 5 tumours are either not methylated or have become demethylated. As the prostate cancer samples used in the preliminary methylation analysis (Figure 46 (B)) by the epigenetic biomarker discovery group were pooled Gleason grades from individual cases which included some Gleason grade 5 tumours, this may account for 35% of prostate cancer samples having no evidence of SFRP-2 methylation in the methylation study. The 11% and 10% methylation frequency observed in BPH samples and histologically normal samples respectively in the methylation study by the epigenetic biomarker discovery group suggests that SFRP-2 may be methylated in a certain amount of benign glands and this may account for the 23% of BPH glands that had negative SFRP-2 expression following immunohistochemistry.

β-Catenin has also been implicated in prostate cancer progression and as this protein is a major player in Wnt signalling it would be interesting to compare SFRP-2 expression with β-Catenin expression to see if the loss of SFRP-2 had a functional affect on β-Catenin expression in prostate cancer cells. However, β-Catenin is a multi-functional protein involved in many cellular processes, including cell-cell adhesion as well as signal transduction (Whitaker *et al.*, 2008). Therefore, β-Catenin is highly abundant in the cell so assessing what effect the loss of SFRP-2 expression in prostate cancer has on β-Catenin expression is difficult to determine. The loss of E-Cadherin- β-Catenin complex at the cell surface has been linked to disease progression in prostate cancer through a loss of cell-cell adhesion and increased metastasis

(Whitaker *et al.*, 2008). When assessing β-Catenin expression in Wnt signalling the general consensus is to examine changes in β-Catenin localization in prostate tissue i.e. examine the expression levels of the protein in the nucleus as the protein translocates to the nucleus to activate TCF and LEF transcription factors. There is a great deal of contradiction and confusion in the literature in reports regarding the expression level of β-Catenin in the nucleus. The majority of groups that have studied β-Catenin localization report that nuclear β-Catenin increases in cancer and with Gleason grade (Chen *et al.*, 2004, Aaltomaa *et al.*, 2005, Jaggi *et al.*, 2005). This finding would support our data and propose that loss of SFRP-2 in prostate cancer results in accumulation of β-Catenin and its translocation to the nucleus to activate cell proliferation transcription factors. However, a significant decrease in β-Catenin nuclear expression has been reported by Whitaker *et al.* (2008) and Horvath *et al.* (2005). It was suggested by Whitaker *et al.* (2008) that a possible loss of nuclear β-Catenin may be reflective of deregulation of β-Catenin and androgen receptor signalling leading to tumourigenesis. They also proposed that the variation on fixation times, antibodies used and antibody concentration are plausible explanations for a significant proportion of the variation seen in β-Catenin immunohistochemistry studies in prostate cancer (Whitaker *et al.*, 2008). Therefore, it is difficult to be definitive in how loss of SFRP-2 expression affects β-Catenin expression in prostate cancer.

The results presented in this study propose SFRP-2 as a possible marker of histologically benign glands and a possible subgroup of Gleason grade 5 tumours that may predict prognosis and biochemical recurrence. However, further methylation and immunohistochemical analysis is required on more Gleason grade 5 tumours with follow up to confirm these results. These findings of discrete differences in SFRP-2 expression and morphological patterns of Gleason grade 5 tumours could be a useful clinical marker to sub-stratify high-risk patients and tailor more appropriate treatment. Proteomic analysis of SFRP-2 in serum and/or urine would also be very beneficial because if SFRP-2 expression correlated at the tissue and serum/urine level

then detection and quantification of SFRP-2 could be performed less invasively.

Chapter 5 - Production of an antigen-grade recombinant SFRP-2 protein

5.1 Summary

The use of well-characterised antibodies is vital for clinical diagnostics and protein studies. One of the major challenges facing researchers and clinicians in the area of cancer research is the lack of high quality, well characterised antibodies to novel target proteins. Successful antibody generation depends on the use and availability of high quality antigen. However, like antibodies to novel proteins in cancer research, there is also a lack of high quality, suitable, commercially available antigens to these proteins. The generation of antibodies to these proteins is not straightforward and often requires heterologous production of recombinant proteins. SFRP-2 is a novel marker in prostate cancer (as discussed in chapter 4) and paucity of quality antigen and antibody is an impediment to research on this marker.

The aim of this study was to design and produce biologically relevant recombinant SFRP-2 protein and to use this protein as an immunogen in an avian immune model to determine whether a recombinant antibody against SFRP-2 can be generated based on the polyclonal serum response of the chicken.

The first strategy taken to produce the SFRP-2 antigen involved using a prokaryotic *(E. coli)* expression system. Both a pGS21-a vector containing a glutathione-s-transferase (GST) tag and a pET-28b(+) vector modified to contain a heart fatty acid binding protein (hFABP) tag were transformed into *E. coli* cells for soluble SFRP-2 recombinant fusion protein expression which could be subsequently used as an immunogen in an avian immune model. However, both fusion proteins were found to be insoluble in the form of bacterial fusion proteins trapped within the bacterial cell periplasm.

The second strategy taken to produce soluble SFRP-2 antigen involved using a "cell-free" translation expression system. "Cell-free" translation is an *in vitro* expression system that does not require the use of a host cell to express the target protein. Soluble expression of SFRP-2 was achieved. However, the

yield and concentration of the soluble protein was very low and, therefore, would be inefficient at generating an immune response in an immune model.

The final phase of this study involved purifying and solubilising SFRP-2 inclusion bodies and using this as an immunogen in an avian immune model to determine whether a recombinant antibody against SFRP-2 can be generated based on the polyclonal serum response of the chicken. Low titres of polyclonal antibodies (pAbs) were obtained in the chicken sera against SFRP-2, indicating that SFRP-2 is not immunogenic in the chicken decreasing the probability of obtaining specific antibodies against SFRP-2 and, thus, of synthesising a recombinant antibody. This implies that the immunisations with crude lysate containing SFRP-2 and purified bacterial SFRP-2 inclusion bodies were not effective in eliciting a good immune response in the chicken to SFRP-2. It suggests that soluble expression of an SFRP-2 conjugated protein is required for immunisations to obtain a good polyclonal antibody response. The challenges and difficulties faced in this study may reflect the lack of high quality, well characterised, commercially available antibodies to novel cancer markers such as SFRP-2.

Overall, the results presented highlight the difficulties faced in producing a soluble antigen suitable for immunisations to challenging proteins for subsequent antibody generation.

5.2 Introduction

5.2.1 Commercially available SFRP-2 antibodies

One of the major challenges facing researchers and clinicians in the area of cancer research is the lack of high quality, suitable antibodies to novel proteins. As described in section 1.2.3, although commercial production of antibodies is well established, the paucity of specific antibodies to "novel" biomarkers is a real impediment to many clinical research advances. Thus, the majority of cancer research studies deal with proteins with accessible commercial antibodies.

Antibody development to novel markers of prostate cancer is a major component of this project. SFRP-2 proved to be a very interesting immunohistochemical marker in prostate cancer, displaying positivity in BPH tissue and negative expression in tumour epithelium (mainly G3 and G4), as discussed in Chapter 4. It is also suggested as a possible surrogate marker of a subgroup of Gleason grade 5 tumours. This protein is novel and it has not previously been evaluated immunohistochemical in prostate cancer and in many other cancers. Thus, it is not surprising that there are few if any specific commercially available antibodies against SFRP-2. In fact, there are only two antibodies to SFRP-2 applicable for immunohistochemistry (IHC) on formalin-fixed paraffin- embedded (FFPE) tissue (see Table 21). The first antibody produced by Atlas antibodies (highlighted in yellow in Table 21). This antibody was used in the immunohistochemical analysis in Chapter 4. The second antibody is recently on the market (since November 2010) and is produced by Proteintech group (highlighted in grey in Table 21). This antibody was not commercially available prior to starting this study.

The use of novel antibodies in clinical diagnostics raises a number of significant issues, largely related to validation. As IHC results directly influence the management and treatment of patients, accurate validation of novel antibody reagents used for IHC is crucial for accurate results. However,

although antibodies are among the most frequently used tools in basic science research and in clinical assays, there are no universally accepted guidelines or standardized methods for determining the validity of these reagents (Bordeaux *et al.*, 2003). Due to the number of pre-analytical factors (e.g. fixation time, inadequate fixation, fixatives used and tissue processing), analytical factors (e.g. antibody clone, dilution, antigen retrieval and detection systems used) and post-analytical factors (variability of interpretation amongst pathologists) known to influence antibody staining on formalin-fixed paraffin embedded tissue, standardization of antibodies for IHC can be a challenge (Bordeaux *et al.*, 2003). This challenge may reflect the lack of antibodies commercially available to SFRP-2 applicable for IHC on FFPE tissue. In general Western blotting is the most commonly used technique to validate antibody specificity by antibody companies. However, this method of validation only guarantees that a given antibody will provide accurate results for Western blot analysis. Many factors can contribute to an antibody displaying good specificity in Western blotting and not in immunohistochemistry. For example, proteins are denatured in Western blotting so post translational modifications to the native protein are not representative of what would be available in tissue.

The choice of using either monoclonal or polyclonal antibodies further complicates the issue of epitope specificity and determining which antibody would be more suitable for IHC (Bordeaux *et al.*, 2003). Polyclonal antibodies are more sensitive as they represent a pool of antibodies against the immunogen and typically show a higher probability for detection in a range of different conditions. However, polyclonal antibody preparations may contain large amounts of non-specific antibodies and also are known to have batch to batch variability. Monoclonal antibodies are produced from a single clone and are specific for only one epitope. Thus, they are more specific antibodies than polyclonal antibodies. Another advantage of monoclonal antibodies is that once a hybridoma is made it is a constant and renewable source; therefore, all batches will be homogenous. Recombinant antibody fragments have also been designed for clinical applications, such as immunohistochemistry, by

some research groups and antibody companies. In comparison with whole antibody fragments, these small antibody fragments such as Fab (antigen binding fragment) and scFv (single chain variable fragment) fragments exhibit better pharmacokinetics for tissue penetration and also provide full binding specificity because the antigen binding region is not altered (Hudson and Saurian, 2003). Also due to the modular structure of recombinant antibodies opposed to the full IgG structure, affinity fine tuning and site specific labelling can be achieved to improve the quality and specificity of these reagents. Interestingly, every antibody commercially available to SFRP-2 is a polyclonal antibody (see Table 21). This may be due to the fact that polyclonal antibodies are most accessible or due to the lack of SFRP-2 antigen sources. This is a "Catch-22" situation as the lack of monoclonal antibodies reflects the lack of antigen source and/or the lack of clinical justification of the marker. However, in order to gain clinical justification or evidence of a marker's relevance the use of well characterised monoclonal antibodies is required.

All the above indicates SFRP-2 as a potentially ideal candidate to generate a recombinant antibody specific for only one epitope on the SFRP-2 protein which can be used for immunohistochemistry on FFPE tissue. .

Table 21: Commercially available SFRP-2 antibodies (results obtained by a Linocut Directory antibody search (http://www.linscottsdirectory.com/)

Specificity	Clone	Source	Application	Supplier	Catalogue Number
SFRP-2	Polyclonal	Rabbit	Western blot	Novus Biologicals LLC	NBP1-31690
SFRP-2	Polyclonal	Goat	Western blot, ELISA	Novus Biologicals LLC	NB110-74715
SFRP-2	Polyclonal	Goat	Western blot, ELISA	Mybiosource LLC	MBS619998
SFRP-2	Polyclonal	Goat	Western blot, ELISA	Mybiosource LLC	MBS421524
SFRP-2	Polyclonal	Goat	Western blot, ELISA	Mybiosource LLC	MBS223561
SFRP-2	Polyclonal	Goat	Immuno- blotting, ELISA	Sigma - Aldrich Corporation	SAB2500934
SFRP-2	Polyclonal	Rabbit	Immuno- blotting, Immunohistochemistry (Formalin-Fixed Paraffin-Embedded sections)	Atlas Antibodies & Sigma - Aldrich Corporation (Prestige antibodies)	HPA002652
Anti-FRP-2	Polyclonal	Rabbit	Western blot, ELISA, Immuno-precipitation, Immuno-fluorescence	Santa Cruz Biotechnology Inc	sc-13940
Anti-FRP-2	Polyclonal	Rabbit	Western blot, ELISA, Immuno-precipitation, Immuno-fluorescence	Santa Cruz Biotechnology Inc	sc-31574
SFRP-2	Polyclonal	Goat	Western blot, ELISA	Mybiosource LLC	MBS619345
SFRP-2	Polyclonal	Goat	Western blot, ELISA	United States Biological	
SFRP-2	Polyclonal	Goat	Western blot, ELISA	AbD Serotec	AHP1685
SFRP-2	Polyclonal	Goat	Western blot, ELISA	Origene Technologies	TA302604
SFRP-2	Polyclonal	Rabbit	Western blot, ELISA	Lifespan Biosciences Inc.	LS-C102708
SFRP-2	Polyclonal	Rabbit	Immunohistochemistry (Formalin-Fixed Paraffin-Embedded sections), Immuno-fluorescence, Western blot	Proteintech group	12189-1-AP

5.2.2 Antibody production

The first step in the generation of an antibody (recombinant, monoclonal or polyclonal) involves immunising an animal with the target protein (antigen). The animal's immune system recognizes the immunised protein (immunogen) as foreign, as described in section 1.3.6, and produces antibodies in response. These mature antibodies are secreted into the plasma by B cells to interact with the immunogen aided by T helper 1 (T_H1) and 2 (T_H2) responses (see section 1.3.2).

The major advantage of using immunised animals over a conventional naive antibody library is that the host animal immune system refines specificity towards the cognate antigen. Therefore, the likelihood of selecting high affinity antibodies from a generated recombinant antibody fragment library due to *in vivo* affinity maturation (Schmitz *et al.*, 2000) is significantly increased. Naive libraries are becoming an increasingly available option for recombinant antibody selection. However, they lack the diversity of the immune system (somatic hypermutation) for generating a large panel of different antibodies (see section 1.3.4). Phage display is the principle technique employed in recombinant antibody selection. This process is described in section 1.3.6.

Several factors determine the magnitude of the antibody response to an immunogen such as the size of the immunogen, its chemical characteristics, and how different it is from the animal's 'self' antigens. The most potent immunogens are generally proteins that come from sources phylogenetically far removed from the host animal (i.e., human proteins injected into rabbits, chickens or goats) and usually have a molecular mass above 5 kDa. The use of highly purified proteins as immunogens is recommended, because the animal will produce antibodies to even small amounts of impurities present as well as to the target protein. Repeated exposure to the immunogen increases the antibody response. Thus, a series of immunisations/boosts at regular intervals is required to achieve high levels of antibody production and antibodies of high affinity.

5.2.3 Adjuvants and conjugated vaccines

Many antigens are not strongly immunogenic on their own. Even immunogenic molecules often do not generate the desired level of antibody response. In order to increase the intensity of the immune response, immunogens are combined with complex mixtures of natural or synthetic compounds called adjuvants. An adjuvant is defined as a substance that enhances the immunogenicity of an antigen (Janeway, 2005). Mineral salts, oil emulsions, microbacterial products, saponins, synthetic products and cytokines are the six categories of commonly used adjuvants. Adjuvants work by tricking the immune system to respond as though an active infection was present in the body. Just as different classes of infectious agent stimulate different types of immune response, different adjuvants may promote different types of responses e.g. an inflammatory T_H1 response or an antibody-dominated T_H2 response (Weeratna *et al.*, 2000).

Adjuvants can be used in immunisations to;

1. stimulate an immune response to an antigen that is not inherently immunogenic
2. increase the potency of the immune response
3. preferentially stimulate either a cellular response (i.e. viral clearance) or a humoral response (i.e. antibody generation)

Adjuvants enhance antigen uptake and localization by antigen presenting cells, extend antigen release, activate macrophages and stimulate T and B cells. Freund's complete adjuvant is a widely used adjuvant in experimental animals to augment antibody responses (Janeway, 2005). It is an oil and water emulsion containing killed mycobacteria.

If an immunogen fails to generate an acceptable response, it may be biologically fused to a carrier protein that is immunogenic. This approach to stimulate the immune system is based on the same principle as conjugating haptens (small molecules that can evade the immune system due to their

small size) to larger carrier protein in order to evoke an immune response for antibody generation. By conjugating the hapten to the larger carrier protein, antigen presenting cells phagocytise the large protein and present peptides representing both the hapten and carrier protein on the MHC molecules. Examples of such carrier proteins are glutathione-s-transferase (GST) and keyhole limpet hemocyanin (KLH). If the target protein is biologically fused to a carrier protein for immunisation, then unconjugated target protein (free-protein) should be used for screening. Alternatively a second carrier protein fused to the target protein should be used for screening. This second carrier protein should be as different as possible to the carrier protein used for immunisations as the animal will form antibodies to this carrier protein as well as to the hapten (see Figure 51).

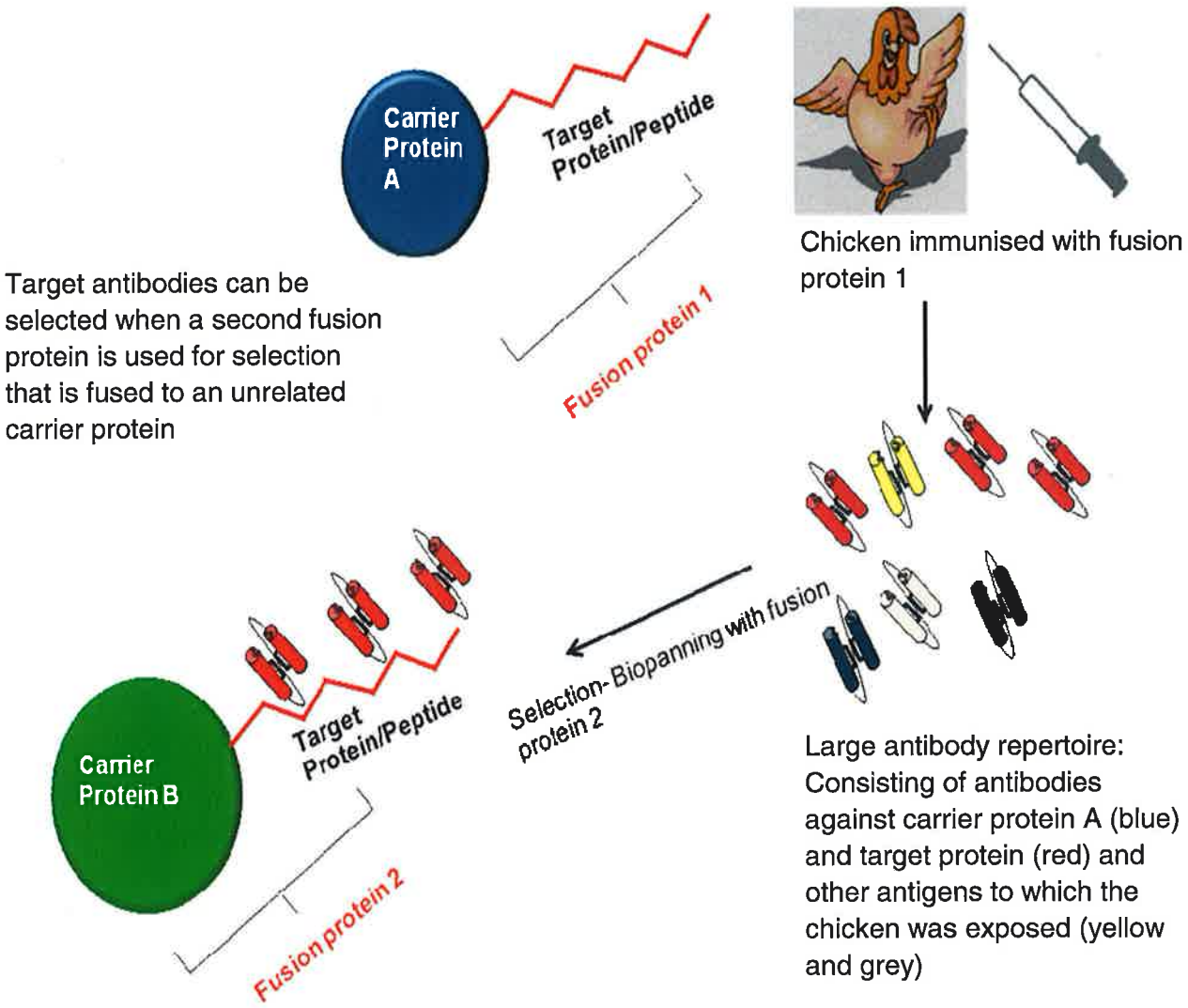

Figure 51: Antibody selection using the antigen (target protein) fused to two different carrier proteins (A and B) for immunisation and selection

5.2.4 SFRP-2 immunogens for commercially available SFRP-2 antibodies

A large number of antigens are highly conserved in mammalian evolution and, therefore, generate a limited immune response in mice and/or rabbits due to immunological tolerance invoked during foetal development (Andris-Widhopf *et al.*, 2000). This is the case for the SFRP-2 human sequence which is 100% conserved across mice (*Mus. musculus*) and rabbits (*Oryctolagus cuniculus*) (see Figure 52). One alternative to overcome this obstacle for successful antibody generation is the use of chickens for immunisations and selection of antibodies. Many highly conserved mammalian proteins are less conserved or absent in non-mamalian species, making animals like chickens a ready source of antibody (Andris-Widhopf *et al.*, 2000). However, although the SFRP-2 human sequence is less homologous in chickens (*Gallus gallus*) compared with mice and rabbits, it also displays high conservation in chickens with 94% homology (see Figure 52). Therefore, SFRP-2 may be less potent as an immunogen and requires the use of a carrier protein to increase its immunogenicity, as discussed in section 5.2.3.

Table 22 documents the SFRP-2 immunogens used to generate the polyclonal antibodies listed in Table 21. The table describes the amino acid peptide sequences used by each immunogen relative to the human SFRP-2 whole sequence (295 amino acids). Almost all the immunogens are 100% conserved across rabbits and mice, yet 6 of these immunogens successfully generated a polyclonal antibody from a rabbit through the use of adjuvants and conjugation to a carrier protein. The least conservative immunogens are HPA002652 (Atlas antibodies), sc-13940 (Santa Cruz Biotechnology) and 12189-1-AP/ ag2853 (Proteintech group) which are 99%, 99% and 94% conserved across chickens, respectively. Ag2853 (Proteintech group) is the only listed commercially available immunogen that is advertised (see Table 22 highlighted in grey). This immunogen became available in November 2010. However, when this immunogen was ordered during the course of this study the company could not synthesise the antigen. Therefore, this antigen is not commercially available to purchase from the company.

Accession	Description	Max score	Total score	Query coverage	E value	Links
AAH08666.1	Secreted frizzled-related protein 2 [Homo sapiens] >gb|AAQ89360.1| sf	597	597	100%	0.0	GM
NP_003004.1	secreted frizzled-related protein 2 precursor [Homo sapiens] >ref|XP_0(	595	595	100%	0.0	UGM
XP_002815272.1	PREDICTED: secreted frizzled-related protein 2-like [Pongo abelii]	595	595	100%	0.0	GM
XP_002716934.1	PREDICTED: secreted frizzled-related protein 2 [Oryctolagus cuniculus]	585	585	100%	0.0	UGM
XP_001366605.1	PREDICTED: secreted frizzled-related protein 2-like [Monodelphis domes	584	584	100%	0.0	UGM
XP_003129182.1	PREDICTED: secreted frizzled-related protein 2-like [Sus scrofa]	580	580	100%	0.0	UGM
NP_001002987.1	secreted frizzled-related protein 2 precursor [Canis lupus familiaris] >sp	578	578	100%	0.0	UG
XP_002913893.1	PREDICTED: LOW QUALITY PROTEIN: secreted frizzled-related protein 2	578	578	100%	0.0	GM
NP_033170.1	secreted frizzled-related protein 2 precursor [Mus musculus] >sp|P9729	573	573	100%	0.0	UGM
AAB70795.1	secreted apoptosis related protein 1 [Mus musculus]	573	573	100%	0.0	GM
BAA09053.1	SDF5 [Mus musculus]	573	573	100%	0.0	GM
NP_001094170.1	secreted frizzled-related protein 2 [Rattus norvegicus] >gb|EDM00833.1	572	572	100%	0.0	UGM
XP_002745425.1	PREDICTED: secreted frizzled-related protein 2-like [Callithrix jacchus]	572	572	100%	0.0	GM
NP_001029565.1	secreted frizzled-related protein 2 [Bos taurus] >gb|AAI04537.1| Secre	571	571	100%	0.0	UGM
BAE23596.1	unnamed protein product [Mus musculus]	570	570	100%	0.0	GM
NP_001156525.1	secreted frizzled-related protein 2 [Ovis aries] >gb|ACR55758.1| secret	569	569	100%	0.0	UG
AAK11319.1	secreted frizzled-related protein 2 [Oryctolagus cuniculus]	565	565	95%	0.0	G
XP_001514431.1	PREDICTED: similar to pancreas tumor-related protein [Ornithorhynchus	561	561	100%	0.0	UG
XP_002808468.1	PREDICTED: LOW QUALITY PROTEIN: secreted frizzled-related protein 2	498	498	84%	3e-177	UGM
NP_989062.1	secreted frizzled-related protein 2 [Xenopus (Silurana) tropicalis] >gb|A	483	483	94%	1e-171	UGM
XP_003257904.1	PREDICTED: secreted frizzled-related protein 2-like [Nomascus leucoger	478	478	80%	1e-170	GM
ACS92629.1	secreted frizzled-related protein 2 [Anas platyrhynchos]	478	478	95%	6e-170	
NP_990104.1	secreted frizzled-related protein 2 precursor [Gallus gallus] >sp|Q9IA96	478	478	94%	1e-169	UGM
NP_001080663.1	secreted frizzled-related protein 2 [Xenopus laevis] >gb|AAH44687.1| S	472	472	94%	2e-167	UG
XP_003221758.1	PREDICTED: secreted frizzled-related protein 2-like [Anolis carolinensis]	471	471	94%	7e-167	UGM
CAF96582.1	unnamed protein product [Tetraodon nigroviridis]	432	432	98%	1e-151	
AAI24708.1	Secreted frizzled-related protein 2 [Danio rerio] >gb|AAI63950.1| Sfrp2	424	424	97%	2e-148	GM
NP_001070852.2	secreted frizzled-related protein 2 [Danio rerio]	423	423	97%	4e-148	UGM
AAB70792.1	secreted apoptosis related protein 1 [Homo sapiens]	415	415	70%	4e-146	GM
NP_001090810.1	secreted frizzled-related protein [Xenopus (Silurana) tropicalis] >gb|AA	303	303	97%	6e-101	UGM
NP_001098737.1	secreted frizzled-related protein [Xenopus laevis] >gb|AAI23153.1| LOC	289	289	89%	3e-95	UG
CAF98709.1	unnamed protein product [Tetraodon nigroviridis]	251	251	90%	7e-80	
XP_002608045.1	hypothetical protein BRAFLDRAFT_74994 [Branchiostoma floridae] >gb|B	251	251	89%	3e-79	UG
NP_571933.1	secreted frizzled-related protein 5 [Danio rerio] >gb|AAL11439.1| secre	241	241	90%	3e-76	UGM
XP_003229116.1	PREDICTED: LOW QUALITY PROTEIN: secreted frizzled-related protein 2	236	236	97%	2e-74	GM
XP_003200152.1	PREDICTED: secreted frizzled-related protein 2-like [Danio rerio]	235	235	89%	6e-74	GM

Figure 52: NCBI (National Centre for Biotechnology Information) screen print of SFRP-2 sequence BLAST (Basic Logical Alignment Search Tool)

Table 22: SFRP-2 immunogen sequences used to generate commercially available SFRP-2 antibodies

Antibody	Supplier	Immunogen: AA sequence on whole SFRP-2 protein	Immunogen AA sequence Homology with Rabbit	Immunogen AA sequence Homology with Mice	Immunogen AA sequence Homology with Chicken
NBP1-31690	Novus Biologicals LLC	231-295	100%	100%	100%
NB110-74715	Novus Biologicals LLC	274-295	100%	100%	100%
MBS619998	Mybiosource LLC	274-295	100%	100%	100%
MBS421524	Mybiosource LLC	274-295	100%	100%	100%
MBS223561	Mybiosource LLC	274-295	100%	100%	100%
SAB2500934	Sigma - Aldrich Corporation	274-295	100%	100%	100%
HPA002652	Atlas Antibodies & Sigma - Aldrich Corporation (Prestige antibodies)	165-295	100%	100%	99%
sc-13940	Santa Cruz Biotechnology Inc.	156-295	100%	100%	99%
sc-31574	Santa Cruz Biotechnology Inc.	None given	–	–	–
MBS619345	Mybiosource LLC	274-295	100%	100%	100%
S1012-87S	United States Biological	274-295	100%	100%	100%
AHP1685	AbD Serotec	274-295	100%	100%	100%
TA302604	Origene Technologies	274-295	100%	100%	100%
LS-C102708	Lifespan Biosciences Inc.	None given	–	–	–
12189-1-AP/ ag2853	Proteintech group	1-295	100%	100%	94%

5.2.5 Aim

The aims of this study were twofold;

(i) to design and produce a SFRP-2 antigen;

- using *E. coli* as an expression system

  and/or

- using "cell-free" translation

(ii) to use the SFRP-2 antigen as an immunogen in an avian immune model and to evaluate the polyclonal antibody response level of the chicken against the immunogen (SFRP-2 fusion protein) to determine whether a recombinant antibody can be generated

5.3 Materials and Methods

The exact materials and methods for this chapter were given in section 2.5.

5.4 Results

5.4.1 Transformation of cloned pGS-21a vector containing SFRP-2 gene into *E. coli* cells and fusion protein expression

An optimised DNA sequence corresponding to amino acids 165-295 on the human SFRP-2 protein was cloned into a pGS-21a vector containing a GST tag using the *Nco* I and *Hind* III restriction sites by Genscript USA Inc., as described in section 2.5.1.1.1.1. Glutathione-s-transferase (GST) is frequently used as a fusion tag due to the fact that it can act as a chaperone to facilitate protein folding and can be expressed as a soluble protein rather than in inclusion bodies (Harper and Speicher, 2011). Also, it is a commonly utilized tag because the GST fusion protein can be affinity purified without denaturation.

The vector was then transformed by "heat shock" into a variety of different chemically competent *E. coli* cells for optimal expression of the SFRP-2-GST fusion protein. The heat shock method requires the use of chemically competent cells which have increased membrane permeability. Approximately 1% of bacterial strains have the ability to naturally take up DNA (Thomas and Nielsen, 2005). However, for the majority of bacterial strains transformation requires the use of artificial competence introduced by laboratory procedures. This can be achieved by calcium chloride transformation (chemical competence) or electroporation. Chemical competence can be obtained by chilling the cells in the presence of divalent cations such as Ca^{++} or Mg^{+}. The heat shock transformation method is commonly used in gene cloning as it is convenient and provides good transformation efficiency.

5.4.1.1 SFRP-2-GST fusion protein expression in BL-21 (DE3) E. coli cells

The pGS-21a vector containing the SFRP-2 gene was transformed into the chemically competent BL-21(DE3) strain of *E. coli* cells following a heat shock protocol (section 2.5.1.1.7). The BL-21 strain of *E. coli* is the most widely used host for protein expression as the strain has the advantage of being deficient in the *lon* and *ompT* proteases. Transformed colonies were randomly picked from carbenicillin-(a semi-synthetic ampicillin analogue) supplemented agar plates to exert selective pressure on cells transformed with the pGS-21a vector containing the ampicillin resistant gene. A total of 5 colonies were picked and grown O/N followed by subsequent 1 mM IPTG induction O/N at 30°C.

The pGS-21a vector contains a *lac* operator spliced together with a T7 promotor. In *E. coli* the *lac* operon is required for the transport and metabolism of lactose. The *lac* operator is a short region of DNA that lies partially within the *lac* promoter and interacts with a regulatory protein that controls the transcription of the operon. The *E. coli* cell can use lactose as an energy source via the use of the *lac* operon. It does this by producing the enzyme β-galactosidase to digest lactose into glucose and galactose. However, when there is no lactose present or if there is an energy source such as glucose readily available to the cell then no enzyme is produced. Therefore, the availability of glucose and lactose to the cell regulates the *lac* operon. T7 polymerase only transcribes DNA downstream of a T7 promoter. The SFRP-2 gene was cloned downstream of the T7 promotor by Genscript in the pGS-21a vector. Isopropyl-β-D-1-thiogalactopyranoside (IPTG) is a molecular mimic of a lactose metabolite, called allolactose, which induces the expression of β-galactosidase by the *lac* operon. The addition of IPTG to the *E. coli* host results in the *lac* repressor being lost from both the host genome and the vector plasmid *lac* operators. The RNA polymerase can then bind the free T7 promoter which is spliced onto the *lac* operator on the plasmid vector.

This results in transcription of the downstream target SFRP-2 gene which, following transcription, is expressed in the bacterial periplasm.

The cultures were sonicated to achieve periplasmic extraction of the SFRP-2 fusion protein which was then analysed by SDS-PAGE and an anti-SFRP-2 Western blot, as described in sections 2.5.1.1.8 and 2.5.1.1.9.

A band was observed in the SDS-PAGE gel in Figure 53 (A) at approximately 40 kDa which is the estimated size of the fusion protein (GST~26 kDA+SFRP-2~14 kDA= 40 kDa) in all 5 transformant lysates which suggests successful transformation. However, the anti-SFRP-2 antibody only detected very weak bands for SFRP-2 protein at 40 kDa in transformant 2, 4 and 6 (lanes 3, 5 and 7, respectively, in Figure 53 (B)). Another SFRP-2-specific band was noted in transformant 2 (lane 3 in Figure 53 (B)) at approximately 32 kDa.

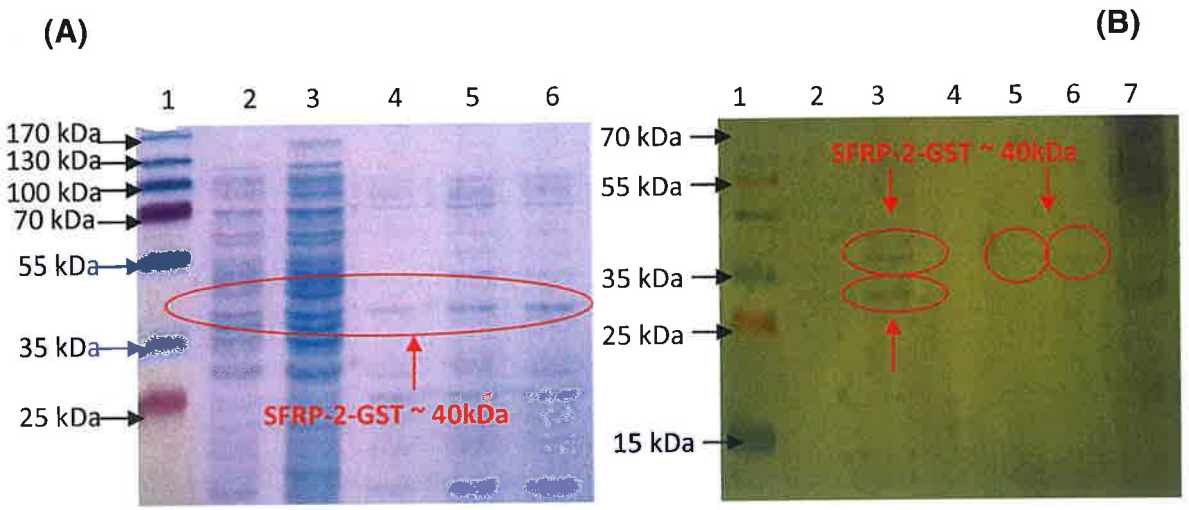

Figure 53: SFRP-2-GST protein expression in BL-21(DE3) *E. coli* cells

(A): SDS PAGE, (B): anti-SFRP-2 Western blot. The lysates from the expressed clones were incubated with sample treatment buffer and analysed on a 12.5% (w/v) SDS-PAGE Gel and by Western blotting using anti-SFRP-2 pAb. In (A) and (B) lane 1 represents prestained protein marker (Fermentas) and lanes 2 to 6 contain lysate from different SFRP-2-GST transformed clones. In (B) lane 7 represents a positive control (SFRP-2 fusion protein conjugated to Albumin Binding Protein (donated by Atlas Antibodies)). A band was observed in the SDS-PAGE gel at approximately 40 kDa which is the estimated size of the fusion protein (GST~26 kDA+SFRP-2~14 kDA= 40 kDa) in all 5 transformant lysates which suggests successful transformation. The anti-SFRP-2 antibody only detected very weak bands for SFRP-2 protein at 40 kDa in transformant 2, 4 and 6 (lanes 3, 5 and 7, respectively). A second band at approximately 32 kDa was noted in transformant 2 (lane 3 (B)).

5.4.1.2 Large-scale SFRP-2-GST fusion protein expression in cells and Immobilized Metal Ion Affinity Chromatography (IMAC) purification of the expressed fusion protein

The SFRP-2-expressing clone (transformant 2) was used for large-scale production of the SFRP-2 fusion protein. A culture volume of 500 mL of transformant 2 was grown up O/N followed by subsequent subculture and induction with 1 mM IPTG O/N at 30°C, as described in section 2.5.1.1.10. The protein lysate following sonication, was centrifuged for removal of cell debris and the supernatant was purified using IMAC, as described in section 2.5.1.1.12.

IMAC is based on the principle that histidine has a high affinity towards nickel ions immobilised onto nitro-triacetic acid (Ni-NTA). Due to the fact that histidine residues are uncommon in proteins (only 2% are present in globular proteins with only half exposed on the protein surface (Ueda *et al.*, 2003)) successful, efficient purification of recombinant fusion proteins with a histidine residue/tag (His6) can easily be achieved by IMAC purification. Non-specifically bound proteins can be removed by washing the resin with running buffer that contains a moderate concentration of imidazole, which forms the side chain of the histidine amino acid. The imidazole (moderate concentration) competes with other proteins containing histidine to bind to the Ni-NTA but cannot inhibit the binding of the fusion protein containing the histidine tag (His6) allowing for elution of a pure recombinant fusion protein. The fusion protein can be successfully eluted using a low pH buffer (10 mM sodium acetate, pH 4.4) or a buffer containing a high concentration of imidazole. These elution buffers reduce the binding affinity between Ni^{2+} and the histidine tag.

The purification was analysed by performing SDS-PAGE (Figure 54 (A)) and an anti-SFRP-2 antibody Western blot (Figure 53 (B)) on the lysate, "flow-through", wash and eluted protein. The large-scale expression and purification of the SFRP-2-GST recombinant fusion protein was unsuccessful as no protein was observed in the lysate (lane 2 in Figure 54 (B)).

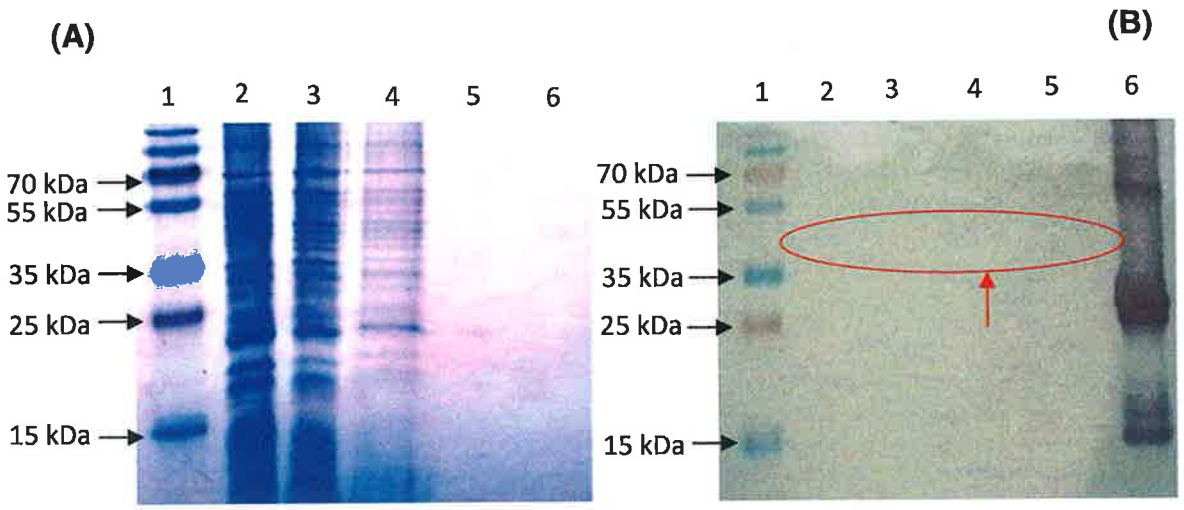

Figure 54: Large-scale SFRP-2-GST fusion protein expression in BL-21(DE3) cells and IMAC purification of the expressed recombinant fusion protein

(A): SDS, (B): anti-SFRP-2 Western blot. In (A) and (B) lane 1 represents the prestained protein marker (Fermentas), lane 2 contains unpurified sonicated lysate of transformant 2 (lane 3 Figure 53) with all the proteins expressed in the bacterial cell lysate, lane 3 contains the "flow-through" with all unbound proteins that passed through the resin, lane 4 contains impure non-specific hydrophobic proteins which may have weakly bound to the resin and were removed using an increased concentration of Tween 20 and lane 5 contains the purified eluted SFRP-2 fusion protein. In (B) lane 6 contains a positive control (SFRP-2 fusion protein conjugated to Albumin Binding Protein (donated by Atlas Antibodies)). The large-scale expression and purification of the SFRP-2-GST recombinant fusion protein was unsuccessful as no protein was observed in the lysate in the Western blot using the anti-SFRP-2 antibody (lane 2 (B)).

5.4.1.3 SFRP-2-GST recombinant fusion protein expression in Tuner E. coli cells

The pGS-21a vector containing the SFRP-2 gene was next transformed into the chemically competent Tuner(DE3) strain of *E. coli* cells following a heat shock protocol (section 2.5.1.1.7). Tuner strains *of E. coli* are *lacZY* deletion mutants of BL-21 *E. coli*, which allows adjustable levels of protein expression throughout the cells in a culture. The *lac Y* mutation allows uniform entry of IPTG into all cells in the population. IPTG can enter the cells in a concentration-dependent fashion that is extremely uniform throughout the culture. Adjusting the concentration of IPTG regulates the protein expression

from very low expression to robust expression. Solubility and activity of difficult target proteins may be enhanced by lower level expression. Tuner cells are also deficient in the *lon* and *ompT* proteases.

Transformed colonies were randomly picked from carbenicillin-supplemented agar plates. A total of 8 colonies were picked and grown O/N followed by subsequent 1 mM IPTG induction O/N at 30°C. The cultures were sonicated to achieve periplasmic extraction of the SFRP-2 recombinant fusion protein which was then analysed by SDS-PAGE electrophoresis and an anti-SFRP-2 and anti-GST Western blot, as described in sections 2.5.1.1.8 and 2.5.1.1.9.

A band was observed in the SDS-PAGE gel in Figure 55 (A) and in the anti-SFRP-2 Western blot in Figure 55 (B) at approximately 35 kDa. This suggests that this is the SFRP-2-GST fusion protein expressing at a slightly lower molecular mass than expected. The anti-GST Western blot in Figure 55 (C) also detected a band at 35 kDa. However bands at approximately 26 kDA and 40 kDa were also detected by the anti-GST Western blot.

5.4.1.3.1 Induction temperature and induction time optimisation for optimal SFRP-2-GST protein expression in Tuner E. coli cells

Transformant 3 (lane 4 in Figure 55) was grown O/N followed by subsequent 1 mM IPTG induction optimisation at different temperatures (25°C and 30°C) and over varying time courses (3 hours, 6 hours and O/N). The cultures were sonicated to achieve periplasmic extraction of the SFRP-2 recombinant fusion protein. The cultures were then analysed by SDS-PAGE electrophoresis and an anti-histidine Western blot, as described in sections 2.5.1.1.8 and 2.5.1.1.9, to determine the optimal induction time and temperature for SFRP-2-GST recombinant fusion protein expression in Tuner (DE3) cells.

A band at approximately 35 kDa in the SDS-PAGE gel in Figure 56 (A) was observed for all induced cultures. A slight increase of protein expression was noted with increasing induction temperature (30°C) and increasing induction time (O/N) in the SDS gel. The anti-histidine Western blot in Figure 56 (B) detected the protein at 35 kDa for all induced cultures. However, no significant decrease or increase in protein expression was noted with increasing induction temperature or increasing induction time in the anti-histidine Western blot. The anti-histidine antibody in the anti-histidine Western blot also detected a weak band at approximately 26 kDa in all induced cultures except the culture induced at 25°C for 3 hours and a band at approximately 40 kDa in transformants 2, 3 and 4 (lanes 3, 4 an 5 in Figure 56 (B)).

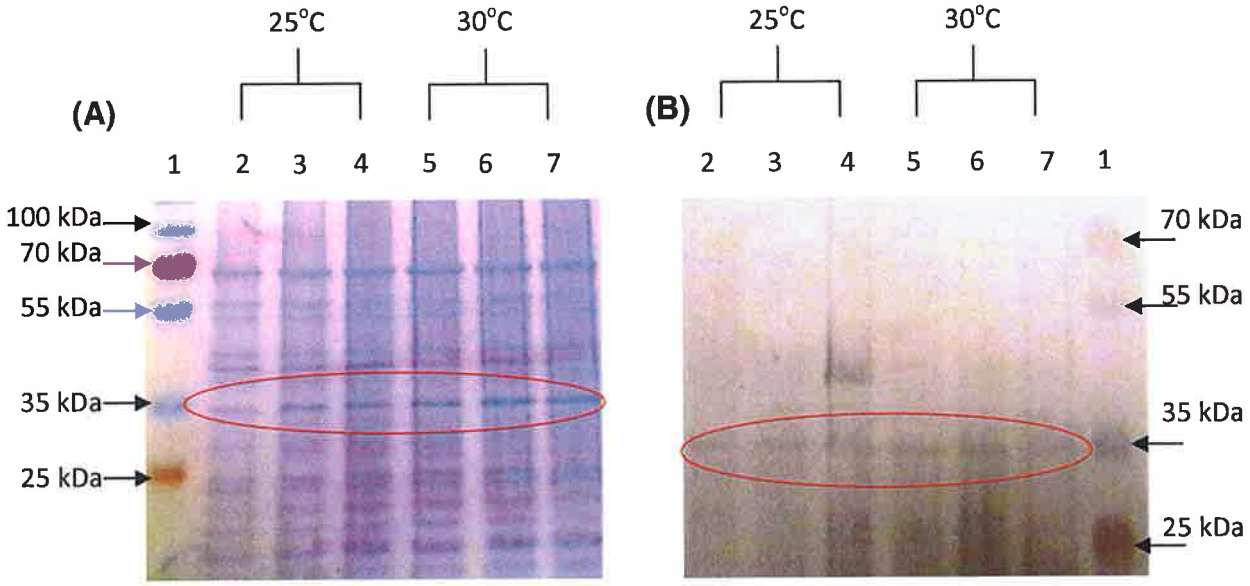

1 = Protein Marker
2 = Transformant 3 following 3 hours 1 mM IPTG induction
3 = Transformant 3 following 6 hours 1 mM IPTG induction
4 = Transformant 3 following O/N 1 mM IPTG induction
5 = Transformant 3 following 3 hours 1 mM IPTG induction
6 = Transformant 3 following 6 hours 1 mM IPTG induction
7 = Transformant 3 following O/N 1 mM IPTG induction

Figure 56: Induction temperature and induction time optimisation for optimal SFRP-2-GST protein expression in Tuner *E. coli* cells

(A): SDS PAGE, (B): anti-histidine Western blot. The lysate from transformant 3 (lane 4 in Figure 55) were incubated with sample treatment buffer and analysed on a 12.5% (w/v) SDS-PAGE Gel and by Western blotting using anti-histidine mAb. In (A) and (B) lane 1: prestained protein marker (Fermentas); lanes 2 to 7: different induction times of SFRP-2-GST transformed clone 3; lanes 2 and 5: 3 hours induction; lanes 3 and 6: 6 hours induction; lanes 4 and 7: O/N induction; lanes 2 to 4: induction at 25°C and lanes 5 to 7: induction at 30°C. A band at approximately 35 kDa in the SDS-PAGE gel was observed for all induced cultures. A slight increase of protein expression was noted with increasing induction temperature (30°C) and increasing induction time (O/N) in the SDS gel. The anti-histidine Western blot detected the protein at 35 kDa for all induced cultures. However, no significant increase or decrease in protein expression was noted with increasing induction temperature or increasing induction time in anti-histidine Western blot. The anti-histidine antibody in the anti-histidine Western blot also detected a weak band at approximately 26 kDa in all induced cultures except the culture induced at 25°C for 3 hours and a band at approximately 40 kDa in transformants 2, 3 and 4 (lanes 3, 4 an 5 (B)).

5.4.1.3.2 IPTG induction concentration optimisation for optimal SFRP-2-GST protein expression in Tuner E. coli cells

Transformant 3 (lane 4 in Figure 57) was grown O/N followed by IPTG induction concentration optimisation O/N at 30°C. The cultures were sonicated to achieve periplasmic extraction of the SFRP-2 recombinant fusion protein. The cultures were then analysed by SDS-PAGE electrophoresis and an anti- Histidine Western blot, as described in sections 2.5.1.1.8 and 2.5.1.1.9, to determine the optimal IPTG concentration for SFRP-2-GST recombinant fusion protein expression in Tuner(DE3) cells.

A band at approximately 35 kDa in the SDS-PAGE gel in Figure 57 (A) was observed for all induced cultures. However, no significant effect was seen in varying IPTG concentration. The anti-histidine Western blot in Figure 57 (B) confirmed these findings where although weak, detection of the protein was observed at 35 kDa with increasing protein expression with increasing IPTG concentration.

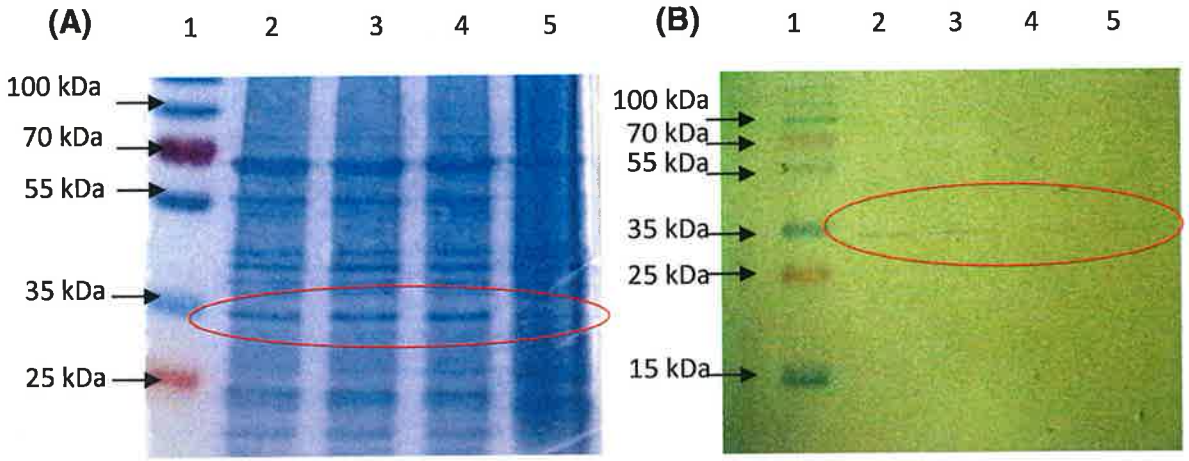

Figure 57: IPTG induction concentration optimisation for optimal SFRP-2-GST protein expression in Tuner *E. coli* cells

(A): SDS PAGE, (B): anti-histidine Western blot. The lysates from the transformant 3 (lane 4 in Figure 55) were incubated with sample treatment buffer and analysed on a 12.5% (w/v) SDS-PAGE Gel and by Western blotting using anti-histidine mAb. In (A) and (B) lane 1: prestained protein marker (Fermentas); lanes 2 to 5: different IPTG induction concentrations for optimal SFRP-2-GST expression in transformed clone 3 following O/N induction at 30°C; lane 2: 1 mM IPTG; lane 3: 0.5 mM IPTG; lane 4: 0.1 mM IPTG and lane 5: 0.05 mM IPTG. A band at approximately 35 kDa in the SDS-PAGE gel was observed for all induced cultures. However, no significant effect was seen in varying IPTG concentration. The anti-histidine Western blot detected a weak band at approximately 35 kDa with increasing protein expression with increasing IPTG concentration.

5.4.1.3.3 Large-scale SFRP-2-GST recombinant fusion protein expression in Tuner E. coli cells and purification of the expressed protein

The SFRP-2-expresing clone (transformant 3) was used for large-scale production of the SFRP-2 fusion protein. A larger culture volume (500 mL) of transformant 3 was grown up O/N followed by subsequent subculture and 1 mM IPTG induction O/N, as described in section 2.5.1.1.10. The protein lysate following sonication was centrifuged for removal of cell debris and the supernatant was purified using immobilized metal affinity chromatography (IMAC), as described in section 2.5.1.1.12 and a GST purification kit described in section 2.5.1.1.11. Glutathione affinity is an efficient method of purification of GST-fusion proteins by affinity chromatography on immobilized glutathione (the substrate of the GST enzyme) followed by competitive elution with excess reduced glutathione.

The IMAC purification was analysed by performing SDS-PAGE (Figure 58 (A)) and an anti-histidine Western blot (Figure 58 (B)) on the lysate, "flow-through", wash and eluted protein. As can be seen in Figure 58, the purification of the SFRP-2-GST recombinant fusion protein using IMAC was unsuccessful as an SFRP-2 recombinant fusion protein band was not observed in the eluted protein lane (lane 5 in Figure 58 (A)). The anti-histidine antibody used in the anti-histidine Western blot generated a band at approximately 35 kDa in the lysate and the "flow-through" suggesting the presence of the SFRP-2-GST fusion protein.

The results of the glutathione affinity purification were analysed by performing SDS-PAGE (Figure 58 (C)), an anti-histidine Western blot (Figure 58 (D)) and an anti-GST Western blot (Figure 58 (E)) on the lysate, "flow-through", wash and eluted protein. The purification of the SFRP-2-GST recombinant fusion protein using the GST purification kit was also unsuccessful as an SFRP-2 recombinant fusion protein band was not observed in the eluted protein lane (lane 5 in Figure 58 (C)). The anti-histidine antibody used for the anti-histidine Western blot generated a band at approximately 35 kDa in the lysate and the "flow-through" and the anti-GST antibody used for the anti-GST Western blot generated a band at approximately 35 kDa in the lysate and the "flow-through" suggesting the presence of the SFRP-2-GST fusion protein. The anti-GST antibody used in the anti-GST Western blot also showed bands at approximately 55 kDa, 26 kDa and 15 kDa in the lysate and the "flow-through" fraction.

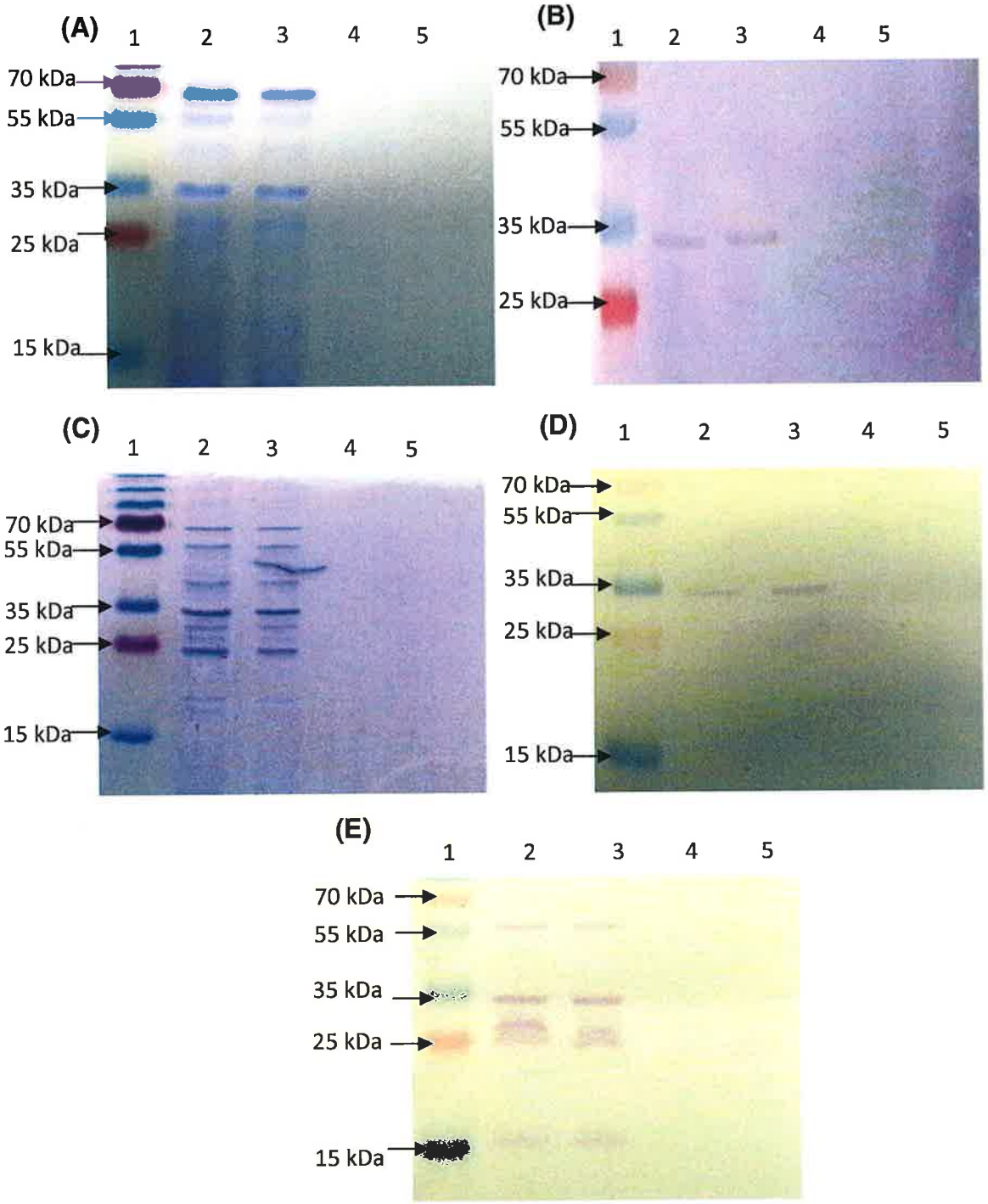

Figure 58: Large-scale SFRP-2-GST recombinant fusion protein expression in Tuner cells and IMAC and GST purification of the expressed protein

(A): SDS (IMAC purification), (B): anti-histidine Western blot (IMAC purification), (C): SDS (GST purification kit), (D): anti-histidine Western blot (GST purification kit), (E): anti-GST Western blot (GST purification kit). In (A)-(E) lane 1 represents the prestained protein marker (Fermentas), lane 2 contains unpurified sonicated lysate from transformant 3 (lane 4 in Figure 55) with all the proteins expressed in the bacterial cell lysate, lane 3 contains the "flow-through" with all unbound proteins that passed through the resin, lane 4 contains any impure non-specific hydrophobic proteins which may have weakly bound to the resin and were removed using an increased concentration of Tween 20 and lane 5 contains the purified eluted SFRP-2 recombinant fusion protein (see section 5.4.1.2.3 for details of results).

The IMAC purification was repeated, as described in section 2.5.1.1.12, using a large-scale production of transformant 3 with 6 M urea and 5 mM dithiothreitol (DTT) added to both the lysis buffer and running buffer. These denaturants were added to ensure that the SFRP-2-GST recombinant fusion protein was not dimerising.

The IMAC purification was analysed by performing SDS-PAGE electrophoresis (Figure 59 (A)), an anti-histidine Western blot (Figure 59 (B)), an anti-SFRP-2 Western blot (Figure 59 (C)) and an anti-GST Western blot (Figure 59 (D)) on the lysate, "flow-through", wash and eluted protein. A protein band was present in the eluted protein lane (lane 5) at approximately 11 kDa, as can be seen in Figure 59 (A). This band was detected by both the anti-histidine antibody in anti-histidine Western blot and the anti-SFRP-2 antibody in the anti-SFRP-2 Western blot along with another protein band at approximately 13 kDa. However, the anti-GST antibody did not detect either bands at 11 kDa and 13 kDa in the anti-GST Western blot in the eluent (lane 5 in Figure 59 (D)). Both the anti-SFRP-2 and the anti-histidine Western blots detected multiple bands in both the lysate and the "flow-through" with the strongest bands appearing between 10 kDa and 15 kDa.

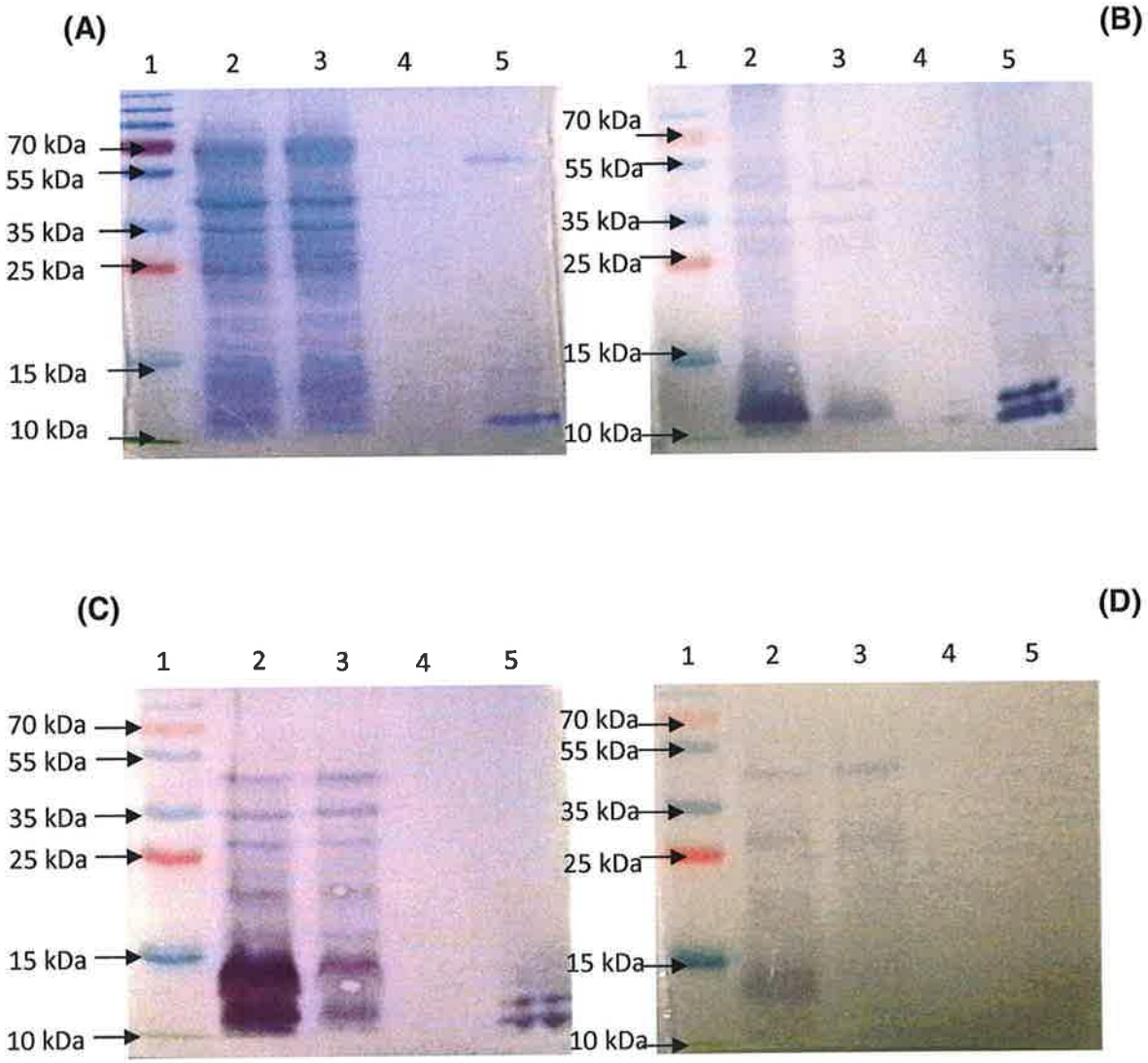

Figure 59: Large-scale SFRP-2-GST fusion protein expression and IMAC purification of the expressed recombinant fusion protein using 6 M urea and 5 mM DTT

(A): SDS, (B): anti-histidine Western blot, (C): anti-SFRP-2 Western blot, (D): anti-GST Western blot. In (A)-(D) lane 1 represents the prestained protein marker (Fermentas), lane 2 contains unpurified sonicated lysate with all the proteins expressed in the bacterial cell lysate, lane 3 contains the "flow-through" with all unbound proteins that passed through the resin, lane 4 contains any impure non-specific hydrophobic proteins which may have weakly bound to the resin and are removed using an increased concentration of Tween 20 and lane 5 contains the purified eluted SFRP-2 recombinant fusion protein. A protein band was present in the eluted protein lane (lane 5) at approximately 11 kDa in (A). This band was detected by both the anti-histidine antibody in anti-histidine Western blot (B) and the anti-SFRP-2 antibody in the anti-SFRP-2 Western blot (C) along with another protein band at approximately 13 kDa. However, the anti-GST antibody did not detect either bands at 11 kDa and 13 kDa in the anti-GST Western blot (D) in the eluent (lane 5). Both the anti-SFRP-2 and the anti-histidine Western blots detected multiple bands in both the lysate and the "flow-through" with the strongest bands appearing between 10 kDa and 15 kDa.

5.4.1.3.4 Analysis of SFRP-2-GST solubilisation in Tuner E. coli cells

A large culture volume (500 mL) of transformant 3 was grown up O/N followed by subsequent subculture and 1 mM IPTG induction O/N, as described in section 2.5.1.1.10. The protein lysate was sonicated and centrifuged. Twenty microlitres of the supernatant (lysate) and 20 µL of the re-suspended cells in PBS were analysed by SDS-PAGE and an anti-SFRP-2 Western blot to determine the solubility of the SFRP-2-GST recombinant fusion protein.

A strong band was visible at 40 kDa in both the SDS-PAGE gel and anti-SFRP-2 Western blot for the re-suspended sonicated cells in Figure 60 (lane 3). A band at 40 kDa was not present in the lysate in the anti-SFRP-2 Western blot (lane 2 in Figure 60 (B)). This result implies the SFRP-2-GST fusion protein is insoluble in the form of inclusion bodies trapped within the periplasm of the *E. coli* cell.

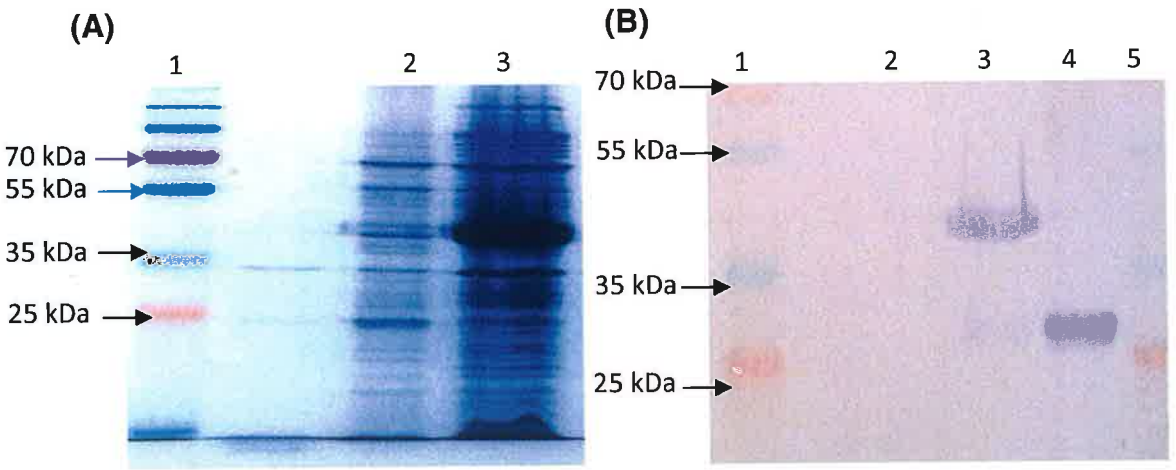

Figure 60: Analysis of SFRP-2-GST solubilisation in Tuner *E. coli* cells

(A): SDS, (B): anti-SFRP-2 Western blot. The lysate and cells of transformant 3 (lane 4 in Figure 55) following sonication were incubated with sample treatment buffer and analysed on a 12.5% SDS-PAGE Gel and by Western blotting using anti-SFRP-2 pAb. In (A) and (B) lanes 1 and 5 represent the prestained protein marker (Fermentas), lane 2 contains unpurified sonicated lysate with all the proteins expressed in the bacterial cell lysate and lane 3 contains unpurified sonicated cells resuspended in PBS. In (B) lane 4 contains a positive control (SFRP-2 recombinant fusion protein fused to Albumin Binding Protein (donated by Atlas Antibodies)). A strong band was visible at 40 kDa in both the SDS-PAGE gel and anti-SFRP-2 Western blot for the re-suspended sonicated cells (lane 3). A band at 40 kDa was not present in the lysate in the anti-SFRP-2 Western blot lane 2.

5.4.1.4 SFRP-2-GST recombinant fusion protein expression in other E. coli strains

To determine if improved soluble SFRP-2-GST expression was possible in other *E. coli* strains, the pGS-21a vector containing the SFRP-2 gene was transformed into other chemically competent DE3 strains of *E. coli* cells following a heat shock protocol (section 2.5.1.1.7). DE3 strains of *E. coli* are lysogenic for a λ prophage that contains an IPTG inducible T7 RNA polymerase. The DE3 *E. coli* strains chosen for transformation were NovaBlue(DE3), BLR(DE3) and HMS174(DE3). The BLR strain of *E. coli* is a *recA* derivative of BL-21. *RecA* is an *E. coli* protein (38 kDa) essential for the repair and maintenance of DNA. This strain of *E. coli* improves plasmid monomer yields and can help stabilise target plasmids containing repetitive sequences or whose products may cause the loss of the DE3 prophage. The HMS174 strains of *E. coli* provide a *recA* mutation in a K-12 background. The HMS174 strain, like the BLR strain, can also stabilise certain target genes whose products may cause the loss of the DE3 prophage. The NovaBlue *E. coli* strain is a K-12 strain containing a *recA* and *endA* (a gene that encodes endonuclease I which degrades double stranded DNA) mutation. It has high transformation efficiency so therefore is an ideal initial cloning host. The NovaBlue(DE3) strain also contains a *lacI* repressor which makes it a stringent host.

Transformed colonies were randomly picked from carbenicillin-supplemented agar plates. A total of 5 NovaBlue and HMS174 colonies were picked and 4 BLR colonies which were then grown O/N followed by subsequent 1 mM IPTG induction O/N at 30°C. The cultures were sonicated to achieve periplasmic extraction of the SFRP-2 recombinant fusion protein which was then analysed by SDS-PAGE electrophoresis, as described in section 2.5.1.1.8.

A band at approximately 35 kDa in all transformants of the BLR strain was noted in the SDS-PAGE gel in Figure 61. This is the molecular mass the SFRP-2-GST recombinant fusion protein expressed in the Tuner *E. coli*

lysates. This protein at 35 kDa was not present in any of the NovaBlue or HMS174 transformants.

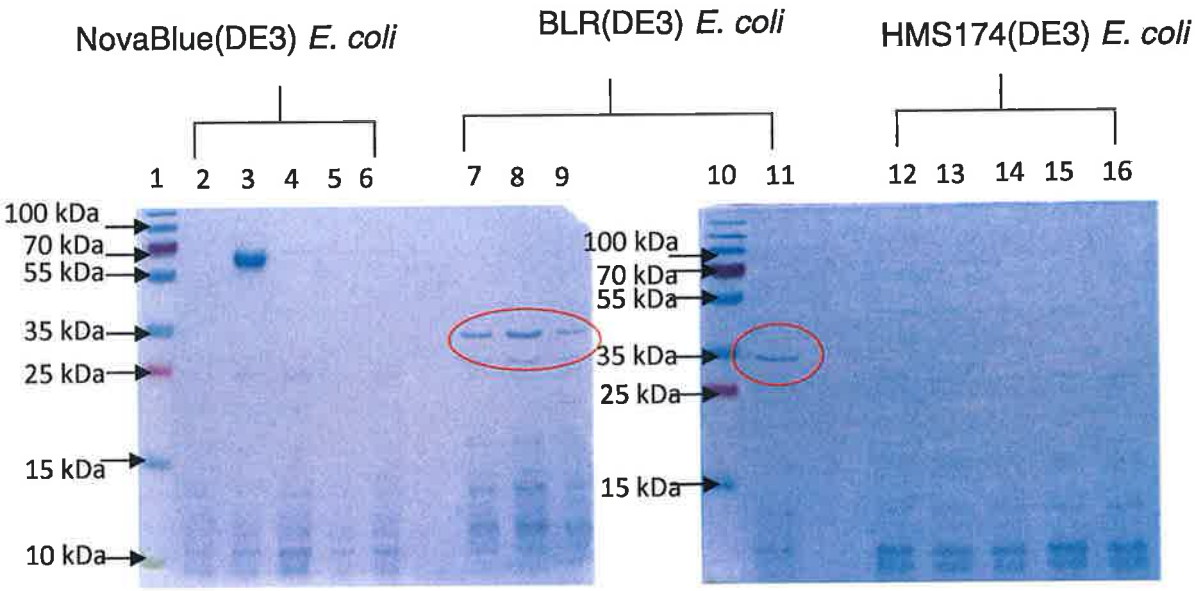

Figure 61: SDS-PAGE analysis for SFRP-2-GST expression in Nova blue, BLR and HMS174 *E. coli* cells

The lysates from expressed clones were incubated with sample treatment buffer and analysed on a 12.5% SDS-PAGE Gel. Lanes 1 and 10: prestained protein marker (Fermentas); lanes 2 to 6: Nova blue *E. coli* transformants; lanes 7 to 11: BLR *E. coli* transformants and lanes 12 to 16: HMS174 *E. coli* transformants. A band at approximately 35 kDa in all transformants of the BLR strain was noted in the SDS-PAGE gel.

5.4.1.5 SFRP-2-GST recombinant fusion protein expression in BLR E. coli cells

To analyse the SFRP-2-GST recombinant fusion protein expression in BLR(DE3) cells the BLR transformants were subject to optimisation experiments including; induction time optimisation, IPTG concentration optimisation and induction temperature optimisation.

5.4.1.5.1 Induction time optimisation for optimal SFRP-2-GST protein expression in BLR E. coli cells

Transformant 4 (lane 11 in Figure 61) was grown O/N followed by subsequent induction optimisation using 1 mM IPTG at 30°C over varying time courses (2 hours, 4 hours, 6 hours and O/N). The cultures were sonicated to achieve periplasmic extraction of the SFRP-2 recombinant fusion protein. The cultures were then analysed by SDS-PAGE electrophoresis and an anti-histidine Western blot, as described in sections 2.5.1.1.8 and 2.5.1.1.9, to determine the optimal induction time and temperature for SFRP-2-GST recombinant fusion protein expression in BLR(DE3) cells.

A band at approximately 35 kDa in the SDS-PAGE gel in Figure 62 (A) was observed for all induced cultures. However, no significant effect was seen in varying induction duration. This observation was supported by the anti-histidine Western blot in Figure 62 (B) where weak histidine bands were observed at approximately 35 kDa with no increase or decrease in expression levels across all induced cultures.

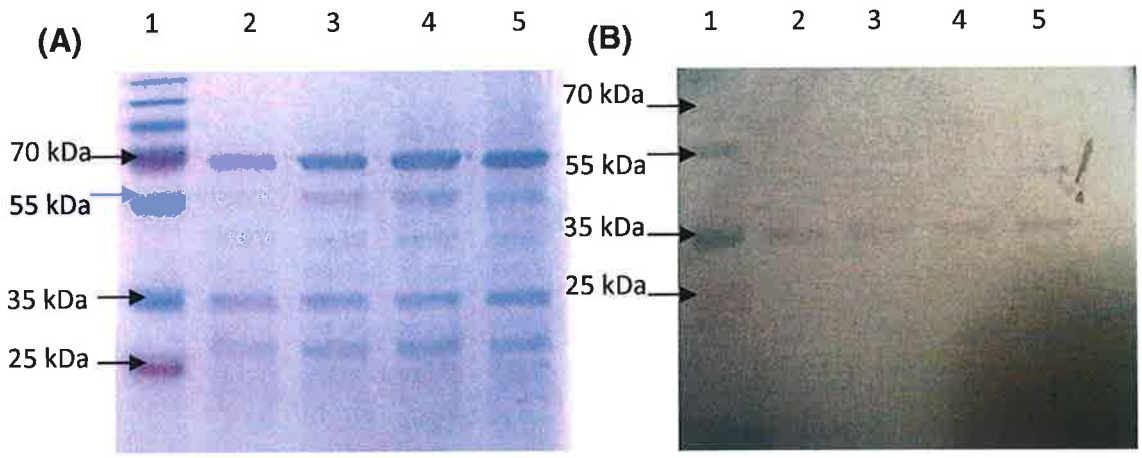

Figure 62: Induction time optimisation for optimal SFRP-2-GST protein expression in BLR *E. coli* cells

(A): SDS PAGE, (B): anti-histidine Western blot. The lysate from transformant 4 (lane 11 in Figure 61) was incubated with sample treatment buffer and analysed on a 12.5% SDS-PAGE Gel and by Western blotting using anti-SFRP-2 pAb. In both (A) and (B) lane 1: prestained protein marker (Fermentas); lanes 2 to 5: different induction times of SFRP-2-GST expression in transformed clone 4; lane 2: 2 hours induction with 1 mM IPTG at 30°C; lane 3: 4 hours induction with 1 mM IPTG at 30°C; lane 4: 6 hours induction with 1 mM IPTG at 30°C and lane 5: O/N induction with 1 mM IPTG at 30°C. A band at approximately 35 kDa in the SDS-PAGE gel was observed for all induced cultures. However, no significant effect was seen in varying induction duration. The anti-histidine Western blot generated weak bands at approximately 35 kDa with no increase or decrease in expression levels across all induced cultures.

5.4.1.5.2 IPTG induction concentration optimisation for optimal SFRP-2-GST protein expression in BLR E. coli cells

Transformant 4 (lane 11 in Figure 61) was grown O/N followed by IPTG induction concentration optimisation O/N at 30°C. The cultures were sonicated to achieve periplasmic extraction of the SFRP-2 recombinant fusion protein. The cultures were then analysed by SDS-PAGE and an anti-SFRP-2 Western blot, as described in sections 2.5.1.1.8 and 2.5.1.1.9, to determine the optimal IPTG concentration for SFRP-2-GST recombinant fusion protein expression in BLR (DE3) cells.

In the SDS-PAGE gel in Figure 63 (A) a band at approximately 35kDa was observed for all induced cultures. The bands for both the cultures induced with 0.1 mM and 1 mM appeared stronger than the band for the culture induced with 0.5 mM. The anti-histidine Western blot in Figure 63 (B)

confirmed these findings where although very weak, detection of the protein was observed at approximately 35 kDa with a slightly weaker band observed in the culture that was induced with 0.5 mM IPTG.

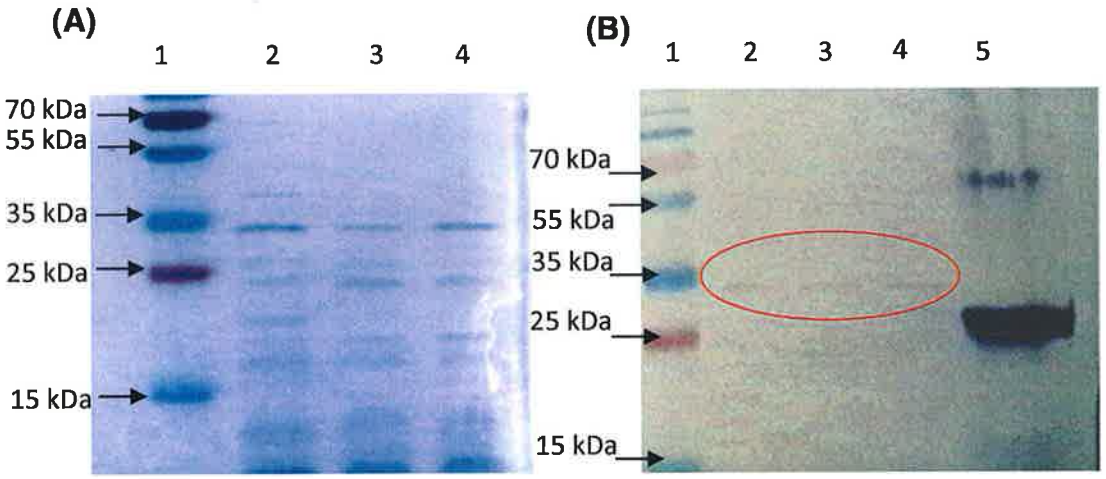

Figure 63: IPTG induction concentration optimisation for optimal SFRP-2-GST protein expression in BLR *E. coli* cells

(A): SDS PAGE, (B): anti-SFRP-2 Western blot. The lysate from transformant 4 (lane 11 in Figure 61) was incubated with sample treatment buffer and analysed on a 12.5% SDS-PAGE Gel and by Western blotting using anti-SFRP-2 pAb. In (A) and (B) lane 1: Prestained protein marker (Fermentas); lanes 2 to 4: different IPTG induction concentrations for optimal SFRP-2-GST expression in transformed clone 4 following O/N induction at 30°C; lane 2: 0.1 mM IPTG; lane 3: 0.5 mM IPTG and lane 4: 1 mM IPTG. In (B) lane 5 contains a positive control (SFRP-2 recombinant fusion protein conjugated to Albumin Binding Protein (donated by Atlas Antibodies)). A band at approximately 35kDa was observed for all induced cultures in the SDS PAGE gel. The bands for both the cultures induced with 0.1 mM and 1 mM appeared stronger than the band for the culture induced with 0.5 mM. The anti-histidine Western blot detected very weak protein bands at approximately 35 kDa with a slightly weaker band observed in the culture that was induced with 0.5 mM IPTG.

5.4.1.5.3 IPTG induction temperature optimisation for optimal SFRP-2-GST protein expression in BLR E. coli cells

Transformant 4 (lane 11 in Figure 61) was grown O/N followed by induction temperature optimisation using 1 mM and 0.1 mM IPTG O/N. The cultures were sonicated to achieve periplasmic extraction of the SFRP-2 recombinant fusion protein. The cultures were then analysed by SDS-PAGE and an anti-SFRP-2 Western blot, as described in sections 2.5.1.1.8 and 2.5.1.1.9, to determine the optimal temperature for SFRP-2-GST recombinant fusion protein expression in BLR(DE3) cells.

Although weak, the optimal temperature for induction of the BLR(DE3) *E. coli* cells was at 30°C using 1 mM IPTG. This was observed in the SDS-PAGE gel in Figure 64 (A) where the strongest band at approximately 35kDa was observed in the culture induced with 1 mM IPTG at 30°C (lane 5 in Figure 64 (A)). The anti-histidine Western blot in Figure 64 (B) confirmed these findings where although very weak, detection of the protein was observed at approximately 35 kDa in all lanes.

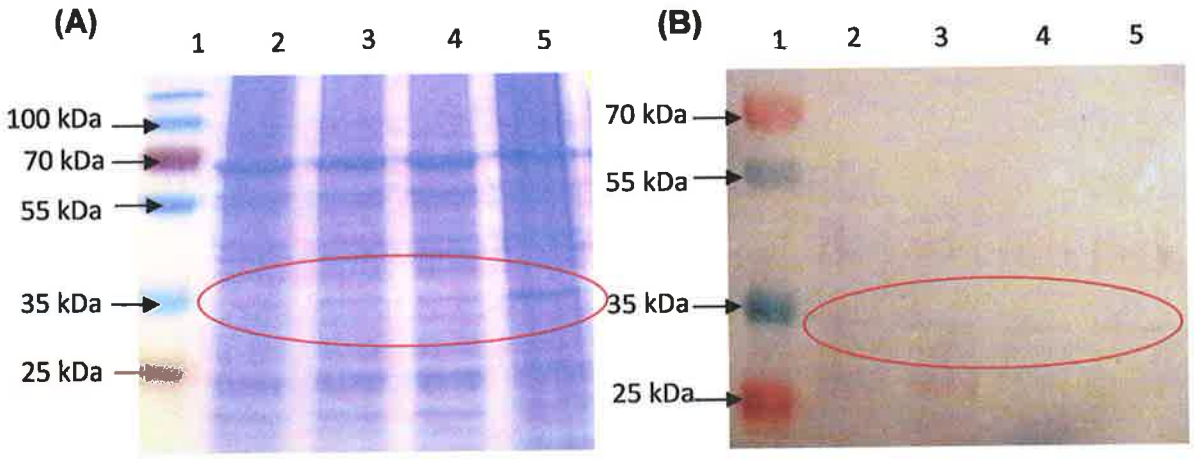

Figure 64: IPTG induction temperature optimisation for optimal SFRP-2-GST protein expression in BLR *E. coli* cells

(A): SDS PAGE, (B): anti-histidine Western blot. The lysate from transformant 4 (lane 11 in Figure 61) was incubated with sample treatment buffer and analysed on a 12.5% SDS-PAGE Gel and by Western blotting using anti-histidine mAb. In (A) and (B) lane 1: prestained protein markers (Fermentas); lanes 2 to 5: different IPTG induction concentrations and temperature for optimal SFRP-2-GST expression in transformed clone 4 following O/N induction; lane 2: 0.1 mM IPTG at 25°C; lane 3: 1 mM IPTG at 25°C; lane 4: 0.5mM IPTG at 30°C and lane 5: 1 mM IPTG at 30°C. Although weak, the optimal temperature for induction of the BLR(DE3) *E. coli* cells was at 30°C using 1 mM IPTG. This was observed in the SDS-PAGE gel where the strongest band at approximately 35kDa was observed in the culture induced with 1 mM IPTG at 30°C (lane (A)). The anti-histidine Western blot confirmed these findings where, although very weak, detection of the protein was observed at approximately 35 kDa.

5.4.1.5.4 Large-scale SFRP-2-GST recombinant fusion protein expression in BLR cells and purification of the expressed protein

The SFRP-2-expresing clone (transformant 4) was used for large-scale production of the SFRP-2 fusion protein. A larger culture volume (500 mL) of transformant 4 was grown up O/N followed by subsequent subculturing and 1 mM IPTG induction O/N at 30°C, as described in section 2.5.1.1.10. The protein lysate following sonication was centrifuged to remove cell debris and the supernatant was purified using IMAC, as described in section 2.5.1.1.12.

The purification was analysed by performing SDS-PAGE (Figure 65 (A)) and an anti-SFRP-2 Western blot (Figure 65 (B)) on the lysate, "flow-through", wash and eluted protein. As can be seen in Figure 65, the large-scale expression and purification of the SFRP-2-GST recombinant fusion protein

was unsuccessful as no protein was observed in the lysate (lane 2 in Figure 65 (B)).

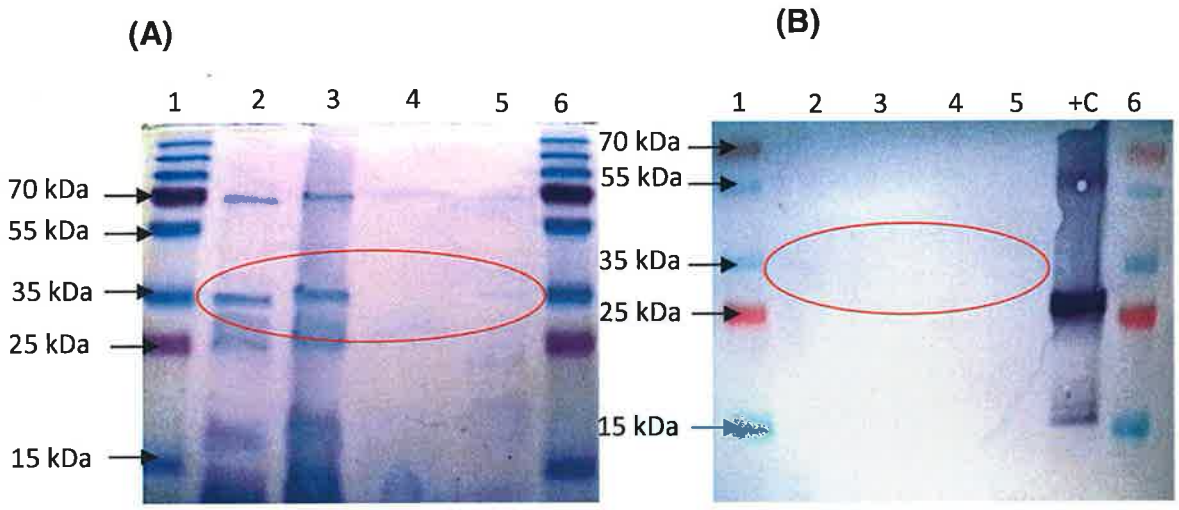

Figure 65: Large-scale SFRP-2-GST recombinant fusion protein expression in BLR cells and IMAC purification of the expressed protein

(A): SDS, (B): anti-SFRP-2 Western blot. In (A) and (B) lanes 1 and 6 represents the prestained protein markers (Fermentas), lane 2 contains unpurified sonicated lysate from transformant 4 (lane 11 in Figure 61) with all the proteins expressed in the bacterial cell lysate, lane 3 contains the "flow-through" with all unbound proteins that passed through the resin, lane 4 contains any impure non-specific hydrophobic proteins which may have weakly bound to the resin and were removed using an increased concentration of Tween 20 and lane 5 contains the purified eluted SFRP-2 recombinant fusion protein. In (B) lane +C contains a positive control (SFRP-2 recombinant fusion protein conjugated to Albumin Binding Protein (donated by Atlas Antibodies)). The large-scale expression and purification of the SFRP-2-GST recombinant fusion protein was unsuccessful as no protein was observed in the lysate.

5.4.2 SFRP-2-hFABP recombinant fusion protein expression in Tuner *E. coli*

The SFRP-2 gene was next cloned into a pET-28b(+) vector which contained a heart fatty acid binding protein (hFABP) gene sequence, a *Sac* I and *Not* I restriction site and a lac operator spliced together with a T7 promotor. This purified vector containing an unrelated peptide sequence in a pET-28b(+) backbone was prepared by Mr. Paul Conroy. This novel fusion construct was designed by Dr. Stephen Hearty and is described in detail in section 2.5.1.1.1.3. Heart fatty acid binding protein is a 15 kDa, hydrophilic protein involved in maintaining myocardial homeostasis via transporting long-chain

fatty acids to different sites of oxidation and esterfication in the cell (Fournier and Richard, 1990). It has become an important early marker of acute myocardial infarction (Kleine *et al.*, 1992). Within the School of Biotechnology hFABP was found to be an excellent expressing protein in an *E. coli* expression system.

5.4.2.1 SFRP-2 gene amplification from the pUC57 vector

The SFRP-2 gene was cloned into a pUC57 vector by Genscript USA Inc. described in detail in section 2.5.1.1.1.2. Primers were designed to amplify the SFRP-2 gene from the pUC57 vector. The sense primer contains a sequence tail that corresponds to the *Sac* I restriction site and the above antisense primer contains a sequence tail that corresponds to the *Not* I restriction site for ligation into pET-28b(+)-hFABP vector described in section 2.5.1.1.2. The PCR was optimised for the predicted annealing temperature and the PCR products were analysed for amplification by agarose gel electrophoresis. All annealing temperatures analysed (54°C, 58°C and 62°C) generated a single defined amplification at the predicted size of 374 bps (SFRP-2 gene = 360 bps + *Sac* I restriction site = 6 bps + *Not* I restriction site = 8 bps) in Figure 66 (A). Large-scale amplification (15X) of the SFRP-2 gene was performed using an annealing temperature of 62°C. The amplified gene was purified by gel extraction resolved by agarose gel electrophoresis. Successful amplification and purification at approximately 374 bps was observed in Figure 66 (B).

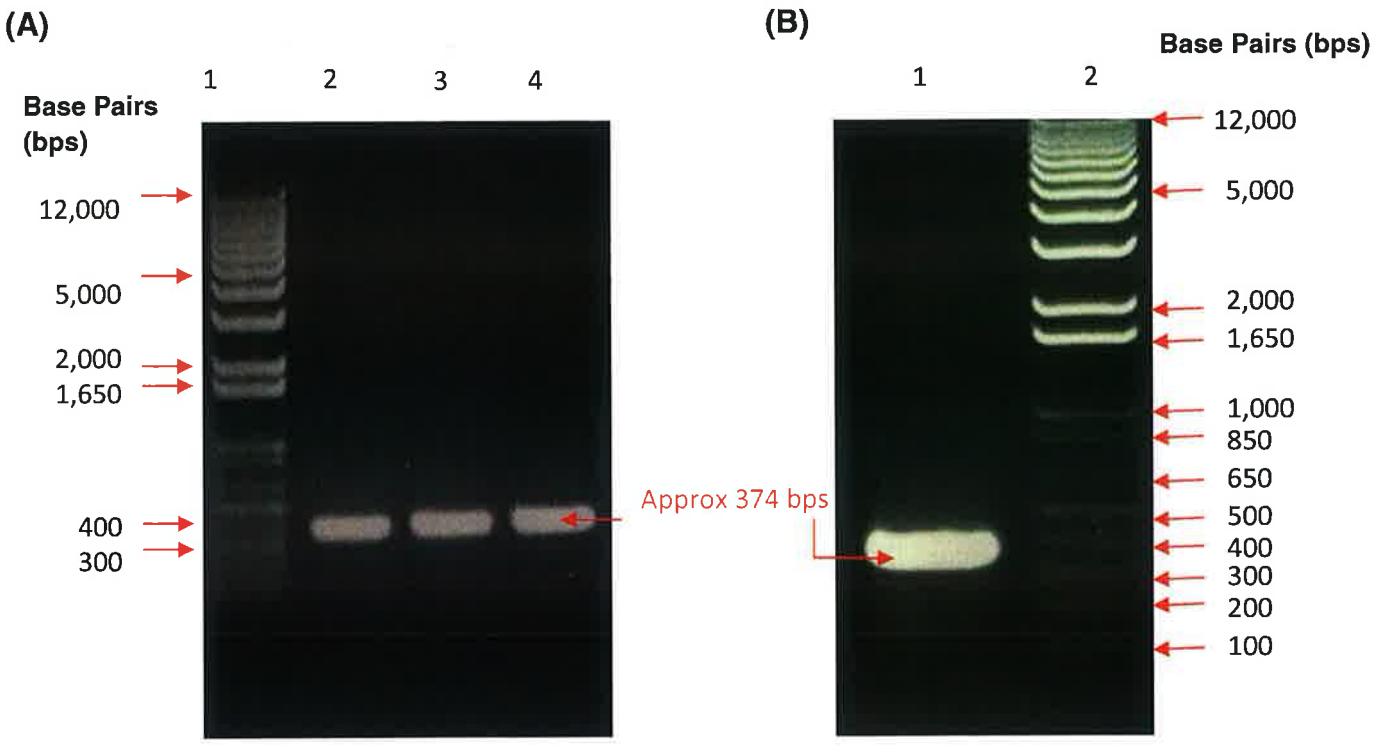

Figure 66: Amplification and purification of the SFRP-2 gene from the pUC57 vector

(A) Annealing temperature optimisation of PCR primers for SFRP-2 amplification from pUC57 vector. Lane 1: 1 kb DNA ladder plus, lane 2: 54°C annealing temperature, lane 3: 58°C annealing temperature, lane 4: 62°C annealing temperature.

(B) Large-scale amplification and purification of the SFRP-2 gene at an annealing temperature of 62°C. Lane 1: purified amplified SFRP-2 gene, lane 2: 1 kb DNA ladder plus.

5.4.2.2 Cloning of the SFRP-2 gene into the pET-28b(+)-hFABP vector

The amplified SFRP-2 gene containing the *Sac* I and *Not* I restriction sites compatible with the pET-28b(+)-hFABP vector was digested with the *Sac* I and *Not* I restriction enzymes, creating cohesive ends. The pET-28b(+)-hFABP vector was also digested with the *Sac* I and *Not* I restriction enzymes, creating cohesive ends and a linear plasmid (see Figure 67). Digesting the SFRP-2 gene with two different enzymes guarantees unidirectional cloning of

the gene into the vector and prevents the vector re-ligating. The pET-28b(+)-hFABP vector and the SFRP-2 gene were mixed in a 3:1 (Vector:insert) and the cohesive ends were ligated by T4 DNA ligase enzyme.

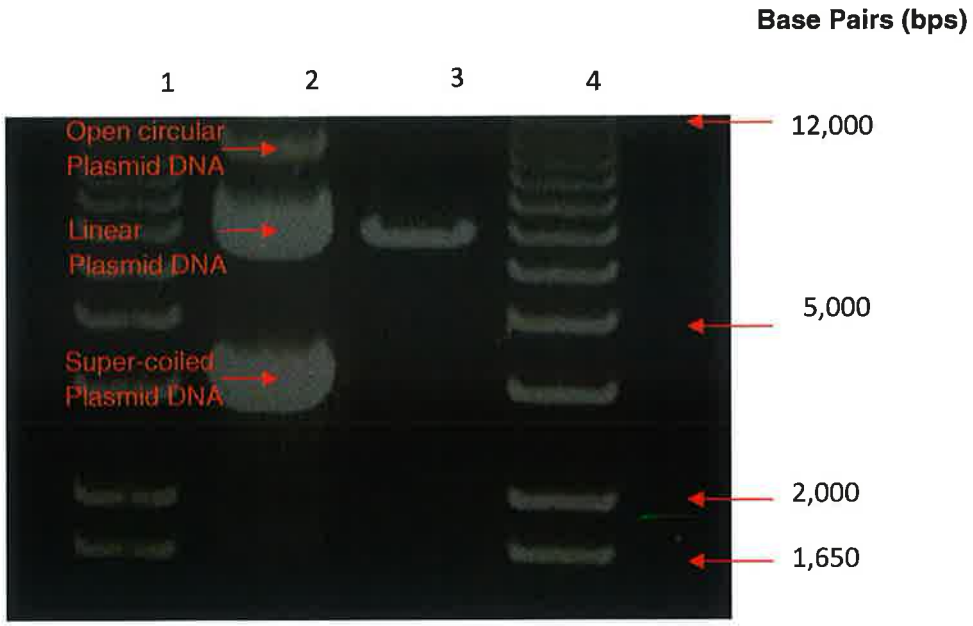

Figure 67: pET-28b(+)-hFABP vector digestion with *Not* I and *Sac* I enzymes

pET-28b(+)-hFABP vector digest. Lanes 1 and 4: 1 kb DNA ladder plus, lane 2: uncut plasmid DNA, lane 3: plasmid DNA cut with *Not* I and *Sac* I enzymes.

5.4.2.3 Transformation of ligated pET-28b(+)-hFABP vector into Tuner cells and SFRP-2 protein expression analysis

The ligated vector containing the SFRP-2 gene was next transformed into the chemically competent Tuner(DE3) strain of *E. coli* cells following a heat shock protocol (section 2.5.1.1.7). Transformed colonies were randomly picked from carbenicillin-supplemented agar plates. A total of 8 colonies were picked and grown O/N followed by subsequent 1 mM IPTG induction O/N at 30°C. The cultures were sonicated to achieve periplasmic extraction of the SFRP-2 recombinant fusion protein which was then analysed by SDS-PAGE and an

anti-SFRP-2 and anti-GST Western blot, as described in sections 2.5.1.1.8 and 2.5.1.1.9.

The predicted size of the SFRP-2-hFABP recombinant fusion was approximately 29 kDa as the SFRP-2 protein is approximately 14 kDa and the hFABP protein is approximately 15 kDa. The anti-histidine antibody used in the anti-histidine Western blot in Figure 68 (B) generated a strong bands at approximately 17 kDa in transformants 2,3,4,6 and 8 (lanes 3,4,5,7 and 9). No histidine was detected for transformants 1, 5 and 7 (lanes 2, 6 and 8 in Figure 68 (B). However, the SFRP-2 antibody generated a strong band at approximately 17 kDa in transformants 1, 5 and 7 (lanes 2,6 and 8) in the anti-SFRP-2 Western blot in Figure 68 (C). A weak band was also noted at approximately 29 kDa (the predicted molecular mass of the SFRP-2-hFABP recombinant fusion protein (SFRP-2~14 kDa + hFABP~15 kDa)) in transformant 1 (lane 2 in Figure 68 (C)).

An anti-cTnI Western blot was also performed. The gene that was cloned into a pET-28b(+) by Genscript consisted of a *Nco* I restriction site, hFABP gene sequence, a *BamH* I restriction site, a linker DNA sequence, a *Sac* I restriction site, a cTnI gene sequence and a *Not* I restriction site, as described in section 2.5.1.1.1.3. The cTnI gene sequence should be cut out from the pET28b-(+)-hFABP vector and replaced with the SFRP-2 gene sequence if the *Not* I and *Sac* I digestion and T4 ligations were successful. Like the anti-histidine Western blot in Figure 68 (B), the anti-cTnI Western blot in Figure 68 (D) also detected strong bands at approximately 17 kDa in transformants 2,3,4,6 and 8 (lanes 3,4,5,7 and 9). Strong bands for hFABP were detected at approximately, 11 kDa, 14kDa and 17 kDa in all transformants in the anti-hFABP Western blot in Figure 68 (E). A weak band for hFABP was also noted in transformant 1 (lane 2 in Figure 68 (E)) at approximately 29 kDa.

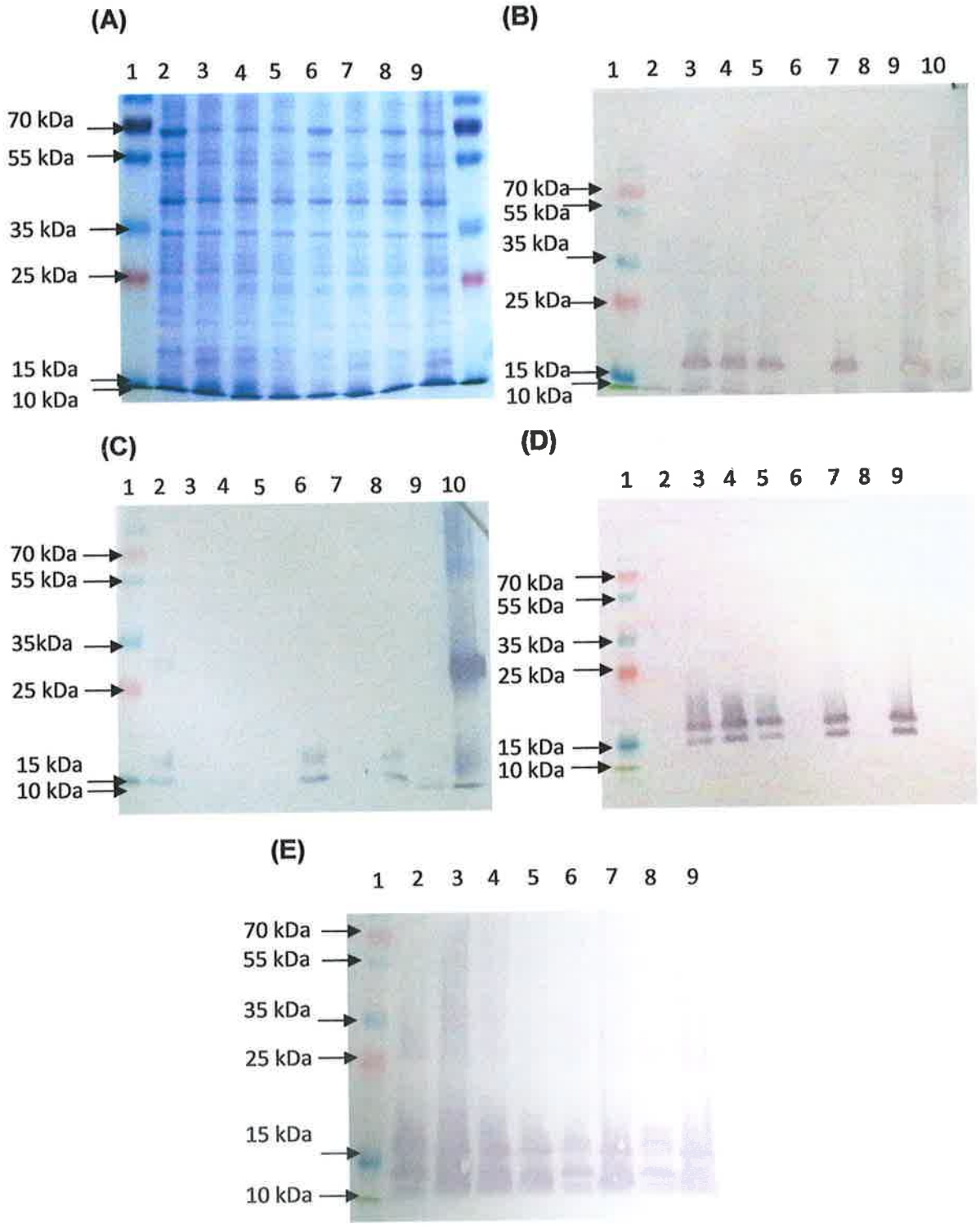

Figure 68: SFRP-2-hFABP protein expression in Tuner *E. coli* cells

(A): SDS PAGE, (B): anti-histidine Western blot, (C): anti-SFRP-2 Western blot, (D): anti-cTnI Western blot, (E): anti-hFABP Western blot. The lysates from the expressed clones were incubated with sample treatment buffer and analysed on a 12.5% SDS-PAGE Gel and by Western blotting. Lane 1: Prestained protein marker (Fermentas) and lanes 2 to 9: different SFRP-2-hFABP transformed clones. In (C) lane 10 contains a positive control (SFRP-2 recombinant fusion protein conjugated to Albumin Binding Protein containing a Histidine tag (donated by Atlas Antibodies)). (See section 5.4.2.3 for details of results)

The entire cloning process was repeated and the ligated vector containing the SFRP-2 gene was transformed into the chemically competent Tuner(DE3) strain of *E. coli* cells following a heat shock protocol (section 2.5.1.1.7). Transformed colonies were randomly picked from carbenicillin supplemented agar plates. Eight colonies were picked and grown O/N followed by subsequent 1 mM IPTG induction O/N at 30°C. The cultures were sonicated and analysed by SDS-PAGE electrophoresis and an anti-SFRP-2 and anti-GST Western blot, as described in sections 2.5.1.1.8 and 2.5.1.1.9.

The anti-histidine antibody in the anti-histidine Western blot in Figure 69 (B) generated strong bands at approximately 17 kDa in transformants 5 and 6 (lanes 6 and 7). No bands were generated by the antibody in all other transformants. However, strong bands were generated by the anti-SFRP-2 antibody at approximately 17 kDa and 14 kDa in transformants 1, 2, 3, 4, 7 and 8 (lanes 2, 3, 4, 5, 8 and 9) in the anti-SFRP-2 Western blot in Figure 69 (C). A weak band at approximately 29 kDa (the predicted molecular mass of the SFRP-2-hFABP recombinant fusion protein) was also noted in transformant 4 and 7 (lanes 5 and 8 in Figure 69 (C)).

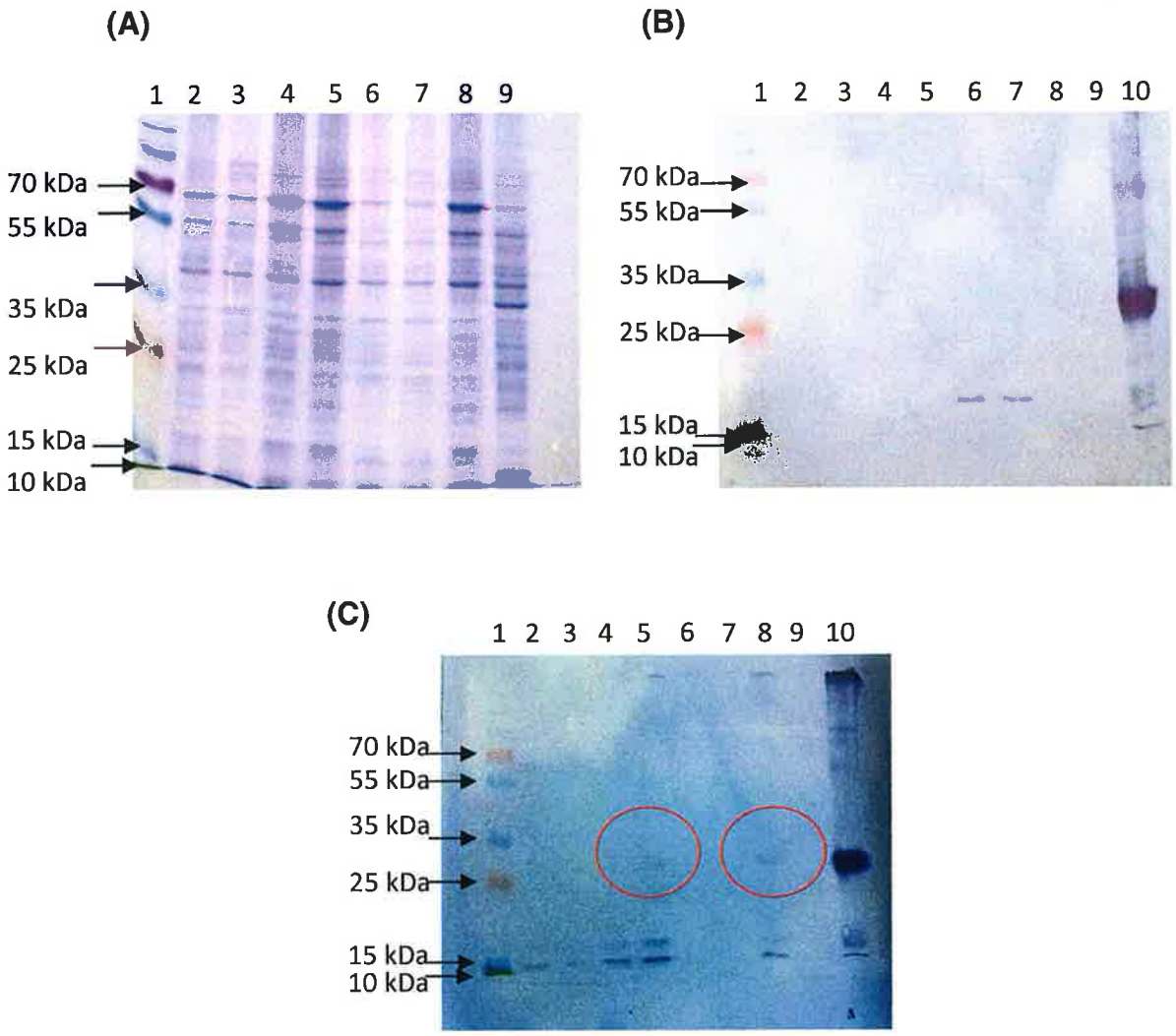

Figure 69: SFRP-2-hFABP protein expression in additional Tuner *E. coli* cells

(A): SDS PAGE, (B): anti-histidine Western blot, (C): anti-SFRP-2 Western blot. The lysates from the expressed clones were incubated with sample treatment buffer and analysed on a 12.5% SDS-PAGE Gel and by Western blotting using anti-SFRP-2 pAb and anti-histidine mAb. In (A)-(C) lane 1: prestained protein marker (Fermentas) and lanes 2 to 9: different SFRP-2-hFABP transformed clones. In (B) and (C) lane 10 contains a positive control (SFRP-2 recombinant fusion protein conjugated to Albumin Binding Protein containing a Histidine tag (donated by Atlas Antibodies)). The anti-histidine antibody in the anti-histidine Western blot generated strong bands at approximately 17 kDa in transformants 5 and 6 (lanes 6 and 7). No bands were generated by the antibody in all other transformants. However, strong bands were generated by the anti-SFRP-2 antibody at approximately 17 kDa and 14 kDa in transformants 1, 2, 3, 4, 7 and 8 (lanes 2, 3, 4, 5, 8 and 9) in the anti-SFRP-2 Western blot in). A weak band at approximately 29 kDa (the predicted molecular mass of the SFRP-2-hFABP recombinant fusion protein) was also noted in transformant 4 and 7 (lanes 5 and 8). The anti-histidine antibody in the anti-histidine Western blot generated strong bands at approximately 17 kDa in transformants 5 and 6 (lanes 6 and 7). No bands were generated by the antibody in all other transformants. However, strong bands were generated by the anti-SFRP-2 antibody at approximately 17 kDa and 14 kDa in transformants 1, 2, 3, 4, 7 and 8 (lanes 2, 3, 4, 5, 8 and 9) in the anti-SFRP-2 Western blot. A weak band at approximately 29 kDa (the predicted molecular mass of the SFRP-2-hFABP recombinant fusion protein) was also noted in transformant 4 and 7 (lanes 5 and 8 68(C)).

5.4.2.4 Sequencing of SFRP-2-hFABP recombinant fusion protein transformant

To ensure that the intact plasmid containing the SFRP-2 sequence was present in transformant 4 (lane 5 Figure 69), a bacterial stock of transformant 4 containing the transformed plasmid was sent for sequencing to Source BioScience LifeSciences. The DNA sequence was received and subsequently translated into its amino acid sequence using ExPASy translation tool.

As can be seen in Figure 70, cloning of the SFRP-2 gene into the pET-28b(+)-hFABP vector was successful. The cTnI gene was successfully excised from the vector via the *Sac* I and *Not* I sites and the SFRP-2 gene was successfully ligated into the vector in its place. This was then successfully transformed into transformant 4.

(A)

MVDAFLGTWKLVDSKNFDDYMKSLGVGFATRQVASMTKPTTIIEKNGDILTLKTHST
FKNTEISFKLGVEFDETTADDRKVKSIVTLDGGKLVHLQKWDGQETTLVRELIDGKLI
LTLTHGTAVCTRTYE***KE***GSGGSSRSSSSGGGGSGGGG***EL***ATEEAPKVCEACKNK
NDDDNDIMETLCKNDFALKIKVKEITYINRDTKIILETKSKTIYKLNGVSERDLKKSVLW
LKDSLQCTCEEMNDINAPYLVMGQKQGGELVITSVKRWQKGQREAAALEHHHHHH

(B)

MVDAFLGTWKLVDSKNFDDYMKSLGVGFATRQVASMTKPTTIIEKNGDILTLKTHST
FKNTEISFKLGVEFDETTADDRKVKSIVTLDGGKLVHLQKWDGQETTLVRELIDGKLI
LTLTHGTAVCTRTYE***KE***GSGGSSRSSSSGGGGSGGGG***EL***NYRAYATEPHAKKKS
KISASRKLQLKTAA

Figure 70: Sequence analysis of transformant 4 (lane 5 in Figure 69)

(A) Plasmid gene sequence transformed into transformant 4 (lane 5 in Figure 69) translated into the amino acid sequence using the ExPASy translation tool. The hFABP sequence is highlighted in blue, the linker is highlighted in grey, the SFRP-2 sequence is highlighted in yellow and the histidine tag is highlighted in green. The amino acid sequences in bold italics correspond to the *Sac* I and *Not* I restriction sites and the AA- sequences is a sequence from the vector that is retained in the construct.

(B) Translated pET-28b(+)-hFABP vector gene sequence containing the cTnI insert, as described in section 2.5.1.1.1.3, using the ExPASy translation tool. The hFABP sequence is highlighted in blue, the linker is highlighted in grey and the cTnI sequence is highlighted in red. The amino acid sequences in bold italics correspond to the *Sac* I and *Not* I restriction sites and the AA- sequences is a sequence from the vector that is retained in the construct

5.4.2.5 IPTG induction time and concentration optimisation for optimal SFRP-2-hFABP protein expression in Tuner E. coli cells

To determine the optimal induction conditions for SFRP-2-hFABP recombinant fusion protein expression in Tuner(DE3) cells, transformant 4 (lane 5 in Figure 69) was grown O/N followed by IPTG induction concentration

optimisation at different time courses at 30°C. The cultures were sonicated to achieve periplasmic extraction of the SFRP-2 recombinant fusion protein. The cultures were then analysed by SDS-PAGE, an anti-histidine Western blot and an anti-SFRP-2 Western blot, as described in sections 2.5.1.1.8 and 2.5.1.1.9, to determine the optimal IPTG concentration and induction time for SFRP-2-hFABP recombinant fusion protein expression in Tuner (DE3) cells.

Bands at approximately 29 kDa were observed for cultures induced with 0.1 mM, 0.5 mM and 1 mM IPTG for 2 hours and also for all the cultures induced for 4 hours in both the anti-SFRP-2 and anti-histidine Western blots in Figure 71. Weak bands were also observed at approximately 14 kDa the anti-histidine Western blot in Figure 71 (B) for the cultures induced with 0.1 mM, 0.5 mM and 1 mM IPTG for 2 hours and the culture induced with 0.05 mM IPTG for 4 hours. The anti-SFRP-2 Western blot also detected SFRP-2 at approximately 14 kDa for all cultures induced for 2 and 4 hours and also at approximately 17 kDa for all the cultures induced for 4 hours.

In Figure 72, only the culture induced for 6 hours with 1 mM IPTG expressed the fusion protein at approximately 29 kDa (lane 5 Figure 72 (C)). This was detected by the anti-SFRP-2 Western blot and a weak band was observed at 29 kDa the anti-histidine Western blot (lane 5 Figure 72 (B)). However, the anti-SFRP-2 and the anti-histidine antibodies did not generate a band at 29 kDa for any of the other cultures induced for 6 hours or O/N in Figure 72 in the anti-SFRP-2 and anti-histidine Western blots. The anti-SFRP-2 antibody also generated a band at approximately 17 kDa and 14 kDa for all cultures induced O/N in the anti-SFRP-2 Western blot Figure 72 (C).

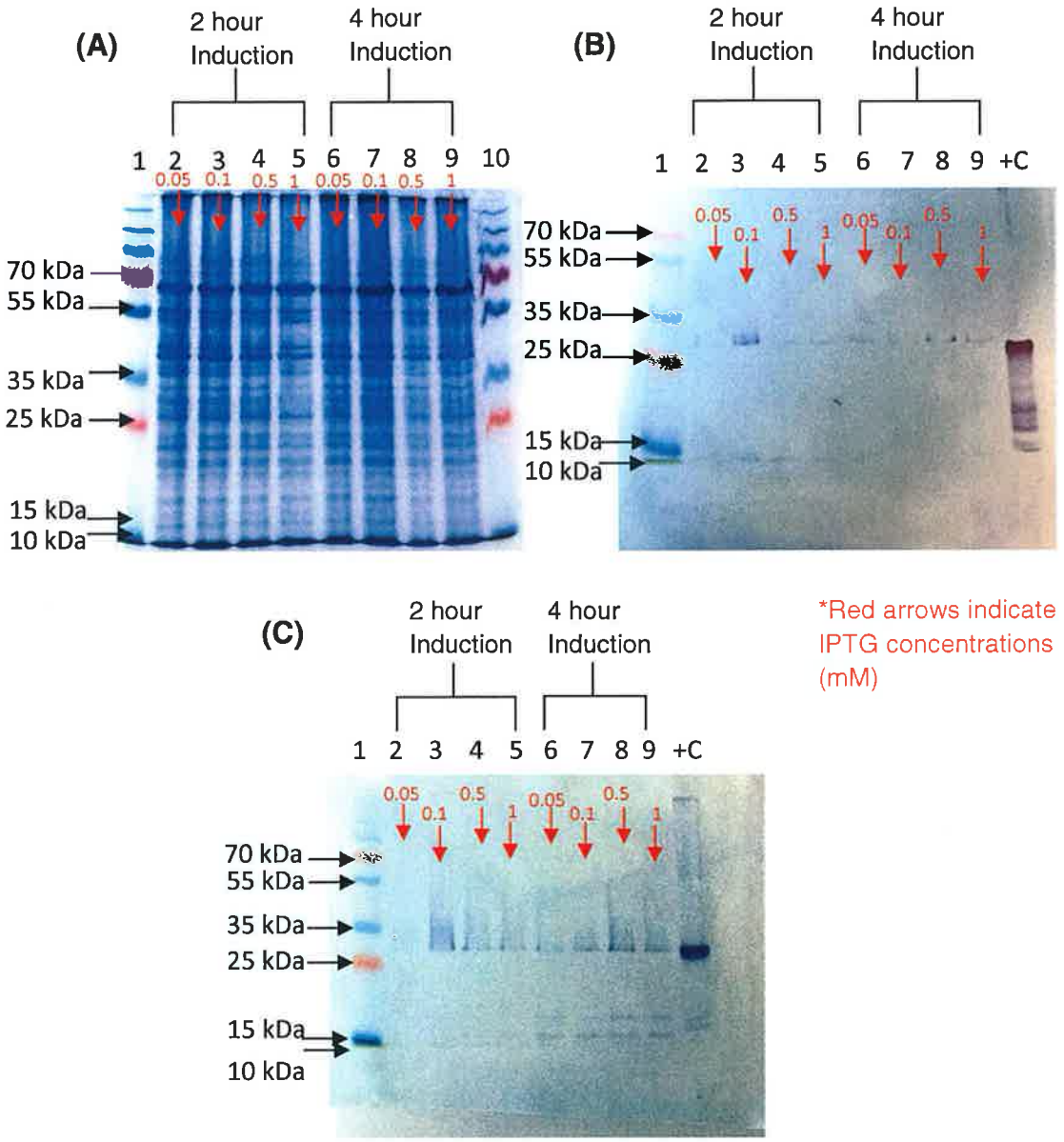

Figure 71: IPTG induction time (2 and 4 hours) and concentration optimisation for optimal SFRP-2-hFABP protein expression in Tuner E. coli cells

(A): SDS PAGE, (B): anti-histidine Western blot, (C): anti-SFRP-2 Western blot. The lysates from the expressed clones were incubated with sample treatment buffer and analysed on a 12.5% SDS-PAGE Gel and by Western blotting using anti-SFRP-2 pAb and anti-histidine mAb. In (A)-(C) lanes 1 and 10: prestained protein markers (Fermentas); lanes 2 to 5: transformant 4 induced with different concentrations of IPTG for 2 hours; lanes 6 to 9: transformant 4 induced with different concentrations of IPTG for 4 hours; lanes 2 and 6: 0,05 mM IPTG; lanes 3 and 7: 0.1 mM IPTG; lanes 4 and 8: 0.5mM IPTG and lanes 5 and 9: 1 mM IPTG. In (B) and (C) lane +C contains a positive control (SFRP-2 recombinant fusion protein conjugated to Albumin Binding Protein containing a Histidine tag (donated by Atlas Antibodies)). Bands at approximately 29 kDa were observed for cultures induced with 0.1 mM, 0.5 mM and 1 mM IPTG for 2 hours and also for all the cultures induced for 4 hours in both the anti-SFRP-2 and anti-histidine Western blots. Weak bands were also observed at approximately 14 kDa the anti-histidine Western blot for the cultures induced with 0.1 mM, 0.5 mM and 1 mM IPTG for 2 hours and the culture induced with 0.05 mM IPTG for 4 hours. The anti-SFRP-2 Western blot also detected SFRP-2 at approximately 14 kDa for all cultures induced for 2 and 4 hours and also at approximately 17 kDa for all the cultures induced for 4 hours.

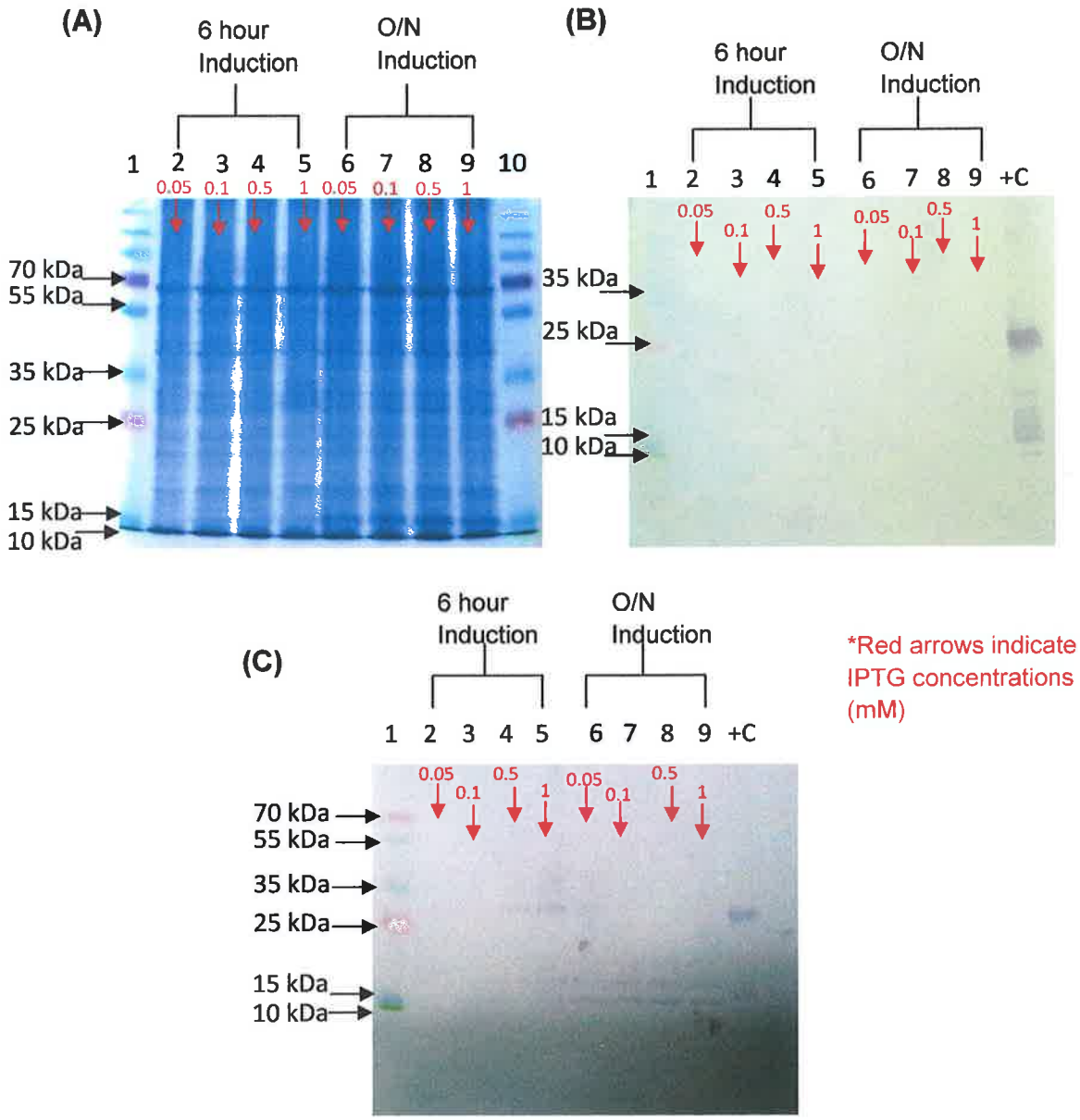

Figure 72: IPTG induction time (6 hours and O/N) and concentration optimisation for optimal SFRP-2-hFABP protein expression in Tuner E. coli cells

(A): SDS PAGE, (B): anti-histidine Western blot, (C): anti-SFRP-2 Western blot. The lysates from the expressed clones were incubated with sample treatment buffer and analysed on a 12.5% (w/v) SDS-PAGE Gel and by Western blotting using anti-SFRP-2 pAb and anti-histidine mAb. In (A)-(C) lanes 1 and 10: Prestained protein markers (Fermentas); lanes 2 to 5: transformant 4 induced with different concentrations of IPTG for 6 hours; lanes 6 to 9: transformant 4 induced with different concentrations of IPTG O/N; lanes 2 and 6: 0,05 mM IPTG; lanes 3 and 7: 0.1 mM IPTG, lanes 4 and 8: 0.5mM IPTG; lanes 5 and 9: 1 mM IPTG. In (B) and (C) lane +C contains a positive control (SFRP-2 recombinant fusion protein conjugated to Albumin Binding Protein containing a Histidine tag (donated by Atlas Antibodies)). Only the culture induced for 6 hours with 1 mM IPTG expressed the fusion protein at approximately 29 kDa (lane 5 (C)). This was detected by the anti-SFRP-2 Western blot and a weak band was observed at 29 kDa the anti-histidine Western blot (lane 5 (B)). However, the anti-SFRP-2 and the anti-histidine antibodies did not generate a band at 29 kDa for any of the other cultures induced for 6 hours or O/N in the anti-SFRP-2 and anti-histidine Western blots. The anti-SFRP-2 antibody also generated a band at approximately 17 kDa and 14 kDa for all cultures induced O/N in the anti-SFRP-2 Western.

5.4.2.6 Large-scale SFRP-2-hFABP recombinant fusion protein expression in Tuner cells and purification of the expressed protein

The SFRP-2-hFABP-expressing clone (transformant 4 (lane 8 in Figure (71)) was used for large-scale production of the SFRP-2 fusion protein. A larger culture volume (500 mL) of transformant 4 was grown up O/N followed by subsequent subculture and 0.5 mM IPTG induction for 4 hours at 30°C, as described in section 2.5.1.1.10. The protein lysate following sonication was centrifuged to remove cell debris and the supernatant was purified using immobilized metal affinity chromatography (IMAC), as described in section 2.5.1.1.12.

The purification was analysed by performing SDS-PAGE (Figure 73 (A)) and an anti-SFRP-2 Western blot (Figure 73 (B)) on the lysate, "flow-through", wash and eluted protein. As can be seen in Figure 73, the large-scale expression and purification of the SFRP-2-hFABP recombinant fusion protein was unsuccessful as no protein was observed in the eluent in lane 5 of the SDS-PAGE gel at approximately 29 kDa (Figure 73 (A)). The anti-SFRP-2 antibody in the anti-SFRP-2 Western blot also did not generate a band in the lysate or "flow-through" at 29 kDa (lane 2 in Figure 73 (B)). However, the anti-SFRP-2 antibody generated weak bands at approximately 17 kDa in both the lysate and "flow-through" (lanes 2 and 3 in figure 73 (B)).

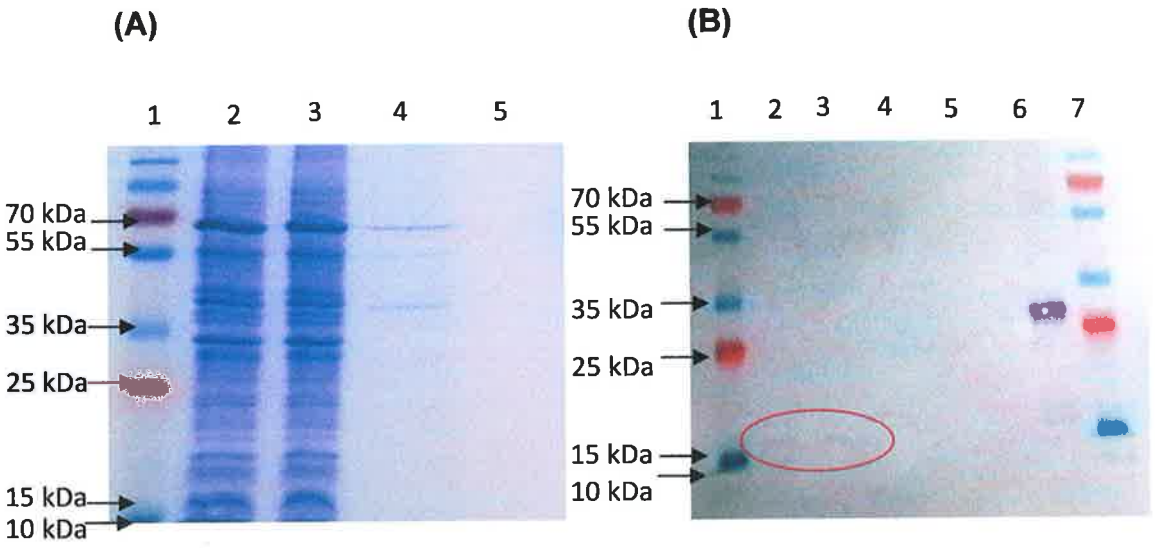

Figure 73: Large-scale SFRP-2-hFABP recombinant fusion protein expression in Tuner cells and IMAC purification of the expressed protein

(A): SDS, (B): anti-SFRP-2 Western blot. In (A) and (B) lanes 1 and 7 represent the prestained protein markers (Fermentas), lane 2 contains unpurified sonicated lysate from transformant 4 (lane 8 in Figure 71, following 0.5 mM IPTG induction for 4 hours), lane 3 contains the "flow-through" with all unbound proteins that passed through the resin, lane 4 contains any impure non-specific hydrophobic proteins which may have weakly bound to the resin and were removed using an increased concentration of Tween 20 and lane 5 contains the purified eluted SFRP-2 recombinant fusion protein. In (B) lane 6 contains a positive control (SFRP-2 recombinant fusion protein conjugated to Albumin Binding Protein (donated by Atlas Antibodies)). The large-scale expression and purification of the SFRP-2-hFABP recombinant fusion protein was unsuccessful as no protein was observed in the eluent in lane 5 of the SDS-PAGE gel at approximately 29 kDa. The anti-SFRP-2 antibody in the anti-SFRP-2 Western blot also did not generate a band in the lysate or "flow-through" at 29 kDa (lane 2 in (B)). However, the anti-SFRP-2 antibody generated weak bands at approximately 17 kDa in both the lysate and "flow-through" (lanes 2 and 3 (B)).

5.4.2.7 Analysis of SFRP-2-hFABP fusion protein solubilisation and induction temperature in Tuner E. coli cells

A large culture volume (500 mL) of transformant 4 (lane 8 in Figure 71) was grown up O/N followed by subsequent subculture and 0.5 mM IPTG induction for 4 hours at 25°C and 30°C, as described in section 2.5.1.1.10. The protein lysate was sonicated and centrifuged. Twenty microlitres of the supernatant (lysate) and 20 µL of the re-suspended cells in PBS were analysed by SDS-PAGE electrophoresis, an anti-histidine Western blot and an anti-SFRP-2 Western blot to determine both the solubility of the SFRP-2-hFABP recombinant fusion protein and the optimal induction temperature.

A strong band is visible at 29 kDa in the SDS-PAGE gel, the anti-histidine Western blot and an anti-SFRP-2 Western blot for the re-suspended sonicated cells in Figure 74 (lanes 3 and 5). This SFRP-2-hFABP fusion protein expression is not noted for either temperature (25°C or 30°C) in the lysates (lanes 2 and 4 in Figure 74). This result implies the SFRP-2-hFABP fusion protein is insoluble in the form of inclusion bodies trapped within the periplasm of the *E. coli* cell.

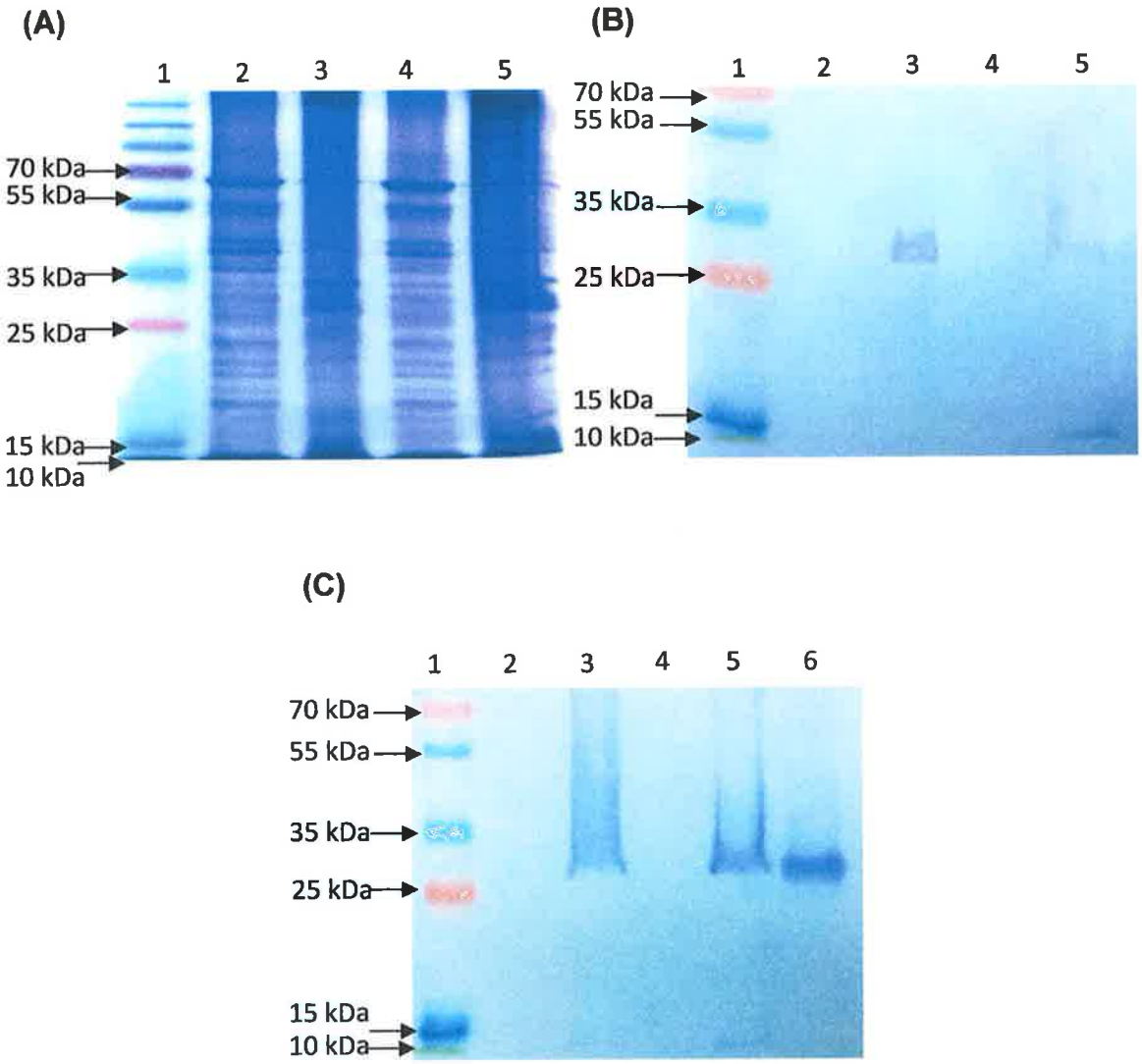

Figure 74: Analysis of SFRP-2-hFABP recombinant fusion protein solubilisation and induction temperature in Tuner *E. coli* cells

(A): SDS, (B): anti-histidine Western blot, (C): anti-SFRP-2 Western blot. The lysate and cells of transformant 4 (lane 8 in Figure 71, 0.5 mM IPTG induction for 4 hours) following sonication were incubated with sample treatment buffer and analysed on a 12.5% (w/v) SDS-PAGE Gel and by Western blotting using anti-SFRP-2 pAb and anti-histidine mAb. In (A)-(C) lane 1 represents the prestained protein marker (Fermentas), lanes 2 and 4 contain unpurified sonicated lysate with all the proteins expressed in the bacterial cell lysate, lane 3 and 5 contain unpurified sonicated cells resuspended in PBS, lanes 2 and 3: Induction at 25°C and lanes 4 and 5: Induction at 30°C. In (C) lane 6 contains a positive control (SFRP-2 recombinant fusion protein conjugated to Albumin Binding Protein (donated by Atlas Antibodies)). A strong band is visible at 29 kDa in the SDS-PAGE gel, the anti-histidine Western blot and an anti-SFRP-2 Western blot for the re-suspended sonicated cells (lanes 3 and 5). This SFRP-2-hFABP fusion protein expression is not noted for either temperature (25°C or 30°C) in the lysates (lanes 2 and 4).

5.4.2.8 Purification of cell-free bacterial SFRP-2 inclusion bodies

Purification of "cell-free" bacterial SFRP-2 inclusion bodies was performed, as described in section 2.5.1.2.8. The pellets were re-suspended in 1 ml of PBS and 20 µL was analysed by SDS-PAGE gel and an anti-SFRP-2 Western blot.

A smear of protein is observed in both the SDS-PAGE gel and the anti-SFRP-2 Western blot. This may be due to the hydrophobic nature of inclusion bodies. However, a strong band at approximately 29 kDa is visible in both the SDS-PAGE gel and the anti-SFRP-2 Western blot.

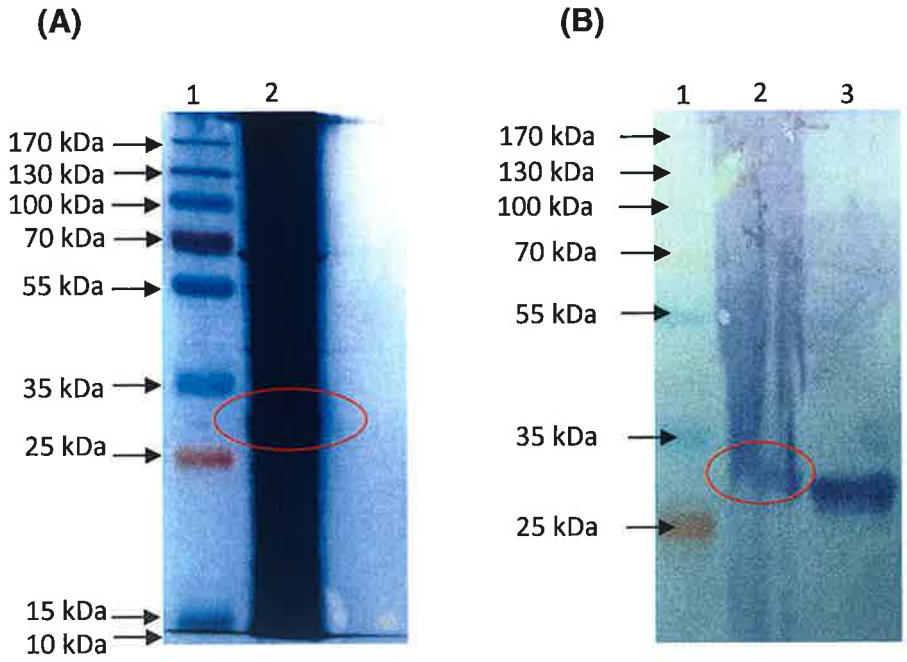

Figure 75: Analysis of SFRP-2-hFABP recombinant fusion protein solubilisation and induction temperature in Tuner *E. coli* cells

(A): SDS, (B): anti-SFRP-2 Western blot. The purified inclusion bodies cell pellet of transformant 4 (lane 8 in Figure 71, 0.5 mM IPTG induction for 4 hours) was resuspended in PBS, incubated with sample treatment buffer and analysed on a 12.5% (w/v) SDS-PAGE Gel and by Western blotting using anti-SFRP-2 pAb and anti-histidine mAb. In (A) and (B) lane 1 represents the prestained protein marker (Fermentas) and lane 2 contains purified SFRP-2 inclusion bodies resuspended in PBS. In (B) lane 3: contains a positive control (SFRP-2 recombinant fusion protein conjugated to Albumin Binding Protein (donated by Atlas Antibodies)). A smear of protein is observed in both the SDS-PAGE gel and the anti-SFRP-2 Western blot. However, a strong band at approximately 29 kDa is visible in both the SDS-PAGE gel and the anti-SFRP-2 Western blot.

5.4.3.1 Amplification of the SFRP-2 gene from pUC57 vector (1st PCR)

Primers were designed to amplify the SFRP-2 gene that was cloned into the pUC57 vector by Genscript USA Inc. described in detail in section 2.5.1.2.1. The PCR was optimised for predicted annealing temperature and the PCR products were analysed for amplification by agarose gel electrophoresis. All annealing temperatures analysed (52°C, 54°C, 58°C and 62°C) had clean amplification at 366 bps (SFRP-2 gene sequence = 360 bps + RBS sequence = 6 bps) in Figure 76 (A). The gene amplification containing no DMSO showed optimal amplification in Figure 76 (B). Larger scale amplification (5X) of the SFRP-2 gene was performed using an annealing temperature of 62°C and no DMSO. The amplified gene was purified by gel extraction resolved by agarose gel electrophoresis. Successful amplification and purification at 365 bps can be observed in Figure 76 (C).

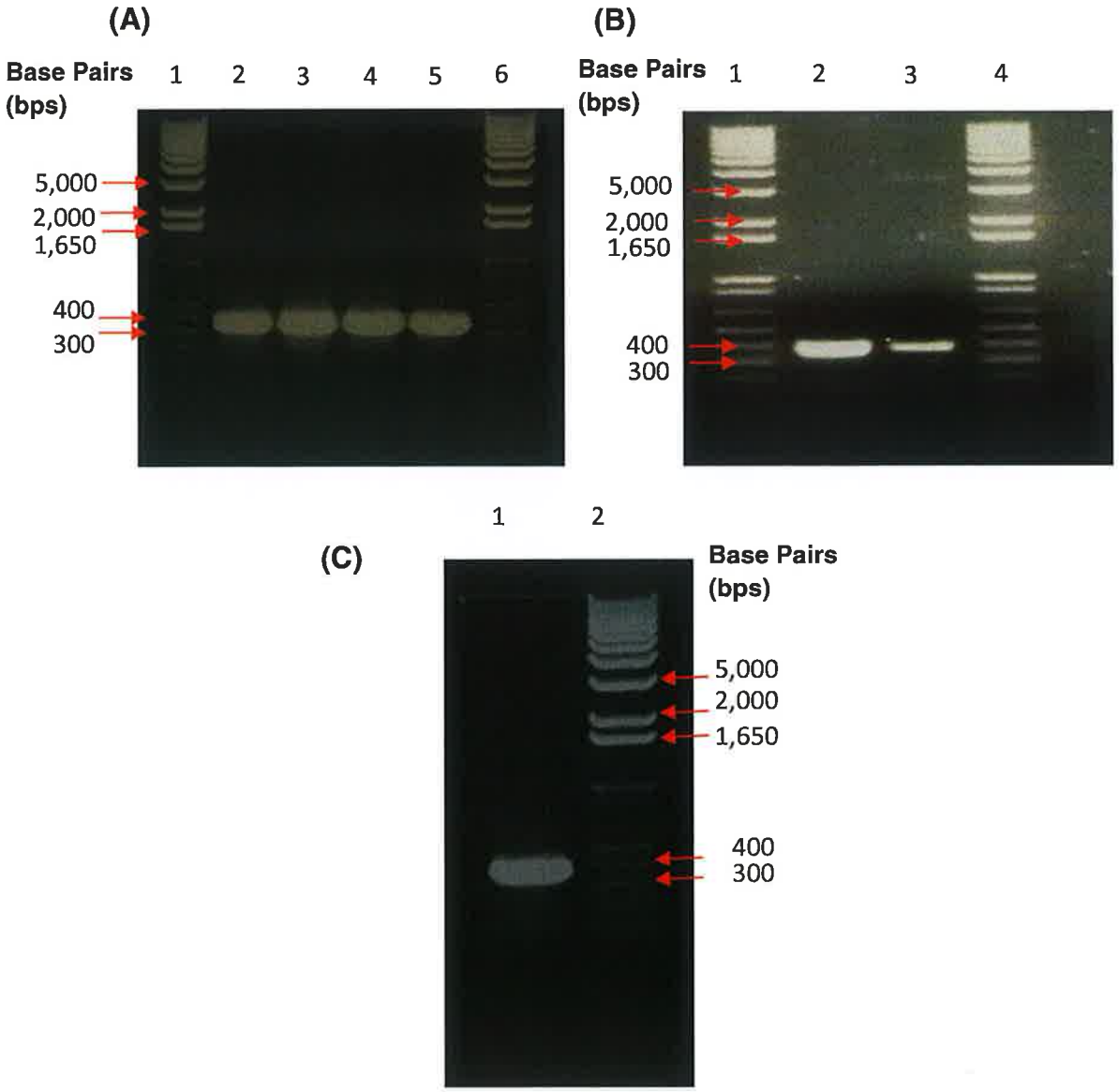

Figure 76: Amplification of the SFRP-2 gene from pUC57 vector for cell-free translation (1st PCR)

(A) Annealing temperature optimisation of the sense and anti-sense primers for SFRP-2 gene amplification from pUC57 vector. Lanes 1 and 6: 1 kb DNA ladder plus, lane 2: 52°C annealing temperature, lane 3: 54°C annealing temperature, lane 4: 58°C annealing temperature, lane 5: 62°C annealing temperature.

(B) DMSO concentration optimisation for SFRP-2 gene amplification from pUC57 vector (62°C Annealing temperature). Lanes 1 and 4: 1 kb DNA ladder plus, lane 2: No DMSO, lane 3: 1.5 µL DMSO.

(C) Amplified SFRP-2 gene (62°C Annealing temperature and no DMSO). Lane 1: Amplified SFRP-2 DNA, lane 2: 1 kb DNA ladder plus.

5.4.3.2 Amplification of the SFRP-2 gene using universal primer (2nd PCR)

The universal primer is designed to attach all the regulatory sequences, including the T7 promotor, to the amplified SFRP-2 gene, as described in detail in section 2.5.1.2.1. The PCR was optimised for annealing temperature and the PCR products were analysed for amplification by agarose gel electrophoresis. All annealing temperatures analysed (52°C, 54°C, 58°C and 62°C) had clean amplification at approximately 436 bps (SFRP-2 gene sequence = 360 bps + RBS sequence = 6 bps + regulatory sequences = 70 bps) in Figure 77 (A). Large-scale amplification (8X) of the SFRP-2 gene containing the regulatory sequences was performed using an annealing temperature of 62°C. The amplified gene was purified by gel extraction resolved by agarose gel electrophoresis. Successful amplification and purification at 436 bps was observed in Figure 77 (B).

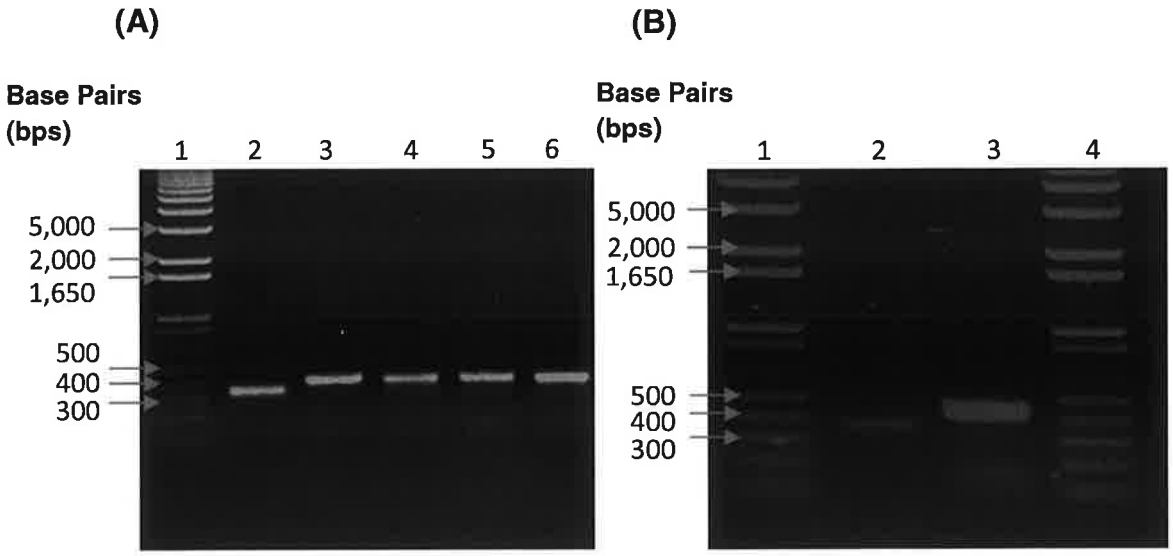

Figure 77: Amplification of the SFRP-2 gene with universal primer for cell-free translation (2nd PCR)

(A) Annealing temperature optimisation of the universal primer for SFRP-2 gene amplification. Lane 1: 1 kb DNA ladder plus, lane 2: 52°C annealing temperature, lane 3: 54°C annealing temperature, lane 4: 58°C annealing temperature, lane 5: 62°C annealing temperature.

(B) Amplified SFRP-2 gene (62°C Annealing temperature and no DMSO). Lanes 1 and 4: 1 kb DNA ladder plus, lane 2: Amplified SFRP-2 DNA from 1st PCR, lane 3: Amplified SFRP-2 DNA using universal primer (2nd PCR).

5.4.3.3 Analysis of SFRP-2 protein expression by cell-free translation

The SFRP-2 protein was translated with the amplified DNA and subsequently purified, as described in section 2.5.1.2.7 and 2.5.1.2.8. Twenty microlitres cell-free translated protein was then analysed by an anti-SFRP-2 Western blot described in 2.5.1.1.9.

A weak band specific to SFRP-2 was detected at approximately 14 kDa (see lane 2 in Figure 78). This indicates that although the yields of the cell-free translation SFRP-2 product were low, the "cell-free" translation of the SFRP-2 gene was successful in so far as it generates a single band at the predicted molecular mass of 14 kDa.

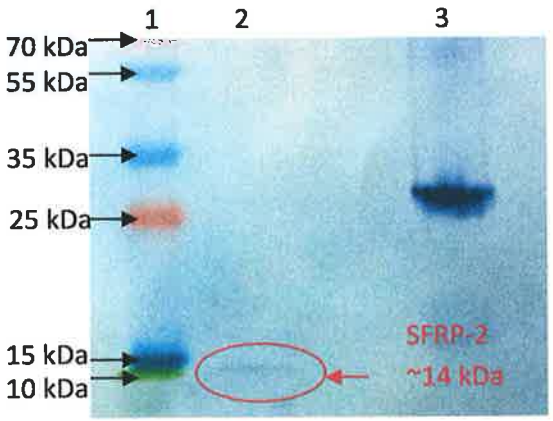

Figure 78: Analysis of SFRP-2 protein expression by "cell-free" translation

The "cell-free" translation product was incubated with sample treatment buffer and analysed by Western blotting using anti-SFRP-2. Lane 1 represents the prestained protein marker (Fermentas), lane 2 contains the "cell-free" translation product and lane 3 contains a positive control (SFRP-2 recombinant fusion protein conjugated to Albumin Binding Protein (donated by Atlas Antibodies)). A weak band was detected at the predicted molecular mass of SFRP-2 at approximately 14 kDa (lane 2).

5.4.3.4 Analysis of Chicken serum titre against SFRP-2 (Polyclonal response)

A chicken (Leghorn female) was immunised in the peritoneal cavity initially with Tuner(DE3) *E. coli* lysate containing SFRP-2 conjugated to GST. Subsequent injections were performed with 200 µg/mL SFRP-2 conjugated to hFABP purified inclusion bodies. A bleed was taken from the chicken 7 days after the second booster administration and an antibody serum titre was performed by ELISA using the SFRP-2-ABP recombinant fusion protein donated by Atlas Antibodies. The antibody serum titre was determined to ensure SFRP-2-specific antibodies were being generated and the titre was sufficiently high for recombinant antibody library production. However, a low specific antibody titre was obtained when screened against SFRP-2-ABP (Figure 79).

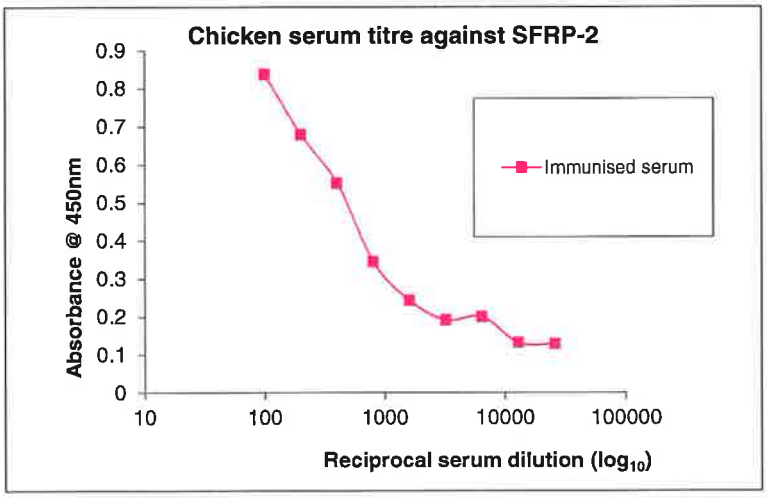

Figure 79: Chicken serum titre against SFRP-2 (Polyclonal response)

Titration of serum antibodies: A chicken was immunised with *E. coli* lysate containing SFRP-2 conjugated to GST and 200 µg/mL SFRP-2 conjugated to hFABP purified inclusion bodies over a period of 3 months. Serum was collected and an antibody serum titre was determined by ELISA. Chicken antibodies were detected using horseradish peroxidase (HRP)-labelled anti-chicken antibody followed by the addition of 3,3',5,5'-Tetramethylbenzidine (TMB) substrate. The absorbance was read at 450 nm. A low signal was observed at the 1:100 dilution gradually decreasing with decreasing concentration of antibody.

5.5 Discussion

Currently, there are only two commercial polyclonal antibodies against SFRP-2 applicable for immunohistochemistry on paraffin embedded formalin fixed tissue, one of which was not available prior to this study. Monoclonal and recombinant antibodies against SFRP-2 do not exist at present for any molecular or diagnostic application. Ag2853 (Proteintech group) is the only advertised commercially available antigen/immunogen. However, this antigen was not available prior to this study and when ordered during the course of this study the Proteintech group were unable to synthesise the antigen. Therefore, there does not exist, at present, a commercially available antigen for SFRP-2.

The main aims of this study were to design and produce an SFRP-2 antigen grade fusion protein, to use this antigen as an immunogen in an avian immune model and to determine whether a recombinant antibody against SFRP-2 can be generated.

The first strategy taken to produce the SFRP-2 antigen involved using *E. coli* as an expression system. This is an appealing approach for recombinant expression of protein due to the relative ease of production of a constant supply of antigen at low cost. The choice of vector plays a significant part in the successful expression of recombinant proteins in *E. coli* expression systems. The SFRP-2 gene was first cloned into a pGS-21a vector containing a GST sequence by Genscript USA Inc. This vector was chosen in the hope that GST as a fusion tag would facilitate protein folding and express SFRP-2 as a soluble fusion protein which could be easily affinity purified. The pGS-21a vector was then transformed into a wide range of DE3 *E. coli* strains for expression analysis. The strain of *E. coli* host is extremely important for recombinant protein expression (Sorensen and Mortensen, 2005). It should be deficient in harmful natural proteases, stably maintain the expression plasmid and confer the genetic elements relevant to the expression system (Sorensen and Mortensen, 2005).

The first strain of *E. coli* the pGS-21a vector was transformed into was the BL-21(DE3) *E. coli* strain. The decision to transform the vector into BL-21 was due to its ability to produce T7 polymerase, its deficiency in *lon* and *Omp T* proteases, its ability to express rare codons and its vigorous growth in minimal media conditions (Sorensen and Mortensen, 2005). Transformation of the pGS-21a vector into BL-21(DE3) cells was successful. Very weak soluble protein expression was observed in the transformed cells at approximately 40 kDa, which is the predicted molecular mass of the SFRP-2-GST recombinant fusion protein (see Figure 53). Another SFRP-2-specific band at approximately 32 kDa was also observed in one of the transformants which could represent some degradation of the fused SFRP-2-GST protein. However, although expression was observed in the transformed BL-21(DE3) cells, this expression was extremely weak and when the positive BL-21(DE3) transformant 2 was grown up in large-scale and purified there was no evidence of the SFRP-2-GST recombinant protein present in the lysate (see Figure 54 (B)). This implies that the fusion protein does not express well in this strain of *E coli* either due to toxicity to the cell or because the fusion protein is in the form of inclusion bodies within the cell.

The pGS-21a vector was next transformed into the Tuner(DE3) strain of *E. coli*. This strain of *E. coli* was chosen for SFRP-2-GST fusion protein expression as it is a *lacZY* deletion mutant of the BL-21 strain. Therefore, like the BL-21 strain, this strain has the ability to produce T7 polymerase, it has deficiency in *lon* and *Omp T* proteases, it has the ability to express rare codons and it has vigorous growth in minimal media conditions. In addition, the *lac Y* mutation results in the loss of the *lac Y* gene product lactose permease which allows uniform entry of IPTG into cell populations and by adjusting the IPTG concentration the protein expression level can be regulated and solubility enhanced. Thus, the Tuner strain of *E. coli* offer a precise control of target protein expression (Sorensen and Mortensen, 2005). The transformation of the pGS-21a vector was successful. Soluble SFRP-2 positivity was observed at approximately 35 kDa in all transformants in Figure 55 (B). This was a slightly lower molecular mass than the predicted sequence

molecular mass of the SFRP-2-GST fusion protein (40 kDa). However, SDS-PAGE provides only a "relative" molecular mass for a protein and discrepancies between protein size in SDS-PAGE gels and sequence analysis are known to occur for some proteins including p53. p53, so called because of its molecular mass of between 53 and 56 kDa when analysed by SDS-PAGE electrophoresis, has a sequence molecular weight of 44 kDa (Zakut-Houri *et al.*, 1985). Factors such as amino acid composition, the charge on the carbohydrate groups and the amount of SDS bound to the protein can affect the molecular mass of the protein when analysed by SDS-PAGE. The presence of the SFRP-2-GST recombinant fusion protein at approximately 35 kDa was also detected by GST Western blotting (see Figure 55 (C)). However, the presence of GST was also detected in all transformants analysed at approximately 26 kDA, which is the predicted molecular mass of the GST protein un-fused to SFRP-2 and two transformants also detected GST at approximately 40 kDA, which is the sequence predicted molecular mass of the SFRP-2-GST recombinant fusion protein. This could imply that the SFRP-2-GST fusion protein could be degrading and the presence of the bands at 26 kDa and 35 kDa could represent some degraded GST/fusion protein. Further evidence of this was observed in the anti-histidine Western blot in Figure 55 (B) which was performed to optimise induction time and temperature. Here, histidine was detected when induced for 6 hours and O/N at 25°C and when induced for 3 hours at 30°C at approximately 26 kDa, 35 kDa and 40 kDa. It is also possible that these bands at approximately 26 kDa and 40 kDa, in both the anti-GST and anti-histidine Western blots, may represent non-specific binding of the antibodies.

Following small-scale induction optimisations of the positive SFRP-2-GST expressing Tuner (DE3) transformant (Transformant 3), the transformant was grown up in large-scale with inducion O/N at 30°C using a concentration of 1 mM IPTG. The lysate was then subjected to IMAC purification which was unsuccessful as noted in Figure 58 (A) and (B) where no purified SFRP-2-GST recombinant protein was present in lane 5. The large-scale production of the fusion protein appeared to be successful as a strong band detected by

the anti-histidine antibody was present at approximately 35 kDa but this band was also present in the "flow-through". This may suggest that the SFRP-2-GST fusion protein is not binding to the IMAC resin due to folding of the protein whereby the histidine tag is not exposed to the resin and, subsequently, in its native state it cannot bind to it. The presence of the 'histidine' band in the Western blot in Figure 58 (B) may be due to the sample being denatured at 95°C prior to loading on the SDS gel.

This process was repeated, using a GST purification kit to facilitate the possibility that the histidine tag was inaccessible due to folding of the native protein. However, a similar result to the IMAC purification was obtained from the immobilised glutathione purification where the presence of the SFRP-2-GST fusion protein was noted in both the lysate and "flow-through" at approximately 35 kDa in the SDS and both the anti-histidine and anti-GST Western blots (see Figure 58 (C), (D) and (E)). The anti-GST Western blot also detected GST bands at approximately 55, 26, 25 and 15 kDa which again could represent some degradation of the SFRP-2-GST fusion protein. However none of these bands were present in the eluted protein lane in the anti-GST Western blot (lane 5) so they may simply represent non-specific binding of the GST antibody.

Two explanations could account for the difficulties encountered with both purification methods. The first explanation could be that there is simply not sufficient yields of the SFRP-2-GST recombinant fusion protein present in the lysate for affinity purification. The second explanation may be that the SFRP-2-GST fusion protein is misfolded. A known disadvantage of using GST as a fusion tag is that GST is a homodimer which can complicate the purification of oligomeric fusion proteins (Waugh, 2005). This suggests that the SFRP-2-GST fusion protein may be forming dimers making it impossible to purify. IMAC purification was repeated using mild denaturants (urea and DTT) in the lysis buffer to reduce any possible dimer formation of the fusion protein in the lysate (see Figure 59). However, the treatment of the lysis buffer with urea and DTT resulted with a purified product appearing between 10 and 15 kDa which both the anti-SFRP-2 and anti-histidine Western blots detected. The

anti-GST Western blot did not detect this purified product which suggests that this product may be degraded/broken down SFRP-2-GST recombinant fusion protein which still retained the SFRP-2 sequence and the histidine tag allowing for IMAC purification. The solubility of the SFRP-2-GST fusion protein was next analysed by SDS-PAGE gel electrophoresis and by anti-SFRP-2 Western blotting (see Figure 60) which revealed a strong band for the fusion protein at approximately 40 kDA (the predicted sequence molecular mass of the fusion protein). This result implies that the SFRP-2-GST recombinant fusion protein is insoluble and forms inclusion bodies and that the inconsistent soluble expression observed at approximately 35 kDa may represent some degraded soluble fusion protein. This may explain the purification problems observed.

The pGS-21a vector was next transformed into NovaBlue(DE3), BLR(DE3) and HMS174(DE3) *E. coli* strains to determine if expressing the vector in other *E. coli* strains would increase protein solubility. The NovaBlue and HMS174 strains of *E. coli* did not express any protein at either 35 kDa or 40kDa (the suspected mass of the SFRP-2-GST fusion protein) in the SDS gel in Figure 61. A strong band was noted at approximately 60 kDa in one of the NovaBlue transformants but this band was at too high a molecular mass to be the SFRP-2 GST fusion protein. All of the BLR transformants displayed protein expression at approximately 35 kDa which was the molecular mass at which the soluble expression of the SFRP-2-GST fusion protein was observed at in the Tuner(DE3) strain. Following further investigation, anti-SFRP-2 and anti-histidine Western blots confirmed the presence of the SFRP-2-GST recombinant fusion protein (Figures 62 and 63). Subsequent induction optimisation experiments were performed to increase the soluble expression of the fusion protein in the BLR cells but the expression was extremely weak and the fusion protein could not be purified from the lysate.

As discussed previously, the choice of vector plays a significant part in the successful soluble expression of recombinant proteins in *E. coli* expression systems. Therefore, the next approach taken was to produce a soluble recombinant SFRP-2 fusion protein using *E. coli* as an expression system was

to clone the SFRP-2 gene sequence into a pET-28b(+) vector containing an hFABP gene sequence. hFABP is a hydrophilic protein that was found to express very well in *E. coli* expression systems. The concept was that by using hFABP as a carrier/conjugate protein, solubility and expression of the recombinant fusion protein would improve in an *E. coli* expression system.

Using specially designed primers the SFRP-2 gene was successfully amplified from the pUC57 vector and a *Sac* I and a *Not* I restriction site was successfully amplified onto the 5'-end and 3'-end of the amplified SFRP-2 gene. The peptide gene sequence was then excised out of the pET-28b(+)-hFABP vector using *Sac* I and *Not* I restriction enzymes and following SFRP-2 gene digestion successful ligation of the SFRP-2 gene into the pET-28b(+)-hFABP vector was achieved (see Figures 66 and 67). The ligated vector was then transformed into Tuner(DE3) *E. coli* cells and transformants were analysed by SDS-PAGE and Western blotting (see Figure 68). The results implied that undigested pET-28b(+)-hFABP vector containing the peptide gene sequence was transformed into five of the transformants as both the anti-histidine and anti-cTnI Western blots detected bands at approximately 17 kDa (the predicted molecular mass of the cTnI-hFABP recombinant fusion protein). However, the three transformants that did not express histidine or cTnI at 17 kDa detected bands specific to SFRP-2 at approximately 17 kDa and 14kDa (molecular mass of un-fused SFRP-2). In one of the SFRP-2 positive transformants a weak band specific to SFRP-2 at approximately 29 kDa (the predicted molecular mass of the SFRP-2-hFABP recombinant fusion protein) was also detected. The anti-hFABP Western blot detected hFABP in all transformants at approximately 17, 14 and 10 kDa. The entire cloning procedure was repeated again to ensure that digestion and ligation of the SFRP-2 gene and pET-28b(+)-hFABP vector were precise. The cloned vector was transformed into additional Tuner(DE3) *E. coli* cells. However, the results were similar to the last transformation with some transformed cells expressing histidine at approximately 17 kDa while the 'histidine-negative' transformants expressed SFRP-2 (see Figure 69). These results imply that undigested pET-28b(+)-hFABP vector was transformed into some of the Tuner(DE3) *E. coli*

cells and that pET-28b(+)-hFABP vector containing the SFRP-2 sequence was transformed into other Tuner(DE3) *E. coli* cells. An explanation for this might be that when the digested pET-28b(+)-hFABP vector was being gel-purified (Figure 67) there were both undigested and digested vectors present n the gel but because the cTnI insert was so small (approximately 81 bps) the two vectors were visible as one single band on the gel. Subsequently this single band was gel-purified which contained two vectors (un-digested and digested).

To ensure the pET-28b(+)-hFABP vector containing the SFRP-2 gene sequence, which was transformed successfully into a number of transformants, was correct and intact, a bacterial stock of transformant 4 was sent for gene sequencing. The results confirmed that an intact pET-28b(+)-hFABP vector containing the SFRP-2 gene sequence was successfully transformed into transformant 4 (see Figure 70). Subsequent induction optimisation experiments were performed to increase the soluble expression of the SFRP-2-hFABP fusion protein at 29 kDa (predicted molecular mass) which revealed that an induction time longer than 4 hours degraded the protein and produced SFRP-2 specific bands at approximately 17 kDa (see Figure 71). This may account for why SFRP-2 detection was observed at 17 kDa in Figures 68 and 69 as these transformants were induced overnight. However, when the transformant was grown up at large-scale, with subsequent induction using the optimised induction conditions, IMAC purification was not successful as the fusion protein degraded to 17 kDa in the lysate (see Figure 73). This may imply that the solubly expressed material (soluble SFRP-2-hFABP fusion protein product) was not very stable.

Insolubility of the SFRP-2-hFABP fusion protein was next analysed which revealed that similar to the SFRP-2-GST recombinant fusion protein, the SFRP-2-hFABP recombinant fusion protein was also insoluble being present in the form of bacterial inclusion bodies (see Figure 74). Bacterial inclusion bodies are water-insoluble protein aggregates. They are formed in the bacterial cytoplasm (and eventually the periplasm) during the overproduction of recombinant proteins, particularly those from viral or mammalian origin

(Rodriguez-Carmona *et al.*, 2010). Inclusion bodies have traditionally been described as biologically inert protein clusters. However, recent research show that inclusion bodies have an important level of molecular organisation and that they are formed by a considerable amount of functional polypeptides (Rodriguez-Carmona *et al.*, 2010). Rodriguez-Carmona *et al.*, (2010) describe inclusion bodies as "pure, structurally organized, mechanically stable and biocompatible protein deposits". For the purpose of immunisation where protein is completely broken down by antigen presenting cells, a fusion protein in the form of inclusion bodies could be used to generate an antibody. For this reason the SFRP-2-hFABP fusion protein which was in the form of inclusion bodies was purified following a detailed optimised protocol by Rodriguez-Carmona *et al.*, (2010) (see Figure 75).

The second strategy explored in order to produce a soluble SFRP-2 antigen was "cell-free" translation. "Cell-free" translation is an *in vitro* expression system that does not require the use of a host cell to express the target protein and is described in detail in section 2.2.2.2. "Cell-free" translation does not require the use of a host cell so that proteins which are toxic or prone to proteolytic degradation can be readily prepared and inclusion body formation is not an issue. This makes "cell-free" translation an attractive method to apply for the soluble expression of SFRP-2. Amplification of the SFRP-2 gene with the ribosomal binding site and regulatory sequences was achieved with specially designed primers (see Figures 76 and 77). Successful translation of the SFRP-2 gene and subsequent soluble expression of the SFRP-2 protein was achieved. A weak specific band for SFRP-2 was visible at approximately 14 kDa (the predicted molecular mass of SFRP-2) in Figure 78. However, this soluble SFRP-2 protein expression is extremely weak and the yields of the protein were too low for use as either an immunogen or in analytical applications. The low yield obtained was probably due to the fact that the protein was translated from a 50 µl reaction using the PURESYSTEM™ classic II mini kit (PURE2004C). Larger quantities of the protein might be obtained using the larger "cell-free" translation kit provided by

Puresystem (PURESYSTEM™ classic II standard (PURE2030C)). However, this kit is much more expensive.

The final aim of this study was to use a SFRP-2 antigen as an immunogen in an avian immune model and to determine whether a recombinant antibody against SFRP-2 can be generated based on the polyclonal serum response of the chicken. As a soluble SFRP-2 conjugated antigen could not be synthesised in this study, a chicken was immunised initially with Tuner(DE3) *E. coli* lysate containing SFRP-2 conjugated to GST. The chicken then received a booster injection with 200 µg/mL of purified SFRP-2 conjugated to hFABP in the form of inclusion bodies which had been solubilised using 8 M urea. Low titres of pAbs obtained in the chicken sera against SFRP-2 (see Figure 79) indicate that SFRP-2 is not immunogenic in the chicken, decreasing the probability of obtaining specific antibodies against SFRP-2 and, thus, of generating a recombinant antibody. This implies that the immunisations with crude lysate containing SFRP-2 and purified bacterial SFRP-2 inclusion bodies were not effective in eliciting a good immune response in the chicken to SFRP-2.

Overall, the results presented in this study highlight the difficulties faced in producing a soluble antigen suitable for immunisations to challenging proteins for subsequent antibody generation. Since SFRP-2 is 100% homologous in mice and rabbits and 99% homologous in chickens, it requires fusion of the least homologous region of the protein to carrier proteins in order to evoke a good antibody response in these common immune hosts. *E. coli* expression systems are the most common strategy used to produce a recombinant fusion protein. However, when this approach was used with SFRP-2, which was cloned into two different vector systems, both recombinant fusion proteins were insoluble. SFRP-2 is a soluble, secreted protein so the hydrophobicity observed here is due to the formation of inclusion bodies which are very common in these expression systems. Soluble expression of SFRP-2 was achieved using "cell-free" translation. However, the "cell-free" translation

yields were very low, the technique was expensive and the protein was unconjugated, limiting its use as an immunogen. The challenges and difficulties faced in this study may reflect the lack of high quality, well characterised, commercially available antibodies to novel cancer markers such as SFRP-2.

Chapter 6 - General discussion, conclusions and future work

This thesis examined the histological expression of a series of potential biomarkers of disease biology and progression in prostate cancer to determine whether these potential biomarkers could permit early diagnosis of disease or provide critical information for stratification and clinical intervention.

6.1 Tissue validation of serum markers

In chapter 3, the tissue expression of up-regulated serum markers of prostate cancer (ZAG, KNG-1, VDBP and PSMB-6) identified within the PCRC was evaluated. The discovery of a novel biomarker of prostate cancer with expression in serum which correlates with expression in tissue and with Gleason grade would be extremely beneficial as it would mean that less invasive diagnostic procedures could be carried out on patients to measure the biomarker's expression level. The results presented in this chapter raise some interesting issues. Although all markers showed an up-regulation in the serum of prostate cancer patients, ZAG, KNG-1 and VDBP did not behave the same way in the tissue. The evaluation of PSMB-6 prostatic tissue expression revealed an interesting result whereby PSMB-6 protein expression was observed in stromal and inflammatory cells around BPH and tumour nests. This result may explain its detection in serum from prostate cancer patients when analyzed by Byrne *et al.* (2009). Prostate cancer is primarily an epithelial malignancy. In BPH, prostate cancer and prostatic disease the imbalance between prostatic cell growth and apoptosis is significantly influenced by the microenvironment around prostate cells (Sciarra *et al.*, 2008). There is growing evidence that carcinogenesis is influenced and controlled by cellular interactions derived from a complex relationship between epithelial, stromal and extracellular matrix components (Micke and Ostman, 2004). "Reactive stroma", which is characterised by modified extra cellular matrix composition, increased microvessel density, inflammatory cells and fibroblasts with an "activated" phenotype, has been identified in breast, lung, colon and prostate cancer (Micke and Ostman, 2004). More recently it has been suggested that prostatic inflammation may contribute to prostate growth

in terms of hyperplasia (BPH) or neoplastic (prostate cancer) changes (Sciarra *et al.*, 2008). Humoral (cytokines) and cellular (leukocytes) components of the inflammatory process can produce a tissue microenvironment with the production of free radicals such as nitric oxide which can alter protein structure, induce gene changes and cause post-translational modifications including those involved in DNA repair and apoptosis (Sciarra *et al.*, 2008). Furthermore, it is suspected that at the site of primary cell growth, prostate cancer cells interact with prostate stromal cells to gain the ability to access to the blood stream and adhere to bone marrow associated endothelial cells (Sung and Chung, 2002). This attachment to bone marrow associated endothelial cells may activate the invasion properties of prostate cancer cells and allow their extravasation into bone marrow space where they interact directly with osteoblasts and osteoclasts and survive, proliferate, migrate and invade and eventually replace the bone marrow components (Sung and Chung, 2002). An immediate question arising from this observation of PSMB-6 expression in prostatic stroma around BPH and tumour areas is; "could PSMB-6 expression be involved in these tumour-stroma, inflammatory interactions involving tumour growth and possible bone metastasis?" The detection and up-regulation of PSMB-6 in the serum of prostate cancer patients with Gleason score 7 compared to Gleason score 5 coinciding with its detection in stromal and inflammatory cells in prostatic tissue, may imply that PSMB-6 could play a role in tumour-stroma interactions in prostatic carcinogenesis, metastasis and/or may be a marker of inflammation.

Further evaluation of PSMB-6 is required on more serum and tissue to elucidate this theory and the design and application of a scoring system for the IHC performed is necessary. As PSMB-6 stromal staining was positive in inflammatory cells and almost all stromal components it may be difficult to devise an unbiased, objective scoring system to evaluate the marker. A new technology that could be used to overcome this problem is a recently developed technique called "Multiplex Tissue Immunoblotting (MTI)". Applying this method of transferring proteins from paraffin-embedded tissue sections to a stack of membranes which can then apply conventional

immunoblotting, permits quantification of markers normalized to total protein content through the use of a fluorescent scanner whilst preserving the morphologic structure of the tissue (Matsuda *et al.*, 2010). RNA *in situ* hybridization is another interesting technique that could be applied to further evaluate PSMB-6 expression in prostatic stromal tissue. LCM and Taqman PCR was used to confirm that PSMB-6 mRNA transcripts were present in prostatic tissue in this study to ensure that what was being observed at a protein level correlated with the mRNA level. However, it was not possible to separate the stroma from the epithelial cells using LCM. Therefore, the mRNA expression of PSMB-6 observed in this study does not definitively confirm the PSMB-6 mRNA expression was located explicitly in the stroma. RNA *in situ* hybridization would overcome this problem by localising the mRNA transcript on the tissue. Further to this, it would be interesting to obtain follow-up information for the patients with Gleason score 7 versus Gleason score 5 in the serum study to establish if PSMB-6 upregulation observed in this cohort is associated with metastasis.

With the exception of PSMB-6, overall the putative serum biomarkers evaluated in chapter 3 did not correlate in serum and tissue at the protein level which implies they may not be good candidates for biomarkers of prostate cancer in serum. One of the factors that could have contributed to the failure of serum and tissue correlation could be that the data from discovery phase which identified these markers (i.e. proteomics on serum) was not strong enough. Only 12 patients were analysed by 2D-DIGE in the initial discovery phase which identified PSMB-6, KNG-1, ZAG and VDBP whilst ZAG was analysed on a further 15 patients following this. Increased numbers in this phase of discovery may improve the correlation rate between serum and tissue protein expression for future discovered putative biomarkers markers in serum.

While major advancements in proteomic and metabolomic research have been seen in the past decade producing potential biomarkers for cancer, most have failed to replace existing markers due to lack of sensitivity and specificity (Issaq *et al.*, 2010). A major reason why proteomic and metabolomic studies

have failed to discover molecules to replace existing clinical tests for cancer is due to errors in either study design and/or experimental execution (Issaq *et al.*, 2010). There are well known limitations associated with 2D-DIGE including low resolution, lack of reproducibility and the requirement of large amounts of sample. Newer methods for large-scale proteomic analysis could be used to measure and identify changes in protein expression in serum/urine in the discovery phase such as comparative mass spectrometry techniques, liquid chromatography, surface-enhanced laser desorption/ionization time-of-flight (SELDI-TOF MS) and matrix-associated laser desorption/ionization time-of-flight (MALDI-TOF MS).

Searching for a protein biomarker in a biofluid is like searching for a needle in a haystack as a single "biomarker" protein could be associated with multiple cancers and diseases resulting in a biomarker with low sensitivity and specificity. A more sound approach is to search for proteins in the cancer tissue prior to looking for the discriminating proteins in the blood or urine (Issaq *et al.*, 2010). This approach could be used to identify sensitive and specific future biomarkers within the PCRC. Additional discovery phases could be introduced into the PCRC also such as reverse phase protein lysate arrays (RPPA), copy number variation studies including *in situ* hybridization (ISH) and/or fluorescent *in situ* hybridization (FISH) and studies on post-translational changes such as glycosylation.

6.2 Tissue validation of the epigenetic marker SFRP-2

In chapter 4, the tissue expression profile of SFRP-2 was evaluated in prostate cancer. This marker had been previously found to be hypermethylated in prostate cancer following Quantitative Methylation-Specific PCR (QMSP) analysis by the epigenetic biomarker discovery group within the PCRC. The immunohistochemical results for SFRP-2 showed cytoplasmic SFRP-2 expression in epithelial cells of benign glands and loss of SFRP-2 expression was observed in tumour epithelium particularly Gleason grade 3 and 4. While 40% of G5 tumours expressed SFRP-2, 60% of G5 tumours did

not express the protein. Further histological evaluation revealed notable morphological differences between G5 acini that corresponded with SFRP-2 staining patterns, leading to a distinction between "Type A" G5 (solid tumours, strong/moderate SFRP-2 expression) and "Type B" G5 (diffuse tumours, weak/negative SFRP-2 expression). Furthermore, "Type A" tumours with strong/moderate SFRP-2 expression were found to be associated with biochemical recurrence (4/4).

These results raise many interesting questions. The first of which is regarding the role of SFRP-2 in androgen-independent phenotype. Mutations in the androgen receptor (AR) lead to "promiscuous" activity of the protein, ultimately proceeding to activation of the androgen-signalling axis with ligands other than testosterone. SFRP-2 is a modulator of Wnt signalling which regulates the levels of cytosolic β-Catenin. The loss of SFRP-2 can result in Wnt signalling dysregulation and subsequent sequestering of cytosolic β-Catenin. β-Catenin has been associated with enhancement of androgen receptor (AR) activity (Chesire and Isaacs, 2003). Androgen-related modes of β-Catenin/AR pathway cross-talk are thought to play an active role in prostate cancer progression (Chesire and Isaacs, 2003). Therefore, one may question if the loss of SFRP-2 expression in prostate cancer and subsequent accumulation of β-Catenin in the cell results in β-Catenin mediated enhancement of AR activity contributing to the transition of androgen-dependent (ADep) phenotype to androgen-independent (AI) disease leading to AR regaining transcriptional function. It would be interesting to obtain androgen ablation resistance follow-up information for the patients in this cohort with both Gleason grade 4 and Gleason grade 5 foci to establish if there is an association between androgen independence and SFRP-2 expression in these tumours. Furthermore, a subset of AI lesions are thought to contain AR activity and do not recruit β-Catenin-mediated stimulation (Chesire and Isaacs, 2003). It could be possible these AI lesions represent the "Type A" subgroup of G5 tumours identified in this study that expressed SFRP-2 possibly due to the reactivation of SFRP-2 through demethylation.

Nearly every prostate cancer patient become resistant to therapy that blocks androgen-mediated cell proliferation (Isaacs and Isaacs, 2004). This is thought to be due to selective pressure on the androgen signalling pathway for mutation development caused by the androgen ablation. This results in a "hypersensitive" pathway with an increased sensitivity of the AR even at very low serum levels of androgen. Recently pivotal phase III studies were undertaken on castration-resistant prostate cancer (CRPC) patients using a combinational drug therapy of abiraterone acetate (a specific inhibitor of CYP17 that is critical to androgen synthesis) and MDV3100 (a novel antagonist of AR). Current data on this trial suggest that the response rate to this therapy targeting the AR is a valid therapeutic strategy in CRPC, imparting overall survival benefit in advanced prostate cancer (Attard *et al.*, 2011). However, an increase of PSA appears to be associated with cancer progression in the majority of patients that received treatment with abiraterone acetate and MDV3100 suggesting that biological mechanisms causing treatment resistance are associated with reactivation of the AR (Attard *et al.*, 2011). The authors of this study conclude that predictive biomarkers could allow patient selection for specific treatment with a preferred agent and substitute for an alternative therapy on objective progression. Could the β-Catenin/AR pathway cross-talk be involved in this treatment resistance through the promiscuous activity of the AR resulting in the activation of the Wnt signalling pathway and loss of SFRP-2? Furthermore, could SFRP-2 be a predictive biomarker allowing patient selection for specific treatment? The differential expression patterns of SFRP-2 within the two identified G5 subgroups in this thesis could represent this stratification. Moreover, SFRP-2 expression with G4 tumours could be more useful.

Furthermore, there is also evidence that the Wnt signalling pathway contributes to prostate cancer–mediated osteoblastic activity (Hall *et al.*, 2005). Prostate cancer bone metastases have both osteolytic and osteoblastic components. There is growing evidence suggesting that there is a shift in the balance from osteolytic to osteoblastic activity as prostate cancer progresses (Hall *et al.*, 2005). It has been suggested by Hall *et al.* 2005 that a

shift in balance between DKK-1 (another regulator of the Wnt signalling pathway) and Wnt expression may contribute to determining which type of bone lesion is predominant at any particular time point in the development of prostate cancer bone metastatic lesions. However, it could be possible that a shift in balance between SFRP-2 and Wnt signal expression could contribute to this bone metastasis. It would be very interesting to obtain follow-up information noting bone metastasis to evaluate whether the two patterns of G5 tumours that expressed SFRP-2 so differently could represent a population of patients that experienced bone metastasis due to an imbalance of the regulatory elements of the Wnt signalling pathway.

The interesting questions raised in chapter 4 could be addressed with more G5 tumours with follow-up information. This follow-up information should include metastasis information, androgen ablation resistance information, survival information and biochemical recurrence information. In addition, follow up information on the G4 patients should also be obtained as certain patients within this subgroup of tumour, although not many displayed SFRP-2 expression. It would be interesting to investigate if SFRP-2 expression or lack of SFRP-2 expression in G4 tumours correlates with any of the above follow-up information characteristics and whether SFRP-2 may in fact be a useful marker to sub-stratify this subgroup of patients.

6.3 Production of an antigen-grade recombinant SFRP-2 protein

The main aim of chapter 5 was to design and produce an antigen-grade recombinant SFRP-2 protein and to use this protein as an immunogen in an avian host model in order to generate a recombinant antibody against SFRP-2. SFRP-2 is a novel marker in prostate cancer and paucity of quality antigen and antibody is an impediment to research on this marker. At present, there are only polyclonal antibodies commercially available to this protein, only two of which can be used for IHC. Polyclonal antibodies are known for batch to batch variation and this can, in turn, affect IHC results. A monoclonal or recombinant antibody would provide more specific and reliable SFRP-2

detection by IHC for clinical utilization. Overall, the results presented in chapter 5 highlight the validation difficulties faced by researchers in the area of cancer research in determining the clinical relevance of novel markers. The research presented in this chapter emphasizes the problems encountered in producing a soluble SFRP-2 antigen suitable for immunizations.

The formation of inclusion bodies was the basis for the insolubility of the produced SFRP-2 protein in this study. Inclusion bodies usually form within prokaryotic systems when heterologous eukaryotic proteins are being over-expressed. An alternative approach to overcome this problem encountered in bacterial models was explored in this chapter by performing "cell-free" translation. However, this approach yielded low concentration of unconjugated SFRP-2 protein. As this SFRP-2 antigen was being synthesised for the purpose of immunisation and the fact the protein itself was extremely conserved across rabbits, mice and humans, it was necessary that the SFRP-2 was conjugated to a carrier protein to increase antigenicity. One approach that could be taken to overcome inclusion body formation in prokaryotic systems whilst employing a carrier tag would be the use of eukaryotic systems such as yeast *Saccharomyces cerevisiae* or mammalian cells which can both accommodate post-translational modifications and protein folding. However, difficulties and disadvantages have been documented with eukaryotic systems owing to the complex genome of eukaryotic cells.

In the design of this study and in determining which amino acid sequence on the SFRP-2 protein to use for antigen synthesis, the approach taken by the Human Protein Atlas (HPA) to generate their SFRP-2 immunogen was closely followed. The reason for this was that HPA, at the time this study commenced, was the only successful group to synthesise an SFRP-2 polyclonal antibody applicable for IHC. The antigen generation approach employed by HPA involved synthesising a 118 amino acid SFRP-2 sequence which had position 162-282 on the SFRP-2 protein (NCBI gene ID: 6423) (Larsson *et al.*, 1996). The conjugated SFRP-2 peptide was synthesised by Human Protein Atlas by cloning the SFRP-2 DNA sequence to the SFRP-2

amino acids 162-282 into a pT7-ABP vector which then was transformed into BL-21-DE3 *E. coli* cells to be expressed (Larsson *et al.*, 1996). However, as HPA's pT7-ABP vector was not available commercially alternative vectors had to be used. Translational difficulties faced in chapter 5 within the *E. coli* model could be due to the large size of the amino acid sequence of the SFRP-2 peptide. A more sound approach to generate a soluble SFRP-2 antigen and subsequent antibody in the future of this study within the PCRC could be to select multiple peptide sequences along the SFRP-2 peptide sequence (within 162-282 amino acid sequence), to clone these sequences into multiple vectors with different affinity tags/carrier protein genes and to transform these into a range of DE3 *E. coli* cells for fusion protein synthesis. This would increase the probability of generating successful soluble SFRP-2 protein. Furthermore, if multiple soluble SFRP-2 fusion proteins were generated then these could be simultaneously immunised into a range of immune models to increase the likelihood of successful antibody response.

Another approach that could be taken to generate a soluble SFRP-2 antigen is to perform SFRP-2 protein extraction from SFRP-2 expressing cell lines (e.g. PC-3 presented in chapter 4) or tissue or serum/blood (if SFRP-2 protein levels were detected in blood by Western blotting). Purification of the SFRP-2 protein from these lysates could be achieved by creating an in-house affinity resin through coupling SFRP-2 antibodies, which can be purchased commercially (listed in Table 21), to a support matrix/resin. High SFRP-2 protein concentrations are unlikely to be achieved using this method for protein extracted in tissue or cell lines but if the protein was found to be expressed in serum then obtaining serum from blood banks may yield higher concentrations of the protein. In addition, immunisations only require 200 µg of pure protein per immunisation so this yield could be possible even from protein extracted from tissue.

6.4 Overall Conclusion

The complexity of bringing a biomarker from early discovery to a well validated clinical tool requires a collective collaborative effort from various organizations and individuals from academia, medicine, government and industry. Putative biomarkers require careful validation and optimisation for their use in clinical screening which requires coordination among clinicians, statisticians and biologists. The PCRC is one such collaboration that provides this coordination. Although some putative biomarkers studied in this thesis failed to have clinical relevance, SFRP-2 was identified as a possible marker of disease progression in prostate cancer pending further analysis. If collaborative effort within this group and others like it continues, in conjunction with the development and implementation of other advancing technologies, adequate funding and the recruitment of skilled researchers, then the likelihood of developing key biomarkers to assist diagnosis and therapies of all cancers, not only prostate cancer, will increase significantly.

Bibliography

Aaltomaa S, Karja V, Lipponen P, Isotalo T, Kankkunen JP, Talja M & Mokka R. Reduced alpha- and beta-catenin expression predicts shortened survival in local prostate cancer. *Anticancer Res* 2005; **25**: 4707-12.

Andris-Widhopf J, Rader C, Steinberger P, Fuller R & Barbas CF, 3rd. Methods for the generation of chicken monoclonal antibody fragments by phage display. *J Immunol Methods* 2000; **242**: 159-81.

Attard G, Richards J & de Bono JS. New strategies in metastatic prostate cancer: targeting the androgen receptor signaling pathway. *Clin Cancer Res* 2011; **17**: 1649-57.

Aus G, Abbou CC, Bolla M, Heidenreich A, Schmid HP, van Poppel H, Wolff J & Zattoni F. EAU guidelines on prostate cancer. *Eur Urol* 2005; **48**: 546-51.

Barbas CF, Burton, D,R., Scott, J,K., Silverman,G,J. *Phage Display: A laboratory manual,* Cold Spring Harbor Laboratory press 2001.

Baumgart LA, Gerling GJ & Bass EJ. Characterizing the range of simulated prostate abnormalities palpable by digital rectal examination. *Cancer Epidemiol* 2010; **34**: 79-84.

Billman-Jacobe H. Expression in bacteria other than Escherichia coli. *Curr Opin Biotechnol* 1996; **7**: 500-4.

Blow N. Antibodies: The generation game. *Nature* 2007; **447**: 741-4.

Bondar OP, Barnidge DR, Klee EW, Davis BJ & Klee GG. LC-MS/MS quantification of Zn-alpha2 glycoprotein: a potential serum biomarker for prostate cancer. *Clin Chem* 2007; **53**: 673-8.

Bordeaux J, Welsh A, Agarwal S, Killiam E, Baquero M, Hanna J, Anagnostou V & Rimm D. Antibody validation. *Biotechniques* 2003; **48**: 197-209.

Bovolenta P, Esteve P, Ruiz JM, Cisneros E & Lopez-Rios J. Beyond Wnt inhibition: new functions of secreted Frizzled-related proteins in development and disease. *J Cell Sci* 2008; **121**: 737-46.

Brawer MK, Meyer GE, Letran JL, Bankson DD, Morris DL, Yeung KK & Allard WJ. Measurement of complexed PSA improves specificity for early detection of prostate cancer. *Urology* 1998; **52**: 372-8.

Brooks JD, Weinstein M, Lin X, Sun Y, Pin SS, Bova GS, Epstein JI, Isaacs WB & Nelson WG. CG island methylation changes near the GSTP1 gene in prostatic intraepithelial neoplasia. *Cancer Epidemiol Biomarkers Prev* 1998; **7**: 531-6.

Brothman AR, Swanson G, Maxwell TM, Cui J, Murphy KJ, Herrick J, Speights VO, Isaac J & Rohr LR. Global hypomethylation is common in prostate cancer cells: a quantitative predictor for clinical outcome? *Cancer Genet Cytogenet* 2005; **156**: 31-6.

Brownback KR, Renzulli J, Delellis R & Myers JR. Small-cell prostate carcinoma: A retrospective analysis of five newly reported cases. *Indian J Urol* 2009; **25**: 259-63.

Byrne JC, Downes MR, O'Donoghue N, O'Keane C, O'Neill A, Fan Y, Fitzpatrick JM, Dunn M & Watson RW. 2D-DIGE as a strategy to identify serum markers for the progression of prostate cancer. *J Proteome Res* 2009; **8**: 942-57.

Chalitchagorn K, Shuangshoti S, Hourpai N, Kongruttanachok N, Tangkijvanich P, Thong-ngam D, Voravud N, Sriuranpong V & Mutirangura A. Distinctive pattern of LINE-1 methylation level in normal tissues and the association with carcinogenesis. *Oncogene* 2004; **23**: 8841-6.

Che M SW, Grignon D. Pathologic features the urologist should expect on a prostate biopsy. *Urologic oncology* 2003; **21**: 153-61.

Chen G, Shukeir N, Potti A, Sircar K, Aprikian A, Goltzman D & Rabbani SA. Up-regulation of Wnt-1 and beta-catenin production in patients with advanced metastatic prostate carcinoma: potential pathogenetic and prognostic implications. *Cancer* 2004; **101**: 1345-56.

Chesire DR & Isaacs WB. Beta-catenin signaling in prostate cancer: an early perspective. *Endocr Relat Cancer* 2003; **10**: 537-60.

Conroy PJ, Hearty S, Leonard P & O'Kennedy RJ. Antibody production, design and use for biosensor-based applications. *Semin Cell Dev Biol* 2009; **20**: 10-26.

Corder EH, Friedman GD, Vogelman JH & Orentreich N. Seasonal variation in vitamin D, vitamin D-binding protein, and dehydroepiandrosterone: risk of prostate cancer in black and white men. *Cancer Epidemiol Biomarkers Prev* 1995; **4**: 655-9.

Correia IR. Stability of IgG isotypes in serum. *MAbs* 2011; **2**: 221-32.

Curran S, McKay JA, McLeod HL & Murray GI. Laser capture microscopy. *Mol Pathol* 2000; **53**: 64-8.

Dabbs D *Diagnostic Immunohistochemistry (2nd Edition),* Elsevier 2006.

Dahlmann B, Ruppert T, Kloetzel PM & Kuehn L. Subtypes of 20S proteasomes from skeletal muscle. *Biochimie* 2001; **83**: 295-9.

Damber JE & Aus G. Prostate cancer. *Lancet* 2008; **371**: 1710-21.

Delker SL, West AP, Jr., McDermott L, Kennedy MW & Bjorkman PJ. Crystallographic studies of ligand binding by Zn-alpha2-glycoprotein. *J Struct Biol* 2004; **148**: 205-13.

DeMarzo AM, Nelson WG, Isaacs WB & Epstein JI. Pathological and molecular aspects of prostate cancer. *Lancet* 2003; **361**: 955-64.

Descazeaud A, de la Taille A, Allory Y, Faucon H, Salomon L, Bismar T, Kim R, Hofer MD, Chopin D, Abbou CC & Rubin MA. Characterization of ZAG protein expression in prostate cancer using a semi-automated microscope system. *Prostate* 2006; **66**: 1037-43.

Downes MR, Byrne JC, Pennington SR, Dunn MJ, Fitzpatrick JM & Watson RW. Urinary markers for prostate cancer. *BJU Int* 2007; **99**: 263-8.

Edwards JL. Diagnosis and management of benign prostatic hyperplasia. *Am Fam Physician* 2008; **77**: 1403-10.

Ehrlich M. DNA methylation in cancer: too much, but also too little. *Oncogene* 2002; **21**: 5400-13.

Epstein JI, Allsbrook WC, Jr., Amin MB & Egevad LL. The 2005 International Society of Urological Pathology (ISUP) Consensus Conference on Gleason Grading of Prostatic Carcinoma. *Am J Surg Pathol* 2005; **29**: 1228-42.

Fitzgerald J, Stapleton, S., Dunne, L., Leonard, P., Madamsetti, N., Danaher, M., Elliot, C., O' Kennedy,R. (2007) Rapid methods for the detection of toxins and anti-protozoan drug residues. *IXth International Conference on AgriFood Antibodies (ICAFA).* Oslo, Norway.

Fournier NC & Richard MA. Role of fatty acid-binding protein in cardiac fatty acid oxidation. *Mol Cell Biochem* 1990; **98**: 149-59.

Gann PH, Ma J, Hennekens CH, Hollis BW, Haddad JG & Stampfer MJ. Circulating vitamin D metabolites in relation to subsequent development of prostate cancer. *Cancer Epidemiol Biomarkers Prev* 1996; **5**: 121-6.

Gerngross TU. Advances in the production of human therapeutic proteins in yeasts and filamentous fungi. *Nat Biotechnol* 2004; **22**: 1409-14.

Hale LP, Price DT, Sanchez LM, Demark-Wahnefried W & Madden JF. Zinc alpha-2-glycoprotein is expressed by malignant prostatic epithelium and may serve as a potential serum marker for prostate cancer. *Clin Cancer Res* 2001; **7**: 846-53.

Hall CL, Bafico A, Dai J, Aaronson SA & Keller ET. Prostate cancer cells promote osteoblastic bone metastases through Wnts. *Cancer Res* 2005; **65**: 7554-60.

Hammarstrom M, Hellgren N, van Den Berg S, Berglund H & Hard T. Rapid screening for improved solubility of small human proteins produced as fusion proteins in Escherichia coli. *Protein Sci* 2002; **11**: 313-21.

Harper S & Speicher DW. Purification of proteins fused to glutathione S-transferase. *Methods Mol Biol* 2011; **681**: 259-80.

Hoogenboom HR, Henderikx P & de Haard H. Creating and engineering human antibodies for immunotherapy. *Adv Drug Deliv Rev* 1998; **31**: 5-31.

Hoque MO, Begum S, Topaloglu O, Jeronimo C, Mambo E, Westra WH, Califano JA & Sidransky D. Quantitative detection of promoter hypermethylation of multiple genes in the tumor, urine, and serum DNA of patients with renal cancer. *Cancer Res* 2004; **64**: 5511-7.

Horvath L & Henshall S. The application of tissue microarrays to cancer research. *Pathology* 2001; **33**: 125-9.

Houlihan LM, Davies G, Tenesa A, Harris SE, Luciano M, Gow AJ, McGhee KA, Liewald DC, Porteous DJ, Starr JM, Lowe GD, Visscher PM & Deary IJ. Common

variants of large effect in F12, KNG1, and HRG are associated with activated partial thromboplastin time. *Am J Hum Genet*; **86**: 626-31.

http://www.cancer.gov/cancertopics/pdq/treatment/prostate/HealthProfessional/page3. Stages in Prostate cancer, National Cancer Institute

http://www.lesc.ic.ac.uk/projects/appp.html. The London e-Science Centre

http://www.microarraystation.com/tissue-microarray/. Tissue Microarray Construction

Hudson PJ & Souriau C. Engineered antibodies. *Nat Med* 2003; **9**: 129-34.

Isaacs JT & Isaacs WB. Androgen receptor outwits prostate cancer drugs. *Nat Med* 2004; **10**: 26-7.

Isaacs W & Kainu T. Oncogenes and tumor suppressor genes in prostate cancer. *Epidemiol Rev* 2001; **23**: 36-41.

Issaq HJ, Waybright TJ & Veenstra TD. Cancer biomarker discovery: Opportunities and pitfalls in analytical methods. *Electrophoresis* 2010; **32**: 967-75.

Jaggi M, Johansson SL, Baker JJ, Smith LM, Galich A & Balaji KC. Aberrant expression of E-cadherin and beta-catenin in human prostate cancer. *Urol Oncol* 2005; **23**: 402-6.

Janeway C, A.,Travers, P., Walport ,M., Shlomchik, M. *Immunobiology: the immune systemin health and disease (6th Edition),* Garland Science Publishing 2005.

Jarrard DF, Bussemakers MJ, Bova GS & Isaacs WB. Regional loss of imprinting of the insulin-like growth factor II gene occurs in human prostate tissues. *Clin Cancer Res* 1995; **1**: 1471-8.

John TT, Bashir J, Burrow CT & Machin DG. Squamous cell carcinoma of the prostate--a case report. *Int Urol Nephrol* 2005; **37**: 311-3.

Jung K, Brux B, Lein M, Rudolph B, Kristiansen G, Hauptmann S, Schnorr D, Loening SA & Sinha P. Molecular forms of prostate-specific antigen in malignant and benign prostatic tissue: biochemical and diagnostic implications. *Clin Chem* 2000; **46**: 47-54.

Jutel M & Akdis CA. T-cell subset regulation in atopy. *Curr Allergy Asthma Rep* 2011; **11**: 139-45.

Kang GH, Lee S, Lee HJ & Hwang KS. Aberrant CpG island hypermethylation of multiple genes in prostate cancer and prostatic intraepithelial neoplasia. *J Pathol* 2004; **202**: 233-40.

Karayi MK & Markham AF. Molecular biology of prostate cancer. *Prostate Cancer Prostatic Dis* 2004; **7**: 6-20.

Katz R. Biomarkers and surrogate markers: an FDA perspective. *NeuroRx* 2004; **1**: 189-95.

Katzen F, Chang G & Kudlicki W. The past, present and future of cell-free protein synthesis. *Trends Biotechnol* 2005; **23**: 150-6.

Kawamoto K, Hirata H, Kikuno N, Tanaka Y, Nakagawa M & Dahiya R. DNA methylation and histone modifications cause silencing of Wnt antagonist gene in human renal cell carcinoma cell lines. *Int J Cancer* 2008; **123**: 535-42.

Keith JC, Jr., Sainz IM, Isordia-Salas I, Pixley RA, Leathurby Y, Albert LM & Colman RW. A monoclonal antibody against kininogen reduces inflammation in the HLA-B27 transgenic rat. *Arthritis Res Ther* 2005; **7**: R769-76.

Kleine AH, Glatz JF, Van Nieuwenhoven FA & Van der Vusse GJ. Release of heart fatty acid-binding protein into plasma after acute myocardial infarction in man. *Mol Cell Biochem* 1992; **116**: 155-62.

Kloetzel PM. Antigen processing by the proteasome. *Nat Rev Mol Cell Biol* 2001; **2**: 179-87.

Kononen J, Bubendorf L, Kallioniemi A, Barlund M, Schraml P, Leighton S, Torhorst J, Mihatsch MJ, Sauter G & Kallioniemi OP. Tissue microarrays for high-throughput molecular profiling of tumor specimens. *Nat Med* 1998; **4**: 844-7.

Lapointe J, Li C, Higgins JP, van de Rijn M, Bair E, Montgomery K, Ferrari M, Egevad L, Rayford W, Bergerheim U, Ekman P, DeMarzo AM, Tibshirani R, Botstein D, Brown PO, Brooks JD & Pollack JR. Gene expression profiling identifies clinically relevant subtypes of prostate cancer. *Proc Natl Acad Sci U S A* 2004; **101**: 811-6.

Larsson M, Brundell E, Nordfors L, Hoog C, Uhlen M & Stahl S. A general bacterial expression system for functional analysis of cDNA-encoded proteins. *Protein Expr Purif* 1996; **7**: 447-57.

Livak KJ & Schmittgen TD. Analysis of relative gene expression data using real-time quantitative PCR and the 2(-Delta Delta C(T)) Method. *Methods* 2001; **25**: 402-8.

Lopez-Beltran A, Mikuz G, Luque RJ, Mazzucchelli R & Montironi R. Current practice of Gleason grading of prostate carcinoma. *Virchows Arch* 2006; **448**: 111-8.

Luster AD, Alon R & von Andrian UH. Immune cell migration in inflammation: present and future therapeutic targets. *Nat Immunol* 2005; **6**: 1182-90.

Lytton B. Prostate cancer: a brief history and the discovery of hormonal ablation treatment. *J Urol* 2001; **165**: 1859-62.

Ma JF, Nonn L, Campbell MJ, Hewison M, Feldman D & Peehl DM. Mechanisms of decreased Vitamin D 1alpha-hydroxylase activity in prostate cancer cells. *Mol Cell Endocrinol* 2004; **221**: 67-74.

Makarov DV, Loeb S, Getzenberg RH & Partin AW. Biomarkers for prostate cancer. *Annu Rev Med* 2009; **60**: 139-51.

Maruvada P, Wang W, Wagner PD & Srivastava S. Biomarkers in molecular medicine: cancer detection and diagnosis. *Biotechniques* 2005; **Suppl**: 9-15.

Matsuda KM, Chung JY & Hewitt SM. Histo-proteomic profiling of formalin-fixed, paraffin-embedded tissue. *Expert Rev Proteomics* 2010; **7**: 227-37.

McCrae KR, Donate F, Merkulov S, Sun D, Qi X & Shaw DE. Inhibition of angiogenesis by cleaved high molecular weight kininogen (HKa) and HKa domain 5. *Curr Cancer Drug Targets* 2005; **5**: 519-28.

McDonald SL & Silver A. The opposing roles of Wnt-5a in cancer. *Br J Cancer* 2009; **101**: 209-14.

McNeal JE. Normal histology of the prostate. *Am J Surg Pathol* 1988; **12**: 619-33.

Micke P & Ostman A. Tumour-stroma interaction: cancer-associated fibroblasts as novel targets in anti-cancer therapy? *Lung Cancer* 2004; **45 Suppl 2**: S163-75.

Miller JR. The Wnts. *Genome Biol* 2002; **3**: REVIEWS3001.

Nadler RB, Humphrey PA, Smith DS, Catalona WJ & Ratliff TL. Effect of inflammation and benign prostatic hyperplasia on elevated serum prostate specific antigen levels. *J Urol* 1995; **154**: 407-13.

Ntais C, Polycarpou A & Tsatsoulis A. Molecular epidemiology of prostate cancer: androgens and polymorphisms in androgen-related genes. *Eur J Endocrinol* 2003; **149**: 469-77.

Perry AS, Loftus B, Moroose R, Lynch TH, Hollywood D, Watson RW, Woodson K & Lawler M. In silico mining identifies IGFBP3 as a novel target of methylation in prostate cancer. *Br J Cancer* 2007; **96**: 1587-94.

Pongracz JE & Stockley RA. Wnt signalling in lung development and diseases. *Respir Res* 2006; **7**: 15.

Pontari MA & Ruggieri MR. Mechanisms in prostatitis/chronic pelvic pain syndrome. *J Urol* 2004; **172**: 839-45.

Purzel J, Schmitt R, Viertlboeck BC & Gobel TW. Chicken IgY binds its receptor at the CH3/CH4 interface similarly as the human IgA: Fc alpha RI interaction. *J Immunol* 2009; **183**: 4554-9.

Roddam AW, Duffy MJ, Hamdy FC, Ward AM, Patnick J, Price CP, Rimmer J, Sturgeon C, White P & Allen NE. Use of prostate-specific antigen (PSA) isoforms for the detection of prostate cancer in men with a PSA level of 2-10 ng/ml: systematic review and meta-analysis. *Eur Urol* 2005; **48**: 386-99; discussion 398-9.

Rodriguez-Carmona E, Cano-Garrido O, Seras-Franzoso J, Villaverde A & Garcia-Fruitos E. Isolation of cell-free bacterial inclusion bodies. *Microb Cell Fact* 2010; **9**: 71.

Rubenstein AB & Rubnitz ME. Transitional cell carcinoma of the prostate. *Cancer* 1969; **24**: 543-6.

Scardino PT, Weaver R & Hudson MA. Early detection of prostate cancer. *Hum Pathol* 1992; **23**: 211-22.

Schmitz U, Versmold A, Kaufmann P & Frank HG. Phage display: a molecular tool for the generation of antibodies--a review. *Placenta* 2000; **21 Suppl A**: S106-12.

Schwartz GG. Correspondence re: E. H. Corder et al., Vitamin D and prostate cancer: a prediagnostic study with stored sera. Cancer Epidemiol., Biomarkers & Prev., 2: 467-472, 1993. *Cancer Epidemiol Biomarkers Prev* 1994; **3**: 183-4.

Schwarz-Romond T, Asbrand C, Bakkers J, Kuhl M, Schaeffer HJ, Huelsken J, Behrens J, Hammerschmidt M & Birchmeier W. The ankyrin repeat protein Diversin recruits Casein kinase Iepsilon to the beta-catenin degradation complex and acts in both canonical Wnt and Wnt/JNK signaling. *Genes Dev* 2002; **16**: 2073-84.

Sciarra A, Mariotti G, Salciccia S, Gomez AA, Monti S, Toscano V & Di Silverio F. Prostate growth and inflammation. *J Steroid Biochem Mol Biol* 2008; **108**: 254-60.

Selius BA & Subedi R. Urinary retention in adults: diagnosis and initial management. *Am Fam Physician* 2008; **77**: 643-50.

Shen MM & Abate-Shen C. Molecular genetics of prostate cancer: new prospects for old challenges. *Genes Dev* 2010; **24**: 1967-2000.

Shimizu Y, Inoue A, Tomari Y, Suzuki T, Yokogawa T, Nishikawa K & Ueda T. Cell-free translation reconstituted with purified components. *Nat Biotechnol* 2001; **19**: 751-5.

Smith GP. Filamentous fusion phage: novel expression vectors that display cloned antigens on the virion surface. *Science* 1985; **228**: 1315-7.

Sorensen HP & Mortensen KK. Advanced genetic strategies for recombinant protein expression in Escherichia coli. *J Biotechnol* 2005; **115**: 113-28.

Steinman L. A brief history of T(H)17, the first major revision in the T(H)1/T(H)2 hypothesis of T cell-mediated tissue damage. *Nat Med* 2007; **13**: 139-45.

Storb U, Shen HM, Michael N & Kim N. Somatic hypermutation of immunoglobulin and non-immunoglobulin genes. *Philos Trans R Soc Lond B Biol Sci* 2001; **356**: 13-9.
Sung SY & Chung LW. Prostate tumor-stroma interaction: molecular mechanisms and opportunities for therapeutic targeting. *Differentiation* 2002; **70**: 506-21.

Tabesh A, Teverovskiy M, Pang HY, Kumar VP, Verbel D, Kotsianti A & Saidi O. Multifeature prostate cancer diagnosis and Gleason grading of histological images. *IEEE Trans Med Imaging* 2007; **26**: 1366-78.

Tada T, Ohkubo I, Niwa M, Sasaki M, Tateyama H & Eimoto T. Immunohistochemical localization of Zn-alpha 2-glycoprotein in normal human tissues. *J Histochem Cytochem* 1991; **39**: 1221-6.

Taichman RS, Loberg RD, Mehra R & Pienta KJ. The evolving biology and treatment of prostate cancer. *J Clin Invest* 2007; **117**: 2351-61.

Tanaka K & Tsurumi C. The 26S proteasome: subunits and functions. *Mol Biol Rep* 1997; **24**: 3-11.

Thomas CM & Nielsen KM. Mechanisms of, and barriers to, horizontal gene transfer between bacteria. *Nat Rev Microbiol* 2005; **3**: 711-21.

Thompson I, Leach RJ, Pollock BH & Naylor SL. Prostate cancer and prostate-specific antigen: the more we know, the less we understand. *J Natl Cancer Inst* 2003; **95**: 1027-8.

Ting AH, McGarvey KM & Baylin SB. The cancer epigenome--components and functional correlates. *Genes Dev* 2006; **20**: 3215-31.

Ueda EK, Gout PW & Morganti L. Current and prospective applications of metal ion-protein binding. *J Chromatogr A* 2003; **988**: 1-23.

Unno M, Mizushima T, Morimoto Y, Tomisugi Y, Tanaka K, Yasuoka N & Tsukihara T. The structure of the mammalian 20S proteasome at 2.75 A resolution. *Structure* 2002; **10**: 609-18.

Varma M & Jasani B. Diagnostic utility of immunohistochemistry in morphologically difficult prostate cancer: review of current literature. *Histopathology* 2005; **47**: 1-16.
Vasan RS. Biomarkers of cardiovascular disease: molecular basis and practical considerations. *Circulation* 2006; **113**: 2335-62.

Veltri RW, Marlow C, Khan MA, Miller MC, Epstein JI & Partin AW. Significant variations in nuclear structure occur between and within Gleason grading patterns 3, 4, and 5 determined by digital image analysis. *Prostate* 2007; **67**: 1202-10.

Verboven C, Rabijns A, De Maeyer M, Van Baelen H, Bouillon R & De Ranter C. A structural basis for the unique binding features of the human vitamin D-binding protein. *Nat Struct Biol* 2002; **9**: 131-6.

Verheyen EM & Gottardi CJ. Regulation of Wnt/beta-catenin signaling by protein kinases. *Dev Dyn* 2010; **239**: 34-44.

Vihinen M. Modeling of prostate specific antigen and human glandular kallikrein structures. *Biochem Biophys Res Commun* 1994; **204**: 1251-6.

Waugh DS. Making the most of affinity tags. *Trends Biotechnol* 2005; **23**: 316-20.

Weeratna RD, McCluskie MJ, Xu Y & Davis HL. CpG DNA induces stronger immune responses with less toxicity than other adjuvants. *Vaccine* 2000; **18**: 1755-62.

Whitaker HC, Girling J, Warren AY, Leung H, Mills IG & Neal DE. Alterations in beta-catenin expression and localization in prostate cancer. *Prostate* 2008; **68**: 1196-205.

Wu J. On the role of proteasomes in cell biology and proteasome inhibition as a novel frontier in the development of immunosuppressants. *Am J Transplant* 2002; **2**: 904-12.

www.ncri.ie. Trends in Irish caner Incidence 1994-2002

www.pdb.org/pdb/home/home.do. Protein Data Bank

www.urology.uci.edu/prostate/prostate.html. The Prostate, Department of Urology, University California

Yang XJ, Tretiakova MS, Sengupta E, Gong C & Jiang Z. Florid basal cell hyperplasia of the prostate: a histological, ultrastructural, and immunohistochemical analysis. *Hum Pathol* 2003; **34**: 462-70.

Zakut-Houri R, Bienz-Tadmor B, Givol D & Oren M. Human p53 cellular tumor antigen: cDNA sequence and expression in COS cells. *EMBO J* 1985; **4**: 1251-5.

Zhu Y, Williams S & Zwiggelaar R. Computer technology in detection and staging of prostate carcinoma: a review. *Med Image Anal* 2006; **10**: 178-99.

Ziada A, Rosenblum M & Crawford ED. Benign prostatic hyperplasia: an overview. *Urology* 1999; **53**: 1-6.